universität wien

MASTERARBEIT

Titel der Masterarbeit

„Can we study cardiomyogenesis in embryonic stem cell or cardiovascular progenitor monolayer cell cultures?
Analysis of reporter gene expression and endogenously expressed marker genes in differentiating embryonic stem cells and cardiovascular progenitor cells"

verfasst von

Marie-Thérèse Konrad, BSc

angestrebter akademischer Grad

Master of Science (MSc)

Wien, 2015

Studienkennzahl lt. Studienblatt:	A 066 834
Studienrichtung lt. Studienblatt:	Masterstudium Molekulare Biologie
Betreut von:	Ao. Univ. Prof. Dr. Georg Weitzer

Table of contents

Danksagung

Ich bedanke mich ganz herzlich bei Ao. Univ. Prof. Dr. Georg Weitzer, der mich sowohl bei der Arbeit im Labor als auch beim Verfassen dieser Masterarbeit hervorragend unterstützt und motiviert hat. Ich habe unendlich viel gelernt.

Ich bedanke mich auch bei meinen LaborkollegInnen für ihre fachliche Unterstützung und Kollegialität. Ganz besonders möchte ich mich bei Hannah und Lucia bedanken, die mir die Zellkultur bzw. das FACS Gerät näher gebracht haben. Eure Hilfsbereitschaft und eure Herzlichkeit schätze ich sehr.

Herzlichen Dank auch an Thomas und Sharif, die mir sehr oft behilflich waren und im Hintergrund hervorragende Arbeit leisten.

Meinen Eltern bin ich unendlich dankbar für ihre Unterstützung auf allen Ebenen. Ich bin sehr glücklich, Eltern wie euch zu haben.
Danke auch an Clara, Clara und Anna, ihr seid die Besten!
Zum Schluss ein riesengroßes Dankeschön an Max, der immer an mich glaubt und für mich da ist.

Acknowledgements

I would like to thank

Lucia Leitner for the production of the Brachyury^{EGFP} and MesP1^{EGFP} reporter ESC and CVPC and of the TOPflash reporter ESC and CVPC lines

Martina Stary for the production of the Nkx2.5^{EGFP} reporter ESC line

Teresa Gottschamel for the production of the Nkx2.5^{EGFP} reporter CVPC line, and

Thomas Sauer for his introduction in the FACSCalibur flow cytometer.

1 Introduction

1.1 Cardiovascular disease and its burdens

As health conditions could be improved over the last century the main causes of death shifted from infectious diseases or nutritional deficiencies to non-communicable diseases such as cancer, diabetes, respiratory and cardiovascular disease (CVD) (Nascimento et al., 2014) with CVD being now the number one cause of death worldwide. At least 75 % of deaths due to CVD occur in low- or middle-income countries (WHO, 2015). More than 30 % of deaths in the USA and nearly 50 % of all deaths in Europe occur as a result of CVD (Go et al., 2014; Nichols et al., 2014).

The definition of CVD by the *International Statistical Classification of Diseases and Related Health Problems* codes comprises all diseases of the circulatory system including congenital CVD. Examples for CVD are ischaemic (coronary) heart disease, pulmonary heart disease, cerebrovascular disease (stroke) or atherosclerosis (Go et al., 2014).

The development of CVD is strongly correlated with the use of tobacco, unhealthy diet, physical inactivity and the harmful use of alcohol (WHO, 2015). Environmental factors such as cold weather and air pollution were also suggested to be associated with CVD (Hopstock et al., 2012; Puett et al., 2009). Ethnicity also plays a role in the burden and outcome of CVD. For example, Hispanics show lower cardiovascular mortality rates than non-Hispanic whites (Cortes-Bergoderi et al., 2013) and South Asian minorities in the UK display a higher incidence of ischaemic heart disease and therefore a higher coronary mortality rate (Zaman and Bhopal, 2013).

Depending on the nature and severity of the disease CVD possible interventions include lifestyle changes; cardiovascular medicines, such as antithrombotic drugs or antihypertensives; and surgery including coronary artery bypass grafting and coronary stenting (NHLBI, 2014). Medical devices such as pacemakers or prosthetic valves might also be needed (WHO, 2015).

Notwithstanding recent progress in the treatment of heart failure, the limited capacity of the heart to renew itself often leaves transplantation as the last intervention to prevent death. However, the amount of donor hearts does not even come close to meeting the needs excluding over 99 % of eligible patients. Even after successful transplantation long term survival rates are rather low. Therefore, there lies great interest and hope in the development of myocardial replacement therapies using stem cells (Bergmann et al., 2009; Chong and Murry, 2014; Yusen et al., 2014).

1.2 Stem cells

Stem cells exist in embryonic, fetal and adult stages of life. They are characterised by the following properties: self-renewal, clonality and the capacity to differentiate into different cell types (potency). According to their differentiation potential stem cells can be divided into five different types (Kolios and Moodley, 2013):

Totipotent stem cells have the ability to differentiate into both embryonic and extra-embryonic tissues, thus to give rise to the embryo and the placenta. Only the fertilized oocyte and cells of the first two divisions of development exhibit these capacities (Rossant, 2001).

Pluripotent stem cells differentiate into cells of all three germ layers, ectoderm, mesoderm and endoderm, eventually forming all tissues and organs. Embryonic stem cells show these characteristics (De Miguel et al., 2010).

Multipotent stem cells can give rise to several cell types of a single germ layer (Ratajczak et al., 2012). An example is the mesenchymal stem cell which is able to develop into different mesodermal tissues like adipose tissue, bone, cartilage and muscle (Augello et al., 2010).

Oligopotent stem cells are capable of differentiating into different lineages of a specific tissue. Hematopoietic stem cells, for example, develop into myeloid and lymphoid lineages (Marone et al., 2002).

Unipotent stem cells develop only into a single cell type. For example, spermatogonial stem cells only differentiate into spermatozoa (De Rooij and Grootegoed, 1998).

Stem cells provide an excellent tool to elucidate mechanisms of organogenesis and regeneration of the body. The most important goal in stem cell research is to fully exploit the potential of these cells to renew damaged tissues or whole organs (Kolios and Moodley, 2013).

1.2.1 Embryonic stem cells

Mammalian embryonic stem cells (ESCs) are derived from the inner cell mass (mouse) or the epiblast (human) of a developing embryo (Evans and Kaufman, 1981; Thomson et al., 1998).

These cells are pluripotent and can therefore develop into cells of all embryonic tissues and organs (De Miguel et al., 2010).

ESCs can be kept in culture indefinitely and are often grown on mitotically inactivated mouse fibroblast feeder cells to inhibit differentiation and to promote self-renewal (Evans and Kaufman, 1981; Thomson et al., 1998).

In mouse ESCs the key molecule in this regulation was found to be secreted leukaemia inhibitory factor (LIF) (Smith et al., 1988; Williams et al., 1988) which activates Janus kinase (JAK) via binding to the LIF receptor/glycoprotein 130 (GP130) heterodimer (Yoshida et al., 1994). One of the down-stream targets of JAKs is the transcription factor Signal transducer and Activator of Transcription 3 (STAT3) which upon phosphorylation activates several target genes (Boeuf et al., 1997) like *Kruppel like factor 4* (*Klf4)*, *Gastrulation brain homeobox 2* (*Gbx2*) or *Transcription factor cp2-like 1* (*Tfcp2l1*). These factors interact with the core pluripotency transcription factor network in ESCs (Hall et al. 2009; Li et al., 2005; Martello et al., 2013; Tai and Ying, 2013) consisting of Octamer binding transcription factor 4 (OCT4), Sex determining region Y-box 2 (SOX2) and Nanog. OCT4, SOX2 and Nanog cross-regulate each other and are essential to keep the ESC in a self-renewing pluripotent state (Young, 2011).

Additionally, JAKs also act via the Phosphoinositide 3-kinase (PI(3)K) – Protein Kinase B (PKB) signalling pathway upon LIF binding, stimulating the transcription of *Tbx3* which subsequently activates Nanog (Niwa et al., 2009). However, STAT3 seems to be the critical transducer of LIF signalling as *Stat3* null ESCs do not show a functional response when exposed to LIF (Martello et al., 2013).

Under serum-free conditions LIF is not sufficient to inhibit differentiation of mouse embryonic stem cells but has to act together with bone morphogenic proteins (BMPs) to successfully impede differentiation processes. BMPs activate *Inhibitor of differentiation* (*Id*) genes via the SMAD signalling pathway which in turn inhibit basic Helix-loop-helix (bHLH) transcription factors (Davies et al., 2013; Ying et al., 2003a; Zhang et al., 2010).

Human ESCs are dependent on basic fibroblast growth factor (bFGF), Nodal/Activin signalling and insulin or insulin-like growth factor (IGF) signalling to remain in a pluripotent and self-renewal state (Bendall et al., 2007; Vallier et al., 2005).

Genetic modification can be easily achieved in ESCs allowing the straightforward production of genetically modified ESC lines. Because of their universal differentiation potential ESCs can be used to study all processes in embryogenesis (Nishikawa et al., 2007).

Even though the potential for therapeutic usage of ESCs is theoretically high major concerns about their possible tumorigenicity and about possible host immune rejection as well as ethical concerns are slowing their clinical translation (Matar and Chong, 2014). For example, a phase I clinical trial investigating the potential of human ESC derived oligodendrocyte progenitor cells in the treatment of spinal cord injury was stopped abruptly in 2011 because the financing company shifted its focus from ESC research to cancer research. None of the four enrolled patients suffered from severe side effects but there was no evidence that the treatment was successful (Alper, 2009; Baker, 2011).

ESC therapy for patients suffering from macular degeneration was investigated in a clinical trial causing no tumorigenic or rejection reactions after 4 months (Schwartz et al., 2012).
Several pre-clinical studies have demonstrated the potential of mouse and human ESC derived cardiomyocytes to repair infarcted cardiac tissue (Chong et al., 2014; Fernandes et al., 2010; Laflamme et al., 2007; Min et al., 2002; Pearl et al., 2011).

1.2.2 Adult stem cells

Adult stem cells reside in most tissues of the body. These cells possess self-renewal capacities and are either multipotent, oligopotent or unipotent (Kolios and Moodley, 2013). Epidermal, blood and intestinal cells are regenerated daily from stem cells residing in these tissues (Hsu and Fuchs, 2012; Li and Clevers, 2010). Cell-type specific stem cells could also be detected in organs with limited regenerative capacity, like the brain or the adult skeletal muscle. These cells are usually found in a dormant state but respond to certain external stimuli, such as learning activity or muscle injury, with differentiation, proliferation or migration (Collins et al., 2005; Doetsch et al., 1999; Zhang et al., 2008a).
Stem cells are located in specific anatomical regions known as niches which provide a micro-environment that influences the characteristics and behaviours of stem cells. Niche cells can both induce or inhibit differentiation and self-renewal. For example, the niche for hair follicle stem cells lies in a region of the hair follicle known as the bulge (Hsu and Fuchs, 2012). Among the many components of this niche are Keratin 6 positive cells which transmit potent quiescence signals to hair follicle stem cells counterbalancing activating signals stemming from the dermal papilla, a cluster of mesenchymal cells (Hsu et al., 2011b).
Adult stem cells are a promising source for tissue repair and cell therapy. For example, several successful results could be obtained in preclinical and clinical studies for bone tissue repair using, among several other types of adult stem cells, mesenchymal stem cells of the bone marrow (Chimutengwende-Gordon and Khan, 2012). Investigations into the possible use of adult stem cells for cell therapy in various degenerative diseases, such as Diabetes mellitus, chronic myeloid leukemia or Crohn's disease, also had encouraging outcomes (Hackanson and Waller, 2011; Oyama et al., 2005; Trivedi et al., 2008).
The usage of adult stem cells in these treatment methods is advantageous as it does not pose the problem of rejection and does not evoke ethical concerns (Kørbling and Estrov, 2003; McCormick and Huso, 2010).

1.2.3 Cardiac stem cells

In 1925 it was published that mitotic structures could not be detected in human cardiomyocytes (Karsner et al., 1925), subsequently leading to the view that the heart is a post-mitotic organ incapable of regeneration (Leri et al., 2014). However, this theory was profoundly challenged by observations that changes in heart weight rarely correlated with changes in cardiomyocyte volume (Anversa and Kajstura, 1998) and the detection of putative endogenous cardiac stem cells in the adult human heart (Nadal-Ginard et al., 2003). In recent years several types of possible cardiac stem cells were identified (Matar and Chong, 2014):

ISL-1+ cardiac stem cells

The transcription factor Islet-1 (ISL-1) is a marker for cardiac progenitors of the secondary heart field (see section 1.4) which develop into cells of the outflow-tract, the right ventricle and the atria and to a small extent into cells of the left ventricle (Cai et al., 2003). ISL-1+ cardiac progenitors were also detected in postnatal rat, mouse and human myocardium (Laugwitz et al., 2005).
Human ESC derived ISL-1+ cardiac progenitors were shown to possess the ability to self-renew and to differentiate into cardiomyocytes, endothelial cells and smooth muscle cells *in vitro* (Bu et al., 2009).

C-KIT+ cardiac stem cells

C-KIT positive cardiac stem cells were identified in the hearts of adult rats, mice, dogs and humans (Bearzi et al., 2007; Beltrami et al., 2003; Linke et al., 2005; Urbanek et al., 2005). In rats, C-KIT+ cardiac stem cells were shown to differentiate into vasculature and immature cardiomyocytes when injected into an infarcted heart (Beltrami et al., 2003).
However, the cardiomyogenic potential of these cells was also valued differently. In a study in mice the ability of these cells to differentiate into cardiomyocytes seemed to decrease over time, being negligible in adult mice (Zaruba et al., 2010). But in a phase I clinical trial with patients undergoing coronary artery bypass surgery after myocardial infarction, stem cell infusion using C-KIT+ cardiac stem cells led to an improved function of the left ventricle and to reduced infarction size in comparison to conventional therapy (Bolli et al., 2011). Concerns about the integrity of certain data of this study were expressed by the Lancet editors (The Lancet Editors, 2014).

Cardiosphere-derived stem cells

Cardiospheres consist of a heterogeneous cell population. C-KIT+ cells are located in its centre and are surrounded by other cells, including cells expressing the stromal cell marker CD105. Upon injection into infarcted murine hearts cardiosphere-derived stem cells differentiated into cardiomyocytes and vasculature (Messina et al., 2004). In a phase I clinical trial with post myocardial infarction patients, it was shown that intracoronary injection of autologous cardiosphere-derived stem cells reduced the scar mass and increased the viable heart mass. The function of the left ventricle, on the other hand, could not be ameliorated (Makkar et al., 2012).

Side-population cardiac progenitors

These cells are characterised by their ability to efflux a DNA binding dye via an ATP-binding cassette transporter (Unno et al., 2012). They could be detected in fetal, neonatal and adult rat hearts (Leri et al., 2011) and were shown to possess cardiomyogenic potential *in vitro* (Hierlihy et al., 2002; Martin et al., 2004). However, a significant proportion of these cells might be bone-marrow derived and not of cardiac origin (Mouquet et al., 2005).

SCA-1+ cardiac stem cells

Stem cell antigen-1 (SCA-1) positive cardiac stem cells were detected in murine adult myocardium (Oh et al., 2003). However, until now it remains unknown whether a true human orthologue of SCA-1 exists (Matar and Chong, 2014).
Upon stimulation with 5-Azacytidine (5-AZA) a small proportion of freshly isolated SCA-1+ cardiac stem cells developed into cells of a phenotype resembling that of cardiomyocytes. When these cells were intravenously administered to mice which had experienced myocardial infarction, they migrated to the infarcted tissue and there developed into cardiomyocytes (Oh et al., 2003).
Knockdown of *Sca-1* in murine SCA-1+ cardiac stem cells caused reduced proliferation and augmented apoptosis of these cells. SCA-1 also seems to be important for the secretion of paracrine effectors in response to hypoxia leading to a stimulation of angiogenesis and a reduction of cardiac apoptosis (Tateishi et al., 2007).

Epicardium-derived cells

The epicardium forms the outer layer of the heart. Epicardium-derived cells play a fundamental role in the developing embryonic heart (Matar and Chong, 2014).

These cells were thought to be dormant in the adult heart but they were shown to respond to injury-related signals after myocardial infarction in mice where they promoted heart regeneration and injury reduction (Zhou et al., 2011). However, it is not entirely clear whether these cells directly contribute to cardiomyocyte and endothelial lineages (Wessels and Pérez-Pomarez, 2004).

SCA-1+/PDGFRα + cardiac stem cells

SCA-1+/Platelet derived growth factor receptor α+ (PDGFRα+) cells were shown to display all stem cell characteristics and were found in murine and human hearts (Chong et al. 2011, 2013). They originate from the epicardium (Chong et al., 2011) and might contribute to its regenerative potential (Matar and Chong, 2014).

Cardiovascular progenitor cells expanded in an *in vitro* niche

In our lab cardiovascular progenitor cells (CVPCs) were isolated from postnatal murine hearts using a strategy to selectively enrich for these cells, as they occur only at low numbers in adult hearts, and to promote their survival.
Heart cells originating from hearts of transgenic newborn mice with a neomycin resistance gene integrated in their genome were mixed with an equal number of murine ESCs which do not carry the neomycin resistance gene. This cell mixture was explanted on LIF secreting fibroblast feeder cells. LIF and other factors secreted by the feeder cells as well as by the ESCs should support the survival and self-renewal not only of the ESCs but also of the CVPCs present in the heart cell population. Cells were then grown at high density for three days followed by 1:3 splitting for 10 passages. During this procedure all cells of the heart cell population except for CVPCs most probably died or were diluted out. As it was assumed that CVPCs would be capable to autonomously self-renew when reaching a certain cell density ESCs were selectively killed after passage 10 using G418 to which CVPCs were resistant. CVPC colonies were isolated and expanded and sub-cloned under G418 conditions.
CVPCs proliferate infinitely on LIF secreting fibroblasts and can be kept in culture for at least 149 passages without altering their phenotype. These cells have the potential to differentiate into cardiomyocytes, endothelial cells and smooth muscle cells *in vitro* (Hoebaus et al., 2013).

1.3 Early mouse development: from fertilization to gastrulation

From fertilization to gastrulation the mouse embryo experiences a series of cell type specifications and body axis determinations (Takaoka and Hamada, 2012).

After three rounds of division the eight cell stage is reached as depicted in figure 1.1. The embryo undergoes a process named compaction which is associated with an increase in cell-cell contacts promoting cell adhesion. At this stage at embryonic day 2.5 (E2.5), known as the early morula stage, the apical-basal polarity of each cell is established (Johnson and Ziomek, 1981, Takaoka and Hamada, 2012). Specific proteins like Ezrin, Protein kinase C (PKC), Partitioning defective 3 (PAR3), PAR6 or atypical Protein kinase C (aPKC) localize to the apical side of the morula (Pauken and Capco, 2000; Plusa et al., 2005; Vinot et al., 2005) while other proteins such as PAR1 localize to the basolateral side (Vinot et al., 2005).

The cells of the morula further divide both symmetrically and asymmetrically (Johnson and Ziomek, 1981).The blastocyst begins to develop through cavitation forming the blastocoel around the 30-cell stage at E3.5 (Smith and McLaren, 1977).

Asymmetric cell divisions occur in a first “wave” from the 8-cell to the 16-cell stage and in a second “wave” from the 16-cell to the 32-cell stage which leads to the generation of outside and inside cells (Tarkowski and Wróblewska, 1967). These cells differ in their Hippo signalling which is only active in inside cells where it leads to the repression of trophectoderm specific genes. These genes are therefore only expressed in the outside cells which subsequently differentiate into trophectoderm (TE). The inside cells, on the other hand, develop into the inner cell mass (ICM) (Nishioka et al., 2008; Yagi et al., 2007). These two distinct cell types are found by E3.5 (Takaoka and Hamada, 2012).

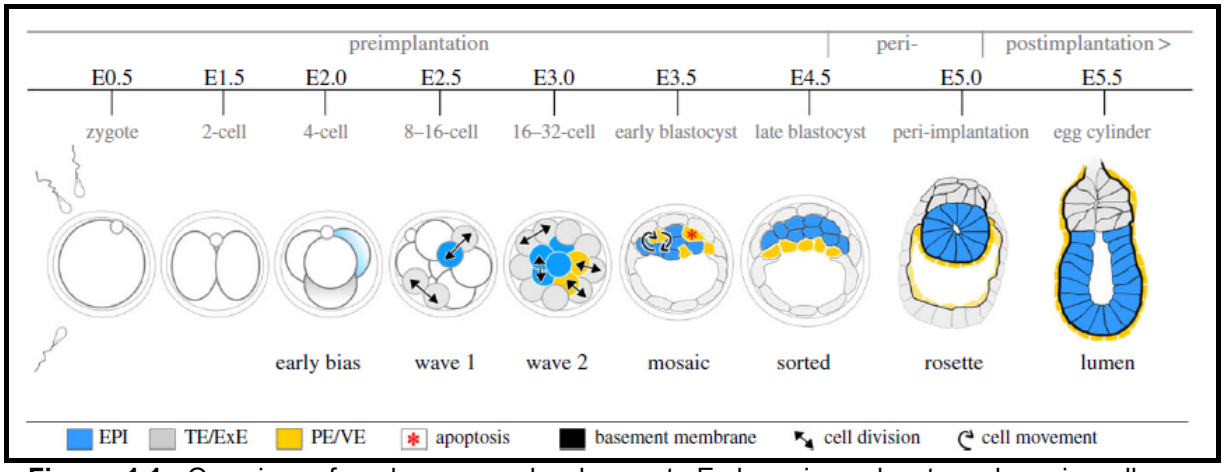

Figure 1.1: Overview of early mouse development. Embryonic and extraembryonic cells are specified in the preimplantation embryo by two cell fate decisions. In the first cell fate decision, waves of cell divisions create inside and outside cells. Outside cells give rise to extraembryonic trophectoderm (TE), while inside cells form the pluripotent inner cell mass (ICM). In the second cell

fate decision, cells of the ICM are segregated into the extraembryonic PE and the pluripotent epiblast (EPI) that will later give rise to all tissues of the body. These fate decisions are influenced but not determined by heterogeneity between individual cells within the embryo that is established by the 4-cell stage (shown by different shading of cells). At E4.5, the embryo initiates implantation and over the next 24 h invades the maternal tissues, rapidly proliferates and transforms into an egg cylinder. This new form serves as a foundation for EPI patterning, laying down the body axis and establishment of the germ layers. ExE, extraembryonic ectoderm; PE, primitive endoderm; VE, visceral endoderm (Bedzhov et al., 2014).

The implantation of the blastocyst in the uterus starts around E4.5 (Plaks et al., 2008). At this stage the ICM has differentiated into two cell types, namely cells of the primitive endoderm (PrE), which form a layer at the outside of the ICM, and cells of the epiblast, which are located inside the ICM as shown in figure 1.2 (Takaoka and Hamada, 2012). However, most of these cells might already be primed for their fate at E3.5 (Chazaud et al., 2006). FGF signalling plays an important role in the segregation of PrE and epiblast (Lanner and Rossant, 2010). While inhibition of FGF signalling shifts the cell fate to the epiblast, stimulation of FGF signalling shifts it towards PrE (Yamanaka et al., 2010).

Upon implantation cells of the mural TE, the part of the TE which is not in contact with the ICM, make contact with the uterine epithelium and subsequently terminally differentiate into trophoblast giant cells. These cells line the developing implantation site (Gardner et al., 1973; Simmons and Cross, 2005). Cells of the polar TE, which overlay the ICM, proliferate and form the extraembryonic endoderm which will eventually give rise to the placenta (Gardner et al., 1973; Simmons et al., 2007).

Cells of the PrE further differentiate into cells of the parietal endoderm (PaE) and cells of the visceral endoderm (VE). The PaE lines the luminal surface of the mural TE and will eventually contribute to the parietal yolk sac. The VE surrounds the extraembryonic ectoderm as well as the epiblast. If located near the extraembryonic endoderm the visceral endoderm is referred to as extraembryonic visceral endoderm (exVE) but if located adjacent to the epiblast it is named embryonic visceral endoderm (emVE) (Gasperowicz and Natale, 2011; Jollie, 1990; Mesnard et al., 2006; Perea-Gomez et al., 2007). At this stage around E5.5 the egg cylinder has formed by the proliferation of embryonic and extraembryonic lineages and their expansion into the blastocyst cavity (Bedzhov et al., 2014).

The embryonic VE can be further distinguished in distal visceral endoderm (DVE) and anterior visceral endoderm (AVE). The DVE is derived from GATA6+ Left-right determination factor 1+ (LEFTY1+) cells which are first present on E4.0 and are located on the upper side of the PrE on E4.2. On E5.5 these cells contribute to the DVE. The AVE arises from GATA binding protein 6+ (GATA6+) LEFTY1- VE cells which move to the

distal tip of the embryo and only begin to express *Lefty1* and *Cerberus-like 1* (*Cer1*) after E5.5 (Takaoka et al., 2006, 2011).

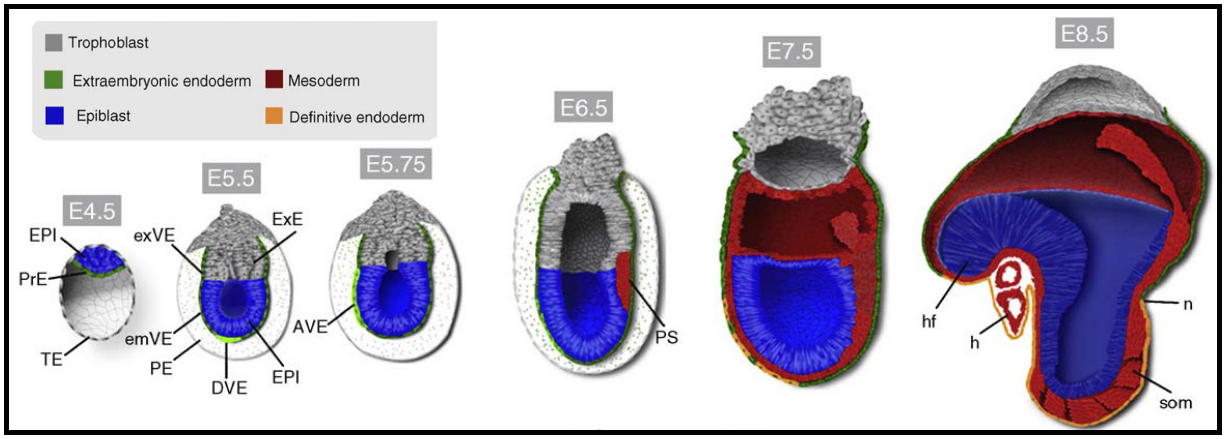

Figure 1.2: Schematic representation of still images depicting different tissue layers in the early mouse embryo: from the late blastocyst (E4.5) to early somite stage (E8.5). Abbreviations: AVE, anterior visceral endoderm; DVE, distal visceral endoderm; E, embryonic day; ExE, extraembryonic ectoderm; EPI, epiblast; emVE, embryonic visceral endoderm; exVE, extraembryonic visceral endoderm; h, heart; hf, headfolds; n, node; PE, parietal endoderm; PrE, primitive endoderm; PS, primitive streak; som, somite; TE, trophectoderm (Nowotschin and Hadjantonakis, 2010).

The anterior-posterior polarity of the embryo is fully established by E6.5 when AVE cells have migrated to the anterior site of the embryo (Stower and Srinivas, 2014; Takaoka and Hamada, 2012). The AVE secretes signals which act on the nearby epiblast and promote its future anterior identity (Takaoka and Hamada, 2012) and which inhibit Nodal and WNT3. Nodal and WNT3A elicit the formation of the primitive streak in the posterior part of the epiblast which is not reached by the inhibitory signals of the AVE (Arnold and Robertson, 2009; Lewis and Tam, 2006; Tam et al., 2006).

The formation of the primitive streak at E6.5 marks the onset of gastrulation, a process that leads to the formation of the three germ layers (Lewis and Tam, 2006).

Endodermal and mesodermal progenitors of the epiblast are internalised by passing through the primitive streak. During the internalisation these cells undergo epithelial-mesenchymal transition (EMT; Williams et al., 2012). In the course of EMT epithelial junctions are disassembled, cell adhesion molecules become down-regulated, the intermediate filament network is established and a rearrangement of the microtubule network takes place (Thiery et al., 2009).

The primitive streak expands along the posterior side of the embryo to the distal tip of the embryo (Arnold and Robertson, 2009). Cells that internalise through the early primitive streak will differentiate into heart mesoderm, prechordal mesoderm and cranial mesoderm. Cells ingressing subsequently at a more anterior aspect of the primitive streak

will form lateral plate mesoderm and paraxial mesoderm (Arnold and Robertson, 2009; Tam et al., 1997). At the most anterior aspect of the primitive streak a structure known as the node is created at E7.5-8 (Solnica-Krezel and Sepich, 2012). Cells which internalise via the node will form parts of the notochord (Yamanaka et al., 2007), which will later play an important role in patterning the neural tube and in establishing the dorsal-ventral axis of the central nervous system (Jessell, 2000).

Nascent endoderm cells intercalate between cells of the VE which leads to an expansion of its surface. Some cells of the VE, which was thought to only contribute to the yolk sac, might also differentiate into embryonic endoderm (Kwon et al., 2008).

Epiblast cells that remain on the anterior side of the embryo and do not migrate through the primitive streak will develop into ectoderm (Lu et al., 2001; Tam and Loebel, 2007).

1.4 Mouse cardiogenesis

The heart is the first functional organ in the developing vertebrate embryo (Gilbert, 2014).

Naïve cardiac mesoderm cells migrate away from the primitive streak to an anterior lateral region where they generate the heart crescent at E7.5 as depicted in figure 1.3 (Buckingham et al., 2005). At this stage two different cell types that will contribute to the heart can be distinguished, cells of the first heart field (FHF) and cells of the second heart field (SHF) (Kelly et al., 2014). The cells of the FHF already differentiate while the cells of the SHF remain undifferentiated (Kelly, 2012).

At E8 the FHF-derived linear heart tube arises from the cardiac crescent which has fused at the midline (Zaffran et al., 2004). The heart tube is composed of an outer myocardial and an inner endocardial layer and possesses an arteriorly positioned outflow tract (OFT), the arterial pole, and a posterior inflow tract, the venous pole (Miquerol and Kelly, 2013).

At E8.5 the heart tube starts beating and loops rightward (Zaffran et al., 2004). During cardiac looping a right-left lateralization is established for the first time in the developing embryo (Männer, 2000). Upon looping the transcription factors Heart and neural crest derivatives 1 (HAND1) and HAND2, which were initially located throughout the whole heart tube, become restricted to the future left and right ventricle, respectively (Biben and Harvey, 1997; Gilbert, 2014). Concomitantly, the heart tube extends by cellular proliferation and the recruitment of cells from the SHF originating from the pharyngeal mesoderm. These cells are added to the arterial and venous poles of the heart tube (Buckingham et al., 2005; Kelly, 2012; Kelly et al., 2014; Mjaatvedt et al., 2001; Waldo et al., 2001). At the arterial pole cells of the SHF generate the OFT, the right ventricle and smooth muscle at the base of the arteries while cells of the FHF contribute to the left ventricle. At the venous pole cells of the SHF develop into atrial, atrial septal and inflow

myocardium (Cai et al., 2003; Galli et al., 2008; Goddeeris et al., 2008; Hoffmann et al., 2009; Kelly et al., 2001; Meilhac et al., 2004; Sun et al., 2007; Waldo et al., 2005). At E9.0 the looped heart tube consists of four anatomical segments, atrium, atrioventricular canal (AVC), ventricle and OFT (Lin et al., 2012).

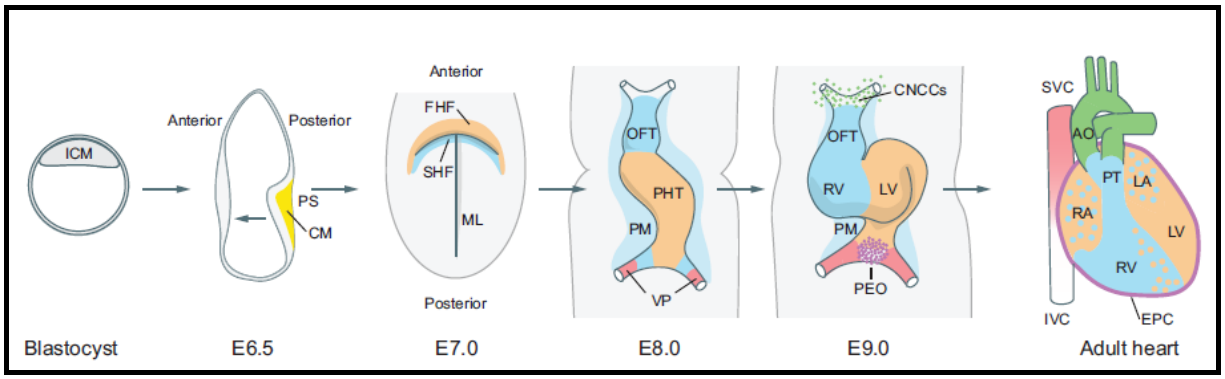

Figure 1.3: Cardiac development in the mouse embryo. Following gastrulation, the cells of the inner cell mass (ICM) are specified into three distinct germlayers: endoderm, ectoderm and mesoderm. The first signs of cardiac development can be detected at ~E6.5 with the formation of the cardiac mesoderm (CM, yellow) at the posterior side of the embryo, along the primitive streak (PS). At E7, the cardiac mesodermal cells migrate towards the anterior side of the embryo to form the two major cardiac progenitor pools: the first heart field (FHF, orange) or cardiac crescent; and the second heart field (SHF, blue), located posterior to the crescent. The FHF gives rise to the beating primitive heart tube (PHT) and eventually to the left ventricle (LV) and parts of the right and left atria (RA and LA, respectively). The SHF progenitors, located behind the PHT within the pharyngeal mesoderm (PM, light blue) by E8, migrate towards the primitive and looping heart tube to contribute to the right ventricle (RV), parts of the atria and outflow tract (OFT), and later to the base of the aorta (AO) and pulmonary trunk (PT). At ~E9.0 the transient proepicardial organ (PEO, purple), which eventually will form the outer lining of the heart known as the epicardium (EPC), becomes apparent. In addition, cardiac neural crest cells (CNCCs, green) migrate in from the dorsal neural tube through the pharyngeal arches, contributing to smooth muscle cells within the aortic and pulmonary arteries. Cells of the venous poles (VP, red), apparent at E8, contribute to the base of the superior and inferior vena cava (SVC and IVC, respectively). ML, midline (Später et al., 2014).

By midgestation the expansion of the heart tube has completed and the heart now grows by proliferation of cells located directly in the heart (Miquerol and Kelly, 2013). The right and left ventricular and atrial working chamber myocardium is formed on the outer curvature of the looped heart by a process of ballooning morphogenesis (Christoffels et al., 2000). At E10.5 well defined chambers are present in the developing heart (Brade et al., 2013).

At the inner curvature of the heart tube, including the OFT and the AVC, proliferation rates remain low (Miquerol and Kelly, 2013). The proliferative differences between the inner and

outer curvature of the heart are regulated by T-box contanining transcription factors. TBX20 and TBX5 mediate chamber myocardial development while TBX2 and TBX3 inhibit this process but instead stimulate the formation of cushions in the AVC and the OFT (Hoogaars et al., 2007). These cardiac cushions prevent bi-directional blood flow in the embryonic heart (Miquerol and Kelly, 2013).

BMP signals from myocardium overlying sites of cushion formation promote EMT in endocardial cells via activation of Notch and Transforming growth factor β (TGF-β) signalling which results in the formation of cushion mesenchyme. This cushion mesenchyme will eventually develop into the definitive cardiac valves concomitantly with heart septation (Combs and Yutzey, 2009).

The outermost layer of the heart, the epicardium, forms between E9.5 and E11.5. It is derived from the proepicardium which arises in close proximity to the venous pole at E8.5 (Brade et al., 2013; Männer et al., 2001).

Adaptation to terrestrial life required the total separation of systemic and pulmonary circulatory systems which is ensured by the formation of septa. The interventricular septum is generated at the interface between FHF- and SHF-derived myocardium. It fuses with the atrioventricular cushions thereby dividing the ventricular chamber into left and right ventricle (Anderson et al. 2003; Koshiba-Takeuchi et al., 2009; Moorman et al., 2003).

The aorticopulmonary septum separates the OFT into aorta and pulmonary trunk. Neural crest cells migrate from the neural tube to the OFT where they merge with other cell lineages to create this septum (Hutson and Kirby, 2003; Kirby et al., 1983).

Anti-clockwise rotation of the anterior pole of the heart leads to the positioning of the base of the pulmonary trunk over the right ventricle and the ascending aorta over the left ventricle (Bajolle et al., 2006; Lomonico et al., 1986).

The primary atrial septum expands from the atrial roof towards the AVC. At its leading edge a structure named mesenchymal cap is located. This cap fuses anteriorly with the atrioventricular cushions and posteriorly with the dorsal mesenchymal protrusion (Mommersteeg et al., 2006; Schroeder et al., 2003; Wessels and Sedmera, 2003; Wessels et al., 1996), which is derived from SHF cells which have migrated through the dorsal mesocardium and have bulged into the atrial chamber (Snarr et al., 2007, 2008). A hole in the primary atrial septum bypasses the pulmonary circulation in the developing embryo (Miquerol and Kelly, 2013; Webb et al., 1996).

At E14.5 the heart is thereby almost fully septated and connected to the aorta and pulmonary trunk (Brade et al., 2013).

At birth the hole in the primary atrial septum is closed by the secondary atrial septum, an infolding of the atrial roof, completing atrial septation and fully separating systemic and

pulmonary circulatory systems (Anderson et al., 2003; Goddeeris et al., 2008; Hoffmann et al., 2009).

1.5 Molecular regulation of cardiomyogenesis

Cardiomyogenesis is tightly regulated by complex transcriptional and molecular machineries.

Mesodermal cells which migrate through the primitive streak are marked by the expression of T-box transcription factor *Brachyury* (Showell et al., 2004). Upon specification into cardiac mesoderm *Brachyury* is down-regulated and the T-box transcription factor Eomesodermin (EOMES) directly activates the bHLH transcription factor Mesoderm posterior 1 (MesP1) (Bondue and Blanpain, 2010; Costello et al., 2011). This model was challenged by another study which showed that *Brachyury* over-expression in mouse ESCs led to a much higher induction of *MesP1* expression when compared to *Eomes* over-expression and that *Brachyury* and *MesP1* were co-expressed in mesoderm precursor cells of the primitive streak in mouse embryos (David et al., 2011). MesP1 plays an important role in the regulation of cardiac specification and migration prior to heart formation (Bondue and Blanpain, 2010; Bondue et al., 2008; Kitajima et al., 2000; Saga et al., 2000).

Once located in the cardiac crescent, FHF cells express key cardiac transcription factors such as *Nk2 homeobox 5* (*Nkx2.5*), *Gata4* and *Tbx5* (Arceci et al. 1993; Harvey, 2002; Heikinheimo et al. 1994; Kelley et al. 1993; Lints et al.,1993; Zeisberg et al. 2005) in response to FGF and BMP signals as well as to inhibitors of Wnt signalling (Marvin et al., 2001; Noseda et al., 2011; Reifers et al., 2000; Schneider and Mercola, 2001; Schultheiss et al., 1997; Tzahor and Lassar, 2001).

Cardiac progenitors of the SHF were thought to be specifically marked by the transcription factor ISL-1 (see section 1.2.3) but ISL-1 could also be detected in the cardiac crescent (Prall et al., 2007). However, ISL-1 has a crucial function in the survival, proliferation and migration into the primitive heart tube of SHF cells (Cai et al., 2003).

SHF progenitors are kept in a proliferative state by FGF signalling within the SHF, Sonic hedgehog (SHH) signals from the endoderm and by canonical Wnt signalling. The latter signalling pathway might also inhibit differentiation of SHF progenitors (Kelly, 2012; Kwon et al., 2009; Vincent and Buckingham, 2010).

SHF cells start to differentiate when contributing to the expansion of the heart tube (Francou et al., 2013). This cardiac differentiation is stimulated by BMP signals from the lateral plate mesoderm as well as by Notch, canonical and non-canonical Wnt signals (Ai

et al., 2007; High and Epstein, 2008; Klaus et al., 2007; Kwon et al., 2007; Schleiffarth et al., 2007; Vincent and Buckingham, 2010; Yang et al., 2006; Zhou et al., 2007).

1.5.1 Brachyury

Brachyury was the first identified T-box gene (Herrmann et al., 1990; Takashima and Suzuki, 2013). A T-box domain functions as a DNA binding domain and contains 180 amino acids (Müller and Herrmann, 1997). In the mouse genome the *Brachyury* gene is located on chromosome 17 and belongs to the 40 cM spanning *t*-complex (Wu et al., 2007).

In the mouse *Brachyury* expression commences shortly after implantation in a group of cells located at the frontier between prospective embryonic and extra-embryonic tissues. At E6.5 *Brachyury* expression becomes restricted to the proximal posterior portion of the embryo where the primitive streak will form (Arnold and Robertson, 2009; Rivera-Pérez and Magnuson, 2005). At the onset of gastrulation Brachyury is detected in the primitive streak and in the node. For a short time it continues to be expressed in newly formed mesodermal cells and adjacent epiblast cells but expression is reduced to a level undetectable by in-situ hybridisation as future paraxial mesoderm cells migrate laterally (Cambray and Wilson, 2007; Herrmann, 1991; Wilkinson et al., 1990). *Brachyury* remains to be expressed in the notochord but its expression will eventually be restricted to a region in the tail that will extend caudally to form the caudal spinal cord and somatic mesoderm (Cambray and Wilson, 2007; Smith, 2004; Wilkinson et al., 1990; Wilson et al., 1993).

Brachyury orthologues could be found in various species including *Xenopus*, zebrafish and chick but also basal chordates such as the ascidians *Halocynthia* and *Ciona* (Corbo et al., 1997; Kispert et al., 1995b; Schulte-Merker et al., 1992, 1994; Smith et al., 1991; Yasuo and Satoh, 1993).

Function

Brachyury functions as a transcriptional activator (Kispert et al., 1995b). It can bind DNA either as a homodimer, recognising palindromic sequences or inverted repeats, or as a monomer (Casey et al., 1998; Di Gregorio and Levine, 1999; Kispert and Herrmann, 1993; Kispert et al., 1995a; Müller and Herrmann, 1997; Tada and Smith, 2001).

Heterozygous mutant *Brachyury* mice show truncated tails and abnormalities in the posterior skeleton (Chesley, 1935; Dobrovolskaïa-Zavadskaïa, 1927). Homozygous mutant *Brachyury* mouse embryos die at E10.5 as a consequence of severe defects in the formation of the allantois, a precursor tissue of the umbilical chord (Gluecksohn-

Schoenheimer, 1944). These embryos show a complete loss of posterior mesoderm including the posterior portion of the notochord. In the anterior portion of the embryo notochordal precursor-like cells are present but they fail to undergo terminal differentiation (Chesley, 1935; Gluecksohn-Schoenheimer, 1938, 1944; Gruneberg, 1958; Yanagisawa, 1990). Most probably these defects are caused by the inability of mesodermal cells to migrate away from the primitive streak in the absence of Brachyury (Rashbass et al., 1991; Wilson and Beddington, 1997; Wilson et al., 1993, 1995). Due to failures in the formation of the notochord severe abnormalities in development of the neural tube and the posterior somites are observed in these embryos (Herrmann, 1991).

Brachyury is also involved in the regulation of the generation of the apical ectodermal ridge, a signalling center organising limb patterning (Liu et al., 2003).

In cultures of mouse ESCs *Brachyury* is expressed in a few cells that induce differentiation towards the mesodermal fate (Suzuki et al., 2006a). In these cells Brachyury up-regulates the expression of *Nanog* in the presence of LIF which leads to an inhibition of BMP-induced mesoderm differentiation (Suzuki et al., 2006b).

Brachyury mutations also influence heart development. *No tail* (*ntl*), a *Brachyury* orthologue, mutant zebrafish show a randomized cardiac left-right orientation (Danos and Yost, 1996). In the mouse Brachyury is required for the correct left-sided expression of *lefty-1* in prospective floorplate and of *lefty-2* in lateral plate mesoderm. As a probable consequence homozygous mutant *Brachyury* mice display randomisation in heart looping and orientation (King et al., 1998). In *Xenopus*, over-expression of *Xenopus Brachyury* (*Xbra*) or inhibition of Xbra function leads to randomised heart and gut looping (Kitaguchi et al., 2002).

Targets

In *Xenopus* several putative Xbra (Brachyury orthologue) target genes could already be identified several years ago. Among these targets are the signalling molecule XWnt11 through which Xbra regulates gastrulation movements, the homeodomain transcription factor Brachyury inducible homeobox 1 (Bix1), the zinc-finger transcription factor Xenopus early growth response protein 1 (Xegr-1) or embryonic Fibroblast growth factor (eFGF) (Casey et al., 1998; Saka et al., 2000; Smith, 2001; Tada and Smith, 2000; Tada et al., 1998). In a recent study additional Xbra targets could be detected in *Xenopus tropicalis* including genes involved in mesoderm development such as *mespa*, *mespb*, *myogenic differentiation* (*myod*) and in neural development such as *paired box 3* (*pax3*) and *sox2* (Gentsch et al., 2013).

In zebrafish Ntl was found to regulate the expression of genes playing a role in a variety of cellular processes including morphogenetic movements (e.g. *wnt11*, s*nail1a*,

connexin43.3, and *tbx16*), muscle specification (e.g. *mesogenin1* and *myoD*) and generation of posterior identity (e.g. *tbx6*, *ventral expressed homeobox* (*vent*), *ventral homeobox* (*vox*), *fgfr4*, and *cdx* genes) (Morley et al., 2009). In a different study the homeodomain transcription factor Floating head (Flh), necessitated for posterior notochord formation, could be identified as an Ntl target (Talbot et al., 1995).

In differentiating mouse ESCs putative Brachyury targets were found to be involved in morphogenesis, cell adhesion and cell polarity among others. Many target genes are components of Wnt, MAPK, JNK, TGF-β, Hedgehog, FGF and G-protein coupled signalling pathways. The expression of the identified Brachyury targets *Wnt3a*, *Axin2* and *Fgf8* was clearly reduced in *Brachyury* mutant mouse embryos and these factors were also targeted by Brachyury in human ESC derived mesodermal cells (Evans et al., 2012).

Functional Brachyury targets in differentiating mouse ESCs or in mouse embryos are components of signalling pathways such as *Fgf8* or *Dual specificity phosphatase 6* (*Dusp6*). They play a role in left right patterning such as *Tbx6*; are involved in haematopoiesis or skeleton muscle and chondrocyte differentiation such as *Mix1 homeobox like 1* (*Mixl1*) or *Mesogenin 1* (*Msgn1*); are expressed in the node, notochord and/or endoderm such as *Forkhead box protein a2* (*Foxa2*) and *Sox17*, function in the cell cycle and in cancer development such as *Retinoblastoma protein* (*Rb1*); influence cell mobility and EMT such as *Sox4*; or are involved in protein synthesis such as *Ribosomal protein s3a* (*Rps3a*) (Lolas et al., 2014).

David and co-workers identified three Brachyury binding elements in the promoter region of the human *MesP1* gene which are bound by Brachyury *in vitro* and can be activated after insertion, as part of a reporter construct, into *Brachyury* over-expressing mouse ESCs (David et al., 2011).

Regulation

Brachyury expression is regulated by several signalling molecules via various pathways. In zebrafish the expression of both *Brachyury* orthologues, *ntl-a* and *ntl-b*, is induced via Nodal signalling. BMP and Wnt signalling additionally regulate *ntl-a* expression (Harvey et al., 2010). Furthermore, NF-κB signalling might also activate *ntl* expression (Correa et al., 2004).

In the *Xbra* promoter an E-box, which can be bound by bHLH transcription factors, and two canonical Tcf1/Lef1 sites, which can be recognised by β-catenin upon canonical Wnt signalling, were detected and are conserved in the mouse (Clements et al., 1996; Latinkić et al., 1997; Lerchner et al., 2000). BMP, TGF-β, Wnt and FGF signalling activate *Xbra* transcription in *Xenopus* (Amaya et al., 1993; Hemmati-Brivanlou and Melton, 1992; Northrop et al., 1995; Vonica and Gumbiner, 2002). FGF signalling is also required to

maintain *Xbra* expression during subsequent development (Isaacs et al., 1994; Schulte-Merker and Smith, 1995; Showell et al., 2004).

In the mouse a mutation in the TCF1/LEF1 site but not in the E-box of the *Brachyury* promoter prohibits *Brachyury* expression (Galceran et al., 2001). Compatibly, Brachyury was found to be a direct target of WNT3A during paraxial mesoderm formation in the mouse (Yamaguchi et al., 1999). Most probably *Brachyury* expression is also activated via different signalling pathways in the mouse as mesoderm can not be induced via Wnt signalling (Showell et al., 2004). BMP-4 as well as, to a minor extent, Activin-A and WNT3A, stimulated *Brachyury* expression in human ESCs (Zhang et al., 2008b).

Negative regulation of *Brachyury* has also been described. For instance, Smad-interacting protein (Sip1) actively inhibited *Xbra* expression (Verschueren et al., 1999). Furthermore, Goosecoid and Xbra repressed each other (Saka et al., 2007) and SOX17 reduced *Brachyury* expression in differentiating mouse ESCs (Lolas et al., 2014).

Autoregulation of Xbra was reported as well (Conlon et al., 1996). Human Brachyury was also shown to bind to its own locus (Nelson et al., 2012). However, in mice an autoregulatory loop was ruled out (Schmidt et al., 1997).

Role in disease

Brachyury was reported to function in EMT in a variety of human cancers including lung cancer, oral squamous cell carcinoma (SCC), adenoid cystic carcinoma (AdCC), breast cancer, chordoma, a malignant skeletal tumour, and prostate cancer (Hu et al., 2014; Imajyo et al., 2012; Palena et al., 2014; Pinto et al., 2014; Roselli et al., 2012; Shimoda et al., 2012).

In human primary lung tumours and adjacent lung tissue *Brachyury* was found to be strongly expressed. Brachyury also contributed to resistance development to the EGF receptor (EGFR) kinase in a human lung cancer cell line. Therefore, Brachyury might be a possible target for immunotherapy against lung cancer (Roselli et al., 2012).

Brachyury expression was associated with EMT as well as with lymph node metastases and distant metastases in oral SCC and thus, might be a useful prognostic marker (Imajyo et al., 2012).

In breast cancer Brachyury over-expression correlated with poor prognosis (Palena et al., 2014).

A copy number gain of *Brachyury* as well as high protein expression levels were detected in sporadic and hereditary chordomas (Oakley et al., 2008; Presneau et al., 2011; Sangoi et al., 2011; Yang et al., 2009b). Furthermore, suppression of Brachyury in chordoma cell lines blocks cell proliferation (Hsu et al., 2011a; Presneau et al., 2011).

Brachyury was highly over-expressed at both the mRNA and the protein level in prostate cancer and associated metastatic tumours which correlated with tumour progression and aggressiveness. Therefore, Brachyury could be used as a prognostic marker in prostate cancer (Pinto et al., 2014).

1.5.2 Mesoderm Posterior 1 (MesP1)

The bHLH transcription factor MesP1 was first identified in a screen for transcripts enriched in the posterior portion of the mouse embryo at E7 to E7.5 (Saga et al., 1996).
From E6.5 *MesP1* is expressed in early mesodermal cells that firstly migrate into and then away from the primitive streak. Upon leaving the primitive streak expression of *MesP1* is rapidly decreasing in these cells (Saga et al., 1996, 1999). After E8.5 *MesP1* expression can still be detected in the presomitic mesoderm.
MesP1 is the earliest known marker of cardiac progenitors and is expressed in precursors of the first as well as the second heart field (Bondue and Blanpain, 2010; Buckingham et al., 2005; Saga et al., 1999; 2000). The majority of cells which have at one point in development expressed *MesP1* contribute to the heart, more precisely to all cardiac lineages including myocardium, endocardium, the conduction cells and the epicardium, the dorsal aorta, the intersomitic and cranial vessels and the amnion at E9.5 (Saga et al., 1999, 2000).
Additionally, MesP1-derived cells will form some muscles and bones of the face (Harel et al., 2009; McBratney-Owen et al., 2008; Yoshida et al., 2008) as well as parts of the embryonic liver (Asahina et al., 2009).
MesP-related genes were identified, among others, in chicken, *Xenopus*, zebrafish as well as in the basal chordate *Ciona* (Buchberger et al., 1998, 2002; Satou et al., 2004; Sawada et al., 2000; Sparrow et al., 1998).

Function

MesP1 can act as both a transcriptional activator and repressor (Bondue et al., 2008).
Transient but not continuous augmented expression of *MesP1* in differentiating mouse ESCs accelerated and increased cardiac differentiation and also stimulated endothelial and smooth muscle differentiation in several studies (Bondue et al., 2008; David et al., 2008; Lindsley et al., 2008).
In yet another study, induction of *MesP1* expression in differentiating mouse ESCs at an early differentiation stage caused the formation of progenitors that will eventually undergo haematopoietic differentiation. In contrast, induction of *MesP1* expression at a later point

in time leads to the generation of precursors, which will subsequently undergo cardiac differentiation. In the absence of serum-derived factors MesP1-derived cells also differentiate into skeletal myocytes in this study (Chan et al., 2013).
Cardiac mesoderm migration is defective in *MesP1*-null mice which, as a consequence, display severe cardiac abnormalities known as “cardia bifida”, the formation of two separate heart tubes instead of one. These defects cause embryonic lethality around E10.5 (Saga et al., 1999; 2000).
MesP2 might be able to partially compensate for the lack of MesP1 as its expression is enhanced in *MesP1*-null mice and these mice still show some myocardium and endocardium differentiation (Bondue and Blanpain, 2010; Kitajima et al., 2000). When both *MesP1* and *MesP2* are inactivated gastrulation is severely hampered as mesodermal cells fail to exit the primitive streak and these mice die around E9.5 (Kitajima et al., 2000).
In humans certain mutations in the *MesP1* gene are associated with congenital heart disease (Lahm et al., 2013).

Targets

In mouse ESCs several cardiac transcription factors including *Hand2*, *Myocardin*, *Nkx2.5*, *Gata4*, *Myocyte-specific enhancer factor 2c* (*Mef2c*), *Tbx20*, *Forkhead box h1* (*Foxh1*), *Foxc1*, and *Foxc2* were identified as MesP1 targets via transcriptional profiling after induction of *MesP1* expression. Furthermore, chromatin immunoprecitipation (ChIP) experiments demonstrated that MesP1 binds to bHLH binding sites within the genomic region of *Hand2*, *Myocardin*, *Nkx2.5* and *Gata4* (Bondue et al., 2008).
In a different study using a similar approach other cardiac structural genes such as *Myosin heavy chain α* (*Mhc-α*), *Mhc-β*, *Myosin regulatory light chain 2* (*Myl2*), *Myl7*, and *cardiac Troponin T (cTnt*) were found to be targets of MesP1 (Lindsley et al., 2008).
MesP1 also modulated the expression of transcription factors implicated in EMT including *Snail1* and *Twist basic helix-loop-helix transcription factor 1* (*Twist1*) and of genes involved in cell migration such as *C-x-c motif chemokine receptor type 4* (*Cxcr4*) and *Chemokine c-x3-x motif ligand 1* (*Cx3cl1*) (Bondue et al., 2008; Lindsley et al. 2008).
MesP1 inhibited the expression of several genes playing a role in the early steps of primitive streak formation such as *Brachyury* and *Fgf8* or in early endoderm specification including *Sox17*, *Nodal*, *Goosecoid* (*Gsc*) and *Foxa2* (Bondue et al., 2008). *MesP2* expression could also be repressed by MesP1 *in vitro* and *in vivo* (Bondue et al., 2008; Kitajima et al., 2000).

Regulation

In the *MesP1* promoter a TCF/LEF-OCT4 composite site was described which mediates the activation of the *MesP1* promoter by Oct4 and canonical Wnt signalling (Li et al., 2013). In accordance with this finding, the addition of Dickkopf1 (DKK1), a soluble Wnt inhibitor, led to the repression of *MesP1* expression in differentiating ESCs whereas the addition of WNT3A strongly activated *MesP1* expression (Bondue et al., 2008; Lindsley et al., 2006; Liu et al., 2007; Ueno et al., 2007).

As already mentioned above, the T-box transcription factors Brachyury and EOMES were both shown to directly bind regions in the *MesP1* promoter and to activate *MesP1* expression (Costello et al., 2011; David et al., 2011). *MesP1* expression could also be up-regulated by the micro RNA (miRNA) let-7c in differentiating mouse ESCs (Coppola et al., 2014).

In differentiating mouse ESCs MesP1 stimulated its own mRNA expression shortly after its expression was induced but later after induction MesP1 inhibited its own mRNA expression. MesP1 was also shown to bind its own promoter, thus, activation and repression of its own gene could be direct (Bondue et al., 2008). Probably, auto-repression of *MesP1* expression occurs *in vivo* as well (Saga et al., 1999).

1.5.3 NK2 transcription factor related, locus 5 (NKX2.5)

The homeobox transcription factor NKX2.5 belongs to a family of transcription factors for which the *Drosophila tinman* protein serves as a prototype (Bartlett et al., 2010). Tinman is indispensable for the development of the dorsal vessel, the fly's heart, (Bodmer, 1993) and related proteins could be detected in several vertebrate species including mouse, (Komuro and Izumo, 1993; Lints et al., 1993), *Xenopus* (Tonissen et al., 1994), chick (Schultheiss et al., 1995), zebrafish (Chen and Fishman, 1996) and human (Shiojima et al., 2000).

NKX2.5 is one of the earliest markers of cardiomyogenic differentiation (Akazawa and Komuro, 2005). In mice, *Nkx2.5* is expressed at high levels in early cardiac progenitors of the FHF and the SHF, then in all developing cardiac regions including left and right ventricle, OFT, atria and sinus venosus and remains to be expressed in the adult heart (Kasahara et al., 1998; Komuro and Izumo, 1993; Lints et al., 1993; Stanley et al., 2002; Zhang et al., 2014). Additionally, *Nkx2.5* is expressed in pharyngeal endoderm adjacent to SHF mesoderm as well as in cells of the proepicardium during murine embryogenesis (Zhang et al., 2014; Zhou et al., 2008).

Function

NKX2.5 is able to bind DNA through its homeodomain as a monomer or as a dimer showing a stronger association with DNA as a dimer (Kasahara et al., 2001a). It can either build homo- or heterodimers (Akazawa and Komuro, 2005). Usually NKX2.5 activates its target genes but it can also have a repressive function depending on its binding partner in a regulatory complex (Ryan et al., 2013).

NKX2.5 is required for normal development of the SHF. *Nkx2.5* null mice die around E9-10 because of circulatory failure (Lyons et al., 1995; Tanaka et al., 1999). These embryos exhibit an arrest in heart development at the looping stage as well as a lack of SHF progenitors resulting in a non-developed right ventricle and a poorly developed OFT (Cambier et al., 2014; Lyons et al., 1995; Tanaka et al., 1999). The initial cardiac differentiation is not hampered in *Nkx2.5*-deficent mice as contracting cardiomyocytes can be found in the normally developed linear heart tube, generated by cells of the FHF, in these mice (Lyons et al., 1995; Tanaka et al., 1999).

After the mid-embryonic stage NKX2.5 is still indispensable for cardiac function and survival. Conditional knock-out of *Nkx2.5* beginning at E12.5 leads to embryonic death by E17.5. At E16.5 mutant embryos exhibit arrhytmias, contraction defects and cardiac malformation including atrial septal defects (ASD) (Terada et al., 2011).

The formation, maturation and maintenance of the conduction system are also dependent on NKX2.5 (Jay et al., 2004; Kasahara et al., 2001b; Pashmforoush et al., 2004). Extinction of *Nkx2.5* in cells committed to ventricular cardiomyocytes in mouse embryos does not cause embryonic lethality. However, at birth these mice show an underdeveloped atrioventricular node, a major component of the cardiac conduction system controlling the heart rate, and at around 6-12 months develop advanced atrioventricular block, i. e. impaired conduction between atria and ventricles, or complete heart block, i. e. absence of atrioventricular conduction (Pashmforoush et al., 2004). Mice carrying a loss-of-function allele for *Nkx2.5* possess structurally normal hearts at birth but also establish complete heart block at 4 weeks of age (Kasahara et al., 2001b). *Nkx2.5* null mice seem to lack the primordium of the atrioventricular node while heterozygous mice only possess half of these cells (Jay et al., 2004).

NKX2.5 also plays a role in cardiac contraction. Hypoplasia and disorganisation of Purkinje fibers, which transmit impulses from the atrioventricular node to the ventricles, leading to abnormal ventricular electrical activation could be detected in *Nkx2.5* heterozygous mice (Meysen et al., 2007).

Targets

Among the known direct downstream targets of NKX2.5 are *Atrial natriuretic peptide* (*Anp*) (Durocher et al., 1996; Lee et al., 1998; Shiojima et al., 1999), *Cardiac α-actin* (*Actc1*) (Chen and Schwartz, 1996), *Cardiac ankyrin repeat protein* (*Carp*) (Zou et al., 1997), *A1 adenosine receptor* (*Adora1*) (Rivkees et al., 1999), *calreticulin* (*Calr*) (Guo et al., 2001), *Connexin40* (*Cx40*) (Bruneau et al., 2001), *Sodium-calcium exchanger-1* (*Ncx-1*) (Müller et al., 2002), *Homeodomain-only protein* (*Hop*) (Chen et al., 2002; Shin et al., 2002), *Myocardin* (Ueyama et al., 2003) and *Mef2c* (von Both et al., 2004). These genes encode structural proteins and transcriptional regulators which convey cardiomyocyte characteristics (Akazawa and Komuro, 2005). Some of these and other cardiac genes including *Anp*, *Carp*, *Hop*, *Mef2c*, *Myosin light chain 2v* (*Mlc2v*), *Brain natriuretic peptide* (*Bnp*), *Hand1*, *N-myc* and *Iroquois homeobox gene 4* (*Irx4*) are also down-regulated in *Nkx2.5* null mice (Biben and Harvey, 1997; Bruneau et al., 2000; Lyons et al., 1995; Shin et al., 2002; Tanaka et al., 1999; Zou et al., 1997).

In mice carrying a loss-of-function allele for *Nkx2.5* the cardiac expression of *Cx40* and *Cx43* was normal at birth and decreased dramatically within three weeks (Kasahara et al., 2001b). The ablation of *Nkx2.5* in mouse embryos beginning at E12.5 resulted in abnormal expression of genes playing a role in conduction and contraction such as *Cardiac voltage-gated Na^+ channel α-subunit* (*Scn5a*), *Cx40*, *Cardiac myosin light chain kinase* (*Cmlck*) and *Sarcolipin* (*Sln*) (Terada et al., 2011).

NKX2.5 also negatively regulates several genes. For instance, in *Nkx2.5*-deficient mouse embryos the expression of various genes including *Isl1*, *Fgf10*, *Insulin-like growth factor binding protein* 5 (*Igfbp5*), *Pdgfra* and *Bmp2* is up-regulated in the cardiac crescent and is maintained in the differentiating heart tube where it would normally be reduced. BMP2 signalling through SMAD proteins was also enhanced in these embryos. Initially, this up-regulation resulted in progenitor over-specification but eventually in diminished SHF proliferation and in a truncated OFT (Prall et al., 2007).

In a study comparing gene expression in *Nkx2.5* null, heterozygous for *Nkx2.5* and *Nkx2.5* over-expressing mouse ESC-derived cardiomyocytes, other possible NKX2.5 target genes were identified. Positively regulated putative targets were for instance cardiac genes such as *Natriuretic peptide precursor type B* (*Nppb*) and *Purkinje cell protein* (*Pcp4*), genes involved in G protein or Wnt signalling including *Regulator of G-protein signalling 4* (*Rgs4*), *G protein-coupled receptor 22* (*Gpr22*) or *R-spondin 3 homolog* (*Rspo3*) and interestingly neuronal genes including *Cell cycle exit and neuronal differentiation 1* (*Cend1*) and *Neuritin 1* (*Nrn1*). Among the negatively regulated possible targets were genes involved in translational initiation such as *DEAD box polypeptide 3* (*Ddx3y*) and *Eukaryotic translation initiation factor 2* (*Eif2s3y*), calcium sensor genes including *Visinin-*

like 1 (*Vsnl1*) and *Stromal interaction molecule 1* (*Stim1*) as well as proteoglycan genes such as *Lumican* (*Lum*) and *Chondroitin sulfate proteoglycan 2* (*Cspg2*) (Nakashima et al., 2009).

Cambier and co-workers confirmed that the Wnt agonist RSPO3 was regulated by NKX2.5 using among other methods ChIP analyses in mouse embryos. *Rspo3* expression was also markedly reduced in mouse embryos in which *Nkx2.5* was conditionally knocked-out in the SHF. Wnt signalling was shown to be generally reduced in the SHF of these embryos and activation of Wnt signalling could significantly ameliorate the phenotype of the *Nkx2.5* mutant embryos (Cambier et al., 2014).

Binding partners

NKX2.5 physically interacts with other transcription factors including GATA4 (Durocher et al., 1997; Lee et al., 1998; Rivkees et al., 1999; Sepulveda et al., 1998; Shiojima et al., 1999), SRF (Serum response factor) (Chen and Schwartz, 1996), TBX5 (Bruneau et al., 2001; Hiroi et al., 2001), TBX2 (Habets et al., 2002), TBX20 (Stennard et al., 2003), HAND2 (Thattaliyath et al., 2002), FOXH1 (von Both et al., 2004) and MEF2C (Vincentz et al., 2008). These interactions modulate its transcriptional activity and regulate cardiac development and processes. For example, the NKX2.5-GATA4 dimer activated the transcription of *Anp* (Durocher et al., 1996) while the NKX2.5-TBX2 dimer inhibited it. Therefore, the expression of *Anp* was repressed in regions of the developing heart expressing *Tbx2* leading to the formation of chamber myocardium in these regions (Habets et al., 2002).

Physical interaction between NKX2.5 and TBX5 regulated gene expression in the cells of the cardiac conduction system (Bruneau et al., 2001; Hiroi et al., 2001). Among the regulated genes was *Id2*, which is required for correct cardiac conduction system development (Moskowitz et al., 2007).

Physical, functional and genetic interactions between NKX2.5 and MEF2C stimulated ventricle formation (Vincentz et al., 2008). Furthermore, NKX2.5 and HAND2 cooperatively activated the expression of *Irx4*, which is required for establishing ventricular identity (Yamagishi et al., 2001).

Cardiac sarcomeric protein gene expression was stimulated by physical interaction of NKX2.5 and SRF as well as by cooperation of NKX2.5 and GATA4 (Sepulveda et al., 2002).

Regulation

Nkx2.5 expression is regulated among others by GATA transcription factors, SRF and ISL-1. In a mouse *Nkx2.5* enhancer, which is active in cardiac precursors, the cardiac crescent, the OFT as well as in the right ventricle, several GATA binding sites as well as an ISL-1 binding site were detected. Mutation of the ISL-1 binding site led to reduced enhancer activity in the right ventricle and the OFT at E9.75 (Lien et al., 1999; Searcy et al., 1998; Takeuchi et al., 2005).

In *Srf* null neonatal cardiomyocytes as well as in a heart specific conditional knock-out of *Srf* in mouse embryos the expression of *Nkx2.5* was down-regulated (Balza and Misra, 2006; Parlakian et al., 2004). Additionally, several conserved SRF binding sites are located in the mouse *Nkx2.5* gene (Balza and Misra, 2006).

BMP signalling plays an important role in the activation of *Nkx2.5* expression in different cell lines. Constitutive expression of *Noggin*, a BMP antagonist, in the P19CL16 cell line, a mouse embryonic carcinoma cell line which predominantly differentiates into cardiomyocytes, impaired the differentiation into cardiomyocytes as well as the induction of the expression of several cardiac transcription factors including *Nkx2.5* (Monzen et al., 1999). In a rat embryonic cardiomyocyte cell line over-expression of human *BMP2* led to hyperacetylation of histone H3 in the promoter region of *Nkx2.5* and stimulation of *Nkx2.5* expression (Zheng et al., 2013).

BMP signals activate SMAD proteins and SMAD binding sites have been identified in a cardiac specific enhancer of the mouse *Nkx2.5* gene (Liberatore et al., 2002; Lien et al., 2002). Deletion of this SMAD consensus region in transgenic mice led to delayed induction of the expression of a *LacZ* reporter during early heart formation (Liberatore et al., 2002). Furthermore, ablation of *Smad4* in cardiomyocytes of mouse embryos impaired the expression of several cardiac transcription factors including *Nkx2.5* (Qi et al., 2007). In the rat embryonic cardiomyocyte system described above, knock-down of *Smad4* reduced BMP2-induced and basal histone acetylation levels in the promoter regions of *Nkx2.5* (Si et al., 2014).

Interestingly, in a different study Wnt/β-catenin signalling but not BMP signalling regulated *Nkx2.5* expression in mouse embryo cultures and in mouse cardiac progenitor cell cultures (Klaus et al., 2012). In P19CL16 cells mimicking the induction of Wnt signalling enhanced *Nkx2.5* expression through inhibition of *Hdac1* expression (Liu et al., 2009).

Phosphatidylinositol 3 (PI3)-kinase was also required for the stimulation of *Nkx2.5* expression in P19CL16 cells (Naito et al., 2003).

Nkx2.5 expression was negatively regulated by *in vivo Pkcε* over-expression in mouse cardiomyocytes (Galli et al., 2013).

In mouse embryonic carcinoma cells, NKX2.5 was shown to interact with the phosphorylated form of Myosin phosphatase (MP) enzyme complex which resulted in a redistribution of NKX2.5 to the cytoplasm and subsequent inhibition of its transcriptional activity as it was absent in the nucleus. Treatment of these cells with WNT3A enhanced the phosphorylation level of MP as well as the nuclear exclusion of NKX2.5 and inhibited terminal cardiomyogenesis (Ryan et al., 2013).

Role in disease

Mutations in the *NKX2.5* gene are associated with about 4% of human cardiovascular malformations (Benson, 2010). Patients with *NKX2.5* mutations most commonly suffer from atrial septal defects with or without atrioventricular block but also from ventricular septal defects (VSD), double-outlet right ventricle, Tetralogy of Fallot, which comprises of four heart defects leading to cyanosis, and right atrioventricular valve abnormalities (Benson, 2010; Benson et al., 1999; Goldmuntz et al., 2001; McElhinney et al., 2003; Reamon-Buettner and Borlak, 2010; Schott et al., 1998; Stallmeyer et al., 2010).
Currently, there are about 40 known mutations in the *NKX2.5* gene, which are connected to disease, and all the patients are heterozygous for the *NKX2.5* mutations (Reamon-Buettner and Borlak, 2010). Mutations in the homeodomain decrease or abolish the DNA-binding activity as well as the transcriptional activation function of NKX2.5 (Kasahara and Benson, 2004; Kasahara et al., 2000). Additionally, in patients with mutations in the *NKX2.5* homeodomain the interaction of NKX2.5 with GATA4 and TBX5 is reduced (Kasahara and Benson, 2004).
A genetic variation in the region of the *NKX2.5* gene might influence the PR interval, which represents atrial and atrioventricular nodal conduction, in the general population (Pfeufer et al., 2010).
NKX2.5 mutations have also been identified in thyroid dysgenesis patients with or without cardiac defects (Dentice et al., 2006).

1.5.4 Wnt signalling

Wnt proteins are cysteine-rich secreted glycoproteins and are homologs of the wingless proteins of *Drosophila* (Cadigan and Nusse, 1997; Tian et al., 2010).
Wnt signalling regulates multiple cellular functions such as proliferation, maintenance of proliferation, differentiation, migration and polarity (Cadigan and Nusse, 1997; Parr and McMahon, 1994; Smalley and Dale, 1999; Tanaka et al., 2011). It is involved, among others, in brain, limb, mammary, skin and cardiovascular development (Baker et al., 1999;

Bradley and Brown, 1995; Cohen et al., 2007; Kispert et al., 1998; Kwon et al., 2007; Lin et al., 2007; Marvin et al., 2001; Pandur et al., 2002; Qyang et al., 2007; Reya et al., 2000; Stark et al., 1994; Ueno et al., 2007).

Wnt ligands can be grouped according to their subcellular signalling elements. The first group predominantly signals via the canonical pathway and consists of WNT1, WNT2, WNT3A and WNT8. WNT4, WNT5A and WNT11 belong to the second group which uses a different signalling network named the non-canonical pathway (Flaherty and Dawn, 2008). However, certain Wnt ligands including WNT5A can actually activate both pathways depending on the cell type (van Amerongen et al., 2008; Mikels and Nusse, 2006).

In the canonical pathway, Wnt binds to a Frizzled (Fz) cell surface receptor and a lipoprotein receptor-related protein 5 or 6 (LRP5/6) co-receptor which eventually leads to the disassembly of the β-catenin destruction complex comprising of Axis inhibition protein (AXIN), Adenomatous polyposis coli (APC), Glycogen synthase kinase-3β (GSK-3β) and Casein kinase 1 (CK1). This disassembly results in the stabilisation and accumulation of β-catenin and its translocation to the nucleus as shown in figure 1.4A. There β-catenin interacts with T-cell factor/lLmphoid enhancement factor (TCF/LEF) transcription factors to induce the expression of target genes. Canonical Wnt signalling can be inhibited by members of the secreted Frizzled-related protein family (SFRPs) and Wnt-inhibitory factor (WIF) which bind Wnt ligands, therefore impairing their signalling activity as well as by DKK-like proteins and Wise and Sclerostin (SOST) which inhibit the generation of the Fz-LRP5 compex (Macdonald et al., 2009; Tanaka et al., 2011; Tian et al., 2010).

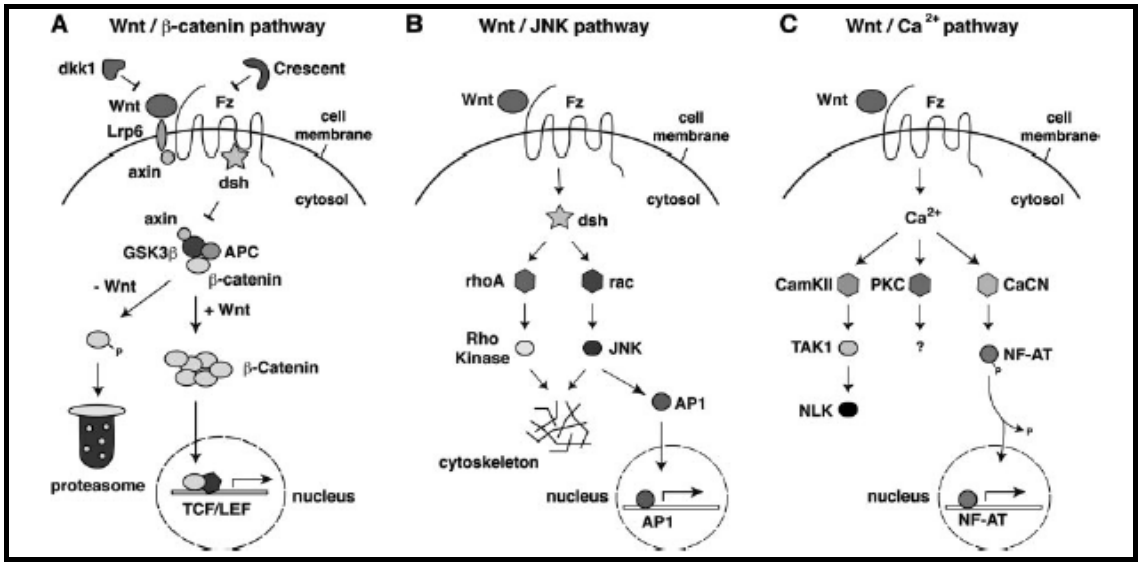

Figure 1.4: A synopsis of Wnt signaling pathways. A, Canonical Wnt or Wnt/β-Catenin pathway. In the absence of Wnt, β-catenin is binding to the destruction complex consisting of axin, APC, and GSK3β and is thereby phosphorylated. This leads to the degradation of

β-catenin by the proteasome. In the presence of Wnt, Wnt interacts with its receptor complex Fz and LRP6. This results in the activation of dsh and in the ablation of axin from the destruction complex, which thereby disintegrates. β-Catenin is accumulating in the cytosol and activating the expression of target genes through its interaction with the TCF/LEF transcription factors. Dkk1 and Crescent are extracellular inhibitors of Wnt/β-catenin signaling. B, Noncanonical Wnt/JNK pathway. The interaction of Wnt with Fz leads to the activation of dsh in the cell. dsh can activate the small GTPases rhoA and rac, which thereby activate Rho kinase and JNK. This results in a rearrangement of the cytoskeleton. JNK can also activate AP1, which participates in the regulation of gene transcription. C, Wnt/$Ca2^{+}$ pathway. In this pathway, the binding of Wnt to the Fz receptor results in an intracellular $Ca2^{+}$ increase. $Ca2^{+}$ thereby can activate CaMKII, PKC, and CaCN. CaMKII itself is regulating TAK1 and NLK, whereas CaCN is regulating NF-AT, which plays a role in transcriptional gene regulation (Gessert and Kühl, 2010).

To track Wnt signalling in the mouse reporter constructs driven by a promoter containing TCF/LEF binding sites or immunostaining for active β-catenin can be used (Maretto et al. 2003; Mohamed et al. 2004).

The non-canonical Wnt pathway functions independently of β-catenin and can be loosely categorised into two pathways, the Wnt/JNK pathway and the Wnt/Ca^{2+} pathway. In the Wnt/JNK pathway Wnt binds to the Frizzled receptor resulting in the activation of Rho-family small GTPases which in turn activate c-Jun kinase (JNK) as depicted in figure 1.4B (Gessert and Kühl, 2010; James et al., 2008; Kühl, 2002; Strutt, 2003; Tada et al., 2002). Wnt/Ca2+ signalling causes the intracellular release of calcium ions and therefore the activation of calcium sensitive enzymes such as PKC, Calcium/Calmodulin dependent kinase (CaMK) II or Calcineurin (CaCN) as shown in figure 1.4C (Gessert and Kühl, 2010; Kohn and Moon, 2005; Kühl et al., 2000a; 2000b; Malbon et al., 2001; Saneyoshi et al., 2002; Sheldahl et al., 2003; Slusarski et al., 1997). The non-canonical Wnt pathway can inhibit canonical Wnt signalling (Maye et al., 2004) and is associated with cell polarity, migration and adhesion (James et al., 2008; Kühl, 2002; Strutt, 2003; Tada et al., 2002; Topol et al., 2003; Westfall et al., 2003).

Role in stem cells

The activation of Wnt/β-catenin signalling in mouse and human ESCs led to increased expression of pluripotency genes and might support the self-renewal of stem cells (Dravid et al., 2005; Lu et al., 2006; Miyabayashi et al., 2007). However, as the stem cells were grown on feeder cells in these studies it might also be possible that Wnt signalling acted via the feeder cells and not directly on the stem cells (Tanaka et al., 2011).

In a different study, treatment with WNT3A was shown to facilitate the pluripotency state in human or mouse ESCs even without feeder cells or LIF, respectively. The same effect could be achieved by artificially inhibiting GSK-3β and thereby augmenting the stability and accumulation of cytosolic β-catenin (Sato et al., 2004).
Over-expression of *Wnt1* or expression of a constantly active variant of *β-catenin* also favoured the self-renewal of mouse ESCs (Aubert et al., 2002; Haegele et al., 2003).
β-catenin was able to enhance the expression of the core pluripotency transcription factors *Tbx3*, *Nanog* and *Oct3/4* in mouse ESCs by activating the expression of *nuclear orphan receptor Nr5a2* in interaction with TCF3 which would then stimulate the transcription of these pluripotency factors (Wagner et al., 2010). When Wnt signalling was up-regulated in mouse ESCs β-catenin interacted with OCT3/4 and enhanced *Tbx3* and *Nanog* expression (Kelly et al., 2011).

Function during mesoderm specification

In the early mouse embryo, Wnt ligands are primarily expressed in the posterior-proximal part of the embryo, the location of mesoderm progenitors and the primitive streak, whereas Wnt inhibitors and FZ receptors are expressed widely or mainly at the anterior or distal regions of the embryo (Kemp et al., 2005, 2007; Pfister et al., 2007; Tanaka et al., 2011).
Canonical Wnt signalling is required for mesoderm development. Depletion of *Wnt3* or *β-catenin* blocked mesoderm formation in mouse embryos (Huelsken et al., 2000; Liu et al., 1999). Additionally, the inhibition of canonical Wnt signalling in mouse ESCs impaired their differentiation into mesoderm precursors (Lindsley et al., 2006).
Primitive streak formation was impaired in mouse embryos depleted of *Wnt3*, *β-catenin* or Wnt co-receptors (Huelsken et al., 2000; Kelly et al., 2004; Liu et al., 1999; Mohamed et al., 2004). The specific deletion of *Wnt3* in the epiblast still permittted a delayed generation of the primitive streak but it could not be preserved (Tortelote et al., 2013). In contrast, expression of a stabilised form of *β-catenin* in the epiblast resulted in premature EMT, a process required for primitive streak formation (Kemler et al., 2004).

Role in cardiac *in vitro* differentiation

Several Wnt ligands including *Wnt2*, *Wnt2b*, *Wnt11* and *Wnt8a* are highly expressed in the developing heart (Eisenberg and Eisenberg, 1999; Jaspard et al., 2000; Monkley et al., 1996; Onizuka et al., 2012; Zakin et al., 1998).
Studies investigating the function of canonical Wnt signalling in cardiogenesis obtained contradictory results. In a mouse embryonic carcinoma cell line, the endogenous

activation of the canonical Wnt pathway was essential for DMSO-induced cardiac differentiation (Nakamura et al., 2003). Over-expression of *Wnt1* in differentiating mouse ESCs increased their ability to form contracting cardiomyocytes in comparison to a control mouse ESC line. The addition of DKK1, a canonical Wnt signalling inhibitor, reduced this ability in *Wnt1* over-expressing and control cells (Weisel et al., 2010). In contrast, DKK1 treatment of differentiating *Mesp1* over-expressing mouse ESCs from day 2 to 6 of differentiation results in the induction of cardiac differentiation (Lindsley et al., 2008). Furthermore, direct inhibition of β-catenin was shown to stimulate cardiac differentiation in mouse ESCs (Singh et al., 2007).

Several studies indicated that canonical Wnt signalling functions bi-phasically during cardiogenesis (Naito et al., 2006; Ueno et al., 2007; Yamashita et al., 2005). Addition of WNT3A early during differentiation enhanced cardiac differentiation of mouse ESCs whereas activation of β-catenin at later points of differentiation has the opposite effect (Ueno et al., 2007). Concomitantly, inhibition of Wnt/β-catenin signalling in differentiating mouse ESCs at early points of differentiation impaired cardiac differentiation while inhibition of the canonical Wnt pathway at a later point enhanced cardiac differentiation (Naito et al., 2006). However, in a different study treatment of differentiating mouse ESCs with the Wnt/β-catenin signalling inhibitor XAV939 immediately after the formation of mesoderm progenitors stimulated the generation of cardiomyocytes at the expense of the development of other mesoderm derived lineages such as endothelial, smooth muscle and haematopoietic lineages (Wang et al., 2011).

Knock-down of *Wnt2* decreased cardiomyocyte differentiation of mouse ESCs while addition of WNT2 enhanced this differentiation. The strongest effect for both treatments was achieved when administered at day 3 of differentiation. Interestingly, WNT2 did not act via the canonical Wnt pathway but via the non-canonical JNK pathway in this context (Onizuka et al., 2012).

Other non-canonical Wnt ligands were also shown to have a stimulatory effect on cardiac differentiation. For example, *Wnt11* over-expression or WNT11 treatment increased cardiac differentiation of mouse ESCs (Terami et al., 2004; Ueno et al., 2007) and addition of WNT11 to murine bone marrow derived adult stem cells induced cardiomyogenic differentiation (Belema Bedada et al., 2005; Flaherty et al., 2008). In a mouse carcinoma cell line WNT11 treatment inhibited canonical Wnt signalling via Cysteinyl-aspartate specific protease3/8 (CASPASE 3/8)-mediated β-catenin degradation, and increased cardiomyocyte differentiation (Abdul-Ghani et al., 2011). Another non-canonical Wnt ligand, WNT5A, stimulated in cooperation with BMP6 and SFRP1 the generation of Troponin-positive cells from murine cardiac progenitors (Chen et al., 2008).

Function in cardiogenesis

SHF progenitor differentiation and proliferation is regulated by Wnt/β-catenin signalling. Specific deletion of *β-catenin* in the SHF resulted in dramatically decreased *Isl1* expression levels as well as numbers of *Isl1* expressing cells in mouse embryos and a subsequent loss of the OFT and the right ventricle (Ai et al., 2007; Cohen et al., 2007; Klaus et al., 2007; Kwon et al., 2007; Lin et al., 2007). β-catenin was shown to bind and activate the *Isl1* promoter using ChIP and *in vitro* reporter assays (Lin et al., 2007). However, in a different study stabilisation of *β-catenin* seemed to negatively regulate the expression of *Isl1* and other cardiac genes at E9 of mouse development (Kwon et al., 2009).

Expression of a stabilised form of *β-catenin* in the SHF also led to defective OFT and right ventricle development due to now enhanced proliferation of SHF progenitors (Ai et al., 2007; Kwon et al., 2007).

Depletion of *β-catenin* using a *MesP1* driver had no effect on FHF derived cardiac crescent formation and the expression of FHF markers. However, conditional knock-out of *β-catenin* around E8.0-8.5 using a specific *Nkx2.5* enhancer led to a reduction in size of both ventricles (Kwon et al., 2007), which rather indicates that Wnt/β-catenin signalling has an effect on both SHF and FHF expansion as the left ventricle is formed by cells of the FHF.

Non-canonical Wnt signalling also plays a role in SHF development. Mutations in *Wnt5a* and *Wnt11* are associated with mild heart defects, for example thinner ventricular walls, because of impaired cell-cell adhesion and cytoskeleton organisation in differentiating cardiomyocytes (Nagy et al., 2010; Schleiffarth et al., 2007; Zhou et al., 2007). However, in a double knock-out of *Wnt5a* and *Wnt11* the number of SHF progenitors in the developing heart was dramatically reduced accompanied by enhanced Wnt/β-catenin signalling. Furthermore, chamber septation, OFT and ventricle formation were defective in these mutant embryos. Treatment with WNT5A or WNT11 increased *Nkx2.5* and *Isl1* expression in differentiating mouse ESCs (Cohen et al., 2012). Furthermore, WNT5A seemed to be a key factor in the partial rescue of the cardiac phenotype of *Id* knock-out mice achieved by intraperitoneal injection of ESCs (Fraidenraich et al., 2004).

1.6 Model systems: Embryoid bodies versus monolayer cell culture

On withdrawal of factors maintaining the stemness of ESCs, such as LIF, ESCs spontaneously differentiate into various cell lineages (Keller, 2005; Wobus and Boheler, 2005). Among the methods for *in vitro* induction of ESC differentiation are monolayer cell culture under appropriate conditions (Ying et al., 2003b), co-culture with heterotypic cell types (Nakano et al., 1994) or generation of cell aggregates in suspension named embryoid bodies (EBs) (Doetschman et al., 1985).

The differentiation processes of ESCs within EBs resemble the development of eutherian embryos during pre- and early gastrulation (Weitzer, 2006). EBs can be produced using several methods such as aggregation in hanging drops (Höpfl et al., 2004; Maltsev et al., 1994) (see section 3.1.8), aggregation in suspension culture in a bacteriological grade Petri dish preventing cell adhesion (Doetschman et al., 1985; Klug et al., 1996; Zhang et al., 2001) or by culture in semi-solid medium, for example in methylcellulose (Keller et al., 1993; Vittet et al., 1996; Wiles, 1993). The generation of EBs is most homogenous and reproducible in hanging drop culture as the drops are formed with a defined number of ESCs but this method is also the most laborious one (Bratt-Leal et al., 2009; Jackson et al., 2010; Weitzer, 2006).

After EB formation the cells can either be kept in suspension or can be adhered to gelatine or similar substances depending on the cell type of interest (Jackson et al., 2010). For instance, haematopoietic cells preferentially develop in suspension (Dang et al., 2002) while differentiation into contracting cardiomyocytes is stimulated in adhesion culture (Wallukat and Wobus, 1991).

The first sign of differentiation within EBs is the creation of a layer of primitive endoderm on the exterior surface of EBs mimicking the hypoblast of a blastocyst (Maurer et al., 2008; Murray and Edgar, 2001; Rula et al., 2007). The inner cells of the EB differentiate into primitive ectoderm and resemble the epiblast and later the early egg cylinder stage of a mouse embryo (Ikeda et al., 1999; Komura et al., 2008). Upon adhesion of EBs to a surface which mimics embryo implantation in the uterus, the primitive endoderm develops into extra-embryonic visceral endoderm and parietal endoderm which, in the mammalian embryo, generate the two yolk sacs (Fuchs et al., 2012). The primitive ectoderm performs EMT leading to mesoderm formation (Behr et al., 2005; Denker et al., 2007; Maranca-Hüwel and Denker, 2010). In some EBs a ridge in the shape of a horseshoe surrounds cells of the centre of the EB (Weitzer, 2006). The cells in the centre will form *Brachyury*-expressing mesodermal precursors eventually developing into hematopoietic cells and beating cardiomyocytes (Bader et al., 2001; Fuchs et al., 2012). These processes resemble gastrulation in the mammalian embryo but the generation of the primitive streak

and gastrulation movements can not be observed in EBs (Jackson et al., 2010). The further development of cell lineages of all three germ layers becomes more and more chaotic (Weitzer, 2006).

In monolayer cell culture, in the absence of feeder cells, ESCs have also been shown to differentiate into several cell types. Under serum-free conditions and without LIF ESCs start to differentiate towards the neuronal lineage (Ying et al., 2003b). Addition of cyclopamine, an antagonist of Shh, at low cell density stimulates ESCs to acquire a neocortical fate (Gaspard et al., 2008; 2009).

In the absence of LIF over-expression of *Id* genes results in the differentiation into epithelial-like cells (Ying et al., 2003a).

In high density monolayer cell culture ESCs spontaneously develop into visceral endoderm (Yasunaga et al., 2005). Definitive endoderm is produced upon addition of retinoic acid or Activin A (Capo-chichi et al., 2005; Yasunaga et al., 2005). Treatment with different small molecules leads to a more efficient generation of definitive endoderm (Borowiak et al., 2009; Zhu et al., 2009).

Activin A treatment also induces mesoderm development (Yasunaga et al., 2005).

Human ESCs differentiate into cardiomyocytes when treated with Activin A and BMP4 under serum-free conditions (Laflamme et al., 2007). Additional activation of Wnt/β-catenin signalling using GSK-3β inhibitors followed by blockage of this signalling pathway strongly enhances the efficiency of cardiomyocyte formation (Lian et al., 2012).

1.7 Flow cytometry

Flow cytometry can be used to measure multiple characteristics of single cells in heterogeneous suspensions such as cell size, cytoplasmic complexity, DNA or RNA content and protein expression in both a qualitative and quantitative manner (Brown and Wittwer, 2000; Rowley, 2012). Tens of thousands of cells can be analysed within minutes (Rowley, 2012). Typical applications for flow cytometry include immunophenotyping (Hwang et al., 2012; Liu et al., 2012), cell sorting and cell counting (Boissière et al., 2012; Fromm and Wood, 2012), ploidy analysis (Lomax et al., 2000; Menten et al., 2009), cancer diagnosis (Lacombe and Belloc, 1996; McCoy and Carey, 1990) and green fluorescent protein (GFP) expression analysis (Kalejta et al., 1997; Sirk et al., 2003).

The most similar prototype to today's flow cytometers was developed in the 1960s by Dittrich and Göhde, Fulwyler, Herzenberg, and Van Dilla, and was named Fluorescence Activated Cell Sorter (FACS) by Herzenberg (Dittrich and Göhde, 1969; Fulwyler, 1965; Givan, 2011; Hulett et al., 1969; Lanier, 2014; Van Dilla et al., 1969). A typical flow cytometer comprises a fluidic system, one or more lasers, optics, electronics and an

external computer system (Figure 1.5). To collect certain cells after the measurement a sorting device can also be added to the flow cytometer.

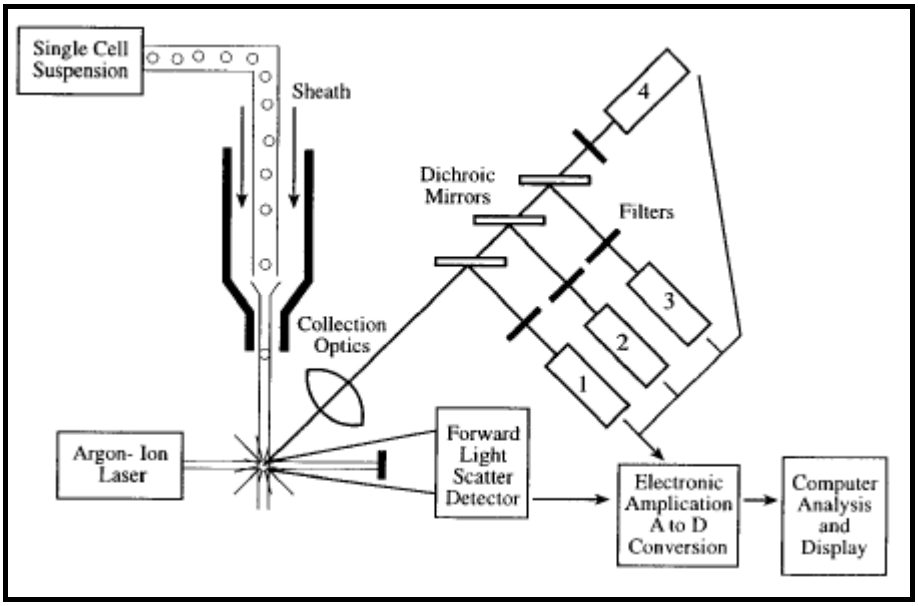

Figure 1.5: Schematic of a flow cytometer. A single cell suspension is hydrodynamically focused with sheath fluid to intersect an argon-ion laser. Signals are collected by a forward angle light scatter detector, a side scatter detector (1), and multiple fluorescence emission detectors (2–4). The signals are amplified and converted to digital form for analysis and display on a computer screen (Brown and Wittwer, 2000).

For the measurement the cells in suspension are loaded onto the collection system of the flow cytometer. The sample then reaches the fluidic system and is transported to the flow chamber where it becomes surrounded by a stream of sheath fluid creating a laminar flow and allowing the cells to pass through an interrogation point one at a time as shown in figure 1.6 (Brown and Wittwer, 2000).

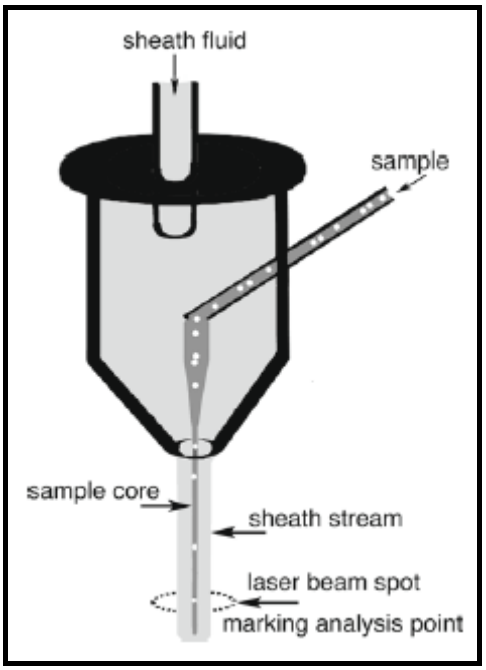

Figure 1.6: A flow cell, with the sample suspension injected into the sheath fluid and forming a central core in the sheath stream. The small diameter of the flow cell at its exit orifice causes the sheath stream and sample core to narrow so that cells flow rapidly and are separated from each other and less likely to coincide in the analysis point (Givan, 2011).

At this interrogation point the cell is intersected by a laser beam of usually 488 nm wavelength in a single laser system. In a multi-laser system more than one interrogation point exists. After colliding with the cell the light is refracted or scattered in all directions and is collected by lenses at two different angles as depicted in figure 1.7. One lens is located in the forward direction, the initial direction of the laser, and collects the forward scattered light. An obscuration bar is positioned before the forward lens to block the laser beam itself. Only light that has been refracted or scattered through contact with a particle in the forward direction reaches the forward lens and will be focused onto a photodiode. The other lens is positioned orthogonal to the first lens and collects the wider scattered light. Forward scatter (FSC) is proportional to cell surface area or size while side scatter (SSC) is proportional to cell granularity or internal complexity. These characteristics can provide information about a peripheral blood sample, for instance, and allow distinguishing between different cell types in this sample.

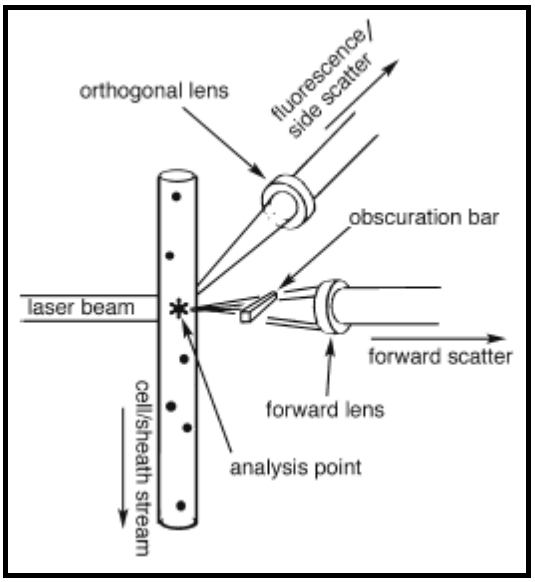

Figure 1.7: The analysis point of a flow cytometer, with the laser beam, the sheath stream, and the lenses for collection of forward scatter and side scatter/fluorescence all at orthogonal angles to each other (Givan, 2011).

Not only SSC but also fluorescent light is collected by the side positioned lens. When a fluorescence molecule is excited to a higher energy state, in flow cytometry by a laser beam, it emits light of a relatively long wavelength upon returning to its resting state. Certain fluorescent dyes such as propidium iodide (PI) bind nucleic acids and can reveal information about the DNA content of a cell. Antibodies conjugated to fluorescent molecules can be used to label specific proteins within a cell which delivers information about their expression level. If cells have been transfected with genes of fluorescent proteins the expression of these fluorescent proteins can also be measured with flow cytometry (Telford et al., 2012).

In this thesis the expression of enhanced green fluorescent protein (EGFP) was analysed. This protein was generated via site-directed mutagenesis and is, in contrast to wild type GFP, optimally enhanced at 488 nm, the wavelength emitted by the long time standard laser in cytometers, as it has an excitation maximum of 484 nm. Its emission maximum lies at 507 nm (Telford et al., 2012).

Additionally, the number of dead cells was determined by flow cytometry using PI in this thesis. PI cannot pass through intact cell membranes and does therefore not stain living cells. In late apoptotic and necrotic cells the cell membrane breaks down and allows PI to enter the cell and to stain nucleic acids. When bound to DNA, PI has an excitation maximum of 535 nm and an emission maximum of 617 nm. Thus, it is possible to excite PI at 488 nm (Martin et al., 2005; Riccardi and Nicoletti, 2006; Rieger et al., 2011).

The side scatter as well as the fluorescent light are focused by the lens located orthogonal to the direction of the laser beam on dichroic mirrors and band-pass filters which split this multicolour light into separate colours and direct the light to different photomultiplier tubes according to its wavelength. The photodetectors, the photodiode and the photomultiplier tubes, convert the light signals into currents which are then transformed into voltage. The voltage will be amplified and, in a last step, digitised. The amplification can either be linear or logarithmic depending on the analysed characteristic. Measurements of DNA content, for example, will usually be amplified in a linear manner while logarithmic amplifiers are often used for data of protein expression because the variation between individual cells might be greater for protein expression levels.

The digital information is analysed by appropriate software. Usually, the data is displayed in a histogram or in a two-dimensional dot plot. The histogram shows the distribution of one parameter over different cells whereas two different parameters can be presented at once in a two-dimensional plot. In a dot plot each dot represents one cell or one event.

Another potential of flow cytometry is the possibility of gating. By gating a certain cell population can be marked and designated for further analysis to obtain information about a subset of cells within a mixed population. In this thesis GFP expressing as well as PI positive cells were gated.

1.8 Working strategy

In vitro cardiomyogenesis is usually initiated and studied in EBs (Boheler et al., 2002; Sun et al., 2015). However, this method is quite laborious (Bratt-Leal et al., 2009; Jackson et al., 2010; Weitzer, 2006) and expensive due to the high volume of medium needed and, in case of an analysis of an effector molecule, the high amount required of this molecule. We therefore wanted to test whether it is possible to study in vitro cardiomyogenesis of ESCs and CVPCs in low-volume monolayer cell culture which is less time consuming and due to the low volume also less expensive than hanging drop culture. Additionally, a smaller amount of effector molecules of interest is required in low-volume monolayer cell culture.

We used ESC and CVPC reporter cell lines carrying a *Brachyury*^{EGFP}, *MesP1*^{EGFP} transgene or an *Nkx2.5*^{EGFP} knock-in allele and analysed the expression of these key genes in mesoderm and/or cardiomyocyte formation (see section 1.5) during differentiation in low-volume monolayer cell culture under different conditions (see section 4) via the expression level of *EGFP* using flow cytometry and assessed the cells' potential to form contracting cardiomyocytes under these conditions. Different cell densities were used and cells were treated with Secreted Protein, Acidic, Rich in Cysteine (SPARC), α-SPARC or CHIR99021. In our group, SPARC was previously shown to enhance

cardiomyogenesis as well as the expression of *Nkx2.5* in EBs (Stary et al., 2005). Similar findings were obtained when using cardiac bodies (CBs) but cardiomyogenesis was only increased at the beginning of cardiomyocyte formation. Additionally, *MesP1* expression slightly rose after SPARC treatment of CBs (Gottschamel, 2010). In contrast, treatment of EBs and CBs with α-SPARC led to reduced formation of contracting cardiomyocytes of both cell types and to a decreased expression of *Nkx2.5* in EBs (Gottschamel, 2010; Stary et al., 2005).

CHIR99021 is an inhibitor of GSK-3β and therefore an activator of canonical Wnt signalling. In previous experiments CHIR was shown to increase *Brachyury* expression in EBs but EBs and CBs did not develop normally under CHIR treatment (Leitner, 2013). However, in a different study treatment of EBs with a different GSK-3β inhibitor during early differentiation led to enhanced cardiomyogenesis (Ueno et al., 2007).

Furthermore, we assessed the activity of the canonical Wnt pathway, required for *Brachyury* expression and probably at the beginning of cardiomyogenesis, during differentiation in low-volume monolayer cell culture using ESC and CVPC reporter cell lines carrying TCF/LEF sites upstream to a luciferase reporter gene allowing us to detect active β-catenin signalling via luminescence measurements. Both, the flow cytometry as well as the luminescence experiments, had already partially been conducted with EBs and CBs (Leitner, 2013) and allowed us to compare the data obtained with EBs/CBs to the data obtained with monolayer cell culture

Finally, we analysed the expression of cardiomyocyte, cardiac fibroblast and endothelial cell markers during differentiation in low-volume monolayer cell culture to investigate whether cells differentiate preferentially in a distinct cell type in low-volume monolayer cell culture.

2 Materials

2.1 General chemicals, buffers and material

Acetic Acid	AppliChem, D
Agarose	Sigma Aldrich, USA
β-Mercaptoethanol	Loba, AUT
Bromphenolblue	Sigma Aldrich, USA
Dithiothreitol (DTT)	Acros, B
DNAse I buffer	Fermentas, Lithuania
dNTPs	Fermentas, Lithuania
EDTA	Acros, B
Ethanol	Sigma Aldrich, USA
Ethidium bromide	Fluka, CH
Gene Ruler 1 kb Plus DNA Ladder	Thermo Fisher Scientific, USA
Glycerin	Merck, D
Hydrochloric acid (HCl)	Acros, B
QIAshredder	Qiagen, D
Sodium chloride (NaCl)	Sigma Aldrich, USA
Reverse Transcriptase Buffer	Invitrogen, USA
Tris Ultrapure	AppliChem, D

2.2 Cell culture

2.2.1 General chemicals and material for cell culture

β-Mercaptoethanol	Loba, AUT
D (+)-Glucose Anhydrous	AppliChem, D
DMEM powder	Gibco, USA
DMEM	Gibco, USA
Dimethyl sulfoxide (DMSO)	Sigma Aldrich, USA
EDTA	Acros, B
Fetal Bovine Serum	HyClone, USA
Fetal Bovine Serum	Gibco, USA
Fetal Bovine Serum	Sigma Aldrich, USA
Gelatine	Difco, USA

L-(+)-Glutamine	Acros, B
Mitomycin C	AG Scientific, USA
Nalgene Filter	Nalgene Labware, USA
Penicillin/Streptomycin	Gibco, USA
Potassium chloride	Sigma Aldrich, USA
Potassium hydrogen phosphate	Fluka, CH
Sodium hydrogen carbonate	Life Technologies, USA
Sodium hydrogen phosphate	Roth, D
Tris Base	LifeTechnologies, USA

2.2.2 Solutions for cell culture

10x Phosphate Buffered Saline (PBS) stock solution

- 80 g NaCl
- 2g KCl
- 10.72 g $Na_2HPO_4x7H_2O$
- 2 g KH_2PO_4
- 800 ml MilliQ water is added.
- The pH is adjusted to 7.2 with saturated Na_2HPO_4.
- The solution is filled up to 1 litre with MilliQ water and is sterile filtered.

100x Glutamine-Penicillin-Streptomycin (GPS)

- 4.25 g NaCl
- 1.5 g Penicillin
- 2.5 g Streptomycin
- 14.6 g L-(+)-Glutamine
- MilliQ water is added to reach a final volume of 500 ml.
- The solution is aliquoted into 50 ml falcons.
- Falcons are stored at -20°C and subsequently at 4°C after thawing.

100x β-Mercaptoethanol (10^{-2}M)

- 200 mL 1x PBS
- 144 µL β-Mercaptoethanol (14 M)
- The solution is sterile filtered and aliquoted into 50 ml falcons.
- Falcons are stored at -20°C and subsequently at 4°C after thawing.

Trypsin solution

- 3.5 g NaCl
- 0.5 g D-Glucose
- 0.09 g $Na_2HPO_4.7H_2O$
- 0.185 g KCl
- 0.12 g KH_2PO_4
- 0.2 g EDTA
- 1.25 g Trypsin
- 1.5 g Tris Base
- MilliQ water is added to reach a final volume of 500 ml.
- The pH is adjusted to 7.6 with concentrated HCl.
- The solution is aliquoted into 50 ml falcons.
- Falcons are stored at -20°C and subsequently at 4°C after thawing.

10x (1%) Gelatine Stock Solution

- 10 g Gelatine
- MilliQ water is added to reach a final volume of 1 litre.
- The solution is sterile filtered.

2.2.3 Media

Dulbecco's Modified Eagle's Medium (DMEM)

- Half a can of DMEM (Gibco, +4500 mg/l Glucose, -$NaHCO_3$, -Pyruvate #52100-039) is dissolved in 4.5 litres MilliQ water in a 5 litre Erlenmayer flask.
- 18.5 g $NaHCO_3$ are added.
- The pH is adjusted to 7.4 with concentrated HCl.
- MilliQ water is added to reach a final volume of 5 litres.
- The medium is sterile filtered into cell culture flasks.
- A small aliquot of each bottle is incubated at 37°C, 5% CO_2 for at least 24 hours and is then checked for contaminations under the microscope.
- Any contaminated bottles need to be sterile filtered again.

M15Hy – Growth medium for ESCs and CVPCs

- 83% DMEM
- 15% Fetal Bovine Serum (HyClone)
- 1% GPS
- 1% β-Mercaptoethanol

M15Si – Growth medium for EBs and CBs as well as for ESCs and CVPCs in monolayer cell culture

- 83% DMEM
- 15% Fetal Bovine Serum (Sigma)
- 1% GPS
- 1% β-Mercaptoethanol

M10Gi – Growth medium for fibroblasts

- 89% DMEM
- 10% Fetal Bovine Serum (Gibco)
- 1% GPS

Freezing Medium (2x stock)

- 60% DMEM
- 20% Fetal Bovine Serum
- 20% DMSO – should be added last and drop wise

2.3 Enzymes

DNAse I RNase free	Fermentas, Lithuania
PCR Master-Mix Gold S	Peqlab, D
Proteinase K	AppliChem, D
RNAseOUT®	LifeTechnologies, USA
RevertAidTM M-MuLV RT	New England Biolabs, USA
Trypsin	LifeTechnologies, USA

2.4 Inhibitors and recombinant proteins

α-SPARC	Santa Cruz Biotechnology, USA
Chir99021	Axon, NL
SPARC	Sino Biological, China

2.5 Kits

ONE-Glo^{TM} Luciferase Assay System	Promega, USA
RNeasy Mini Kit	Qiagen, D

2.6 PCR Primers

Gene or vector	Primer name	Sequence (5' to 3')	Ta [°C]	Product length [bp]	
				cDNA	gDNA
Brachyury	Bra fw Bra rv	GTGGCGAGAGAAGTGAAGGT GCGAGTCTGGGTGGATGTAG	62	461	915
c-Kit	c-kit fw c-kit rv	GCCCTAATGTCGGAACTGAA TTGCGGATCTCCTCTTGTCT	50	319	6,478
Cd31	CD31 iso1 fw CD31 iso1 rv	AGAGCCACAGAGACGGTGTA TTACTGCTTTCGGTGGGGAC	57	196	16,775
Cd34	CD34 fw CD34 rv	GCTGATGCTGGTGCTAGT GCTCCCGATATCTTGTTTA	58	183	622
Ddr2	Ddr2 fw Ddr2 rv	ATGGCGGAACGAAAGTGCTA CTTGGTGATGAGGAGCGGTT	59	615	11,362
Desmin	Desmin fw Desmin rv	TGACAACCTGATAGACGA TTCTTATTGGCTGCCTGA	51	390	1,972
EGFP	EGFP fw EGFP rv	GGGCACAAGCTGGAGTACAA CTCAGGTAGTGGTTGTCGGG	60	194	194
eNos	eNOS fw eNOS rv	GCATGGGCAACTTGAAGAGTG CAGCGTCTTGAGGTACAGGG	58	295	2,388
Gata4	GATA4 fw GATA4 rv	GCCTGTATGTAATGCCTGCG CCGAGCAGGAATTTGAAGAGG	60	500	3,364
Gapdh	GAPDH fw GAPDH rv	CGTCTTCACCACCATGGAGA CGGCCATCACGCCACAGTTT	55	300	300
Hprt	hprt fw hprt rv	GGGCTTACCTCACTGCTTTC TCTCCACCAATAACTTTTATGTCC	57	450	20,561
Mef2c	Mef2C iso 1 fw Mef2C iso 2 rv	CTTATCCCACCTGGCAGCAA GTGGTACGGTCTCTAGGAGGA	61	413	9,467
MesP1	Mesp fw Mesp rv	AGGATAAAGCTACAGCGGACC GTTGCATTGTCCCCTCCACT	58	797	1,070
Nkx2.5	Nkx2.5 fw Nkx2.5 rv	TGCGTCGCCACCATGTTCCC TGCGCCTGCGAGAAGAGCAC	57	455	1,832
Pim1	Pim1 fw Pim1 rv	GAGTGCCCATGGAAGTGGTC CTTCAAAGGAGGGCCGATCT	59	594	2,975
pMesP1-EGFP	Mesp-Vektor fw EGFP rv	TCGTTTTTCTGACCCCGCTT CTCAGGTAGTGGTTGTCGGG	60		937
pT-Bra-Puro-IRES2-EGFP	Puro fw Puro rv	ATGACCGAGTACAAGCCCAC CTCGTAGAAGGGGAGGTTGC	60	516	516
pT-Bra-Puro-IRES2-EGFP	Puro 2 fw Puro 2 rv	GAGCTGCAAGAACTCTTCCTCA CCGGGAACCGCTCAACTC	60	165	165

Gene or vector	Primer name	Sequence (5' to 3')	Ta [°C]	Product length [bp] cDNA	gDNA
pT-Bra-Puro-IRES2-EGFP	Bra-Vektor fw Puro 3 rv	TACTTCAAAGGGTGTCCCGC CGGTGACCCGCTCGATG	62		548
pT-Bra-Puro-IRES2-EGFP	Bra-Vektor 2 fw Puro 3 rv	GCTGTTGGGTAGGGAGTCAAG CGGTGACCCGCTCGATG	60	254	254
pT-Bra-Puro-IRES2-EGFP	Bra-Vektor 3 fw Puro 3 rv	AGCTTTTATGTGGGACGCGA CGGTGACCCGCTCGATG	64		1,130
pT-Bra-Puro-IRES2-EGFP	T-NK1 fw Puro 3 rv	TGCTCTTTGTCACCTTCCCC CGGTGACCCGCTCGATG	66		1,323
Tropomyosin-α	Tropo-myosin-α fw Tropo-myosin-α rv	CAAGCGGAGGCTGATAAGAAGG TGCCTCTCTCACTCTCATCTGC	60	310	13,074
Vimentin	Vimentin fw Vimentin rv	AGAGAGGAAGCCGAAAGCAC AGCCACGCTTTCATACTGCT	60	255	3,146
VE-Cadherin	VE-Cadherin fw VE-Cadherin rv	AAGACATCCGAGTGGGCAAG CTGTCACTGGTCTTGCGGAT	58	442	7,465

2.7 Cell lines

2.7.1 SNL76/7 fibroblast cell line

The murine SNL76/7 fibroblast cell line is derived from the murine STO fibroblast cell line but additionally carries a LIF gene and a Neomycin resistance gene. This cell line was established by Allan Bradley (McMahon and Bradley, 1990).

2.7.2 Embryonic stem cells

2.7.2.1 Ab2.2 cell line

This *hprt*-deficient ESC line was isolated by Allan Bradley from the 129S5/SvEvBrd mouse strain (Adams et al., 2005; Ramírez-Solis et al., 1995).

2.7.2.2 W4 cell line

This wild type ESC line was isolated by Georg Weitzer from the C3H mouse strain (Lauss et al., 2005).

2.7.2.3 W4-bra-R cell line

This cell line is derived from the W4 cell line and was established by Lucia Leitner. It carries an EGFP reporter gene which is regulated by the 5' UTR region of the *Brachyury* gene (Leitner, 2013). Unless otherwise stated clone c3 of this cell line was used for the experiments of this thesis. This cell line is referred to as Brachyury^{EGFP} reporter ESC line in this thesis.

2.7.2.4 W4-MesP-R cell line

This cell line is derived from the W4 cell line and was established by Lucia Leitner. It carries an EGFP reporter gene under the control of the *MesP1* promoter region (Leitner, 2013). Unless otherwise stated clone cA of this cell line was used for the experiments of this thesis. This cell line is referred to as MesP1^{EGFP} reporter ESC line in this thesis.

2.7.2.5 MS15 cell line

This cell line is derived from the Ab2.2 cell line and was established by Martina Stary. It carries an EGFP reporter gene as well as a Puromycin resistance gene in one allele of the gene *Nkx2.5*. This cell line is referred to as Nkx2.5^{EGFP} reporter ESC line in this thesis.

2.7.2.6 W4-TOPflash cell line

This cell line is derived from the W4 cell line and was established by Lucia Leitner. It carries 8 copies of TCF/LEF sites upstream of a firefly luciferase open reading frame (Leitner, 2013). This cell line is referred to as TOPflash reporter ESC line in this thesis.

2.7.3 Cardiovascular progenitor cells

2.7.3.1 A5 cell line

This CVPC cell line was isolated by Wolfgang Weber and Matthias Scheinast from the hearts of new-born mice which harbour a Neomycin resistance gene in one allele of the gene *Hdac1* (Hoebaus et al., 2013). The isolation of this cell line is described in more detail in section 1.2.3.

2.7.3.2 A5-bra-R cell line

This cell line is derived from the A5 cell line and was established by Lucia Leitner. It carries an EGFP reporter gene which is regulated by the 5' UTR region of the *Brachyury* gene (Leitner, 2013). Unless otherwise stated clone cB of this cell line was used for the experiments of this thesis. This cell line is referred to as Brachyury^{EGFP} reporter CVPC line in this thesis.

2.7.3.3 A5-MesP-R cell line

This cell line is derived from the A5 cell line and was established by Lucia Leitner. It carries an EGFP reporter gene under the control of the *MesP1* promoter region (Leitner, 2013). Unless otherwise stated clone c1 of this cell line was used for the experiments of this thesis. This cell line is referred to as MesP1^{EGFP} reporter CVPC line in this thesis.

2.7.3.4 A5-Csx4 cell line

This cell line is derived from the A5 cell line and was established by Teresa Gottschamel (Gottschamel, 2010). It carries an EGFP reporter gene as well as a Puromycin resistance gene in one allele of the gene *Nkx2.5*. This cell line is referred to as Nkx2.5^{EGFP} reporter CVPC line in this thesis.

2.7.3.5 A5-TOPflash cell line

This cell line is derived from the A5 cell line and was established by Lucia Leitner. It carries 8 copies of TCF/LEF sites upstream of a firefly luciferase open reading frame (Leitner, 2013). This cell line is referred to as TOPflash reporter CVPC line in this thesis.

3 Methods

3.1 Cell culture

As detergents are cytotoxic for ESCs and CVPCs all glass ware used in stem cell culture needs to be cleaned separately from glass ware used in standard cell culture.

3.1.1 Cleaning of pipettes

After usage pipettes are kept in a water/hypochlorite solution for at least 10 minutes but can also be stored in this solution for several days. Then pipettes are rinsed with tap water for 3 hours and are then kept in a container containing milliQ water over night. Subsequently pipettes are dried at 60°C, fitted with a piece of cotton wool and autoclaved.

3.1.2 Cleaning of bottles

Glass bottles are filled with a water/hypochlorite solution and let stand for about 15 minutes. Bottles are then rinsed with tap water for another 15 to 20 minutes, filled with milliQ water and stored over night. The next day bottles are air-dried and autoclaved when completely dry.

3.1.3 Maintenance of ESCs and CVPCs

ESCs and CVPCs are grown in 24-well plates on mitotically inactivated SNL76/7 fibroblast feeder cells (see sections 1.2.1 and 2.7.1). They are fed every 24 hours with 1.5 ml M15Hy. Old medium is removed gently and new medium is added drop wise to not detach the cells from the surface. Cells are incubated at 37°C, 5 % CO_2.

3.1.4 Splitting of ESCs and CVPCs

ESCs and CVPCs are usually split 1:3 every three days. Two hours prior to splitting cells are pre-fed with 0.5 ml M15Hy and required wells containing feeder cells are pre-fed with 2 ml M15Hy. For splitting the medium is aspirated away completely and cells are carefully washed with 1 ml 1x PBS. Subsequently 200 µl of trypsin are added and cells are incubated at 37°C, 5 % CO_2 for 15 to 20 minutes until detached from the surface. Trypsinisation is stopped with 1 ml M15Hy from the pre-fed wells containing feeder cells and cells are resuspended thoroughly in the medium. 400 µl for 1:3 or 600 µl for 1:2 splitting of the cell suspension are then transferred drop wise in each pre-fed well

containing feeder cells. Cells should be incubated for at least 24 hours to let them attach completely before feeding them again.

3.1.5 Splitting of SNL76/7 fibroblasts

SNL76/7 fibroblasts are grown in 10 cm cell culture dishes and are usually split 1:6 about every 3 days or 1:8 about every 4 days. These cells do not have to be pre-fed prior to splitting. The medium is aspirated away and cells are washed with 5 ml of 1x PBS. 1 ml of trypsin is added and the cells are then incubated for 5-7 minutes at 37°C, 5 % CO_2. In the meantime the required number of dishes is filled with the appropriate amount of M10Gi. The final volume in the 10 cm dish should be 8 ml, hence if 1 ml cell suspension will be added to the dish, 7 ml of M10Gi should be provided. Trypsinisation is stopped with at least twice the amount of M10Gi compared to the amount of trypsin. For 1:6 splitting usually 5 ml of M10Gi are added, cells are resuspended thoroughly and 1 ml of the cell suspension is added to each of the prepared dishes. Cells are then incubated at 37°C, 5 % CO_2.

3.1.6 Production of feeder cells

First SNL76/7 feeder cells need to be mitotically inactivated. For this purpose most of the medium in the cell culture dish is discarded except for 4 ml and 80 µl of Mitomycin C is added. Cells are incubated for 4 hours at 37°C, 5 % CO_2. The required number of 24-well plates is coated with 0.1% gelatine and incubated for 2 hours at room temperature in the laminar flow hood.

After the 4 hour incubation time the medium is aspirated away from the cells and cells are washed with 5 ml 1x PBS. Cells are trypsinised as described in section 3.1.5. The trypsinisation is stopped with 4 ml M10Gi and cells are resuspended thoroughly. All the cells are then pooled in a 50 ml falcon and centrifuged at 1000 rpm for 7 minutes. Subsequently, the supernatant is aspirated away and cells are resuspended thoroughly in 20 to 30 ml of M10Gi; the dilution should allow for precise cell counting. The cell number is determined using a counting chamber and cells are diluted to a final concentration of $3.5x10^5$ cells/ml. 0.5 ml of the cell suspension are transferred to each well of the prepared 24-well plates. Cells are incubated at 37°C, 5 % CO_2.

3.1.7 Establishment of monolayer cell culture

ESCs or CVPCs are separated from LIF secreting feeder cells to and transferred onto 48-well plates to stimulate differentiation. For that purpose the required number of wells containing ESCs or CVPCs is pre-fed with 1 ml M15Si and cells are incubated for 2 hours

at 37°C, 5 % CO_2. The appropriate number of 6 cm or 10 cm dishes (depending on the required cell number) are gelatinised and incubated for 2 hours at room temperature in the laminar flow hood.

Following the incubation period the medium is aspirated away from the cells and cells are washed with 1 ml 1x PBS and then trypsinised as described in section 3.1.4. The trypsinisation is stopped with 1 ml M15Si and cells are resuspended thoroughly. Then cells are pooled in the gelatinised 6 cm or 10 cm dish and incubated for 45 minutes at 37°C, 5 % CO_2. During this period of time only the feeder cells but not the ESCs or CVPCs will attach to the surface resulting in the separation of ESCs or CVPCs from feeder cells. In the meantime the required number of 48-well plates is gelatinised and incubated for 2 hours at room temperature in the laminar flow hood.

After incubation of the cells the medium containing only ESCs or CVPCs is transferred to a 15 ml or 50 ml falcon (depending on the cell number). The 6 cm or 10 cm dish is rinsed with 3 or 5 ml M15Si, respectively, to collect remaining ESCs or CVPCs which are subsequently transferred into the same 15 ml or 50 ml falcon. Next, cells are centrifuged at 1000 rpm for 7 minutes. The supernatant is aspirated away, an appropriate amount of M15Si (depending on the cell number) is added and cells are resuspended thoroughly. Then the cells are counted in a counting chamber and are brought to the desired concentration. Finally, 500 µl of cell suspension is transferred into each of the required wells on the gelatinised 48-well plates. Cells can then be fed with M15Si after 24 hours at the earliest.

3.1.8 Production of embryoid and cardiac bodies

ESCs are used to produce EBs while CVPCs are used for CBs but apart from that there is no difference in the procedure. In this thesis only CBs were generated.

Cells need to be split 1:2 on the previous day to assure that cells are in the best condition possible. On the next day (at least 24 hours later) cells are pre-fed with 1 ml M15Si and are incubated for 2 hours at 37°C, 5 % CO_2. The required number of 10 cm cell culture dishes (depending on the number of different cell lines used) is gelatinised and incubated for 2 hours at room temperature in the laminar flow hood. ESCs or CVPCs are then trypsinised and separated from feeder cells on the gelatinised 10 cm dishes as described in section 3.1.7 except that cells are incubated for 1 hour.

For EB or CB production bacterial culture 10 cm dishes are used because they are hydrophobic and therefore, prevent cell attachment and facilitate droplet formation. The required number of these dishes is filled with autoclaved milliQ water to prevent drying-out of the cells.

After the incubation period ESCs or CVPCs are transferred to a 50 ml falcon and centrifuged for 7 minutes at 1000 rpm. The supernatant is then aspirated away, an appropriate amount of M15Si is added (depending on the expected cell number) and cells are resuspended thoroughly. Next, cells are counted and brought to a final concentration of $9x10^4$ cells/ml.
80-100 drops of 80 µl are placed in regular intervals at the inner surface of each lid of the prepared bacterial culture dishes and the dishes are then carefully covered with the lids again. Dishes should be kept in the laminar flow hood for some time as the vibrations created by the flow facilitate the aggregation process. Finally, cells are incubated at 37°C, 5 % CO_2. After 4.5 days the aggregated EBs or CBs are rinsed onto gelatinised 10 cm cell culture dishes (see also section 1.6).

3.1.9 Freezing of ESCs and CVPCs

Cells are trypsinised as described in section 3.1.4. In the mean time the freezing medium is prepared (see section 2.2.3). Trypsinisation is stopped with 800 µl M15Hy. Next, 200 µl freezing medium is added drop wise to each well which is to be frozen. After each drop the plate is moved for 5 seconds. Then 800 µl of freezing medium are added in the same manner resulting in the appropriate dilution of the 2x freezing medium. Cells are transferred to cryotubes (1 ml cell suspension/tube) which are subsequently put into a styrofoam box. This box is tightly sealed and incubated at -80°C for 24-48 hours allowing for slow and thus gentle freezing of the cells. Finally, cells can be transferred to liquid nitrogen for long term storage.

3.1.10 Thawing of ESCs and CVPCs

The required number of 24-wells containing feeder cells is pre-fed with 1.5 ml M15Hy and cells are incubated for 2 hours at 37°C, 5 % CO_2. ESCs or CVPCs which are to be thawed are removed from liquid nitrogen and quickly thawed at 37°C in a water bath. The thawed cell suspension is then transferred to a 15 ml falcon. 200 µl M15Hy are added drop-wise using a 200 µl pipette. After each drop the falcon is gently shaken. 800 µl and then 1 ml M15Hy are added in the same way using a 1000 µl pipette. Finally, 5 ml M15Hy are added in the same manner using a 5 ml glass pipette. Cells are subsequently centrifuged for 7 minutes at 1000 rpm. The supernatant is aspirated away; cells are resuspended in 1 ml M15Hy from pre-fed wells containing feeder cells and transferred to the same wells.

3.1.11 Thawing of SNL76/7 feeder cells

The procedure is very similar to thawing of ESCs and CVPCs described in section 3.1.10 except that pre-feeding is not required. Furthermore, after centrifugation the cell pellet is resuspended in 4 ml M10Gi and transferred to a 10 cm cell culture dish. Subsequently the falcon is rinsed with another 4 ml M10Gi which are added to the 10 cm cell culture dish.

3.2 Molecular biology methods

3.2.1 Genomic DNA isolation from ESCs or CVPCs

The cells are washed with 1x PBS. Subsequently, 600 µl of lysis buffer (see below) are added directly to each required 24-well. The vicious cell suspension is then transferred to a 15 ml tube (several wells can be pooled) and is incubated over night at 60°C.
The next day twice the amount of previously added lysis buffer 75mM NaCl solution (diluted in 96% ethanol) is added to the lysed cells. This solution is incubated at -20°C for at least 20 minutes or over night to precipitate the DNA. The next day the tube is centrifuged for 10 minutes at maximum speed. The supernatant is aspirated away and the pellet is washed twice with ice cold 70% ethanol and is again centrifuged for 5 minutes at full speed. The supernatant is again discarded; the probably small DNA pellet is dried at room temperature for about 10 minutes and then suspended in 100 µl milliQ water. The DNA can now be stored at -20°C.

Lysis Buffer

- 10 mM Tris-HCl pH 7.5
- 10 mM EDTA pH 8.0
- 10 mM NaCl
- 0.5% Sarcosyl
- 1 mg/ml Proteinase K (added shortly before usage)

3.2.2 Messenger RNA isolation from ESCs or CVPCs

ESCs or CVPCs are separated from feeder cells as described in section 3.1.7 except that M15Hy is used here instead of M15Si. Cells are then pooled in a falcon and centrifuged for 7 minutes at 1000 rpm. The supernatant is aspirated away and cells are washed with 4°C cold 1x PBS and are centrifuged for 7 minutes at 1000 rpm at 4°C. The supernatant is discarded and the cell pellet is suspended in 1 ml 4°C cold 1x PBS and the solution is

transferred to a 1.5 ml tube. Next, the tube is centrifuged at 4°C for 5 minutes at 13.000 rpm.

RNeasy Mini Kit, QIA-shredder protocol

The supernatant is aspirated away and cells are suspended in 600 µl RLT buffer/β-mercaptoethanol (100:1). Subsequently the solution is transferred onto a QIA-shredder column (purple) and is centrifuged for 2 minutes at 13.000 rpm. Next, 600 µl RNAse free-ethanol are added; the solution is mixed very well and transferred onto an RNeasy column (pink). The column is centrifuged for 15 seconds at 13.000 rpm resulting in the binding of the RNA to the column. The flow-through is discarded and 700 µl RWI buffer are added. The column is then centrifuged for 15 seconds at 13.000 rpm. Subsequently, the RNA is washed twice with 500 µl RPE. After each washing step the tube is centrifuged 15 seconds at 13.000 rpm and then the column is dry spun for 2 minutes at 13.000 rpm. The column is placed into a new 1.5 ml tube; 30 µl RNAse-free water are added and the column is centrifuged for 1 minute at 13.000 rpm to elute the RNA.

DNA digestion

To remove possible DNA contamination from the RNA sample DNA digestion is performed following the mRNA isolation procedure. For that purpose 3.75 µl RNAse-free DNAse I and 3.75 µl RNAse-free DNAse I buffer are added to the sample. The tube is incubated at 37°C for 30 minutes. After the incubation period the digest is stopped with 3.75 µl EDTA and the sample is incubated for 10 minutes at 65°C. To collect any condensed liquid the sample is short-spun and can then be stored at -80°C. To check whether the DNA digestion was successful a PCR reaction (see section 3.2.5) using *Gapdh* or *Hprt* primers should be performed.

3.2.3 Messenger RNA isolation from differentiating ESCs or CVPCs in monolayer cell culture

The procedure is almost identical to the one described in section 3.2.2 except that cells do not have to be separated from feeder cells. Instead cells are washed once with 4°C cold 1x PBS and are then again covered with 4°C cold 1x PBS. Cell culture plates are placed on ice. Cells are subsequently scraped off with a scraper or a pipette tip and are transferred to a falcon. The sample is centrifuged at 4°C for 7 minutes at 1000 rpm. Next, the supernatant is discarded; cells are suspended in 1 ml 4°C cold 1x PBS and are

transferred to a 1.5 ml tube. Subsequently, the tube is centrifuged at 4°C for 5 minutes at 13.000 rpm. The procedure can now be continued according to the RNeasy Mini Kit and DNA digestion protocols described in section 3.2.2.

3.2.4 Reverse transcription

RT-mix for 1 reaction

- 10 µl 5x RT buffer
- 5 µl 0.1 M DTT
- 1.5 µl RNAse OUT
- 2 µl 10 mM dNTPs

To reverse transcribe mRNA into cDNA 1 µl oligo dT is added to the mRNA sample. Subsequently, the sample is incubated at 70°C for 10 minutes and then incubated on ice for 3 minutes. The sample is then centrifuged for 30 seconds at 13.000 rpm. 18.5 µl of the RT-mix (see above) are added and the tube is incubated at 42°C for 2 minutes. Next, 1 µl reverse transcriptase is added and the sample is again incubated at 42°C for 50 minutes followed by a 5 minute incubation on ice. The sample is centrifuged at 13.000 rpm for 2 minutes. The nucleic acid concentration can now be measured using a NanoDrop instrument and then the sample is stored at -20°C.

3.2.5 Polymerase chain reaction (PCR)

PCR is used to specifically amplify certain DNA regions of interest.

Mix for 1 PCR reaction

- 10 µl Peqlab Master Mix Gold S
- 5 µl ddH_2O
- 4 µl Primer mix (forward and reverse primers) diluted 1:10
- 1 µl template DNA

Depending on the reaction setup a master mix for several reactions is prepared only from Peqlab Master Mix and ddH_2O or, either the primers or the DNA are additionally added to the first two components. The master mix is distributed into the required number of PCR reaction tubes and the missing component/s is/are added individually to each reaction

tube. A negative control, which does not contain DNA but all the other solutions needed in a PCR reaction, should also be prepared.
All the samples are transferred to the PCR machine and the according program is started (see also below).

General PCR conditions

1) 95°C for 5 minutes
2) 95°C for 1 minute
3) x°C for 1 minute } x 30-40
4) 72°C for 1-4 minutes
5) 72°C for 5 minutes
6) 4°C as long as required

The annealing temperature x in the third step (see above) is dependent on the primers used (see section 2.6) and usually lies between 55°C and 65°C. The elongation time in the fourth step (see above) depends on the length of the desired fragment and is typically 1 minute per kilobase (kb). The PCR products can either be stored at 4°C or -20°C or can be directly analysed on an agarose gel.

3.2.6 Gel electrophoresis

Gel electrophoresis is a method to visualise PCR products or other DNA samples and to simultaneously separate these DNA molecules according to their size.

Agarose gel

To produce an agarose gel the appropriate amount of agarose (see table 3.1) is weighed out and mixed with 1x TAE buffer in an Erlenmayer flask. This solution is heated in the microwave until the agarose is completely dissolved. During the heating the solution is swirled from time to time. The solution is then cooled down to about 60°C and approximately 5 µl of ethidium bromide are added per 100 ml of gel solution. Ethidium bromide is a fluorescent DNA dye and is suspected to be mutagenic. Therefore, ethidium bromide should only be used in designated areas of the lab and nitril gloves have to be worn whenever working with this substance or with gels containing it. The agarose solution is then poured into a gel tray and the well comb is put in place. Bubbles in the gel are pushed away from the well comb or to the sides of the gel with a pipette tip. When the

gel has completely solidified after about 20 - 30 minutes the well comb can be removed and the samples can be loaded.

Proportion of agarose [%]	Range of separation [bp]
0.5	1,000 – 30,000
0.7	800 – 12,000
1.0	500 – 10,000
1.2	400 – 7,000
1.4	200 – 4,000
2.0	50 – 2,000

Table 3.1: Separation range of agarose gels.

Sample loading and running of gel

The hardened gel is placed into the gel box which is filled with 1x TAE buffer until the gel is covered.
Before loading onto the gel 4 µl 6x Loading Dye (see below) are added to each 20 µl PCR sample. Next, a DNA size marker is carefully loaded into the first well and the samples are then loaded into the additional wells.
The lid is placed onto the gel box and connected to the power supply. The gel is run at 80 V for about 1 hour.

6x Loading dye

- 505 µl 88% Glycerin
- 600 µl 0.5 M EDTA
- 0.0022 g Bromphenolblue
- Fill up to 5 ml with dH_2O

Observation of DNA fragments

The gel is exposed to UV light to visualise the DNA samples and a picture of the gel is taken. The gel can then be disposed in specific ethidium bromide waste.

3.3 Flow cytometry

The principles of this method are described in section 1.7. All measurements are performed on the BD FACSCalibur flow cytometer. Settings are adapted accordingly as described in section 3.3.2. FSC, SSC and EGFP as well as PI fluorescence are detected and appropriate gates for the fluorescence parameters were set as shown in figure 3.2. All settings are maintained during the whole experiment. EGFP and PI fluorescence data are used for further analysis.

3.3.1 Preparation of cells

Cells are trypsinised as described in section 3.1.4. If cells are grown in monolayer culture on 48-well plates only 80 µl of trypsin are used. 1 ml cell suspension is transferred into a FACS measuring tube. If cells are grown at high density the cell suspension should be diluted accordingly to allow for reliable measurements.

3.3.2 Measurement

Instrument and software settings

The instrument settings were adopted from Lucia Leitner (Leitner, 2013) and are presented in table 3.2. The voltage is adjusted accordingly to allow for the production of a significant signal which can be further adapted and amplified via the setting amplification gain (AmpGain). As fluorescence signals can vary greatly between different samples the logarithmic mode was chosen for the fluorescence channels (FL1 and 2; see also section 1.7).

Parameter	Detector	Voltage	AmpGain	Mode
P1	FSC	0.10	6.00	Lin
P2	SSC	350	1.00	Lin
P3	FL1	456	1.00	Log
P4	FL2	456	1.00	Log

Table 3.2: Flow cytometer settings.

A threshold of the value 53 is determined for the FCS channel to only analyse cells but not cellular fragments which are smaller than whole cells. In figure 3.1 these smaller fragments are not displayed and thus, a gap between the y-axis and the cloud of dots representing the measured events can be seen. The analysed cells are displayed in a two-dimensional dot plot according to their SSC and FSC in figure 3.1; EGFP positive cells are also shown and are marked in green.

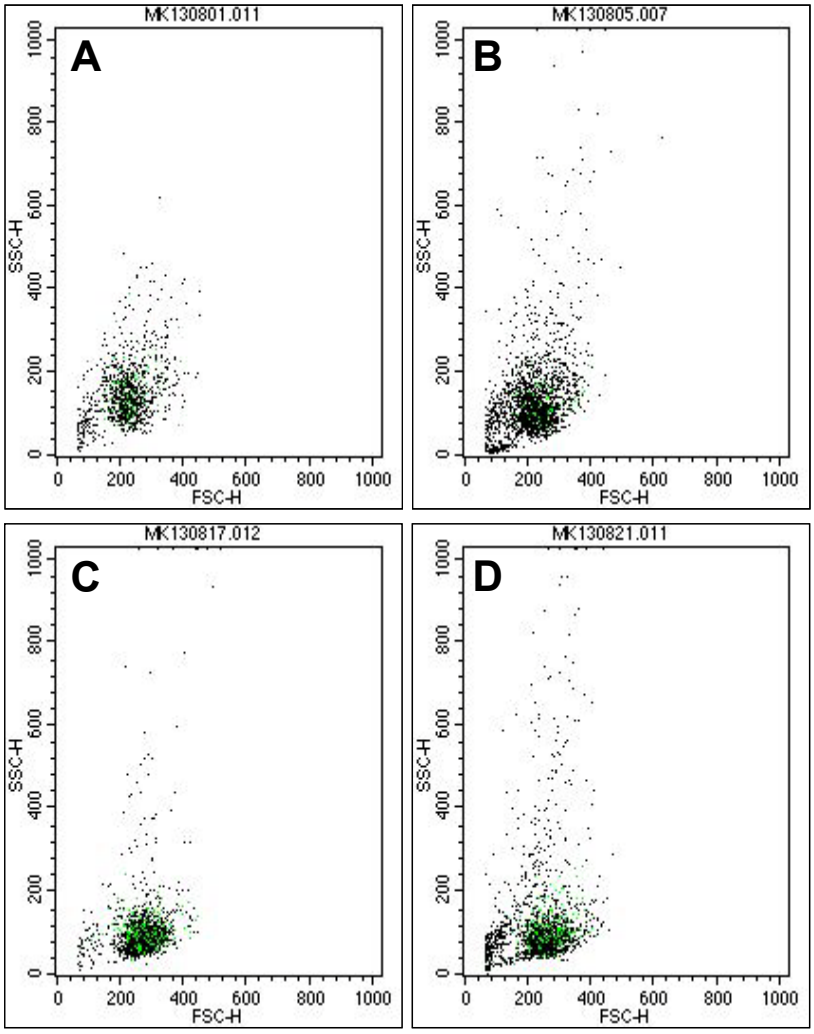

Figure 3.1: Graphical presentation of FACS analysis in two-dimensional dot plot. Displayed parameters: SSC and FSC. Dot: Event (cell). Green dot: EGFP positive cell.

A) MesP1^{EGFP} reporter ESC line on day 3 of differentiation.
B) MesP1^{EGFP} reporter ESC line on day 7 of differentiation.
C) MesP1^{EGFP} reporter CVPC line on day 3 of differentiation.
D) MesP1^{EGFP} reporter CVPC line on day 7 of differentiation.

EGFP and PI gates were manually set by the experienced user Thomas Sauer and are depicted in figure 3.2.

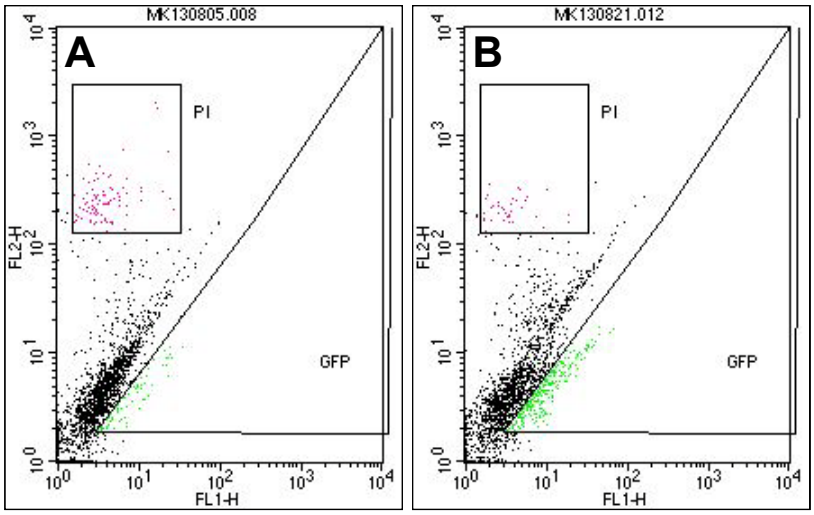

Figure 3.2: Gates for EGFP and PI positive cells in flow cytometry experiments.

A) MesP1^{EGFP} reporter ESC line on day 7 of differentiation.

B) MesP1^{EGFP} reporter CVPC line on day 7 of differentiation.

Actual measurement

The flow cytometer is switched on according to the procedure indicated on the instrument. Next, the computer connected to the instrument is booted up and the software BD CellQuest^{TM} Pro is started. The appropriate analysis file is opened and applicable instrument settings (Table 3.2) are loaded. A new folder to save the measurements is created.

The sample is vortexed and is subsequently loaded onto the collection system of the cytometer. The measurement is started by clicking on the 'Acquire' button in the 'Browser' window of the software. After 10,000 analysed events the measurement is stopped automatically. To determine the proportion of dead cells 1 µl PI is added to the sample and the measurement is repeated. EGFP and PI fluorescence cannot be analysed simultaneously as the PI signal influences the EGFP signal.

After the measurements the cytometer is shut down according to the procedure indicated on the instrument. The acquired data can be exported and saved as a Microsoft Excel File.

3.4 Luminescence assay

This assay was used to monitor Wnt signalling in TOPflash reporter cell lines carrying β-catenin responsive elements upstream of a firefly luciferase reporter gene (see also section 4.6). When the luciferase gene is expressed the enzyme can convert a provided substrate into a luminescent reagent whose luminescence is detected during the assay.
All measurements are performed using the Victor^{3}V multilabel plate reader. An adapted version of the 'luminescence' program of the software Wallac 1420 (version 3.4) is used.

3.4.1 Preparation of cells

Cells are trypsinised as described in sections 3.1.4 and 3.3.1. 50 µl of cell suspension is then transferred onto a non-transparent 96-well plate and mixed with 50 µl ONE-Glo^T *M* luciferase substrate solution. Each sample is analysed in triplicate but once the luciferase substrate is not added and this probe thus serves as a negative control (see also section 4.6). The measurement should be performed at least three minutes after addition of the substrate.

3.4.2 Measurement

The computer as well as the plate reader is switched on. The lid of the non-transparent 96-well plate is removed and the plate is placed into the plate reader. Next, the program Wallac 1420 is opened and luminescence settings are loaded. The wells of the plate which are to be analysed are defined. The measurement is started and should then be repeated another two times. Finally, the data can be exported and saved as a Microsoft Excel file.

4 Results

The aim of this thesis was to test the possibility whether cardiomyogenesis and its molecular regulation can be studied in a 2D monolayer cell culture system. We used embryonic stem or cardiovascular progenitor reporter cell lines with *Brachyury*^{EGFP} and *MesP1*^{EGFP} transgenes and an *Nkx2.5*^{EGFP} knock-in allele to monitor expression of *Brachyury*, *MesP1* and *Nkx2.5* respectively at different differentiation time points under various conditions using FACS analysis.

4.1 Influence of SPARC on expression of *Brachyury*, *MesP1* and *Nkx2.5*

SPARC was previously shown to increase *Nkx2.5* expression levels in differentiating ESCs in a hanging drop cell culture system and to enhance the number of beating cardiomyocytes developing from these cells (Stary et al., 2005).

To test whether SPARC has an effect on the expression of *Brachyury*, *MesP1* and *Nkx2*.5 in ESCs or CVPCs at an early differentiation time point in a monolayer cell culture system Brachyury^{EGFP}, MesP1^{EGFP} and Nkx2.5^{EGFP} reporter cell lines were separated from feeder cells and placed onto gelatinised 48-well plates at increasing cell numbers. On the next day (day 1 of differentiation) either 2 µg/ml SPARC was added to the cells or the cells were left untreated. After 24 h the proportion of *EGFP* expressing cells and the mean *EGFP* intensity of an EGFP positive cell was determined by FACS. To determine the percentage of living cells, dead cells were identified by PI staining and FACS analyses after the EGFP measurement. Thus, EGFP positive cells might be comprised of a certain amount of dead cells.

For reliable FACS data 10,000 cells should be measured. However, this was only possible for 10^5 cell samples. 5,000 events were measured where $5x10^4$ cells were present, 800 for 10^4 cells and 300 for $5x10^3$ cells. Each sample variant was analysed in triplicate.

Measuring only a low number of events reduces the significance of the statistical analysis of the obtained FACS data.

4.1.1 Effects of SPARC on expression of *Brachyury*^{EGFP}, *MesP1*^{EGFP} and *Nkx2.5*^{EGFP} reporter genes in embryonic stem cell lines

First we analysed the influence of SPARC treatment on *Brachyury*^{EGFP}, *MesP1*^{EGFP} and *Nkx2.5*^{EGFP} expression in differentiating ESCs in low volume monolayer cell culture investigating the proportions of *Brachyury*^{EGFP}, *MesP1*^{EGFP} and *Nkx2.5*^{EGFP} expressing

cells as well as the mean expression intensity of these genes. Additionally, we determined the proportions of dead cells after SPARC treatment.

Proportion of Brachyury^{EGFP}, MesP1^{EGFP} and Nkx2.5^{EGFP} expressing cells

The proportions of Brachyury^{EGFP}, MesP1^{EGFP} and Nkx2.5^{EGFP} expressing cells in low volume monolayer ESC culture were determined using FACS analysis after 24 hour SPARC treatment and compared to the same proportions in untreated cells.

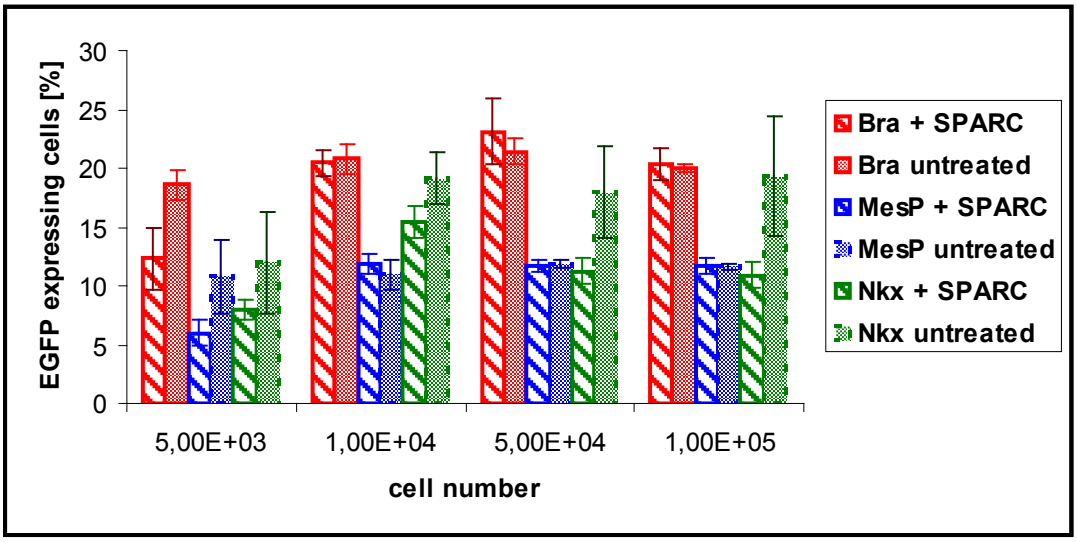

Figure 4.1: The influence of SPARC on *Brachyury*, *MesP1* or *Nkx2.5* expression in **ESCs**. FACS analyses of Brachyury^{EGFP}, MesP1^{EGFP} and Nkx2.5^{EGFP} reporter ESC lines after treatment with 2 µg/ml SPARC for 24 h (shaded bars). Proportion of ESCs expressing *Brachyury^{EGFP}* (red bars), *MesP1^{EGFP}* (blue bars) or *Nkx2.5^{EGFP}* (green bars) at different cell numbers seeded on 48-well plates one day before the addition of SPARC. Error bars: SD.

Under the conditions described above the addition of SPARC showed no effect on the expression of *Brachyury^{EGFP}* and *MesP1^{EGFP}* at cell numbers between 10^4 and 10^5 cells within 24 hours but significantly reduced *Nkx2.5^{EGFP}* expression as shown in figure 4.1. The latter result contradicts previous findings obtained with EBs but SPARC treatment was only started at day 7 of differentiation in these previous experiments (Stary et al., 2005).

The negative effect of SPARC on all reporter genes at low cell numbers is of low significance due to the low number of cells analysed by FACS.

Mean intensity of *Brachyury*^{EGFP}, *MesP1*^{EGFP} and *Nkx2.5*^{EGFP} expression

The mean intensity of *Brachyury*^{EGFP}, *MesP1*^{EGFP} and *Nkx2.5*^{EGFP} expression after SPARC treatment was investigated by flow cytometry in low volume monolayer ESC culture.

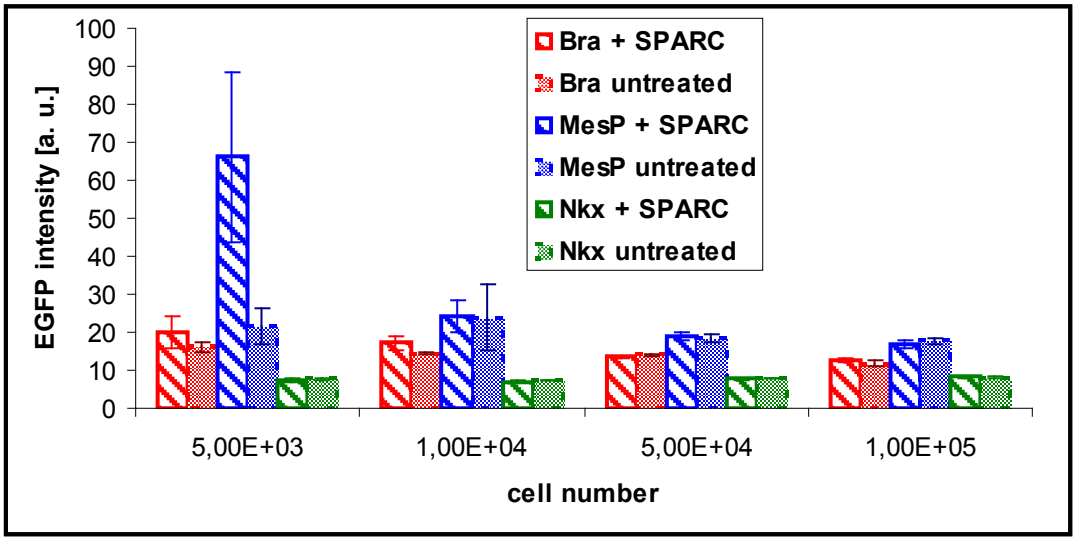

Figure 4.2: The influence of SPARC on *Brachyury*, *MesP1* or *Nkx2.5* expression in **ESCs**. FACS analyses of Brachyury^{EGFP}, MesP1^{EGFP} and Nkx2.5^{EGFP} reporter ESC lines after treatment with 2 µg/ml SPARC for 24 h (shaded bars). Mean intensity of *Brachyury*^{EGFP} (red bars), *MesP1*^{EGFP} (blue bars) or *Nkx2.5*^{EGFP} (green bars) expression in ESCs at different cell numbers seeded on 48-well plates one day before the addition of SPARC. Error bars: SD.

As depicted in figure 4.2 SPARC did not alter the mean intensity of *Brachyury*^{EGFP}, *MesP1*^{EGFP} and *Nkx2.5*^{EGFP} expression in most samples. Addition of SPARC led to an increase of *MesP1*^{EGFP} expression at 5x10^3 cells. However, due to the low cell count on the FACS machine this finding is not significant.

Proportion of PI positive cells

We investigated the proportion of dead cells, which stain positively for PI, in our samples using FACS analysis.

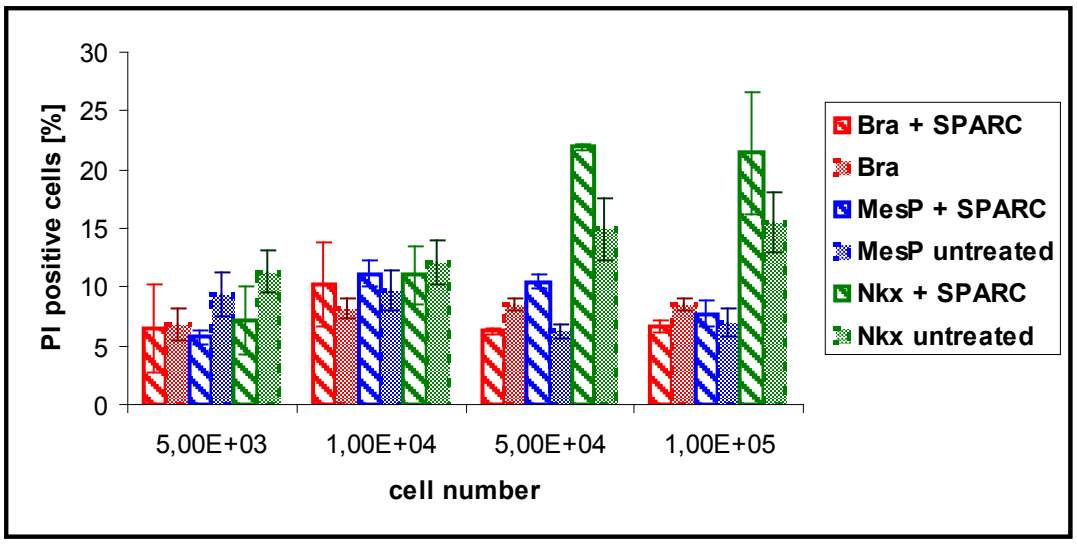

Figure 4.3: The influence of SPARC on *Brachyury*, *MesP1* or *Nkx2.5* expression in **ESCs**. FACS analyses of Brachyury^{EGFP}, MesP1^{EGFP} and Nkx2.5^{EGFP} reporter ESC lines after treatment with 2 µg/ml SPARC for 24 h (shaded bars). Proportion of PI positive (dead) cells in Brachyury^{EGFP} (red bars), MesP1^{EGFP} (blue bars) and Nkx2.5^{EGFP} (green bars) reporter ESC lines at different cell numbers seeded on 48-well plates one day before the addition of SPARC. Error bars: SD.

SPARC treated cells of the ESC Nkx2.5^{EGFP} or MesP1^{EGFP} reporter lines showed a higher proportion of PI positive (dead) cells compared to untreated cells at $5x10^4$ and 10^5 cells or at $5x10^4$ cells respectively as can be seen in figure 4.3. However, this finding might not be significant as only three samples were tested for each cell number and each condition, respectively.

As addition of SPARC did not enhance the proportion of dead cells in other samples SPARC did probably not have a toxic effect on the cells but cell death might have rather been caused by harsh treatment of the cells.

4.1.2 Effects of SPARC on *Brachyury^{EGFP}*, *MesP1^{EGFP}* and *Nkx2.5^{EGFP}* expression in cardiovascular progenitor cell lines

The influence of SPARC on *Brachyury^{EGFP}*, *MesP1^{EGFP}* and *Nkx2.5^{EGFP}* expressing cells was also observed in low volume monolayer CVPC culture and the proportion of dead cells after SPARC treatment was measured.

Proportion of *Brachyury*^{EGFP}, *MesP1*^{EGFP} and *Nkx2.5*^{EGFP} expressing cells

CVPCs in low volume monolayer cell culture were treated with SPARC for 24 hours. Subsequently the proportions of *Brachyury*^{EGFP}, *MesP1*^{EGFP} and *Nkx2.5*^{EGFP} expressing cells were determined using FACS analysis.

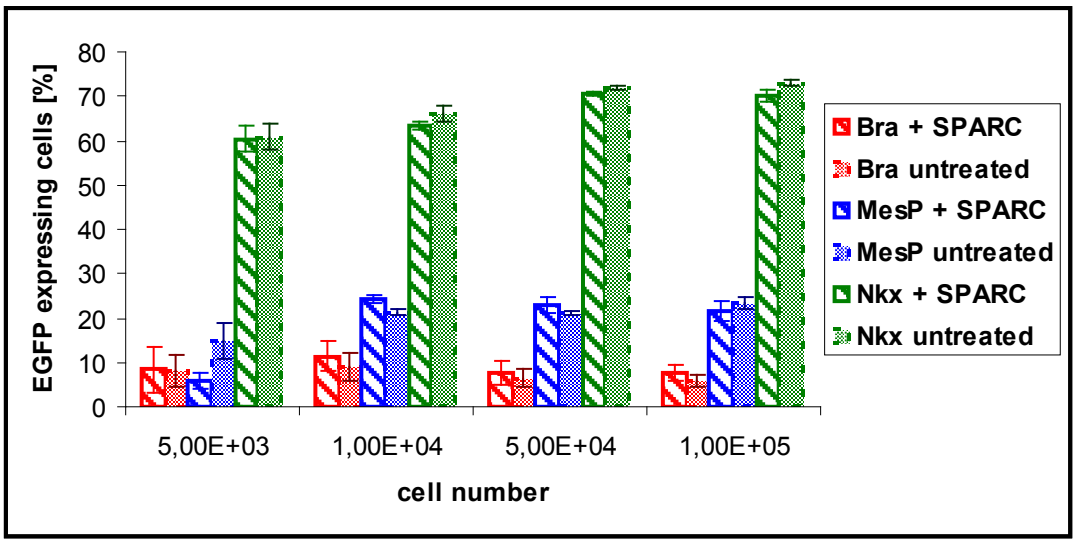

Figure 4.4: The influence of SPARC on *Brachyury*, *MesP1* or *Nkx2*.5 expression in **CVPCs**. FACS analyses of Brachyury^{EGFP}, MesP1^{EGFP} and Nkx2.5^{EGFP} reporter CVPC lines after treatment with 2 µg/ml SPARC for 24 h (shaded bars). Proportion of CVPCs expressing *Brachyury*^{EGFP} (red bars), *MesP1*^{EGFP} (blue bars) and *Nkx2.5*^{EGFP} (green bars) at different cell numbers seeded on 48-well plates one day before the addition of SPARC. Error bars: SD.

As depicted in figure 4.4, addition of SPARC did not influence the expression of *Brachyury*^{EGFP}, *MesP1*^{EGFP} and *Nkx2.5*^{EGFP} in all three CVPC lines tested within 24 hours. This result is not in line with previous results demonstrating that SPARC up-regulates expression of *Brachyury*, *MesP1* and *Nkx2.5* mRNA in an undifferentiated CVPC line (Gottschamel, 2010).

Mean *Brachyury*^{EGFP}, *MesP1*^{EGFP} and *Nkx2.5*^{EGFP} intensity

The mean expression intensity of *Brachyury*^{EGFP}, *MesP1*^{EGFP} and *Nkx2.5*^{EGFP} expression in monolayer CVPC culture after 24 hour SPARC treatment was investigated using flow cytometry.

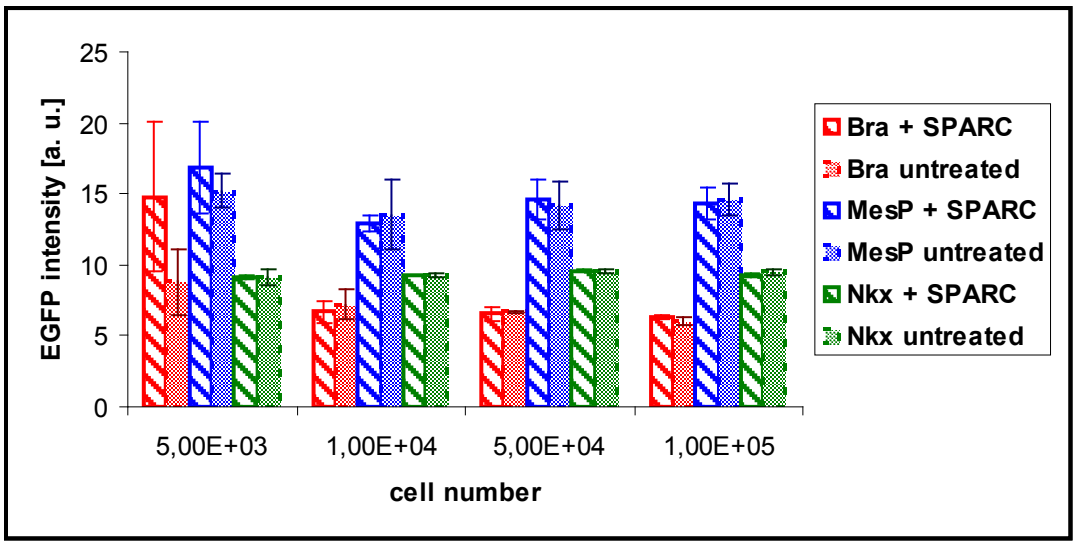

Figure 4.5: The influence of SPARC on *Brachyury*, *MesP1* or *Nkx2.5* expression in **CVPCs**. FACS analyses of Brachyury^{EGFP}, MesP1^{EGFP} and Nkx2.5^{EGFP} reporter CVPC lines after treatment with 2 µg/ml SPARC for 24 h (shaded bars). Mean intensity of *Brachyury^{EGFP}* (red bars), *MesP1^{EGFP}* (blue bars) or *Nkx2.5^{EGFP}* (green bars) expression in CVPCs at different cell numbers seeded on 48-well plates one day before the addition of SPARC. Error bars: SD.

Figure 4.5 shows that expression of *Brachyury^{EGFP}*, *MesP1^{EGFP}* and *Nkx2.5^{EGFP}* did not differ greatly between untreated cells and cells treated with SPARC except for *Brachyury^{EGFP}* expression at 5x10^3 cells. But again, the number of cells analysed by FACS in these samples was too low for a trustworthy statistical analysis.

Proportion of PI positive cells

The proportion of dead cells after SPARC treatment was observed in low volume monolayer cell culture using FACS analysis.

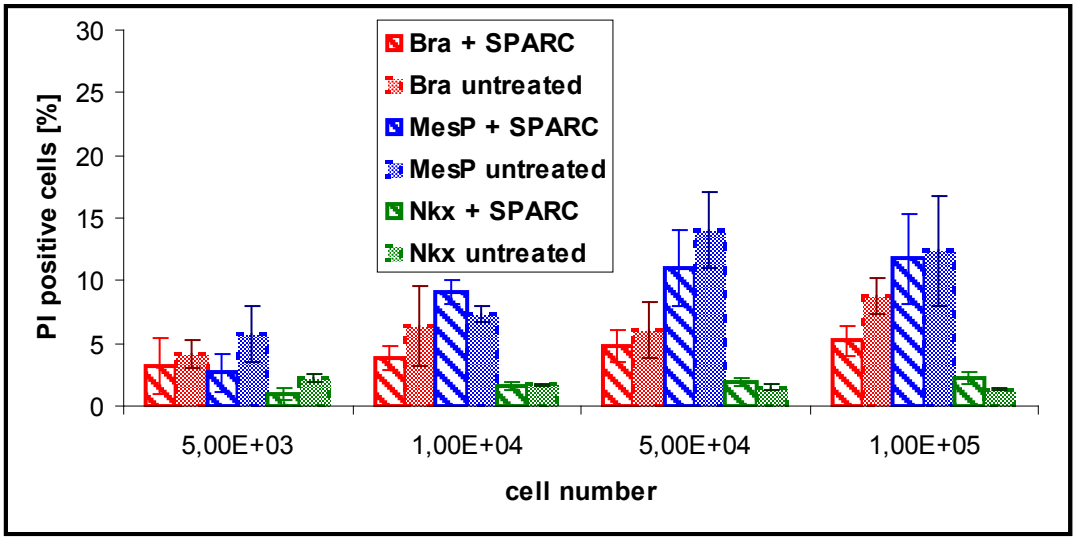

Figure 4.6: The influence of SPARC on *Brachyury*, *MesP1* or *Nkx2.5* expression in **CVPCs**. FACS analyses of Brachyury^{EGFP}, MesP1^{EGFP} and Nkx2.5^{EGFP} reporter CVPC lines after treatment with 2 µg/ml SPARC for 24 h (shaded bars). Proportion of PI positive (dead) cells in *Brachyury^{EGFP}* (red bars), *MesP1^{EGFP}* (blue bars) and *Nkx2.5^{EGFP}* (green bars) reporter CVPC lines at different cell numbers seeded on 48-well plates one day before the addition of SPARC. Error bars: SD.

The proportion of dead (PI positive) was comparable between untreated and with SPARC treated CVPCs as depicted in figure 4.6 which is another evidence that SPARC does not display a cytotoxic effect at the concentration used in this experiment.

4.1.3 Comparison between cardiovascular progenitor and embryonic stem cells

Overall, SPARC did not change expression patterns of *Brachyury^{EGFP}* and *MesP1^{EGFP}* in ESC and CVPC reporter cell lines. SPARC reduced the expression of *Nkx2.5^{EGFP}* in ESCs but it had no effect on its expression in CVPCs (Figures 4.1, 4.2, 4.4 and 4.5).

Brachyury^{EGFP} expression was higher in differentiating ESCs than in CVPCs (Figures 4.1, 4.2, 4.4 and 4.5). As Brachyury is an early mesodermal marker it was not surprising that it was already expressed to a lower extent in further differentiated CVPCs.

The CVPC MesP1^{EGFP} reporter cell line showed a higher proportion of *MesP1^{EGFP}* expressing cells than the corresponding ESC line (Figures 4.1 and 4.4) which could be expected as MesP1 is a marker of cardiovascular precursors. However, the intensity of *MesP1^{EGFP}* expression was slightly lower in CVPCs compared to ESCs (Figures 4.2 and 4.5). It might be possible that a higher amount of MesP1 is required in ESCs than in CVPCs to drive cardiovascular differentiation.

As expected a much higher percentage of CVPCs was expressing *Nkx2.5*^{EGFP} compared to their ESC counterparts (Figures 4.1 and 4.4) because *Nkx2.5* is only expressed in cardiac but not in mesodermal progenitors. Interestingly, the mean intensity of *Nkx2.5*^{EGFP} expression was similar in ESCs and CVPCs (Figures 4.2 and 4.5).

4.2 Expression of *Brachyury*, *MesP1* and *Nkx2.5* at different time points of differentiation

SPARC did not have a great effect on the expression of *Brachyury*^{EGFP}, *MesP1*^{EGFP} and *Nkx2.5*^{EGFP} in ESCs and CVPCs at an early time point of differentiation.

We then were interested in the expression pattern of *Brachyury*^{EGFP}, *MesP1*^{EGFP} and *Nkx2.5*^{EGFP} in ESCs and CVPCs over time in monolayer cell culture and whether that pattern was comparable to previous results obtained with EBs and CBs. For that purpose we evaluated the proportion of *Brachyury*^{EGFP}, *MesP1*^{EGFP} and *Nkx2.5*^{EGFP} expressing cells, the proportion of PI positive cells as well as the mean intensity of *Brachyury*^{EGFP}, *MesP1*^{EGFP} and *Nkx2.5*^{EGFP} expression in ESC and CVPC Brachyury^{EGFP}, MesP1^{EGFP} and Nkx2.5^{EGFP} reporter cell lines at days 0 (undifferentiated), 1, 3, 5, 7, 9 and 11 of differentiation using FACS analysis.

Cells were separated from feeder cells and were either analysed directly with flow cytometry (day 0) or placed onto a gelatinised 48-well plate and used for FACS analysis at the time points mentioned above. As an appropriate number of events for statistical analysis can be measured with $5x10^4$ cells per 48-well this cell number was chosen for this experiment.

10,000 events of each sample were measured except for days 0, 1 and 3 of differentiation in the Brachyury^{EGFP} and MesP1^{EGFP} ESC lines as well as in the Nkx2.5^{EGFP} CVPC line and days 0 and 1 of differentiation in the Brachyury^{EGFP} and MesP1^{EGFP} CVPC lines as well as in the Nkx2.5^{EGFP} ESC line where only 5,000 events were evaluated. Each sample was measured in triplicate. The experiment was repeated once for the Brachyury^{EGFP} reporter ESC line and twice for the Brachyury^{EGFP} CVPC line during the experiment described in section 2.3.

4.2.1 *Brachyury*^{EGFP}, *MesP1*^{EGFP} and *Nkx2.5*^{EGFP} expression in embryonic stem cell reporter lines at different time points of differentiation

Brachyury^{EGFP}, *MesP1*^{EGFP} and *Nkx2.5*^{EGFP} expression patterns over time were investigated in differentiating ESCs in low volume monolayer cell culture. The proportions of dead cells during differentiation in monolayer cell culture were also determined.

Proportion of *Brachyury*^{EGFP}, *MesP1*^{EGFP} and *Nkx2.5*^{EGFP} expressing cells

We evaluated the proportions of *Brachyury*^{EGFP}, *MesP1*^{EGFP} and *Nkx2.5*^{EGFP} expressing cells over time in differentiating ESCs in low volume monolayer cell culture using flow cytometry.

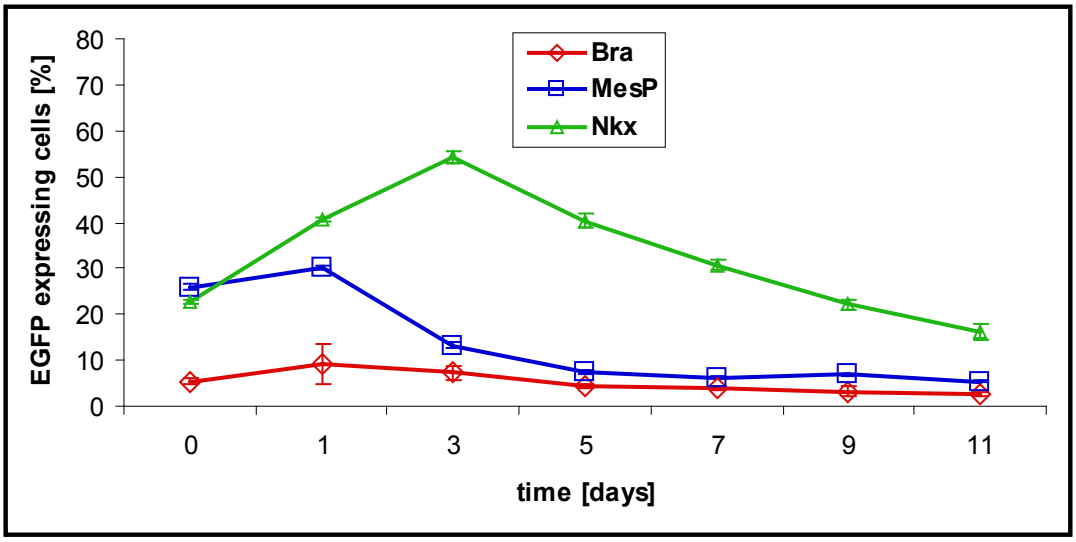

Figure 4.7: Analysis of expression of *Brachyury*, *MesP1* or *Nkx2.5* in **ESCs** at different time points. FACS analyses of Brachyury^{EGFP}, MesP1^{EGFP} and Nkx2.5^{EGFP} reporter ESC lines on different time points of differentiation. Proportion of ESCs expressing *Brachyury*^{EGFP} (red line), *MesP1*^{EGFP} (blue line) and *Nkx2.5*^{EGFP} (green line) seeded on 48-well plates ($5x10^4$ cells per well) on day 0 of differentiation. Data for *Brachyury*^{EGFP} expression obtained from two independent experiments and six samples in total. Error bars: SD.

As depicted in figure 4.7 *Brachyury*^{EGFP} and *MesP1*^{EGFP} expression in ESCs showed a peak on day 1 of differentiation which could be a stress response to the establishment procedure of the monolayer cell culture. After day 1 the proportions of *Brachyury*^{EGFP} and *MesP1*^{EGFP} expressing cells were declining and did practically not change after day 5 of differentiation.

The proportion of *Nkx2.5*^{EGFP} expressing ESCs peaked on day 3 of differentiation and continually decreased from that time point on. The proportion of *Nkx2.5*^{EGFP} expressing cells was highest at all time points compared to the expression of *Brachyury*^{EGFP} and *MesP1*^{EGFP} except for day 0 of differentiation where it was similar to *MesP1*^{EGFP} expression.
There was no great difference between *Brachyury*^{EGFP} and *MesP1*^{EGFP} expression except for the first three time points where the proportion of *MesP1*^{EGFP} expressing cells was higher.

Additionally, the proportions of *Brachyury*^{EGFP} and *MesP1*^{EGFP} expressing cells at different time points of differentiation were compared between monolayer ESC culture and EBs.

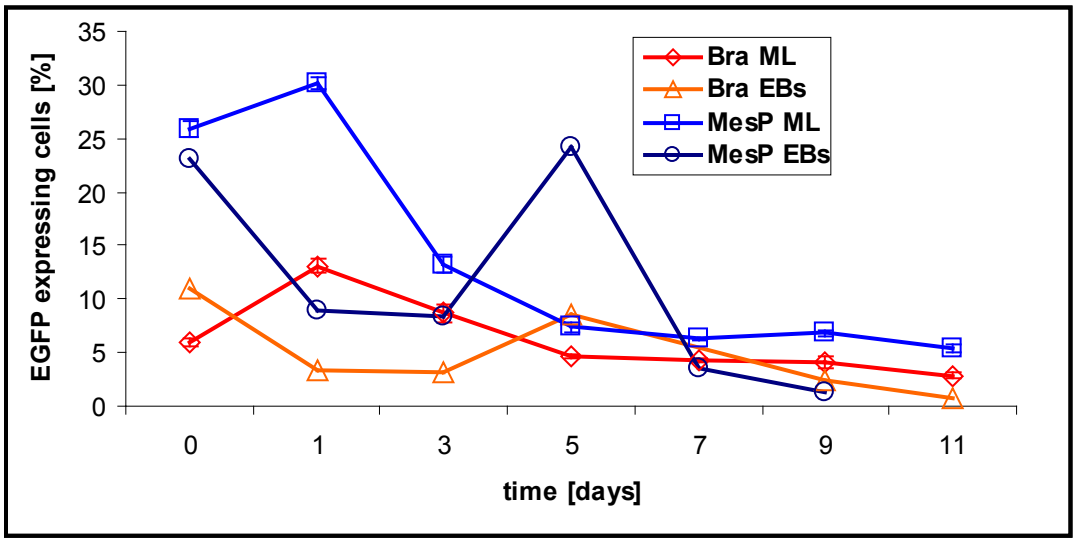

Figure 4.8: Analysis of expression of *Brachyury* or *MesP1* in **ESCs** at different time points. Comparison between monolayer cell culture and the EB system. FACS analyses of Brachyury^{EGFP} and MesP1^{EGFP} reporter ESC lines on different time points of differentiation. Proportion of ESCs expressing *Brachyury*^{EGFP} and *MesP1*^{EGFP} either seeded on 48-well plates ($5x10^4$ cells per well) or placed into hanging drop cell culture on day 0 of differentiation. Error bars: SD. Data for *Brachyury*^{EGFP} expression obtained from two independent experiments and six samples in total. Data for EBs was produced by Lucia Leitner in the course of her diploma thesis (Leitner, 2013). ML: monolayer cell culture.

Figure 4.8 shows that in former experiments with EBs a clear peak of the proportion of *Brachyury*^{EGFP} and *MesP1*^{EGFP} could be seen on day 5 of differentiation which was not observed in this experiment. The proportion of *Brachyury*^{EGFP} and *MesP1*^{EGFP} expressing cells was very high on day 0 or day 1 of differentiation in EBs or low volume monolayer cell culture, respectively. Both of these high values could result from trypsinisation stress

on the previous day (day 0 for monolayer experiment, one day before day 0 for hanging drop culture experiment) of FACS analysis.

As ESCs were capable to differentiate into contracting cardiomyocytes in the EB system but failed in this differentiation process in low volume monolayer cell culture, the expression profile in the EB system probably better reflected the *in vivo* situation.

Mean *Brachyury*^{EGFP}, *MesP1*^{EGFP} and *Nkx2.5*^{EGFP} intensity

The mean intensity of *Brachyury*^{EGFP}, *MesP1*^{EGFP} and *Nkx2.5*^{EGFP} expression was determined in low volume monolayer ESC culture at different time points of differentiation.

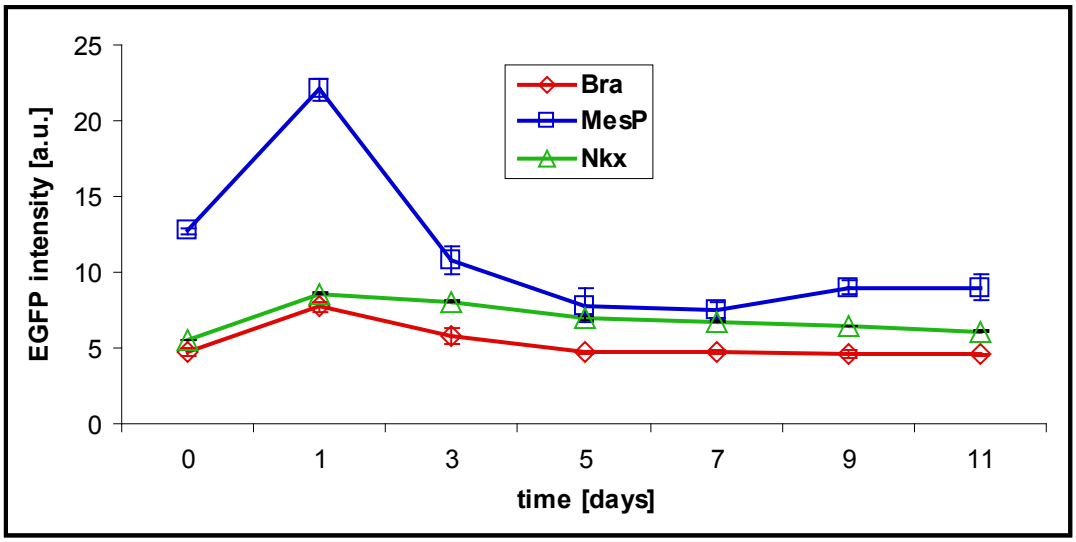

Figure 4.9: Analysis of expression of *Brachyury*, *MesP1* or *Nkx2.5* in **ESCs** at different time points. FACS analyses of Brachyury^{EGFP}, MesP1^{EGFP} and Nkx2.5^{EGFP} reporter ESC lines on different time points of differentiation. Mean intensity of *Brachyury*^{EGFP} (red line), *MesP1*^{EGFP} (blue line) or *Nkx2.5*^{EGFP} (green line) expression in ESCs seeded on 48-well plates (5x10^4 cells per well) on day 0 of differentiation. Data for *Brachyury*^{EGFP} expression obtained from two independent experiments and six samples in total. Error bars: SD.

The mean intensity of *MesP1*^{EGFP} expression in ESCs distinctly peaked on day 1 of differentiation as shown in figure 4.9 which could also result from stress because of trypsinisation. This intensity level was similar in all tested samples indicated by the small error bar.

Peaks of *Brachyury*^{EGFP} and *Nkx2.5*^{EGFP} expression levels were only small on that time point. Mean intensities of *Brachyury*^{EGFP}, *MesP1*^{EGFP} and *Nkx2.5*^{EGFP} expression were declining after day 1 of differentiation with *MesP1*^{EGFP} expression levels rising again after day 7 of differentiation.

Interestingly, the mean intensity of *Brachyury*^{EGFP}, *MesP1*^{EGFP} and *Nkx2.5*^{EGFP} expression in ESCs was similar at most time points. Only on days 0 and 1 of differentiation *MesP1*^{EGFP} expression levels exceeded *Brachyury*^{EGFP} and *Nkx2.5*^{EGFP} expression levels.

We also investigated whether *Brachyury*^{EGFP} and *MesP1*^{EGFP} expression intensities differed between monolayer ESC culture and EBs.

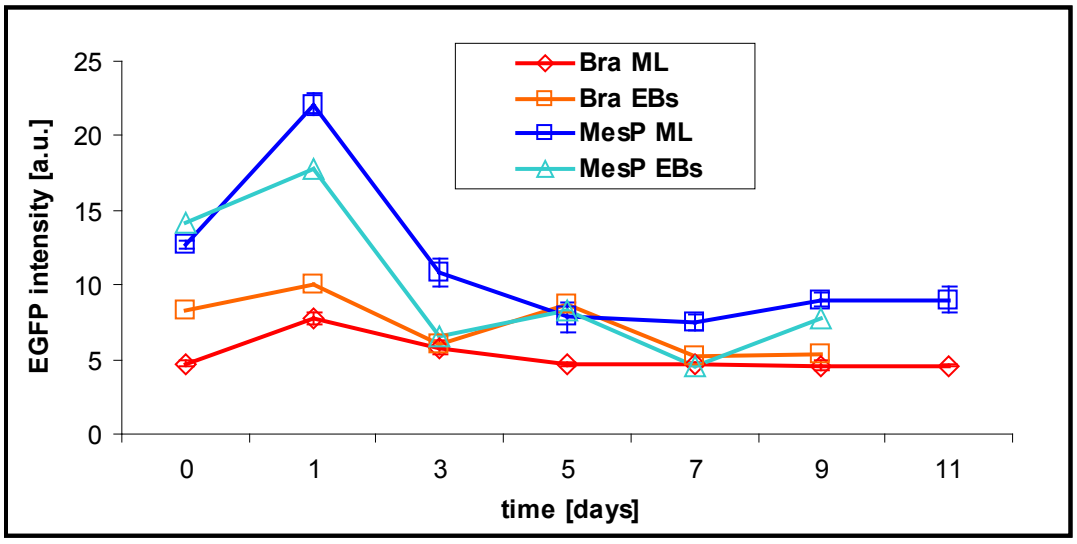

Figure 4.10: Analysis of expression of *Brachyury* or *MesP1* in **ESCs** at different time points. Comparison between monolayer cell culture and the EB system. FACS analyses of Brachyury^{EGFP} and MesP1^{EGFP} reporter ESC lines on different time points of differentiation. Mean intensity of *Brachyury*^{EGFP} or *MesP1*^{EGFP} expression in ESCs either seeded on 48-well plates ($5x10^4$ cells per well) or placed into hanging drop cell culture on day 0 of differentiation. Error bars: SD. Data for *Brachyury*^{EGFP} expression obtained from two independent experiments and six samples in total. Data for EBs was produced by Lucia Leitner in the course of her diploma thesis (Leitner, 2013). ML: Monolayer cell culture.

In former experiments with EBs the cell lines also showed a peak of the mean intensity of *Brachyury*^{EGFP} and *MesP1*^{EGFP} expression at day 5 of differentiation which was missing in our experiments in low volume monolayer cell culture as depicted in figure 4.10. On all the other time points the expression pattern was quite similar in the two systems.
However, as ESCs did not develop into contracting cardiomyocytes in the low volume monolayer system the expression peaks of *Brachyury* and *MesP1* on day 5 of differentiation seem to be favourable for *in vitro* cardiomyogenesis.

Proportion of PI positive cells

The proportions of dead cells in low volume monolayer ESC cultures were measured at different time points of differentiation using FACS analysis.

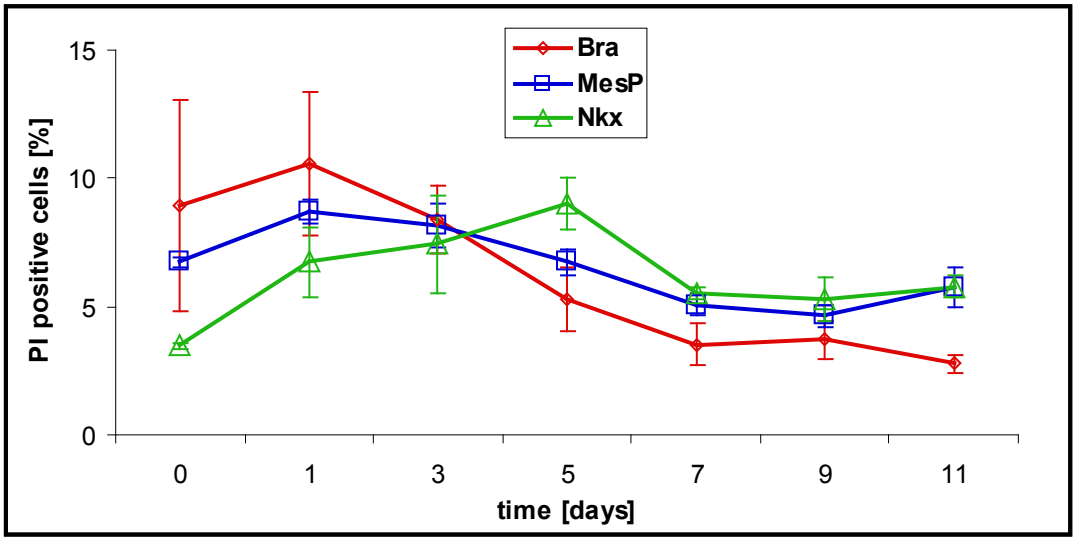

Figure 4.11: Analysis of expression of *Brachyury*, *MesP1* or *Nkx2.5* in **ESCs** at different time points. FACS analyses of Brachyury^{EGFP}, MesP1^{EGFP} and Nkx2.5^{EGFP} reporter ESC lines on days 0-11 of differentiation. Proportion of PI positive (dead) cells in Brachyury^{EGFP} (red line), MesP1^{EGFP} (blue line) and Nkx2.5^{EGFP} (green line) reporter ESC lines seeded on 48-well plates (5x10^4 cells per well) on day 0 of differentiation. Error bars: SD.

As can be seen in figure 4.11 the proportion of PI positive (dead) cells remained rather low during the whole experiment indicating that the increasing cell density in low media volume in the monolayer cell culture system did not lead to increased cell death at the time points analysed and the cell number used in this experiment.

On day 1 of differentiation the proportion of dead cells peaked in ESC Brachyury^{EGFP} and MesP1^{EGFP} reporter cell lines which was probably the result from the stressful procedures necessary for the establishment of a monolayer cell culture system.

The high variation in the proportion of dead cells indicated by the large error bars in Brachyury^{EGFP} and Nkx2.5^{EGFP} reporter cell lines at certain time points could be explained by differences in trypsinisation times or in other handling procedures during the experiment.

4.2.2 *Brachyury*^{EGFP}, *MesP1*^{EGFP} and *Nkx2.5*^{EGFP} expression in cardiovascular progenitor reporter cell lines at different time points of differentiation

In differentiating CVPCs in low volume monolayer cell culture, *Brachyury*^{EGFP}, *MesP1*^{EGFP} and *Nkx2.5*^{EGFP} expression patterns were analysed over time. Additionally, the proportion of dead cells was detected at different time points of differentiation.

Proportion of *Brachyury*^{EGFP}, *MesP1*^{EGFP} and *Nkx2.5*^{EGFP} expressing cells

In low volume monolayer CVPC culture, we also investigated the percentages of *Brachyury*^{EGFP}, *MesP1*^{EGFP} and *Nkx2.5*^{EGFP} expressing cells over time.

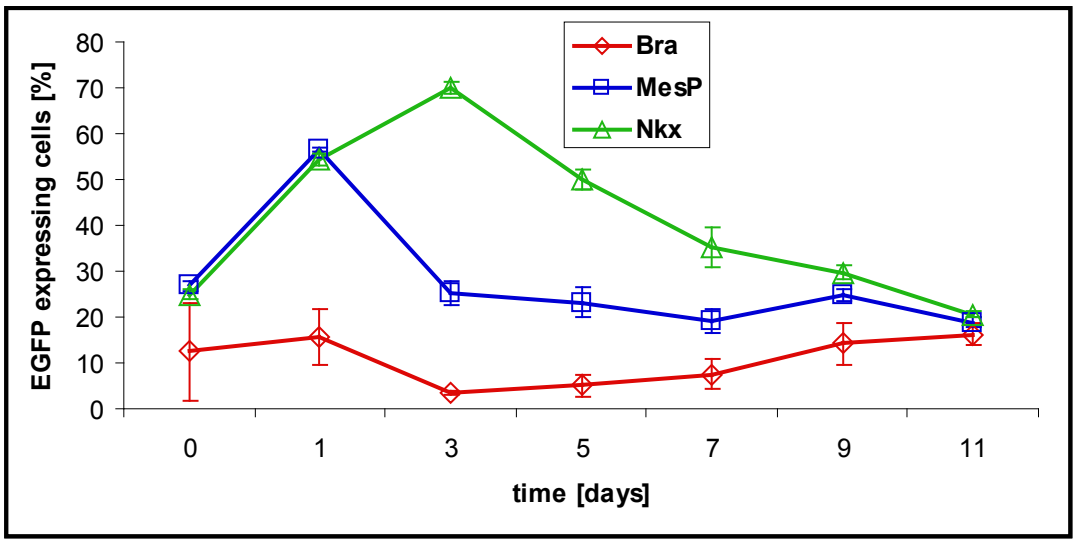

Figure 4.12: Analysis of expression of *Brachyury*, *MesP1* or *Nkx2.5* in **CVPCs** at different time points. FACS analyses of Brachyury^{EGFP}, MesP1^{EGFP} and Nkx2.5^{EGFP} reporter CVPC lines on different time points of differentiation. Proportion of CVPCs expressing *Brachyury*^{EGFP} (red line), *MesP1*^{EGFP} (blue line) and *Nkx2.5*^{EGFP} (green line) seeded on 48-well plates (5x10^4 cells per well) on day 0 of differentiation. Data for *Brachyury*^{EGFP} expression obtained from three independent experiments and nine samples in total. Error bars: SD.

As can be seen in figure 4.12 the proportion of *Brachyury*^{EGFP} expressing CVPCs remained constant between day 0 and 1 of differentiation followed by a decrease on day 3. From day 5 on the proportion of *Brachyury*^{EGFP} expressing cells rose steadily until the last experimental time point.

A distinct peak of *MesP1*^{EGFP} expressing CVPCs was observed on day 1 of differentiation. The percentage of *MesP1*^{EGFP} expressing cells was then declining.

The proportion of Nkx2.5^{EGFP} expressing CVPCs peaked on day 3 of differentiation and was steadily decreasing afterwards.
Brachyury^{EGFP} expression was lowest on most time points compared to *MesP1*^{EGFP} and *Nkx2.5*^{EGFP} expression in CVPCs while *Nkx2.5*^{EGFP} expression was highest between days 3 and 7 of differentiation.

Next, we compared the proportions of Brachyury^{EGFP}, MesP1^{EGFP} and Nkx2.5^{EGFP} expressing cells at different time points of differentiation between monolayer CVPC culture and CVPC hanging drop culture.

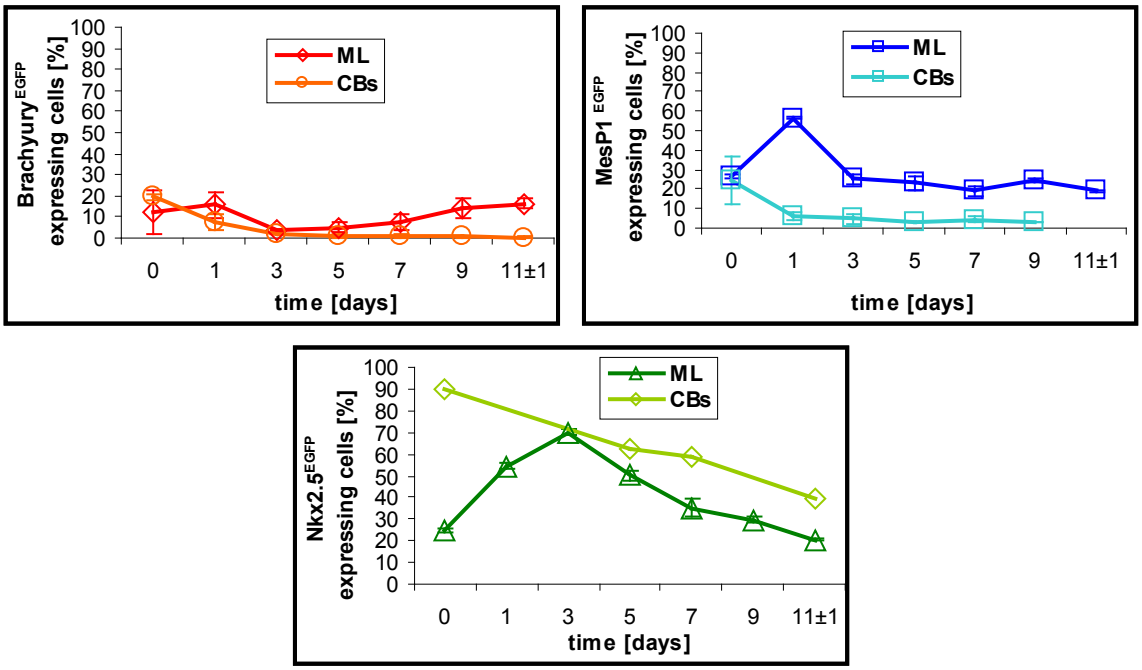

Figure 4.13: Analysis of expression of *Brachyury* (upper left panel), *MesP1* (upper right panel) or *Nkx2.5* (lower panel) in **CVPCs** at different time points. Comparison between monolayer cell culture and the CB system. FACS analyses of Brachyury^{EGFP}, MesP1^{EGFP} and Nkx2.5^{EGFP} reporter CVPC lines on different time points of differentiation. Proportion of CVPCs expressing *Brachyury*^{EGFP}, *MesP1*^{EGFP} and *Nkx2.5*^{EGFP} either seeded on 48-well plates (5x10^4 cells per well) or placed into hanging drop cell culture on day 0 of differentiation. Error bars: SD. Data for *Brachyury*^{EGFP} expression obtained from three independent experiments and nine samples in total. Data for CBs of Brachyury^{EGFP} and MesP1^{EGFP} reporter cell lines or the Nkx2.5^{EGFP} reporter cell line were produced by Lucia Leitner or Diana Walder, respectively, in the course of their diploma theses (Leitner, 2013; Walder, 2011). ML: monolayer cell culture.

In contrast to our experiments in low volume monolayer cell culture a constant decrease in the proportion of *Brachyury*^{EGFP}, *MesP1*^{EGFP} and *Nkx2.5*^{EGFP} expressing cells was detected in previous experiments using CBs as shown in figure 4.13. Proportions of *Brachyury*^{EGFP}

expressing cells were lower, proportions of *MesP1*^{EGFP} expressing cells much lower and proportions of *Nkx2.5*^{EGFP} expressing cells were higher in CBs.
Similar to ESCs no beating cardiomyocytes could be observed in low monolayer CVPC culture indicating that the expression profile of *Brachyury*, *MesP1* and *Nkx2.5* observed in monolayer cell culture did not accurately copy the *in vivo* situation.

Mean *Brachyury*^{EGFP}, *MesP1*^{EGFP} and *Nkx2.5*^{EGFP} intensity

We determined the mean intensity of *Brachyury*^{EGFP}, *MesP1*^{EGFP} and *Nkx2.5*^{EGFP} expression in monolayer CVPC culture at different time points of differentiation using flow cytometry.

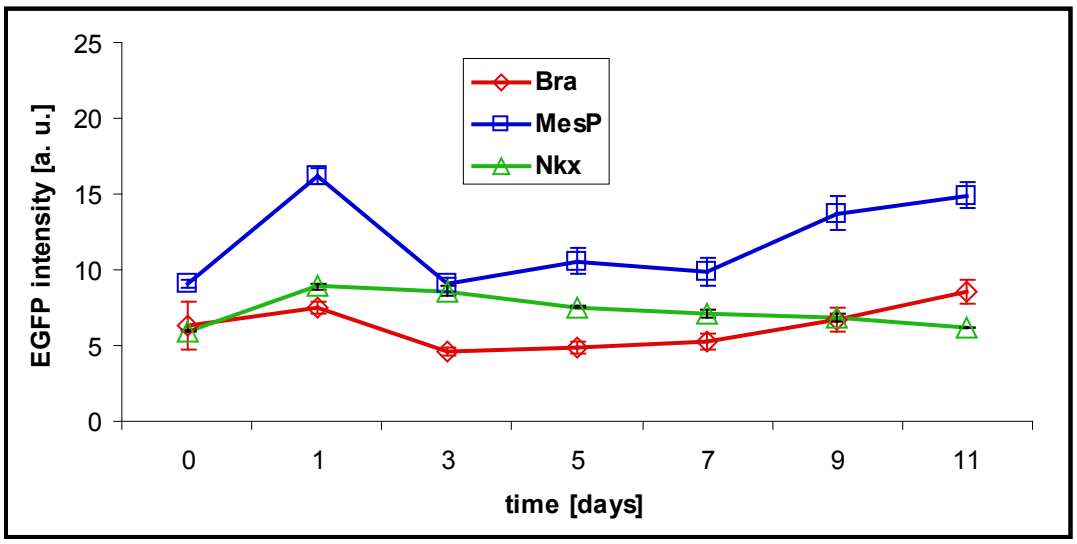

Figure 4.14: Analysis of expression of *Brachyury*, *MesP1* or *Nkx2.5* in **CVPCs** at different time points. FACS analyses of Brachyury^{EGFP}, MesP1^{EGFP} and Nkx2.5^{EGFP} reporter CVPC lines on different time points of differentiation. Mean intensity of *Brachyury*^{EGFP} (red line), *MesP1*^{EGFP} (blue line) or *Nkx2.5*^{EGFP} (green line) expression in CVPCs seeded on 48-well plates (5x10^4 cells per well) on day 0 of differentiation. Data for *Brachyury*^{EGFP} expression obtained from three independent experiments and nine samples in total. Error bars: SD.

Figure 4.14 shows that mean intensities of *Brachyury*^{EGFP} and *MesP1*^{EGFP} expression peaked on day 1 of differentiation probably in response to the trypsinisation stress of the previous day and rose again after day 3 of differentiation. *Nkx2.5*^{EGFP} expression levels did not change to a great extent during the experiment.
Brachyury^{EGFP}, *MesP1*^{EGFP} and *Nkx2.5*^{EGFP} expression levels were rather similar but on days 1, 9 and 11 of differentiation the mean intensity of *MesP1*^{EGFP} expression clearly exceeded those of *Brachyury*^{EGFP} and *Nkx2.5*^{EGFP} expression.

The difference of *Brachyury*^{EGFP} and *MesP1*^{EGFP} expression between monolayer CVPC culture and CBs was also evaluated.

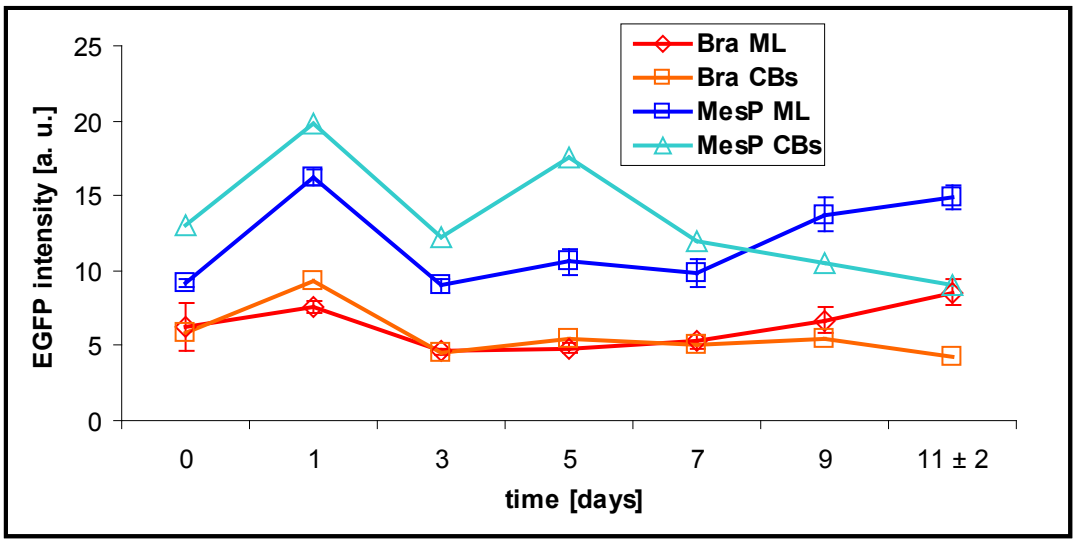

Figure 4.15: Analysis of expression of *Brachyury* or *MesP1* in **CVPCs** at different time points. Comparison between monolayer cell culture and the CB system. FACS analyses of Brachyury^{EGFP} and MesP1^{EGFP} reporter CVPC lines on different time points of differentiation. Mean intensity of *Brachyury*^{EGFP} or *MesP1*^{EGFP} expression in CVPCs either seeded on 48-well plates ($5x10^4$ cells per well) or placed into hanging drop cell culture on day 0 of differentiation. Data for *Brachyury*^{EGFP} expression obtained from three independent experiments and nine samples in total. Data for CBs was produced by Lucia Leitner in the course of her diploma thesis (Leitner, 2013). Error bars: SD. ML: Monolayer cell culture.

Similar to low volume monolayer cell culture a peak of the mean intensity of *Brachyury*^{EGFP} and *MesP1*^{EGFP} expression on day 1 of differentiation could also be observed in former experiments with CBs as shown in figure 4.15 which might be a result of stress during the establishment of the hanging drop culture system. After day 3 of differentiation the mean intensity of *Brachyury*^{EGFP} expression stayed relatively stable in CBs and in monolayer cell culture but at later time points of differentiation it dropped in CBs while it rose in the monolayer system.

The mean intensity of *MesP1*^{EGFP} expression peaked on day 5 of differentiation exclusively in CBs and was then decreasing while it increased in the monolayer system starting from day 7 of differentiation.

The mean intensity levels *Brachyury*^{EGFP} expression were similar between CBs and CVPCs in monolayer cell culture whereas the mean intensity levels of *MesP1*^{EGFP} expression were higher in CBs except for later time points of differentiation.

Both *Brachyury*^{EGFP} and MesP1^{EGFP} expression increased at later time points of differentiation in low volume monolayer CVPC culture (Figures 4.12 and 4.14) which might indicate that CVPCs start differentiation at varying time points in this system but that this differentiation is arrested at a certain time.

Proportion of PI positive cells

The proportions of PI positive cells in low volume monolayer CVPC culture were determined at different time points of differentiation using flow cytometry.

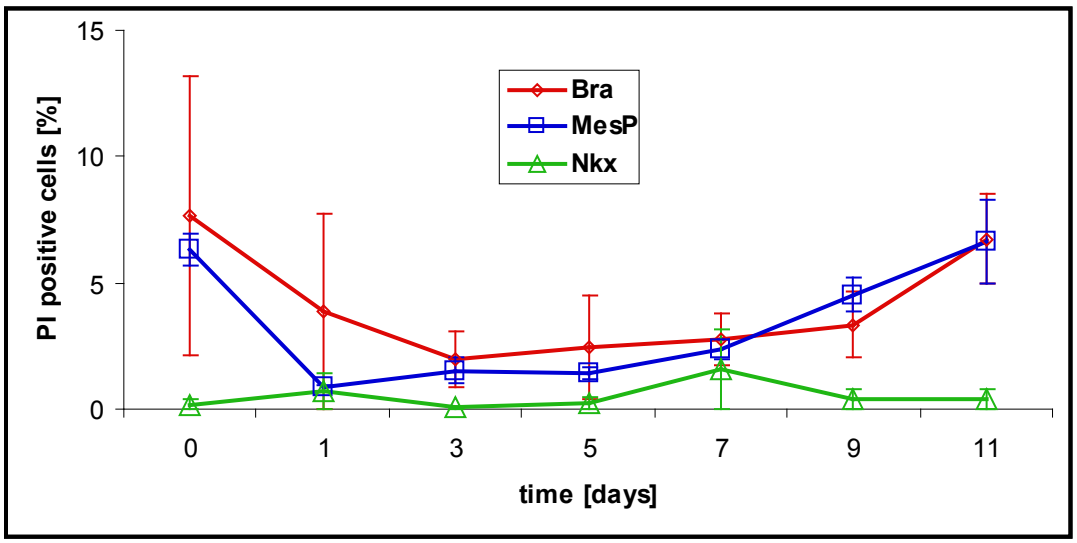

Figure 4.16: Analysis of expression of *Brachyury*, *MesP1* or *Nkx2.5* in **CVPCs** at different time points. FACS analyses of Brachyury^{EGFP}, MesP1^{EGFP} and Nkx2.5^{EGFP} reporter CVPC lines on days 0-11 of differentiation. Proportion of PI positive (dead) cells in Brachyury^{EGFP} (red line), MesP1^{EGFP} (blue line) and Nkx2.5^{EGFP} (green line) reporter CVPC lines seeded on 48-well plates ($5x10^4$ cells per well) on day 0 of differentiation. Error bars: SD.

Generally the proportion of PI positive cells remained rather low throughout the whole experiment as depicted in figure 4.16.

The proportion of PI positive cells was already highest on day 0 of differentiation in CVPC Brachyury^{EGFP} and MesP1^{EGFP} reporter cell lines probably caused by harsh handling of the cells. Due to increasing cell density the number of dead Brachyury^{EGFP} and MesP1^{EGFP} cells rose again at later time points.

The inverse peak of the proportion of PI positive cells in the MesP1^{EGFP} reporter cell line on day 1 of differentiation correlated with a peak in *MesP1*^{EGFP} expression on that time point.

The number of dead Nkx2.5^{EGFP} cells remained surprisingly low during the whole experiment.

There was quite large variation in the proportion of dead cells indicated by the large error bars between the individual samples in the CVPC Brachyury^{EGFP} reporter cell line which could be explained by the fact that the data for this cell line was produced in three individual experiments where unintended differences in the handling of the cells could have occurred.

4.2.3 Comparison between cardiovascular progenitor and embryonic stem cells

Brachyury^{EGFP} expression peaked on day 1 of differentiation in ESCs and CVPCs. While *Brachyury^{EGFP}* expression was declining starting from day 1 in ESCs it was increasing between day 3 and 11 of differentiation in CVPCs as depicted in figure 4.17.

Both cell types showed an aberrant *Brachyury^{EGFP}* expression pattern in low volume monolayer cell culture as *Brachyury^{EGFP}* expression had been previously shown to peak on day 5 in EBs and to be constantly decreasing in CBs. Thus, *Brachyury* expression levels might decrease too early in low volume monolayer ESC culture and might increase inappropriately in low volume monolayer CVPC culture which could lead to a blockage of cardiomyogenesis. The proportion of *Brachyury^{EGFP}* expressing cells was higher in ESCs than in CVPCs at most time points.

Mean intensity levels of *Brachyury^{EGFP}* expression did not differ greatly between ESCs and CVPCs at most time points but were lower in ESCs at later differentiation time points.

These findings also indicate that, at later time points of differentiation, *Brachyury* expression might be too high for correct development of contracting cardiomyocytes in low volume monolayer CVPC culture.

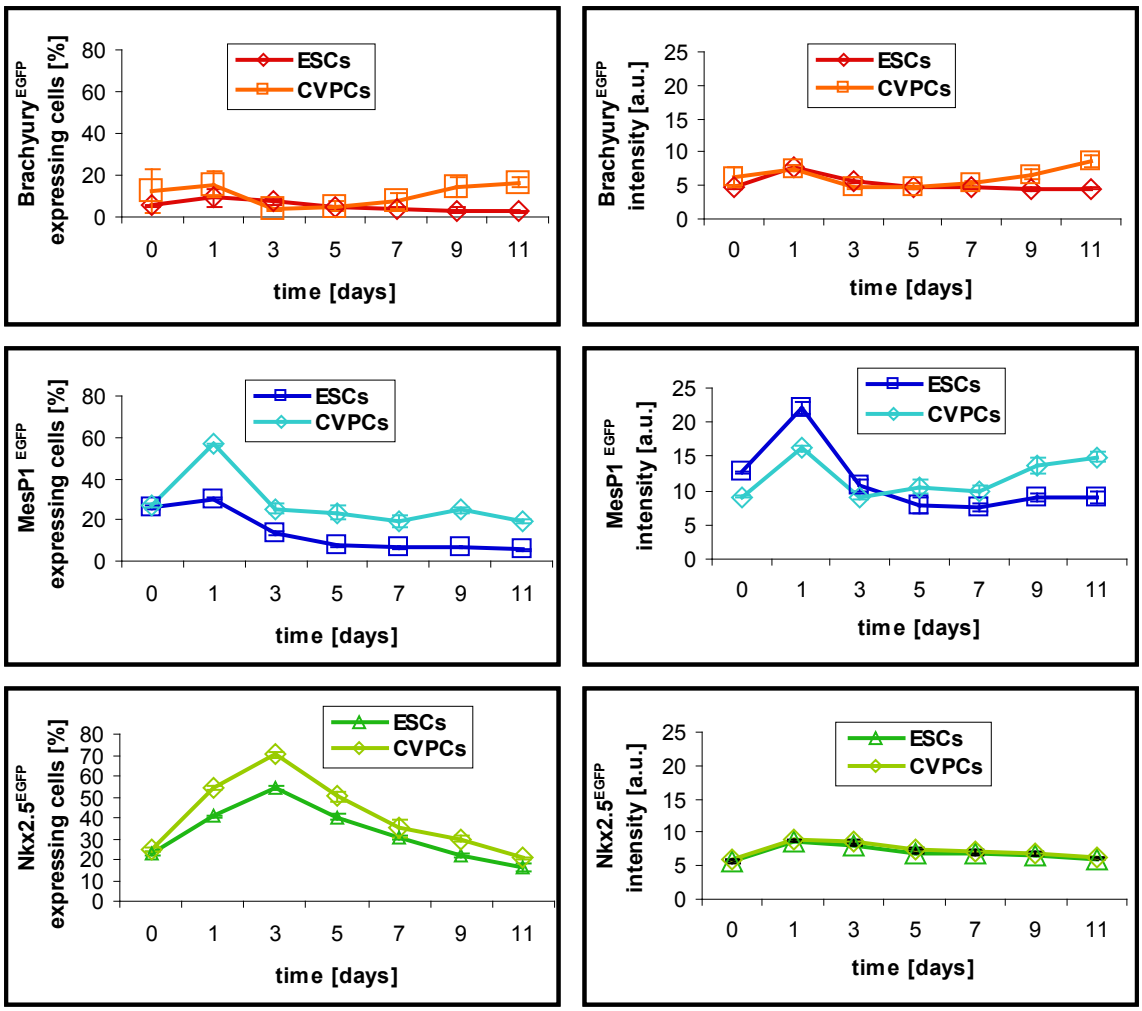

Figure 4.17: Analysis of expression of *Brachyury* (upper panels), *MesP1* (middle panels) or *Nkx2.5* (lower panels) in **ESCs and CVPCs** at different time points. FACS analyses of Brachyury^{EGFP}, MesP1^{EGFP} and Nkx2.5^{EGFP} reporter ESC and CVPC lines on day 0-11 of differentiation. Proportion of ESCs and CVPCs expressing Brachyury^{EGFP}, MesP1^{EGFP} and Nkx2.5^{EGFP} (left panels) and mean intensity of Brachyury^{EGFP}, MesP1^{EGFP} or Nkx2.5^{EGFP} expression in ESCs and CVPCs (right panels) seeded on 48-well plates ($5x10^4$ cells per well) on day 0 of differentiation. Data for *Brachyury^{EGFP}* expression in ESCs and CVPCs obtained from two independent experiments and six samples in total and from three independent experiments and nine samples in total, respectively. Error bars: SD.

As shown in figure 4.17 a peak of *MesP1^{EGFP}* expression could be observed on day 1 of differentiation in ESCs and CVPCs.

In both, ESCs and CVPCs, the proportion of *MesP1^{EGFP}* expressing cells was decreasing after day 1 of differentiation. However, the mean intensity of *MesP1^{EGFP}* expression was decreasing in ESCs after day 1 of differentiation while it rose between day 3 and 11 of differentiation in CVPCs. *MesP1^{EGFP}* expression levels were lower in differentiating ESCs than in differentiating CVPCs at most time points.

MesP1^{EGFP} expression did not peak on day 5 of differentiation in neither ESCs nor in CVPCs in low volume monolayer cell culture as it had been observed in EBs and CBs. Additionally, *MesP1*^{EGFP} expression was increasing at later time points of differentiation in CVPCs in monolayer cell culture while it was decreasing in CBs. Therefore, the *MesP1* expression pattern in monolayer cell culture of both ESCs and CVPCs was not appropriate for successful cardiomyogenesis.

The proportion of *Nkx2.5*^{EGFP} expressing cells peaked on day 3 of differentiation in ESCs and CVPCs as can be seen in figure 4.17. The mean intensity of *Nkx2.5*^{EGFP} expression rose between day 1 and 0 of differentiation and then stayed rather constant in both cell types suggesting that mature cardiomyocytes do not form as this would probably be accompanied by an up-regulation of *Nkx2.5* expression in these cells.

The intensity levels of *Nkx2.5*^{EGFP} expression were similar in ESCs and CVPCs but the proportion of *Nkx2.5*^{EGFP} expressing cells was lower in ESCs at most time points.

In CBs the proportion of *Nkx2.5*^{EGFP} expressing cells was constantly decreasing while it was increasing between day 0 and 3 of differentiation in low volume monolayer CVPC culture. Furthermore, a smaller number of CVPCs was expressing *Nkx2.5*^{EGFP} in monolayer cell culture compared to CBs. These observations might indicate that differentiation into contracting cardiomyocytes fails to advance in CVPCs in low volume monolayer cell culture.

In none of the cell lines any contracting cardiomyocytes were found in low volume monolayer cell culture.

4.3 Effects of CHIR99021 and α-SPARC on expression of *Brachyury*

As SPARC treatment did not influence the expression of *Brachyury*^{EGFP} in low volume monolayer cell culture we wanted to test whether its inhibitor, α-SPARC, had an effect on *Brachyury*^{EGFP} expression in ESCs and CVPCs under these conditions. α-SPARC had been shown to decrease the number of developing contracting cardiomyocytes in EBs and CBs (Gottschamel, 2010; Stary et al., 2005).

We were also interested in the influence of constantly active Wnt signalling on *Brachyury*^{EGFP} expression and whether it might have a positive effect on the development of contracting cardiomyocytes in ESCs and CVPCs in low volume monolayer cell culture. For that purpose we used CHIR99021, a GSK-3β inhibitor and therefore an activator of Wnt signalling.

In our group CHIR treatment was previously shown to enhance the expression of *Brachyury* in EBs and of *MesP1* in EBs and CBs but to inhibit the formation of contracting

cardiomyocytes in CBs (Leitner, 2013). Still, we also wanted to test whether CHIR treatment had a positive effect on the development of beating cardiomyocytes in low volume monolayer cell culture.

Brachyury^{EGFP} ESCs and CVPCs were separated from feeder cells and 5x10^4 cells per well were placed on a gelatinised 48-well cell culture plate. Cells were either treated with 2.5 µM CHIR99021 or α-SPARC diluted 1:100 throughout the whole experiment or left untreated. The proportion of *Brachyury^{EGFP}* expressing and PI positive cells as well as the mean intensity of *Brachyury^{EGFP}* expression were determined with FACS analysis on days 0 (undifferentiated), 1, 3, 5, 6, 7, 9 and 11 of differentiation.

The experiment was repeated once for untreated ESCs and twice for untreated CVPCs, partly during the experiment described in section 4.2. Each sample was analysed in triplicate.

4.3.1 Influence of CHIR99021 and α-SPARC on *Brachyury^{EGFP}* expression in embryonic stem cell reporter line

We investigated the effects of α-SPARC and CHIR treatment on *Brachyury^{EGFP}* expression in differentiating ESCs in low volume monolayer cell culture measuring the proportion of *Brachyury^{EGFP}* expressing cells and the mean intensity of *Brachyury^{EGFP}* expression. The proportion of dead cells after α-SPARC or CHIR treatment were also analysed at different time points.

Proportion of *Brachyury^{EGFP}* expressing cells

ESCs in low volume monolayer culture were treated with α-SPARC for 0-11 days and the proportions of *Brachyury^{EGFP}* expressing cells were evaluated at different time points of differentiation using FACS analysis.

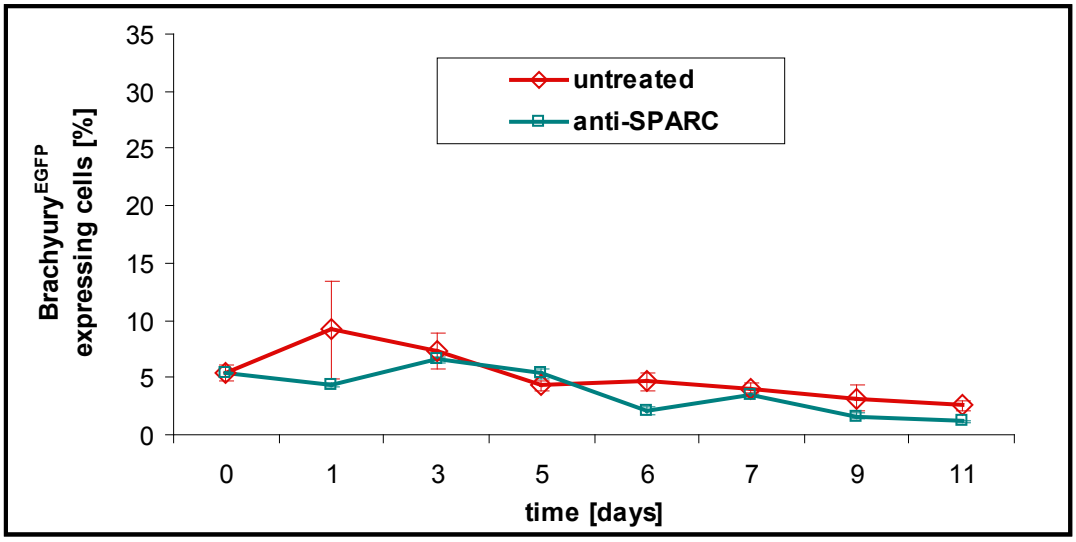

Figure 4.18: Effects of α-SPARC on *Brachyury* expression in **ESCs** on different differentiation time points. FACS analyses of Brachyury^{EGFP} reporter ESC line on days 0–11 of differentiation after treatment with α-SPARC dil. 1:100 for 0-11 days. Proportion of untreated (red line) or α-SPARC treated (blue line) ESCs expressing *Brachyury*^{EGFP} seeded on 48-well plates ($5x10^4$ cells per well) on day 0 of differentiation. Data for *Brachyury*^{EGFP} expression in untreated cells obtained from two independent experiments and six samples in total. Error bars: SD.

As depicted in figure 4.18, α-SPARC treatment showed no effect on the proportion of *Brachyury*^{EGFP} expressing ESCs in low volume monolayer cell culture. The proportion of *Brachyury*^{EGFP} expressing cells was decreasing starting from day 3 of differentiation in α-SPARC treated differentiating ESCs.

We also assessed the influence of CHIR treatment on the proportion of *Brachyury*^{EGFP} expressing cells in monolayer ESC culture on several time points of differentiation and compared it to the effects of CHIR on the same parameters in EBs.

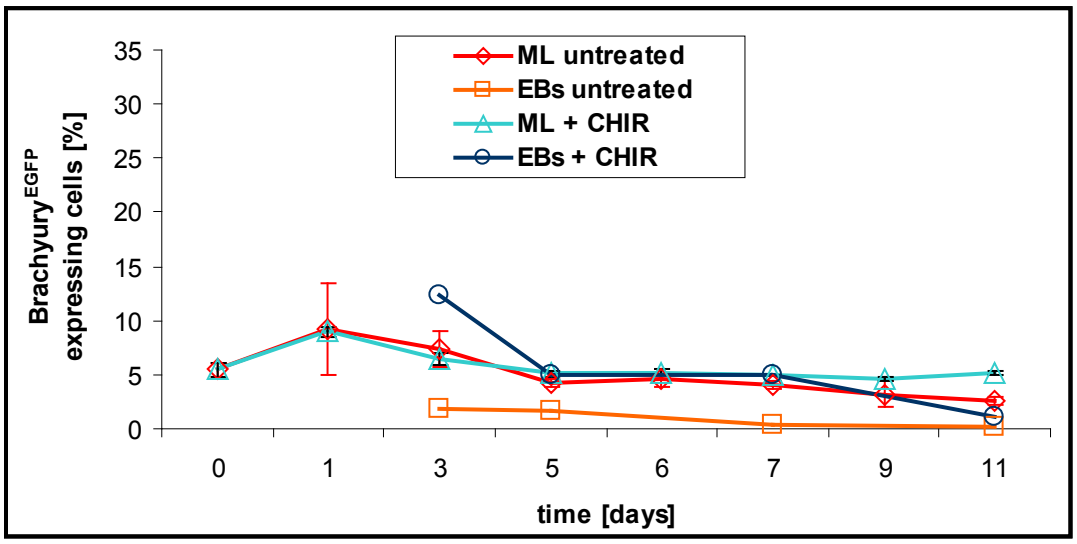

Figure 4.19: Effects of CHIR99021 on *Brachyury* expression in **ESCs** on different differentiation time points. Comparison between monolayer cell culture and the EB system. FACS analyses of Brachyury^{EGFP} reporter ESC line on days 0–11 of differentiation after treatment with 2.5 µM CHIR99021 for 0-11 days. Proportion of untreated or CHIR99021 treated ESCs expressing *Brachyury*^{EGFP} either seeded on 48-well plates (5x10^4 cells per well) or placed into hanging drop cell culture on day 0 of differentiation. Data for *Brachyury*^{EGFP} expression in untreated cells obtained from two independent experiments and six samples in total. Data for EBs was produced by Lucia Leitner in the course of her diploma thesis (Leitner, 2013). Error bars: SD. ML: monolayer cell culture.

Figure 4.19 shows that CHIR treatment did not influence the proportion of *Brachyury*^{EGFP} expressing ESCs in low volume monolayer cell culture. The proportion of *Brachyury*^{EGFP} expressing cells was declining starting from day 1 of differentiation in untreated cells and starting from day 3 of differentiation in CHIR treated cells.

In former experiments using EBs CHIR treatment led to an increase in the proportion of *Brachyury*^{EGFP} expressing ESCs on days 3, 5 and 7 of differentiation compared to untreated cells having the largest effect on day 3 which is the only time point where a small increase in the proportion of *Brachyury*^{EGFP} expressing ESCs could be observed in monolayer cell culture as demonstrated in figure 4.19.

ESCs seem to be more sensitive to external stimuli in the hanging drop cell culture system than in the monolayer cell culture system.

Again, no contracting cardiomyocytes could be detected in low volume monolayer cell culture under these conditions which did not seem to favour cardiomyogenesis.

Mean *Brachyury*^{EGFP} intensity

The effect of α-SPARC and CHIR treatment on the mean intensity of *Brachyury*^{EGFP} expression in differentiating ESCs in low volume monolayer cell culture was determined at different time points using flow cytometry.

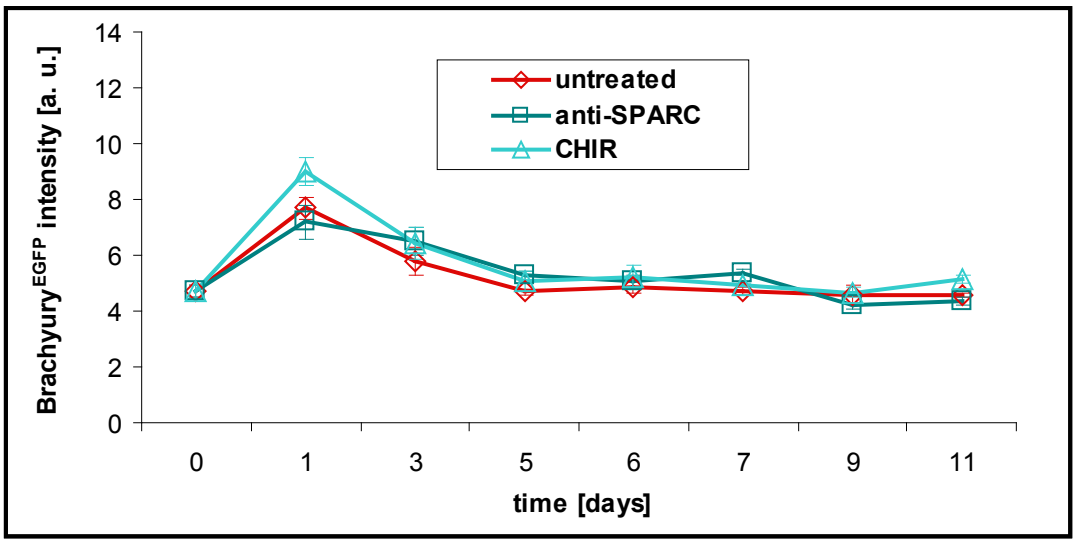

Figure 4.20: Effects of CHIR99021 or α-SPARC on *Brachyury* expression in **ESCs** on different differentiation time points. FACS analyses of Brachyury^{EGFP} reporter ESC line on days 0–11 of differentiation after treatment with 2.5 µM CHIR99021 or α-SPARC dil. 1:100 for 0-11 days. Mean intensity of *Brachyury*^{EGFP} expression in untreated (red line), α-SPARC (blue line) or CHIR99021 (light blue line) treated ESCs seeded on 48-well plates (5x10^4 cells per well) on day 0 of differentiation. Data for *Brachyury*^{EGFP} expression in untreated cells obtained from two independent experiments and six samples in total. Error bars: SD.

CHIR99021 and α-SPARC did not influence the intensity of *Brachyury*^{EGFP} expression in ESCs in low volume monolayer cell culture as can be seen in figure 4.20. The intensity of *Brachyury*^{EGFP} expression was declining between day 1 and 5 of differentiation and then stayed rather constant under all tested conditions.

Proportion of PI positive cells

The proportion of dead cells in ESC low volume monolayer culture after α-SPARC and CHIR treatment was measured at different time points of differentiation.

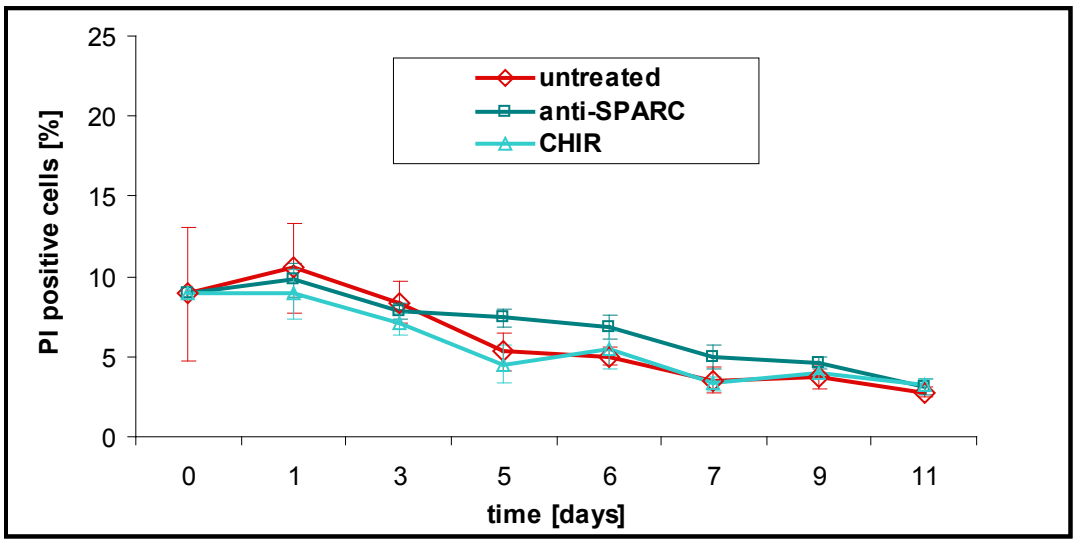

Figure 4.21: Effects of CHIR99021 or α-SPARC on *Brachyury* expression in **ESCs** on different differentiation time points. FACS analyses of Brachyury^{EGFP} reporter ESC line on days 0–11 of differentiation after treatment with 2.5 µM CHIR99021 or α-SPARC dil. 1:100 for 0-11 days. Proportion of PI positive (dead) cells in untreated (red line), α-SPARC (blue line) or CHIR99021 (light blue line) treated ESCs seeded on 48-well plates (5x10^4 cells per well) on day 0 of differentiation. Error bars: SD.

As depicted in figure 4.21 the proportions of PI positive cells were quite similar between untreated, CHIR99021 and α-SPARC treated cells indicating that neither CHIR99021 nor α-SPARC had a toxic effect on the cells.
Untreated Brachyury^{EGFP} ESC samples varied greatly in the proportion of dead cells on the first few time points which might have been due to differences in cell handling during the two separate experiments.

4.3.2 Influence of CHIR99021 and α-SPARC on *Brachyury^{EGFP}* expression in cardiovascular progenitor reporter line

We determined the effects of α-SPARC and CHIR treatment on *Brachyury^{EGFP}* expression as well as on cell death in differentiating CVPCs in low volume monolayer cell culture.

Proportion of *Brachyury^{EGFP}* expressing cells

The proportion of *Brachyury^{EGFP}* expressing cells after α-SPARC treatment for 0-11 days was evaluated in differentiating CVPCs in monolayer culture at different time points using FACS analysis.

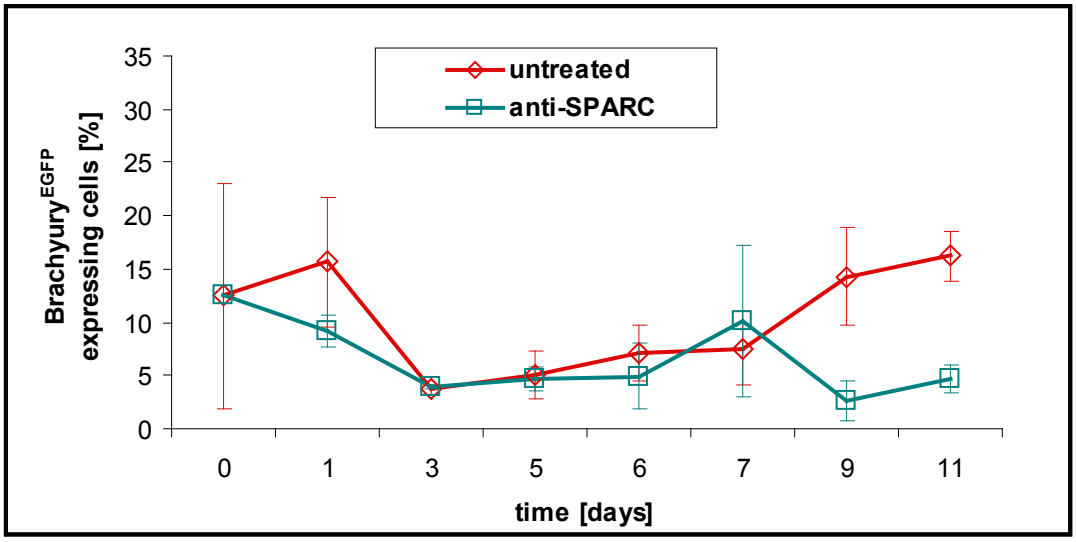

Figure 4.22: Effects α-SPARC on *Brachyury* expression in **CVPCs** on different differentiation time points. FACS analyses of Brachyury^{EGFP} reporter CVPC line on days 0–11 of differentiation after treatment with 2.5 µM CHIR99021 or α-SPARC dil. 1:100 for 0-11 days. Proportion of untreated (red line) or α-SPARC (blue line) CVPCs expressing *Brachyury*^{EGFP} seeded on 48-well plates (5x10^4 cells per well) on day 0 of differentiation. Data for *Brachyury*^{EGFP} expression in untreated cells obtained from three independent experiments and nine samples in total. Error bars: SD.

As shown in figure 4.22 the proportion of *Brachyury*^{EGFP} expressing differentiating CVPCs was only reduced on days 9 and 11 of differentiation upon α-SPARC treatment indicating that this treatment only becomes effective after 7 to 9 days in CVPCs. A decrease of the proportion of *Brachyury*^{EGFP} expressing cells at early time points of differentiation followed by an increase could be observed in both untreated and α-SPARC treated cells but the proportion of *Brachyury*^{EGFP} expressing cells declined again at later time points in α-SPARC treated cells.

Differentiating CVPCs in low volume monolayer culture were also treated with CHIR for 0-11 days and the proportion of *Brachyury*^{EGFP} expressing cells were assessed following this treatment at different time points of differentiation. This data was compared to the proportion of Brachyury^{EGFP} expressing cells in CHIR treated CBs.

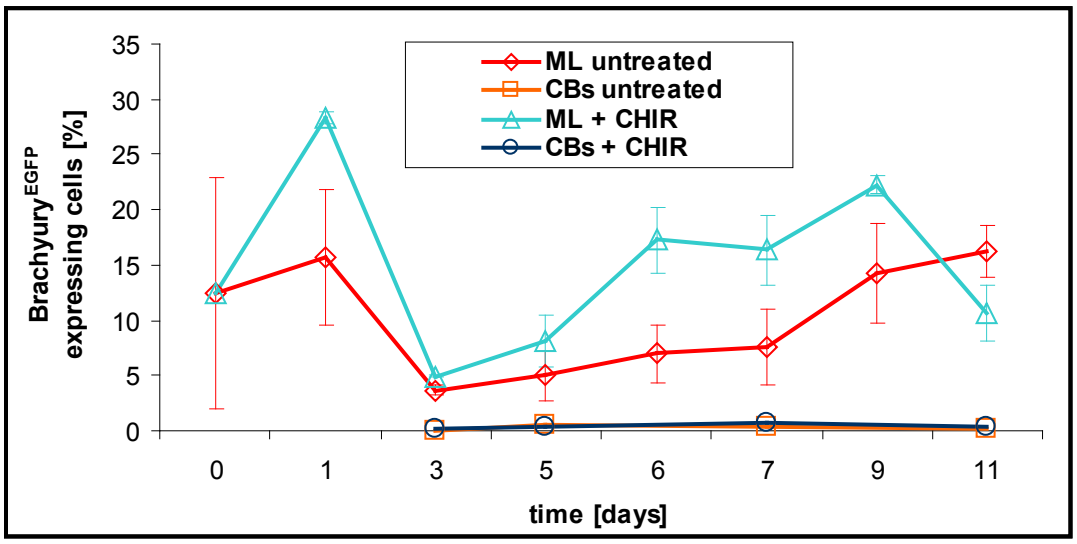

Figure 4.23: Effects of CHIR99021 on *Brachyury* expression in **CVPCs** on different differentiation time points. Comparison between monolayer cell culture and the CB system. FACS analyses of Brachyury^{EGFP} reporter CVPC line on days 1–11 of differentiation after treatment with 2.5 µM CHIR99021 for 1-11 days. Proportion of CHIR99021 treated CVPCs expressing Brachyury^{EGFP} either seeded on 48-well plates ($5x10^4$ cells per well) or placed into hanging drop cell culture on day 0 of differentiation. Data for *Brachyury^{EGFP}* expression in untreated cells obtained from three independent experiments and nine samples in total. Data for CBs was produced by Lucia Leitner in the course of her diploma thesis (Leitner, 2013). Error bars: SD. ML: monolayer cell culture.

Figure 4.23 shows that CHIR treatment significantly augmented the proportion of *Brachyury^{EGFP}* expressing CVPCs compared to untreated cells on days 1, 6, 7 and 9 of differentiation and slightly decreased this proportion on day 11 of differentiation.

The proportion of *Brachyury^{EGFP}* expressing CVPCs peaked on day 1 of differentiation and increased again starting from day 3 of differentiation under both conditions. However, at late time points of differentiation the proportion of *Brachyury^{EGFP}* expressing cells was declining upon CHIR treatment which could not be observed in untreated cells.

In CBs CHIR99021 did not affect the proportion of *Brachyury^{EGFP}* expressing CVPCs compared to untreated cells. The proportions of *Brachyury^{EGFP}* expressing CVPCs were much lower in untreated or CHIR treated CBs than in similarly treated CVPCs in monolayer cell culture as demonstrated in figure 4.23.

In contrast to the situation in EBs, CVPCs seem to be less sensitive to CHIR treatment in CBs than in monolayer cell culture. An explanation for this observation could be found in the fact that most differentiating CVPCs in CBs do not express *Brachyury* while a certain proportion of CVPCs in monolayer cell culture show *Brachyury* expression. As the effects of CHIR probably only lie in the enhancement of *Brachyury* expression and not in its

initiation CHIR can only influence cells in an environment where *Brachyury* is already expressed.

Importantly, the cells did not develop into beating cardiomyocytes in low volume monolayer CVPC culture under any condition showing that none of the treatments had a positive effect on cardiomyogenesis.

Mean *Brachyury*^{EGFP} intensity

The mean intensity of *Brachyury*^{EGFP} expression after α-SPARC or CHIR treatment in differentiating CVPCs in monolayer culture was determined at different time points of differentiation.

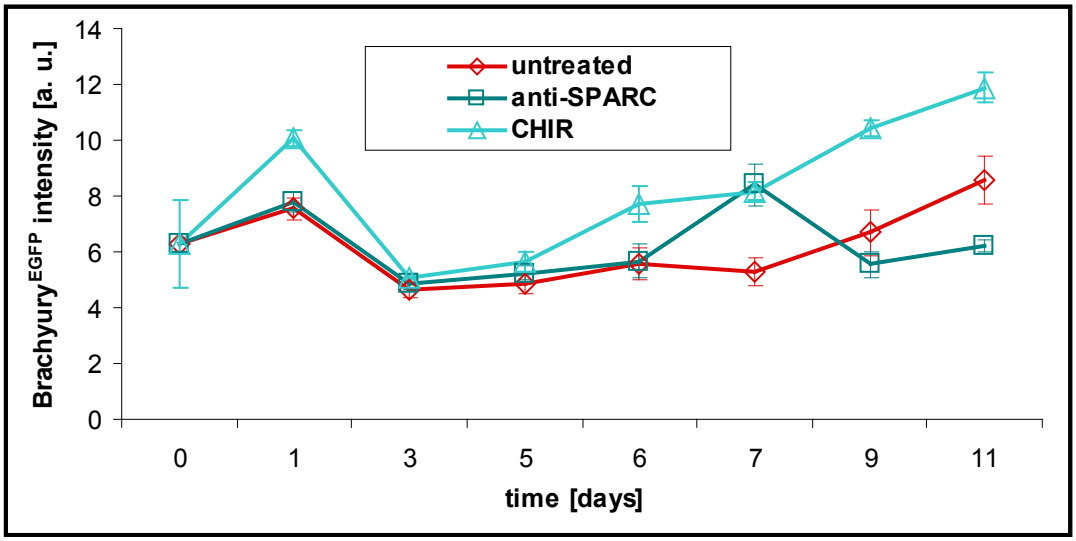

Figure 4.24: Effects of CHIR99021 or α-SPARC on *Brachyury* expression in **CVPCs** on different differentiation time points. FACS analyses of Brachyury^{EGFP} reporter CVPC line on days 0–11 of differentiation after treatment with 2.5 µM CHIR99021 or α-SPARC dil. 1:100 for 0-11 days. Mean intensity of *Brachyury*^{EGFP} expression in untreated (red line), α-SPARC (blue line) or CHIR99021 (light blue line) treated CVPCs seeded on 48-well plates ($5x10^4$ cells per well) on day 0 of differentiation. Data for *Brachyury*^{EGFP} expression in untreated cells obtained from three independent experiments and nine samples in total. Error bars: SD.

CHIR treatment also enhanced the intensity of *Brachyury*^{EGFP} expression in CVPCs in low volume monolayer cell culture at most time points as depicted in figure 4.24.

Interestingly, α-SPARC treatment led to an increase in the intensity levels of *Brachyury*^{EGFP} expression on day 7 of differentiation but again to a decrease on day 11 of differentiation compared to untreated cells.

The mean intensity of *Brachyury*^{EGFP} expression declined between day 1 and 3 of differentiation and increased afterwards under all three conditions but decreased again after day 7 of differentiation in α-SPARC treated cells.

Proportion of PI positive cells

We analysed the proportion of dead cells following α-SPARC or CHIR treatment in CVPC monolayer culture at different time points of differentiation using FACS analysis.

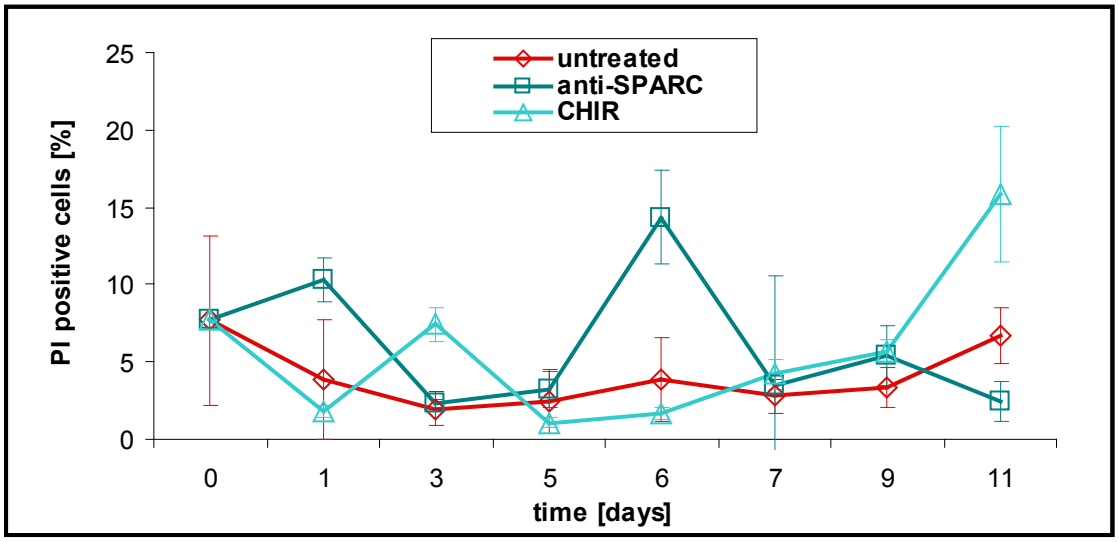

Figure 4.25: Effects of CHIR99021 or α-SPARC on *Brachyury* expression in **CVPCs** on different differentiation time points. FACS analyses of Brachyury^{EGFP} reporter CVPC line on days 0–11 of differentiation after treatment with 2.5 µM CHIR99021 or α-SPARC dil. 1:100 for 0-11 days. Proportion of PI positive (dead) cells in untreated (red line), α-SPARC (blue line) or CHIR99021 (light blue line) treated CVPCs seeded on 48-well plates (5x10^4 cells per well) on day 0 of differentiation. Error bars: SD.

The proportion of dead cells was similar at most time points in the three different tested conditions as can be seen in figure 4.25 demonstrating that CHIR99021 and α-SPARC did not have a cytotoxic effect on CVPCs. However, on day 6 of differentiation the proportion of PI positive cells was significantly higher in α-SPARC treated than in untreated cells. Therefore, the proportion of *Brachyury*^{EGFP} expressing α-SPARC treated CVPCs might have been underestimated on that time point.

4.3.3 Comparison between cardiovascular progenitor and embryonic stem cell Brachyury^{EGFP} reporter cell lines

As shown in figure 4.26, CHIR and α-SPARC treatment influenced the expression of *Brachyury*^{EGFP} only in CVPCs but not in ESCs indicating that in low volume monolayer cell culture CVPCs are more sensitive to effector compounds than ESCs.

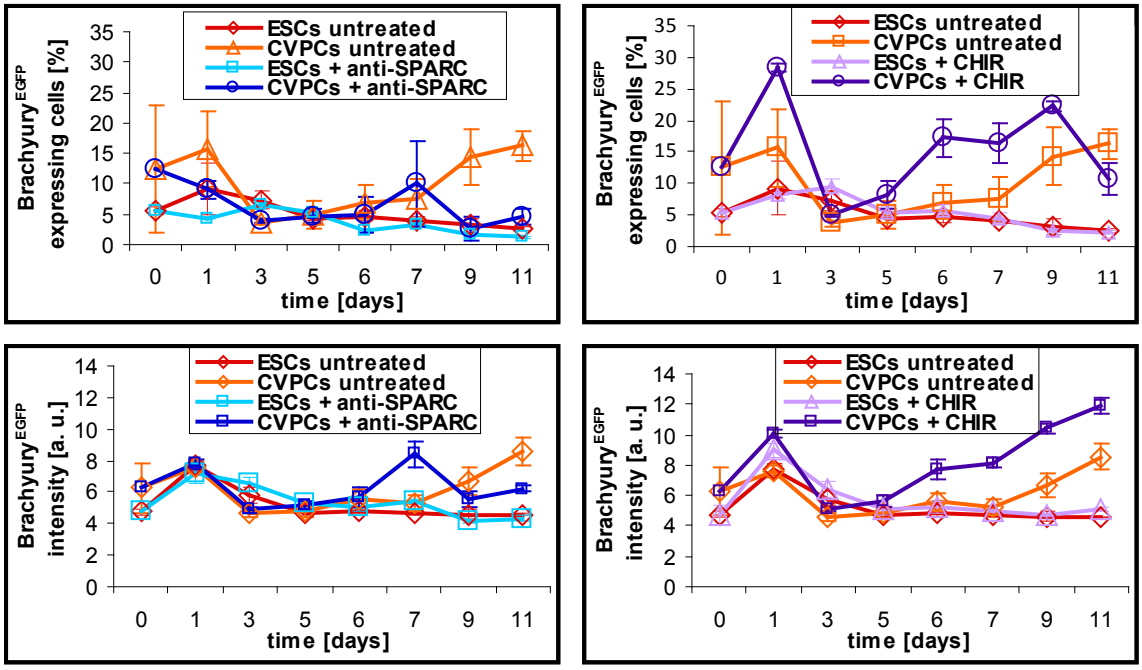

Figure 4.26: Effects of α-SPARC (left panels) or CHIR99021 (right panels) on *Brachyury* expression in **ESCs and CVPCs** on different differentiation time points. FACS analyses of Brachyury^{EGFP} reporter ESC and CVPC line on days 0–11 of differentiation after treatment with 2.5 µM CHIR99021 or α-SPARC dil. 1:100 for 0-11 days. Proportion of *Brachyury*^{EGFP} expressing ESCs and CVPCs (upper panels) and mean intensity of *Brachyury*^{EGFP} expression in ESCs and CVPCs (lower panels) in untreated, α-SPARC or CHIR99021 treated conditions seeded on 48-well plates ($5x10^4$ cells per well) on day 0 of differentiation. Data for *Brachyury*^{EGFP} expression in untreated ESCs and CVPCs obtained from two independent experiments and six samples in total and from three independent experiments and nine samples in total, respectively. Error bars: SD.

The proportion of *Brachyury*^{EGFP} expressing cells was higher in untreated CVPCs than in untreated ESCs at most time points while the mean intensity of *Brachyury*^{EGFP} expression in untreated CVPCs was higher than in untreated ESCs only at later time points of differentiation as depicted in figure 4.26.

In CHIR treated CVPCs both the proportion of *Brachyury*^{EGFP} expressing cells as well the mean intensity of *Brachyury*^{EGFP} expression were enhanced at most time points compared to CHIR treated ESCs.

On day 1 and 7 of differentiation the proportion of *Brachyury*^{EGFP} expressing cells in α-SPARC treated CVPCs exceeded that in α-SPARC treated ESCs while it was similar between the two cell types on the other time points. The mean intensity of *Brachyury*^{EGFP} expression was higher in α-SPARC treated CVPCs than in α-SPARC treated ESCs at later time points of differentiation.

Irrespective of the treatment conditions, *Brachyury*^{EGFP} expression tended to decrease in ESCs starting from day 1 of differentiation and to increase in CVPCs starting from day 3 of differentiation. However, *Brachyury*^{EGFP} expression in α-SPARC treated CVPCs showed the lowest increase compared to differently treated CVPCs and decreased again after day 7 of differentiation. Thus, *Brachyury*^{EGFP} expression patterns in α-SPARC treated CVPCs came closer to those previously found in CBs (cf. Figure 4.23) even though the proportions of *Brachyury*^{EGFP} expressing CVPCs were higher in low volume monolayer cell culture.

However, in both CVPCs and ESCs no beating cardiomyocytes were detected in any of the three conditions tested.

4.4 Impact of cell density on expression of *Brachyury* and *MesP1*

Contracting cardiomyocytes did not form in any of the conditions we had tested so far. As cells form 3D-aggregates in hanging drop culture systems we reasoned that the cells might require a higher cell density in monolayer cell culture to show appropriate expression patterns (cf. Leitner, 2013) and to develop into beating cardiomyocytes.

Therefore, we used 10^5, $5x10^5$ or 10^6 cells per 48-well. ESC and CVPC Brachyury^{EGFP} and MesP1^{EGFP} reporter cell lines were separated from feeder cells and placed on gelatinised 48-well plates at the according cell numbers mentioned above. Please note, that the cell number 10^6 was not used for the CVPC MesP1^{EGFP} reporter cell line.

The proportion of *Brachyury*^{EGFP} and *MesP1*^{EGFP} expressing cells, the mean intensity of *Brachyury*^{EGFP} and *MesP1*^{EGFP} expression and the proportion of PI positive (dead) cells were determined on days 0, 1, 3, 5, 6, 7, 9 and 11 of differentiation using FACS. 10,000 events of each sample were measured and samples were analysed in triplicate except for samples of the MesP1^{EGFP} reporter CVPC line which were only analysed in duplicate.

The data was compared with the results obtained with $5x10^4$ cells per 48-well in the experiment described in section 4.2.

4.4.1 Influence of cell density on *Brachyury*^{EGFP} and *MesP1*^{EGFP} expression in embryonic stem cell reporter lines

Brachyury^{EGFP} and *MesP1*^{EGFP} expression patterns in differentiating ESCs in low volume monolayer cell culture at increasing cell numbers were evaluated over time using flow cytometry. The proportion of dead cells at different cell densities was also determined.

Proportion of *Brachyury*^{EGFP} and *MesP1*^{EGFP} expressing cells

We analysed the percentage of *Brachyury*^{EGFP} expressing cells in ESC monolayer culture at stated cell numbers between days 0 and 11 of differentiation.

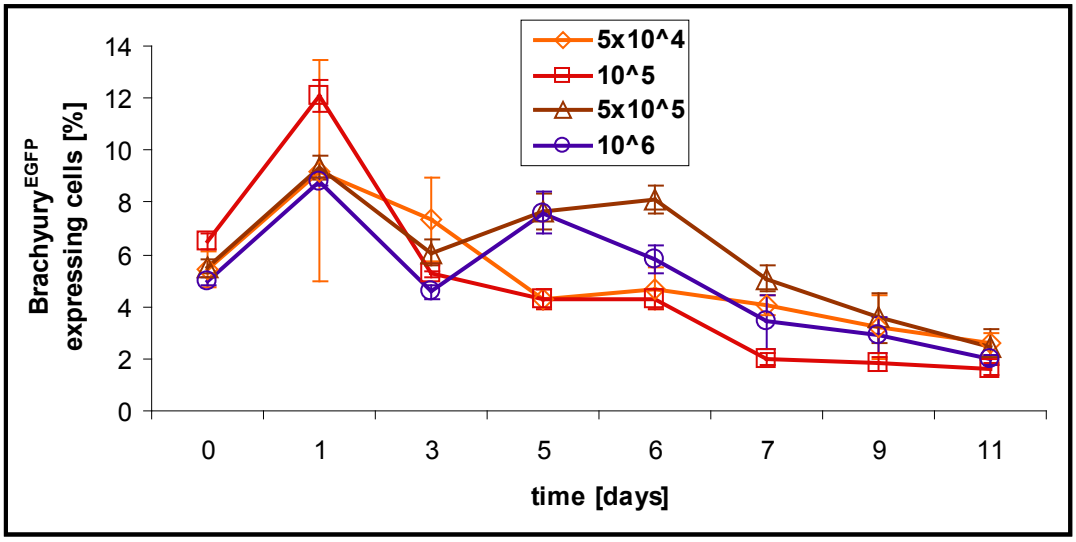

Figure 4.27: Influence of cell density on *Brachyury* expression in **ESCs** on different time points of differentiation. FACS analyses of Brachyury^{EGFP} reporter ESC line on days 0–11 of differentiation. Proportion of ESCs expressing *Brachyury*^{EGFP} seeded on 48-well plates with 5x10^4 (orange line), 10^5 (red line), 5x10^5 (brown line) or 10^6 (purple line) cells per well on day 0 of differentiation. Data for *Brachyury*^{EGFP} expression in ESC samples with 5x10^4 cells obtained from two independent experiments and six samples in total and also described in section 4.2. Error bars: SD.

As depicted in figure 4.27, in low volume monolayer cell culture a peak in the proportion of *Brachyury*^{EGFP} expressing ESCs could be observed at all four tested cell numbers on day 1 of differentiation. In samples of the cell number 5x10^4 and 10^5 the proportion of *Brachyury*^{EGFP} expressing cells was then constantly declining while it peaked on day 5 and 6 in samples of the cell numbers 5x10^5 and 10^6, respectively, before it then decreased as well.

We also assessed the proportion of *MesP1*^{EGFP} expressing cells in ESC monolayer culture at increasing cell numbers at different time points.

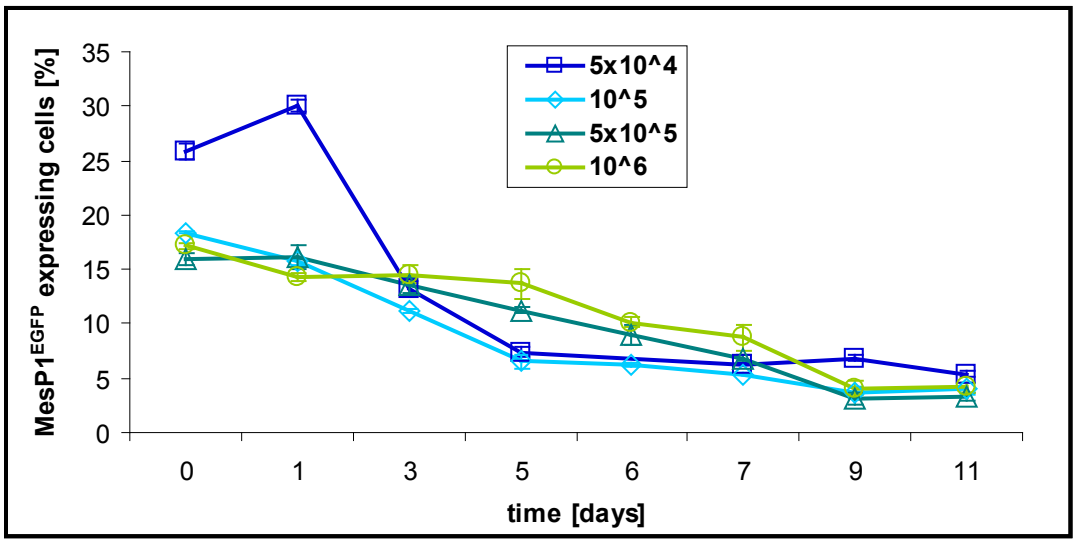

Figure 4.28: Influence of cell density on *MesP1* expression in **ESCs** on different time points of differentiation. FACS analyses of MesP1^{EGFP} reporter ESC line on days 0–11 of differentiation. Proportion of ESCs expressing *MesP1*^{EGFP} seeded on 48-well plates with 5x10^4 (blue line), 10^5 (light blue line), 5x10^5 (turquoise line) or 10^6 (green line) cells per well on day 0 of differentiation. Data for *MesP1*^{EGFP} expression in ESC samples with 5x10^4 cells also described in section 4.2. Error bars: SD.

Figure 4.28 shows that the proportion of *MesP1*^{EGFP} expressing ESCs was decreasing during the whole time course at all cell numbers but at cell number 5x10^4, where it peaked on day 1 of differentiation, in low volume monolayer cell culture.
At most time points the proportion of *MesP1*^{EGFP} expressing ESCs was higher than that of *Brachyury*^{EGFP} expressing ESCs but at later time points of differentiation these proportions were rather similar in low volume monolayer cell culture (Figures 4.27 and 4.28).

Next, we compared the proportion of *Brachyury*^{EGFP} expressing cells between ESC monolayer cell culture and EBs at different time points. The data for monolayer cell culture comprises mean values of the results for cell numbers 10^5 to 10^6.

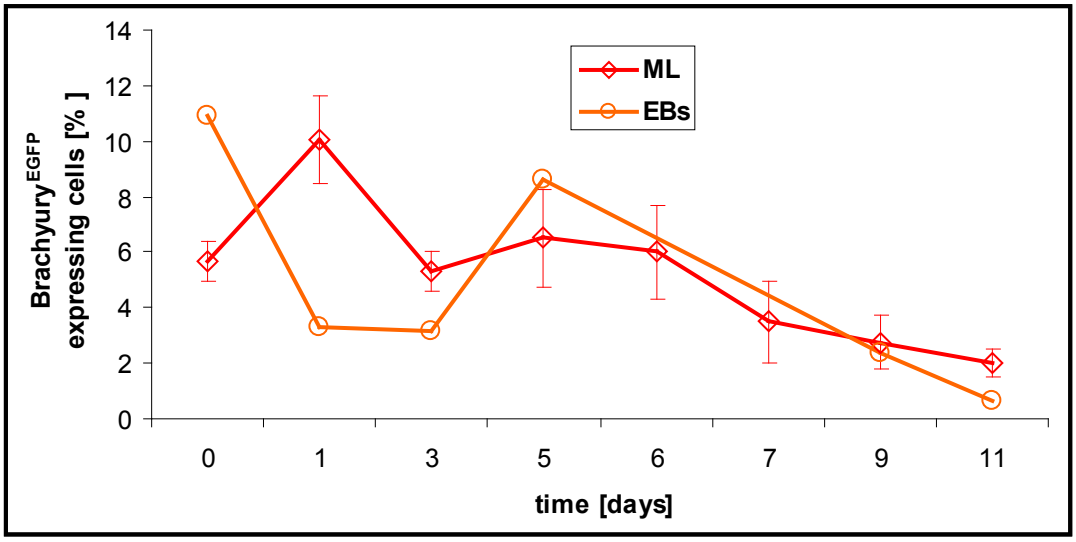

Figure 4.29: Comparison between **ESC** monolayer (ML) cell culture and the **EB** system. FACS analyses of Brachyury^{EGFP} reporter ESC line on days 0–11 of differentiation. Proportion of ESCs expressing *Brachyury*^{EGFP} either seeded on 48-well plates in ML cell culture (red line) or placed into hanging drop cell culture (orange line) on day 0 of differentiation. Data for ML comprised of mean values from samples with cell numbers 10^5, $5x10^5$ and 10^6. Data for EBs was produced by Lucia Leitner in the course of her diploma thesis (Leitner, 2013). Error bars: SD.

As shown in figure 4.29 differentiating ESCs in monolayer cell culture showed a peak of the proportion of *Brachyury*^{EGFP} expressing cells on day 1 of differentiation which could not be seen in former experiments with EBs. However, the high values on day 1 in this experiment could be comparable with the high values on day 0 in former experiments which might be caused by trypsinisation stress among other factors. The peak of the proportion of *Brachyury*^{EGFP} expressing cells in EBs on day 5 of differentiation could also be observed at the highest cell density in low volume monolayer ESC culture (Figure 4.27).

The difference between the proportion of *MesP1* expressing cells in ESC monolayer culture and the same proportion in ESC hanging drop culture was also determined.

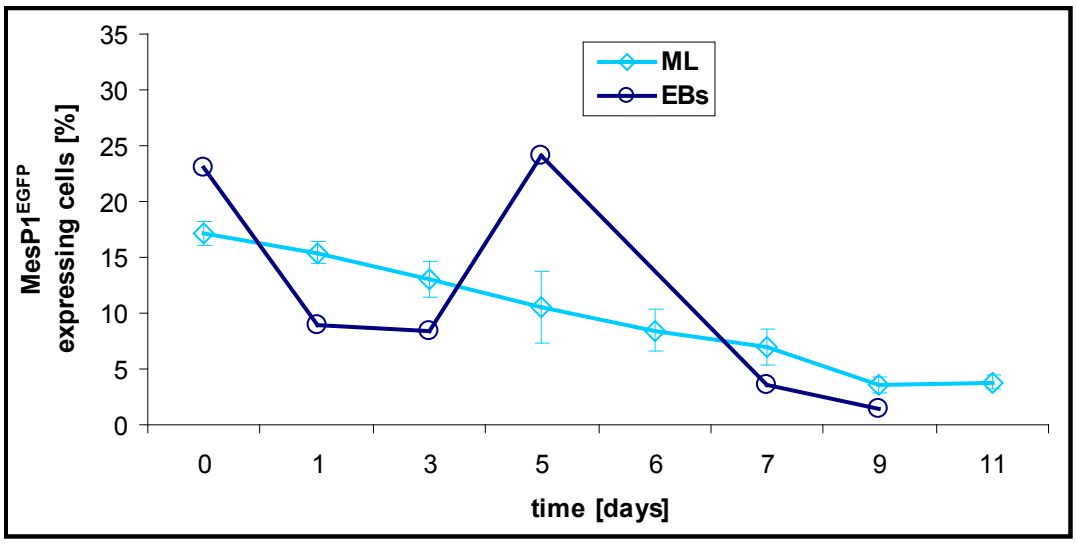

Figure 4.30: Comparison between **ESC** monolayer (ML) cell culture and the **EB** system. FACS analyses of MesP1^{EGFP} reporter ESC line on days 0–11 of differentiation. Proportion of ESCs expressing *MesP1*^{EGFP} either seeded on 48-well plates in ML cell culture (light blue line) or placed into hanging drop cell culture (blue line) on day 0 of differentiation. Data for ML comprised of mean values from samples with cell numbers 10^5, $5x10^5$ and 10^6. Data for EBs was produced by Lucia Leitner in the course of her diploma thesis (Leitner, 2013). Error bars: SD.

As demonstrated in figure 4.30 a peak of the proportion of *MesP1*^{EGFP} expressing ESCs could not be detected in monolayer cell culture on day 5 of differentiation, not even at high cell density (Figure 4.29), while in former experiments using EBs this peak was present. This finding could indicate that cardiac precursors, which normally express *MesP1* at some point, do not develop in low volume monolayer ESC culture.

The proportions of *Brachyury*^{EGFP} and *MesP1*^{EGFP} expressing ESCs were rather similar in EBs and monolayer cell culture except for early time points of differentiation for *Brachyury*^{EGFP} expression and for day 5 for *MesP1*^{EGFP} expression (Figures 4.29 and 4.30).

In low volume monolayer ESC culture cell density seemed to have an influence on the expression patterns of *Brachyury*^{EGFP} and *MesP1*^{EGFP} as well as on the percentage values of cells expressing these genes as these properties differed between samples with different cell numbers. Interestingly, differences seemed to be greater for *Brachyury*^{EGFP} expression. Additionally, the pattern of *Brachyury*^{EGFP} expression at high cell density in monolayer cell culture resembled that observed in EBs suggesting that differentiation processes might be more similar between high density monolayer cell culture and hanging drop culture than between low density monolayer cell culture and hanging drop culture.

However, also in this experiment beating cardiomyocytes could never be observed indicating that a certain expression pattern of *Brachyury*^{EGFP} and *MesP1*^{EGFP} was not sufficient for successful cardiomyogenesis.

Mean *Brachyury*^{EGFP} and *MesP1*^{EGFP} intensity

The mean intensity of *Brachyury*^{EGFP} expression in differentiating ESCs in low volume monolayer cell culture at different cell densities was determined over time using FACS analysis.

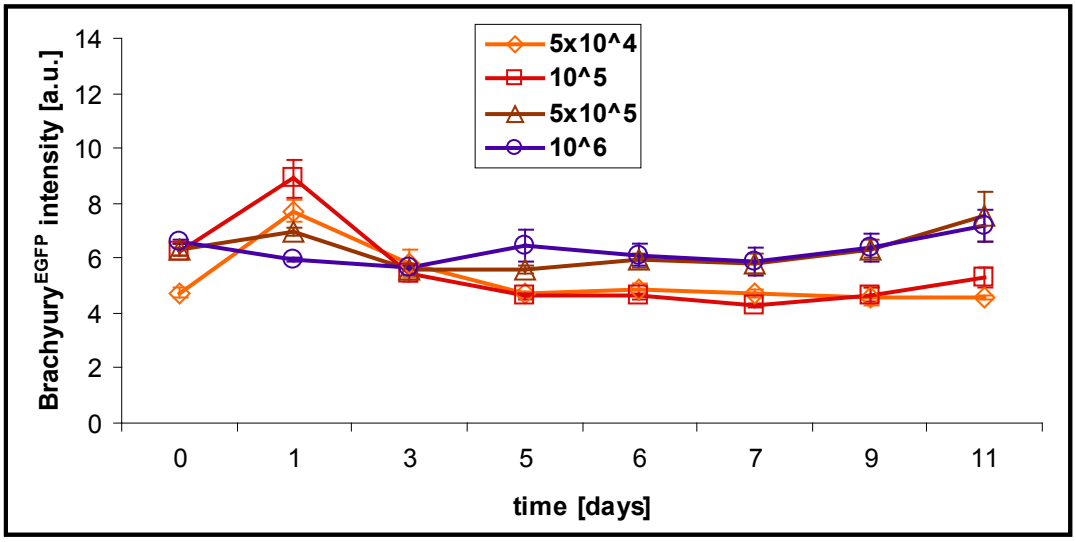

Figure 4.31: Influence of cell density on *Brachyury* expression in **ESCs** on different time points of differentiation. FACS analyses of Brachyury^{EGFP} reporter ESC line on days 0–11 of differentiation. Mean intensity of *Brachyury*^{EGFP} expression in ESCs seeded on 48-well plates with 5x10^4 (orange line), 10^5 (red line), 5x10^5 (brown line) or 10^6 (purple line) cells per well on day 0 of differentiation. Data for *Brachyury*^{EGFP} expression in ESC samples with 5x10^4 cells obtained from two independent experiments and six samples in total and also described in section 4.2. Error bars: SD.

In contrast to the proportion of *Brachyury*^{EGFP} expressing cells the mean intensity of *Brachyury*^{EGFP} expression only peaked in samples with the cell numbers 10^5 and 5x10^5 at day 1 of differentiation in low volume monolayer ESC culture as shown in figure 4.31. Furthermore, samples with the cell number 10^6 only showed a tiny peak of the mean intensity of *Brachyury*^{EGFP} expression on day 5 of differentiation. In all samples the mean intensity of *Brachyury*^{EGFP} expression rose slightly between day 7 and 11 of differentiation except for samples with the cell number 5x10^4.

Simlarly, we analysed the mean intensity of *MesP1*^{EGFP} expression at different time points of differentiation in low volume monolayer ESC culture at different cell densities.

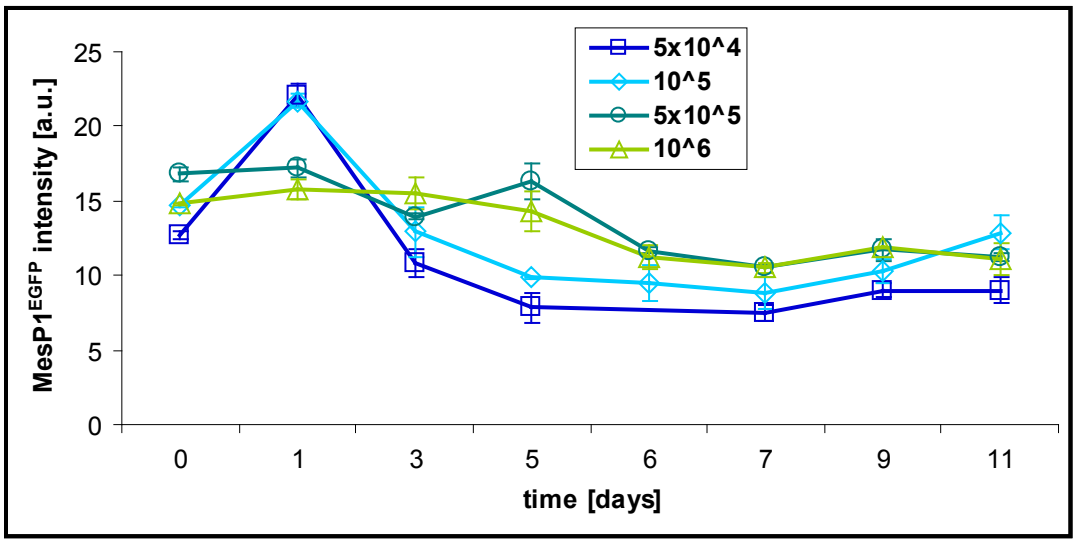

Figure 4.32: Influence of cell density on *MesP1* expression in **ESCs** on different time points of differentiation. FACS analyses of MesP1^{EGFP} reporter ESC line on days 0–11 of differentiation. Mean intensity of MesP1^{EGFP} expression in ESCs seeded on 48-well plates with 5x10^4 (blue line), 10^5 (light blue line), 5x10^5 (turquoise line) or 10^6 (green line) cells per well on day 0 of differentiation. Data for *MesP1*^{EGFP} expression in ESC samples with 5x10^4 cells also described in section 4.2. Error bars: SD.

Figure 4.32 demonstrates that the mean intensity of *MesP1*^{EGFP} expression behaved differently over time dependent on the cell density used in low volume monolayer ESC culture. At cell numbers 5x10^4 and 10^5 the mean intensity of *MesP1*^{EGFP} expression peaked on day 1 of differentiation, then decreased and increased again at later time points of differentiation. Samples of the cell number 5x10^5 showed a peak in the mean intensity of *MesP1*^{EGFP} expression at day 5 of differentiation followed by a decrease of *MesP1*^{EGFP} expression intensity. At the highest cell density, the intensity of *MesP1*^{EGFP} expression was slightly decreasing over most of the time course.

The intensity of *MesP1*^{EGFP} expression was much higher than that of *Brachyury*^{EGFP} expression in monolayer ESC culture (Figures 4.31 and 4.32).

The mean intensities of *Brachyury*^{EGFP} and *MesP1*^{EGFP} expression were compared between monolayer ESC culture and EBs at different time points of differentiation.

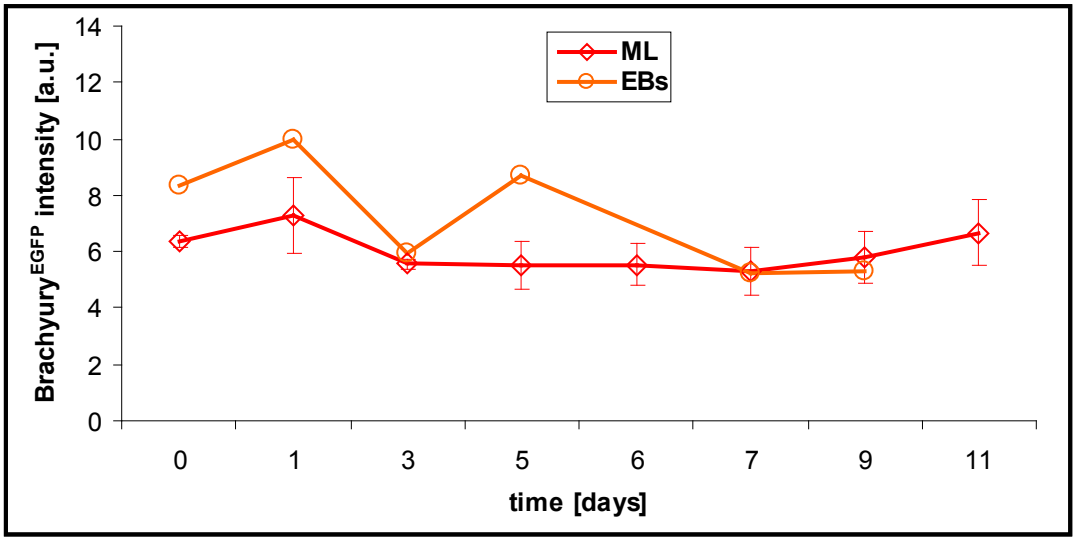

Figure 4.33: Comparison between **ESC** monolayer cell (ML) culture and the **EB** system. FACS analyses of Brachyury^{EGFP} reporter ESC line on days 0–11 of differentiation. Mean intensity of *Brachyury*^{EGFP} expression in ESCs either seeded on 48-well plates in ML cell culture (red line) or placed into hanging drop cell culture (orange line) cells per well on day 0 of differentiation. Error bars: SD. Data for ML comprised of mean values from samples with cell numbers 10^5, $5x10^5$ and 10^6. Data for EBs was produced by Lucia Leitner in the course of her diploma thesis (Leitner, 2013).

As depicted in figures 4.33 and 4.34, in former experiments using EBs the mean intensities of *Brachyury*^{EGFP} and *MesP1*^{EGFP} expression peaked on day 1 of differentiation which could also be detected in monolayer cell culture. In both cases these findings might be explained by a cellular stress response. Additionally the peaks of the mean intensity of *Brachyury*^{EGFP} and *MesP1*^{EGFP} expression on day 5 of differentiation in EBs could generally not be copied in monolayer cell culture but only at cell number 10^6 and $5x10^5$ (Figures 4.31 and 4.32), respectively, indicating that higher cell density monolayer cell culture favours *Brachyury* and *MesP1* expression patterns resembling those in EBs.
The mean intensity of *Brachyury*^{EGFP} expression was rather similar in EBs and monolayer cell culture while that of *MesP1*^{EGFP} expression was lower in EBs as shown in figures 4.33 and 4.34.

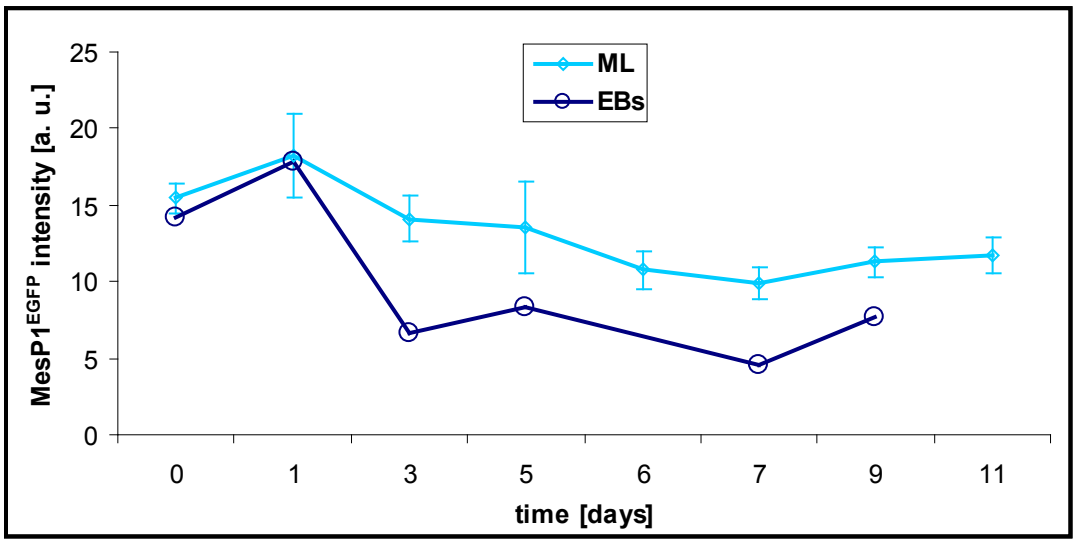

Figure 4.34: Comparison between **ESC** monolayer (ML) cell culture and the **EB** system. FACS analyses of MesP1^{EGFP} reporter ESC line on days 0–11 of differentiation. Mean intensity of *MesP1^{EGFP}* expression in ESCs either seeded on 48-well plates in ML cell culture (light blue line) or placed into hanging drop cell culture (blue line) on day 0 of differentiation. Error bars: SD. Data for ML comprised of mean values from samples with cell numbers 10^5, $5x10^5$ and 10^6. Data for EBs was produced by Lucia Leitner in the course of her diploma thesis (Leitner, 2013).

Cell density barely influenced the mean intensity of *Brachyury^{EGFP}* but had an impact on *MesP1^{EGFP}* expression as the pattern and level of *MesP1^{EGFP}* expression intensity varied between samples of different cell numbers.

Proportion of PI positive cells

We assessed the proportions of dead cells in low volume monolayer cell culture of Brachyury^{EGFP} and MesP1^{EGFP} reporter ESC lines at increasing cell densities at different time points of differentiation.

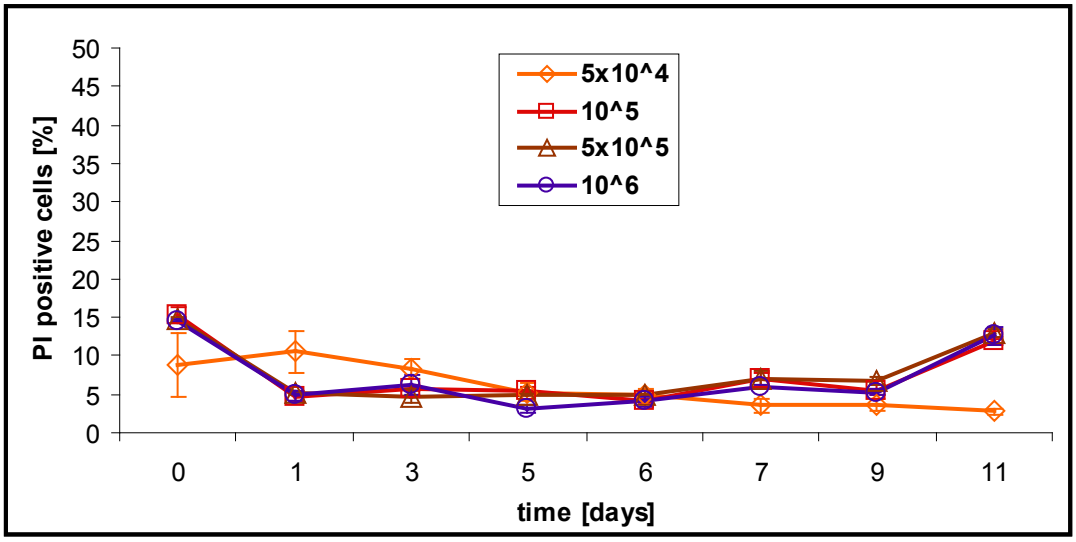

Figure 4.35: Influence of cell density on *Brachyury* expression in **ESCs** on different time points of differentiation. FACS analyses of Brachyury^{EGFP} reporter ESC line on days 0–11 of differentiation. Proportion of PI positive (dead) ESCs seeded on 48-well plates with 5x10^4 (orange line), 10^5 (red line), 5x10^5 (brown line) or 10^6 (purple line) cells per well on day 0 of differentiation. Error bars: SD.

As demonstrated in figures 4.35 and 4.36 the proportions of dead cells were rather low and only increasing at later time points in both reporter ESC lines.

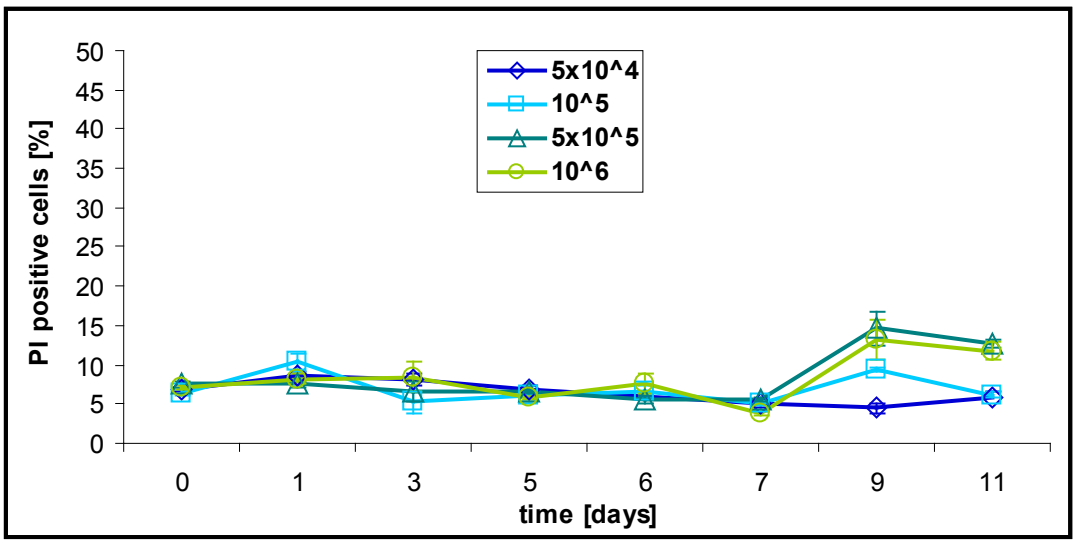

Figure 4.36: Influence of cell density on *MesP1* expression in **ESCs** on different time points of differentiation. FACS analyses of MesP1^{EGFP} reporter ESC line on days 0–11 of differentiation. Proportion of PI positive (dead) ESCs seeded on 48-well plates with 5x10^4 (blue line), 10^5 (light blue line), 5x10^5 (turquoise line) or 10^6 (green line) cells per well on day 0 of differentiation. Error bars: SD.

Higher cell density only led to a higher proportion of dead cells at late time points of differentiation (Figures 4.35 and 4.36). The increase in the proportion of dead cells was probably caused by insufficient supply with nutrients because of the the high cell numbers present at these late time points.

4.4.2 Influence of cell density on *Brachyury*^{EGFP} and *MesP1*^{EGFP} expression in cardiovascular progenitor reporter cell lines

In low volume monolayer CVPC culture the impact of cell density on *Brachyury*^{EGFP} and *MesP1*^{EGFP} expression patterns as well as on cell death was also determined by measuring the proportions of *Brachyury*^{EGFP} and *MesP1*^{EGFP} expressing cells, the mean intensity of *Brachyury*^{EGFP} and *MesP1*^{EGFP} expression as well as the proportion of dead cells using flow cytometry.

Proportion of *Brachyury*^{EGFP} and *MesP1*^{EGFP} expressing cells

We analysed the proportion of *Brachyury*^{EGFP} expressing cells in low volume monolayer CVPC culture at increasing cell numbers over time.

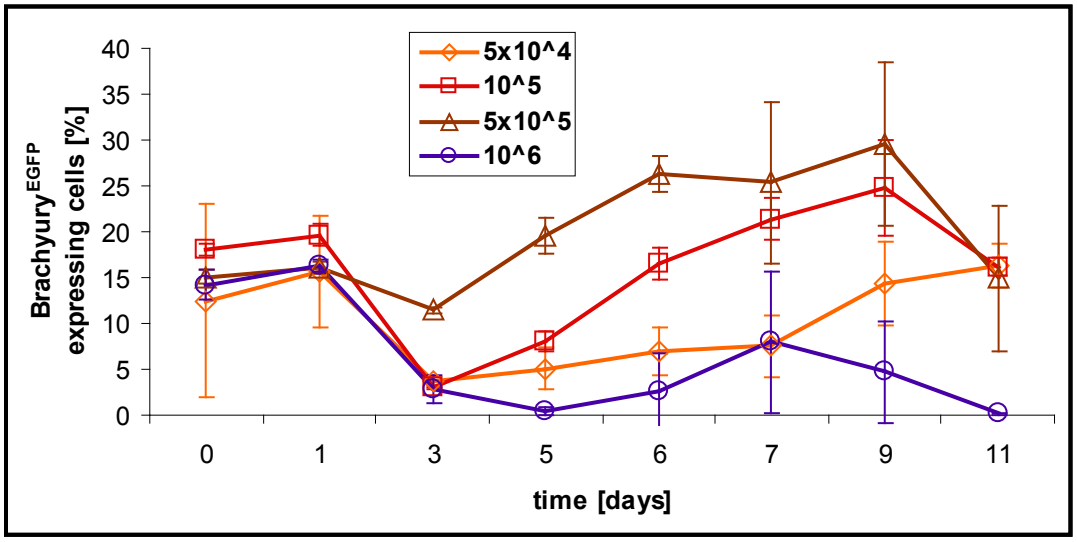

Figure 4.37: Influence of cell density on *Brachyury* expression in **CVPCs** on different time points of differentiation. FACS analyses of Brachyury^{EGFP} reporter CVPC line on days 0–11 of differentiation. Proportion of CVPCs expressing *Brachyury*^{EGFP} seeded on 48-well plates with 5x10^4 (orange line), 10^5 (red line), 5x10^5 (brown line) or 10^6 (purple line) cells per well on day 0 of differentiation. Data for *Brachyury*^{EGFP} expression in CVPC samples with 5x10^4 cells obtained from three independent experiments and nine samples in total and also described in section 4.2. Error bars: SD.

As depicted in figure 4.37 the proportion of *Brachyury*^{EGFP} expressing CVPCs decreased between day 0 and 3 of differentiation, then steeply rose until day 9 and declined again on day 11 of differentiation at cell numbers 5x10^4, 10^5 and 5x10^5. At the highest cell density tested, a decrease in the proportion of *Brachyury*^{EGFP} expressing CVPCs could be observed between day 0 and 5 of differentiation which was followed by a flatter increase than at lower cell densities only until day 7 of differentiation.

The proportion of *MesP1*^{EGFP} expressing cells in monolayer CVPC culture at different cell numbers was also determined at various time points of differentiation.

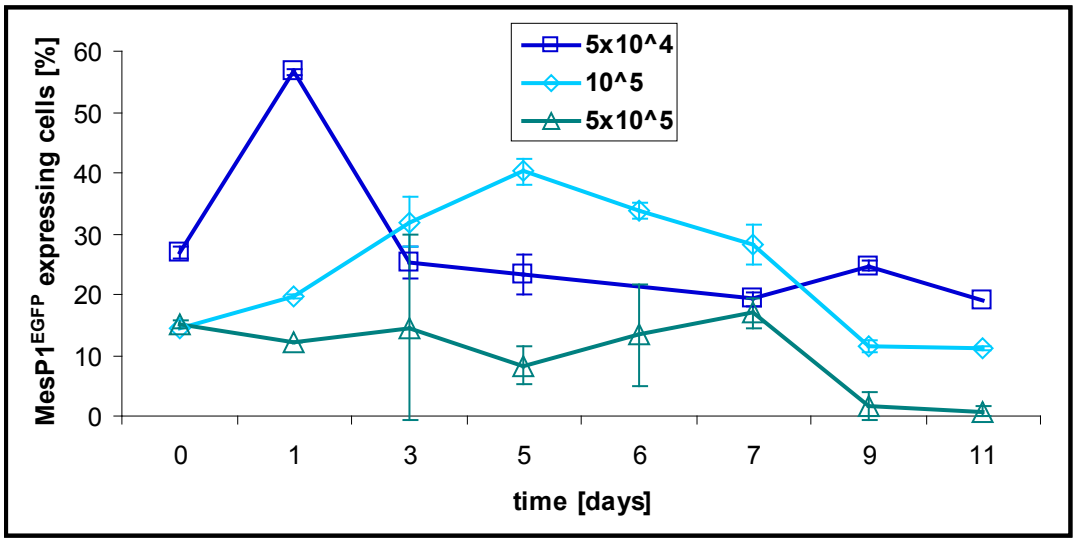

Figure 4.38: Influence of cell density on *MesP1* expression in **CVPCs** on different time points of differentiation. FACS analyses of MesP1^{EGFP} reporter CVPC line on days 0–11 of differentiation. Proportion of CVPCs expressing *MesP1*^{EGFP} seeded on 48-well plates with 5x10^4 (blue line), 10^5 (light blue line) or 5x10^5 (turquoise line) per well on day 0 of differentiation. Data for *MesP1*^{EGFP} expression in CVPC samples with 5x10^4 cells also described in section 4.2. Error bars: SD.

As depicted in figure 4.38 CVPCs showed a distinct peak of the proportion of *MesP1*^{EGFP} expressing cells on day 5 of differentiation at the cell number 10^5 which was absent at the other two cell numbers tested. At cell number 5x10^4 the proportion of *MesP1*^{EGFP} expressing cells peaked on day 1 of differentiation and then decreased. In samples of the cell number 5x10^5 the proportion of *MesP1*^{EGFP} expressing cells declined at early time points of differentiation and then started to rise at day 5 of differentiation resulting in a peak on day 7 of differentiation.

Generally, the proportions of *MesP1*^{EGFP} expressing CVPCs were lower at higher cell density than at lower cell density and at later time points of differentiation the proportion of *MesP1*^{EGFP} expressing CVPCs were very low at the cell number 5x10^5.

At lower cell densities the proportion of *MesP1*^{EGFP} expressing CVPCs tends to be larger than that of *Brachyury*^{EGFP} expressing cells while at higher cell densities the opposite is the case (Figures 4.37 and 4.38).

We also compared the proportion of *Brachyury*^{EGFP} expressing cells between high density monolayer CVPC culture (mean values of data derived from samples of cell numbers 10^5 to 10^6) and CVPC hanging drop culture.

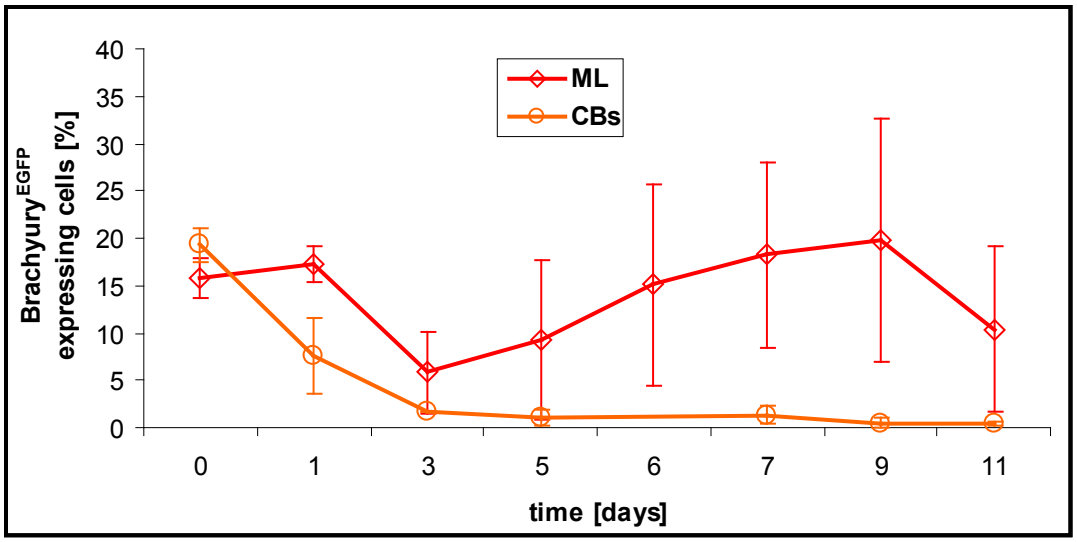

Figure 4.39: Comparison between **CVPC** monolayer cell (ML) culture and the **CB** system. FACS analyses of Brachyury^{EGFP} reporter CVPC line on days 0–11 of differentiation. Proportion of CVPCs expressing *Brachyury*^{EGFP} either seeded on 48-well plates in ML cell culture (red line) or placed into hanging drop cell culture (orange line) on day 0 of differentiation. Data for ML comprised of mean values from samples with cell numbers 10^5, $5x10^5$ and 10^6. Data for CBs was produced by Lucia Leitner in the course of her diploma thesis (Leitner, 2013). Error bars: SD.

In previous experiments using CBs the proportion of *Brachyury*^{EGFP} expressing cells had been declining between day 0 and 3 of differentiation which could also be seen in this experiment using monolayer cell culture as demonstrated in figure 4.39. However, in CBs the proportions of *Brachyury*^{EGFP} expressing cells had stayed at low levels on the remaining time points whereas they increased again in monolayer CVPC culture.
At high cell density the pattern of *Brachyury*^{EGFP} expression of CBs could be partially copied in monolayer CVPC culture. Also the percentage values of *Brachyury*^{EGFP} expressing cells were most similar between CBs and highest cell density monolayer cell culture compared to lower cell densities.

The proportion of *MesP1*^{EGFP} expressing cells in high density CVPC monolayer culture was also compared to the same proportion in CBs at different time points of differentiation.

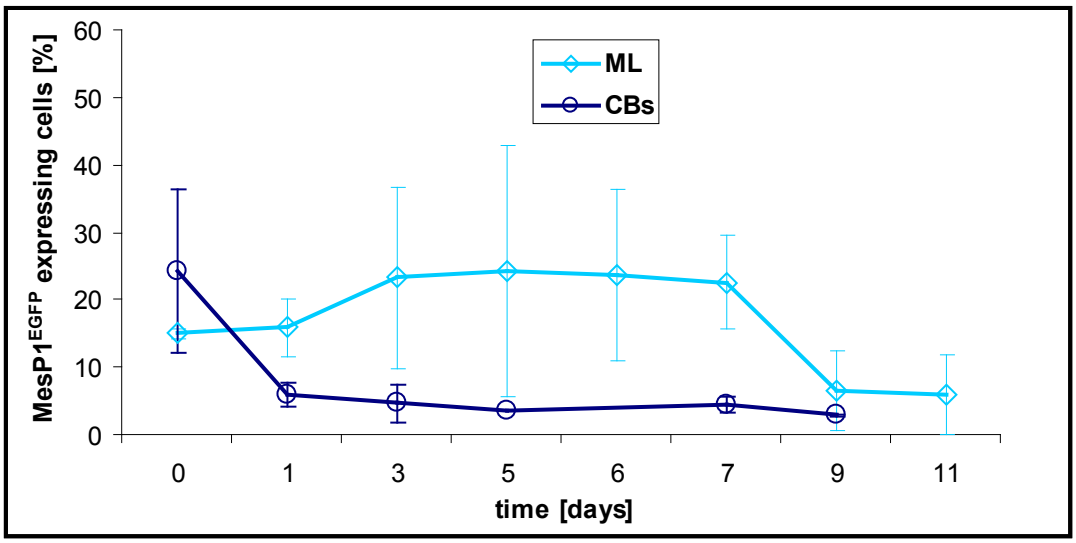

Figure 4.40: Comparison between **CVPC** monolayer (ML) cell culture and the **CB** system. FACS analyses of MesP1^{EGFP} reporter CVPC line on days 0–11 of differentiation. Proportion of CVPCs expressing *MesP1*^{EGFP} either seeded on 48-well plates in ML cell culture (light blue line) or placed into hanging drop cell culture (blue line) on day 0 of differentiation. Data for ML comprised of mean values from samples with cell numbers 10^5 and $5x10^5$. Data for CBs was produced by Lucia Leitner in the course of her diploma thesis (Leitner, 2013). Error bars: SD.

Figure 4.40 shows that the proportion of *MesP1*^{EGFP} expressing cells had been constantly decreasing in previous experiments using CBs while it only declined at later time points in monolayer CVPC culture. The proportions of *MesP1*^{EGFP} expressing cells were lower in CBs than in monolayer cell culture.

Similar to the situation in differentiating ESCs cell density had an impact on the pattern and the proportion of *Brachyury*^{EGFP} and *MesP1*^{EGFP} expression in CVPCs as they differed in otherwise comparable samples with different cell densities.

Noteworthy, no beating cardiomyocytes could be detected in this experiment not even at the highest cell density.

Mean *Brachyury*^{EGFP} and *MesP1*^{EGFP} intensity

The mean *Brachyury*^{EGFP} expression intensity in CVPC monolayer culture at different cell numbers was investigated over time.

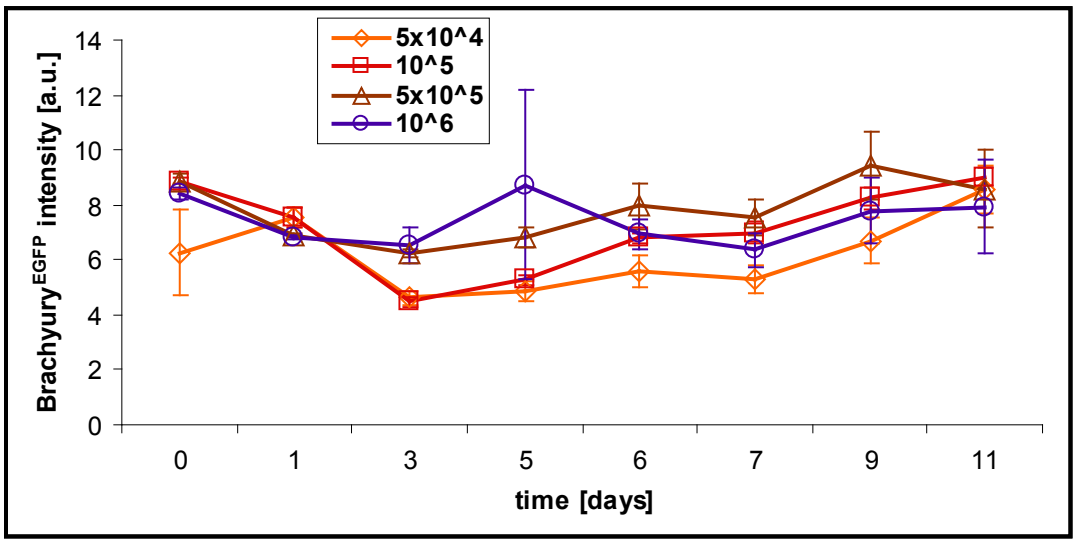

Figure 4.41: Influence of cell density on *Brachyury* expression in **CVPCs** on different time points of differentiation. FACS analyses of Brachyury^{EGFP} reporter CVPC line on days 0–11 of differentiation. Mean intensity of *Brachyury^{EGFP}* expression in CVPCs seeded on 48-well plates with 5x10^4 (orange line), 10^5 (red line), 5x10^5 (brown line) or 10^6 (purple line) cells per well on day 0 of differentiation. Data for *Brachyury^{EGFP}* expression in CVPC samples with 5x10^4 cells obtained from three independent experiments and nine samples in total and also described in section 4.2. Error bars: SD.

In low volume monolayer cell culture the mean intensity of *Brachyury^{EGFP}* expression in CVPCs decreased between day 0 and 3 and then increased for the remaining time at all cell numbers as shown in figure 4.41. Additionally, a distinct peak of the mean intensity of *Brachyury^{EGFP}* expression could be observed on day 5 of differentiation at cell number 10^6.

Furthermore, we analysed the mean intensity of *MesP1^{EGFP}* expression in low volume monolayer CVPC culture at increasing cell densities at different time points.

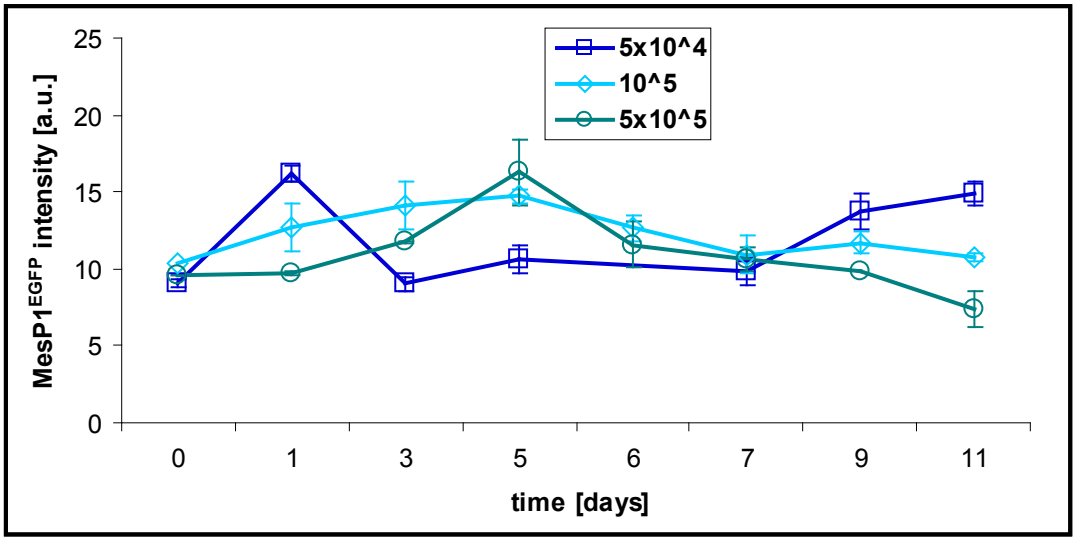

Figure 4.42: Influence of cell density on *MesP1* expression in **CVPCs** on different time points of differentiation. FACS analyses of MesP1^{EGFP} reporter CVPC line on days 0–11 of differentiation. Mean intensity of *MesP1*^{EGFP} expression in CVPCs seeded on 48-well plates with 5x10^4 (blue line), 10^5 (light blue line) or 5x10^5 (turquoise line) cells per well on day 0 of differentiation. Data for *MesP1*^{EGFP} expression in CVPC samples with 5x10^4 cells also described in section 4.2. Error bars: SD.

As depicted in figure 4.42 the mean intensity of *MesP1*^{EGFP} expression increased between day 0 and 5 of differentiation and then decreased at cell numbers 10^5 and 5x10^5 but at cell number 5x10^5 a more distinct peak appeared on day 5 of differentiation. At cell number 5x10^4 the mean intensity of *MesP1*^{EGFP} expression only peaked on day 1 of differentiation followed first by a decrease and then again by an increase at later time points of differentiation.

The mean intensity of *MesP1*^{EGFP} expression was higher than that of *Brachyury*^{EGFP} expression at most time points in CVPCs. Only at the cell number 5x10^5 levels of mean *MesP1*^{EGFP} expression were similar to those of *Brachyury*^{EGFP} expression at later time points of differentiation (Figures 4.41 and 4.42).

Cell density did not influence the level and the trend of the intensity of *Brachyury*^{EGFP} and *MesP1*^{EGFP} expression to a great extent in low volume monolayer CVPC culture.

We also analysed the difference in the mean intensity of *Brachyury*^{EGFP} expression between high density monolayer CVPC culture and CBs at various time points.

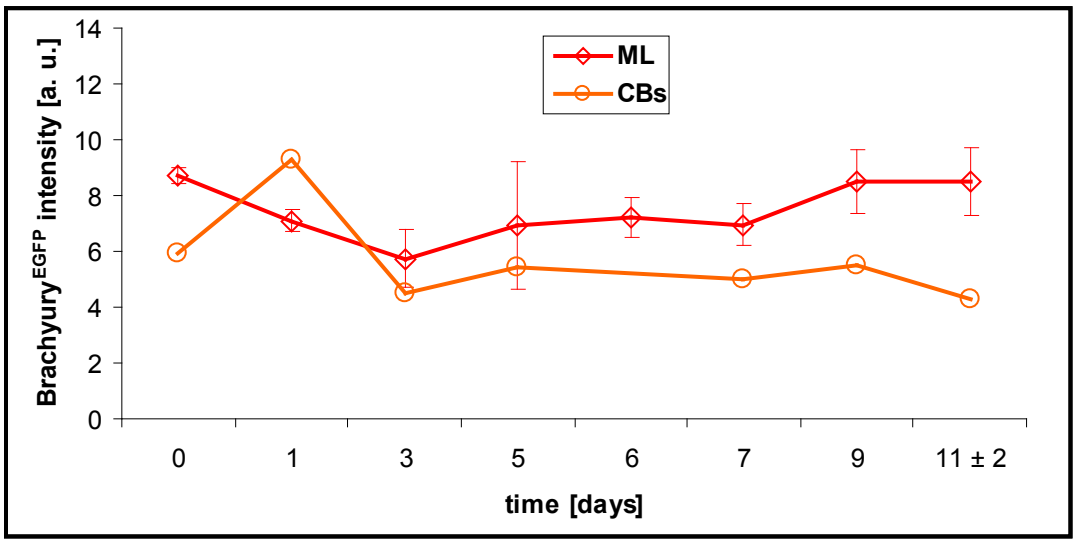

Figure 4.43: Comparison between **CVPC** monolayer (ML) cell culture and the **CB** system. FACS analyses of Brachyury^{EGFP} reporter CVPC line on days 0–11 of differentiation. Mean intensity of *Brachyury*^{EGFP} expression in CVPCs either seeded on 48-well plates in ML cell culture (red line) or placed into hanging drop cell culture (orange line) cells per well on day 0 of differentiation. Data for ML comprised of mean values from samples with cell numbers 10^5, $5x10^5$ and 10^6. Data for CBs was produced by Lucia Leitner in the course of her diploma thesis (Leitner, 2013). Error bars: SD.

In former experiments with CBs the mean intensity of *Brachyury*^{EGFP} expression had peaked on day 1 of differentiation as depicted in figure 4.43. This peak could not be detected in monolayer cell culture but a local maximum of the intensity of *Brachyury*^{EGFP} expression was seen on day 0 of differentiation. Both of these high values might be due to a stress response to rough handling or trypsinisation.
Between day 3 and 9 of differentiation the mean intensity of *Brachyury*^{EGFP} expression had stayed relatively stable in CBs while it tended to increase in low volume monolayer CVPC culture. Starting from day 9 the intensity of *Brachyury*^{EGFP} expression had decreased in CBs which could be observed only at higher cell densities in monolayer CVPC culture (Figure 4.41).

The mean intensity of *MesP1*^{EGFP} expression over time was also compared between high density monolayer CVPC culture and hanging drop CVPC culture.

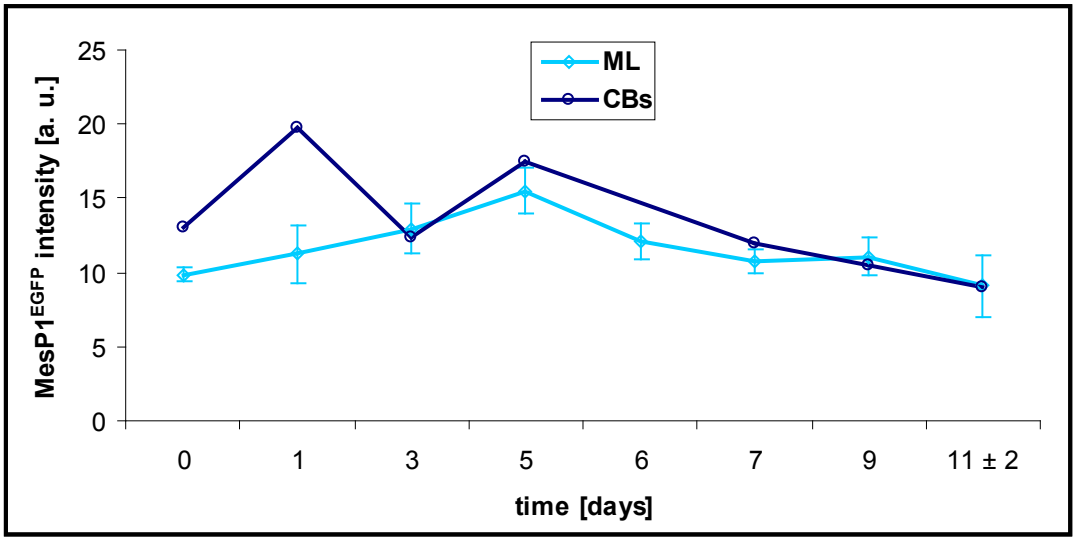

Figure 4.44: Comparison between **CVPC** monolayer (ML) cell culture and the **CB** system. FACS analyses of MesP1^{EGFP} reporter CVPC line on days 0–11 of differentiation. Mean intensity of *MesP1*^{EGFP} expression in CVPCs either seeded on 48-well plates in ML cell culture (light blue line) or placed into hanging drop cell culture (blue line) on day 0 of differentiation. Data for ML comprised of mean values from samples with cell numbers 10^5 and $5x10^5$. Data for CBs was produced by Lucia Leitner in the course of her diploma thesis (Leitner, 2013). Error bars: SD.

As shown in figure 4.44 CBs had shown peaks of the mean intensity of *MesP1*^{EGFP} expression on days 1 and 5 of differentiation in former experiments. The peak on day 5 could also be detected in monolayer CVPC culture especially at high cell density (Figure 4.42).

Generally, in high density monolayer CVPC culture, the mean intensity pattern of *MesP1*^{EGFP} expression came closer to the situation in CBs than the mean intensity pattern of *Brachyury*^{EGFP} expression.

Proportion of PI positive cells

We assessed the proportion of dead cells of Brachyury^{EGFP} and MesP1^{EGFP} reporter CVPC lines in low volume monolayer culture at increasing cell densities at certain time points of differentiation.

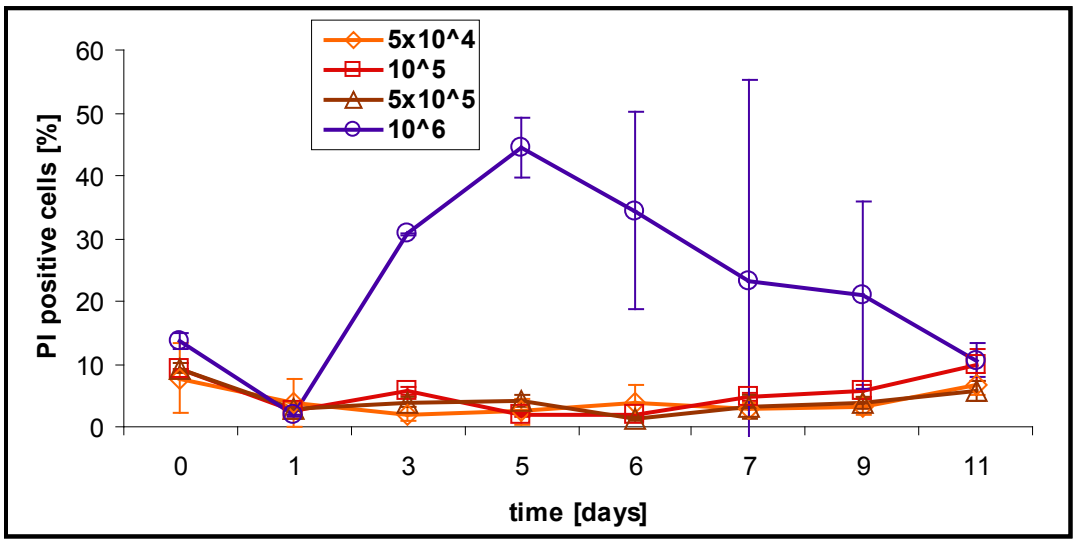

Figure 4.45: Influence of cell density on *Brachyury* expression in **CVPCs** on different time points of differentiation. FACS analyses of Brachyury^{EGFP} reporter CVPC line on days 0–11 of differentiation. Proportion of PI positive (dead) CVPCs seeded on 48-well plates with 5x10^4 (orange line), 10^5 (red line), 5x10^5 (brown line) or 10^6 (purple line) cells per well on day 0 of differentiation. Error bars: SD.

At higher cell density the proportions of dead CVPCs were very high already at rather early time points of differentiation in low volume monolayer cell culture as shown in figures 4.45 and 4.46.

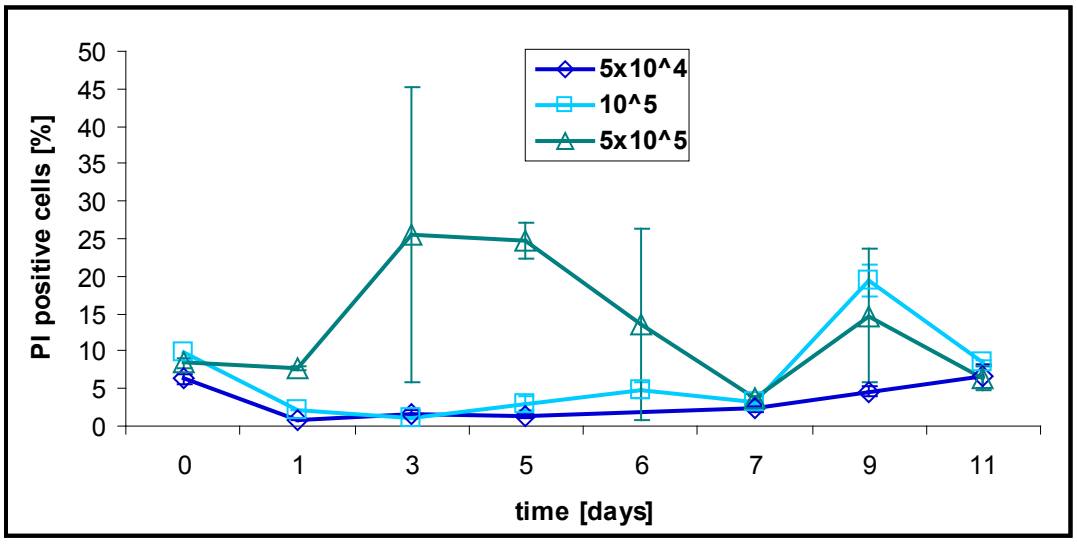

Figure 4.46: Influence of cell density on *MesP1* expression in **CVPCs** on different time points of differentiation. FACS analyses of MesP1^{EGFP} reporter CVPC line on days 0–11 of differentiation. Proportion of PI positive (dead) CVPCs seeded on 48-well plates with 5x10^4 (blue line), 10^5 (light blue line) or 5x10^5 (turquoise line) cells per well on day 0 of differentiation. Error bars: SD.

In the monolayer CVPC culture system high cell density rather seemed to cause cell death than to promote the development of contracting cardiomyocytes.

4.4.3 Comparison between cardiovascular progenitor and embryonic stem cell reporter cell lines

As shown in the two upper left panels of figure 4.47 a distinct peak of the proportion of *Brachyury*^{EGFP} expressing ESCs could be observed on day 1 of differentiation which was only small in the corresponding CVPC lines on that time point.

At the cell numbers 5x10^4 and 10^5 the proportion of *Brachyury*^{EGFP} expressing ESCs was then decreasing while the proportion of *Brachyury*^{EGFP} expressing CVPCs was increasing starting from day 3 at these cell numbers.

Similarly, at the cell number 5x10^5 the proportion of *Brachyury*^{EGFP} expressing CVPCs rose starting from day 3 of differentiation while the proportion of *Brachyury*^{EGFP} expressing ESCs declined starting from day 6 of differentiation. Additionally, on day 6 of differentiation a peak of the proportion of *Brachyury*^{EGFP} expressing ESCs could be observed at this cell number which could not be detected for the proportion of *Brachyury*^{EGFP} expressing CVPCs.

At the cell number 10^6 the proportion of *Brachyury*^{EGFP} expressing CVPCs decreased between day 1 and 5 of differentiation before peaking on day 7 of differentiation and then declining further while the proportion of *Brachyury*^{EGFP} expressing ESCs only decreased between day 1 and 3 of differentiation before peaking on day 5 of differentiation and declining afterwards.

The pattern of *Brachyury*^{EGFP} expression in the hanging drop culture system could only be copied in high density monolayer ESC culture but not in high density monolayer CVPC culture (see also figures 4.29 and 4.39).

Proportions of *Brachyury*^{EGFP} expressing CVPCs at the cell numbers 5x10^4, 10^5 and 5x10^5 were higher than those of ESCs at all cell numbers while the proportions of *Brachyury*^{EGFP} expressing CVPCs at the cell number 10^6 were lower or similar compared to those of ESCs at all cell number as depicted in figure 4.47. In CBs the proportions of *Brachyury*^{EGFP} expressing cells were also lower than in EBs (see also figures 4.29 and 4.39) indicating that a lower proportion of Brachyury expressing CVPCs compared to ESCs comes closer to the *in vivo* situation.

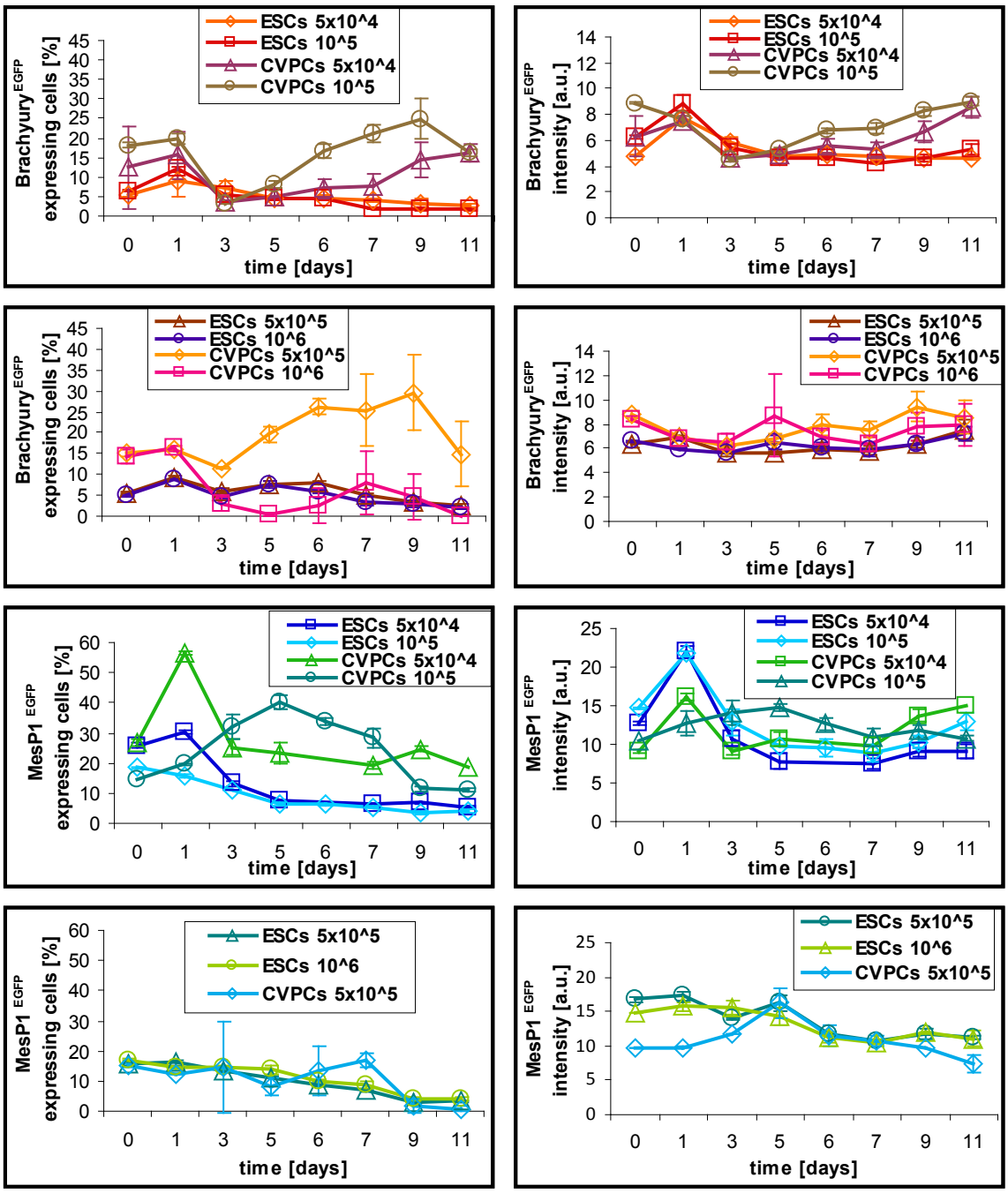

Figure 4.47: Influence of cell density on *Brachyury* and *MesP1* expression in **ESCs and CVPCs** on different time points of differentiation. FACS analyses of Brachyury^{EGFP} (two upper rows) and MesP1^{EGFP} (two lower rows) reporter ESC and CVPC lines on days 0–11 of differentiation. Proportion of ESCs and CVPCs expressing *Brachyury^{EGFP}* or *MesP1^{EGFP}* (left panels) and mean intensity of *Brachyury^{EGFP}* or *MesP1^{EGFP}* expression in ESCs and CVPCs (right panels) seeded on 48-well plates with 5x10^4, 10^5, 5x10^5 or 10^6 cells per well on day 0 of differentiation. Data for Brachyury^{EGFP} expression in ESC and CVPC samples with 5x10^4 cells obtained from two independent experiments and six samples in total and from three independent experiments and nine samples in total, respectively, and also described in section 4.2. Data for MesP1^{EGFP} expression in ESC and CVPC samples with 5x10^4 cells also described in section 4.2. Error bars: SD.

As demonstrated in the two left lower panels of figure 4.47 the proportion of *MesP1*^{EGFP} expressing ESCs was decreasing over the whole time course in monolayer cell culture similarly to that of CVPCs at the cell number 5x10^4, while the proportion of *MesP1*^{EGFP} expressing CVPCs peaked on day 5 at the cell number 10^5 and on day 7 at the cell number 5x10^5.

At the cell numbers 5x10^4 and 10^5 the proportions of *MesP1*^{EGFP} expressing CVPCs exceeded that of ESCs at most time points while at the cell number 5x10^5 the proportions of *MesP1*^{EGFP} expressing CVPCs and ESCs were similar at most time points.

The pattern of *MesP1*^{EGFP} expression in hanging drop culture did not resemble that in high density monolayer ESC or CVPC culture (cf. Figures 4.30 and 4.40).

At cell numbers 5x10^4, 10^5 and 5x10^5 ESCs showed a peak of the mean intensity of *Brachyury*^{EGFP} expression on day 1 of differentiation while CVPCs showed a decrease in the mean intensity of *Brachyury*^{EGFP} expression at all cell numbers between day 0 and 3 of differentiation as depicted in the two upper right panels of figure 4.47. The mean intensity of *Brachyury*^{EGFP} expression was then increasing in CVPCs but stayed rather constant in ESCs. Therefore, the pattern of mean intensity of Brachyury^{EGFP} expression in high density monolayer ESC culture resembled that in CBs while the pattern of mean intensity of Brachyury^{EGFP} expression in high density monolayer CVPC culture resembled that in EBs.

At early time points of differentiation the mean intensity of *Brachyury*^{EGFP} expression in CVPCs at cell numbers 5x10^4, 10^5 and 5x10^5 was similar to that in ESCs at these cell numbers while at later time points of differentiation it was higher in CVPCs than in ESCs at those cell numbers. At the cell number 10^6 the mean intensity of *Brachyury*^{EGFP} expression was similar between CVPCs and ESCs at most time points which reflected the situation between EBs and CBs (see also figures 4.33 and 4.43).

The two lower right panels of figure 4.47 demonstrate that a peak of the mean intensity of *MesP1*^{EGFP} expression could be observed in ESCs at the cell numbers 5x10^4 and 10^5 on day 1 of differentiation which could also be detected in CVPC samples with the cell number 5x10^4 but was absent in CVPCs at the cell number 10^5 on that time point. The pattern of *MesP1*^{EGFP} expression intensity was quite similar between ESCs at the cell numbers 5x10^4 and 10^5 and CVPCs at the cell number 5x10^4.

The mean intensity of *MesP1*^{EGFP} expression was increasing in CVPCs at the cell number 10^5 between day 0 and 5 of differentiation while it was declining in ESCs between day 1 and 5 of differentiation. A decrease of the mean intensity of *MesP1*^{EGFP} expression could then be observed in ESCs and CVPCs at the cell number 10^5 but on days 9 and 11 of differentiation the mean intensity of *MesP1*^{EGFP} expression rose again in ESCs.

At the cell number 5x10^5 CVPCs showed an increase in the mean intensity of *MesP1*^{EGFP} expression between day 0 and 5 of differentiation while ESCs showed a decrease between day 0 and 3 of differentiation at the same cell number. In ESCs and CVPCs at the cell number 5x10^5 the mean intensity of *MesP1*^{EGFP} expression peaked on day 5 of differentiation and was decreasing afterwards.

At early time points of differentiation the mean intensity of *MesP1*^{EGFP} expression was lower in CVPCs than in ESCs but for the remaining time points it was similar between CVPCs and ESCs. In CBs the mean intensity of *MesP1*^{EGFP} expression was mostly higher than in EBs (see also figures 4.34 and 4.44).

At higher cell densities the pattern of the mean intensity of *MesP1*^{EGFP} expression in monolayer CVPC culture resembled that in CBs at most time points while in monolayer ESC culture this resemblance to EBs could be seen at a lower cell density on most time points (see also figures 4.34 and 4.44).

As shown in figures 4.35, 4.36, 4.45 and 4.46, at high cell density the proportion of dead cells was much larger in CVPCs than in ESCs which is probably due to the lower doubling time and a therefore faster increase in cell density of CVPCs.

Importantly, neither ESC nor CVPC lines developed into beating cardiomyocytes even in a high cell density monolayer system.

4.5 Correlation between reporter gene (*EGFP*) expression and expression of gene of interest (*Brachyury*, *MesP1* or *Nkx2.5*)

In the Brachyury^{EGFP} and MesP1^{EGFP} reporter cell lines the EGFP gene is only coupled to the promoter region of *Brachyury* and *MesP1* but not to their whole genes. This construct is randomly integrated in an unknown locus of the genome, therefore other regulatory DNA sequences than the promoter regions of our genes of interest might act *in cis* or *in trans* on the EGFP gene and influence its expression. Thus, we wanted to test whether *EGFP* expression detected with flow cytometry could be effectively compared to the actual expression of *Brachyury* or *MesP1*. As the EGFP gene is directly integrated into the NKX2.5 gene in the Nkx2.5^{EGFP} reporter cell lines it should be exposed to the same regulatory elements as the NKX2.5 gene and *EGFP* expression should directly correlate with *Nkx2.5* expression. Therefore, the Nkx2.5^{EGFP} cell lines were used as a control.

We isolated mRNA from undifferentiated Brachyury^{EGFP}, MesP1^{EGFP} and Nkx2.5^{EGFP} reporter CVPC and ESC lines as well as from other undifferentiated ESC (W4 and Ab2.2) and CVPC lines (A5) and reverse transcribed it into cDNA. We then performed semi-quantitative PCR analyses with *Brachyury*, *MesP1*, *Nkx2.5* and *EGFP* primers after samples had been normalised using primers for the housekeeping gene *Hypoxanthine*

phosphoribosyl transferase (*Hprt*). The Ab2.2 cell line carries a mutation introduced via retroviral integration between exon 5 and 6 of the HPRT gene (Kuehn et al., 1987; Ramírez-Solis et al., 1995; Roy et al., 2009). As we used *Hprt* primers spanning the region between exon 1 and 4 of the HPRT gene the mutation in the Ab2.2 cell line should not affect the results of the normalisation PCR analyses.

PCR reactions were repeated once with *Brachyury*, *MesP1* and *Nkx2*.5 primers respectively and only one PCR reaction was performed with *EGFP* primers. Positive as well as negative controls were included in PCR analyses. Samples were separated on an agarose gel. The intensity of the bands was detected by measuring the integrated density of the signal on the agarose gel with the programme ImageJ and adjusting it to the background signal.

FACS analysis was performed with the same undifferentiated reporter cell lines measuring the proportion of *Brachyury*^{EGFP}, *MesP1*^{EGFP} or *Nkx2.5*^{EGFP} expressing cells, the proportion of PI positive cells as well as the mean intensity of *Brachyury*^{EGFP}, *MesP1*^{EGFP} or *Nkx2.5*^{EGFP} expression.

ESCs or CVPCs were separated from feeder cells before mRNA isolation or FACS analysis. Two confluent wells of a 24-well cell culture plate were used for mRNA isolation and an aliquot from each of three confluent 24-wells was taken for FACS analysis.

Please note that, unlike in other experiments of this thesis, different clones of Brachyury^{EGFP} and MesP1^{EGFP} reporter CVPC and ESC lines were used in this experiment.

4.5.1 Expression of reporter gene and gene of interest in Brachyury^{EGFP}, MesP1^{EGFP} and Nkx2.5^{EGFP} reporter or wild type embryonic stem cell lines

To test whether *Brachyury*^{EGFP}, *MesP1*^{EGFP} and *Nkx2.5*^{EGFP} expression correlates with endogenous *Brachyury*, *MesP1* and *Nkx2*.5 expression in undifferentiated ESCs we investigated *EGFP*, *Brachyury*, *MesP1* and *Nkx2.5* mRNA levels as well as the proportions of *Brachyury*^{EGFP}, *MesP1*^{EGFP} and *Nkx2.5*^{EGFP} expressing cells and the mean intensity of *Brachyury*^{EGFP}, *MesP1*^{EGFP} and *Nkx2.5*^{EGFP} expression in undifferentiated reporter ESC lines.

mRNA levels of *EGFP*, *Brachyury*, *MesP1* and *Nkx2.5*

We analysed *EGFP* mRNA levels in different clones of Brachyury^{EGFP}, MesP1^{EGFP} and Nkx2.5^{EGFP} reporter ESC lines and compared it with *Brachyury*, *MesP1* and *Nkx2.5* mRNA levels in these cell lines. Additionally, we determined *Brachyury*, *MesP1* and *Nkx2.5*

mRNA levels in the ESC lines Ab2.2 and W4 which had been used to generate our reporter cell lines.

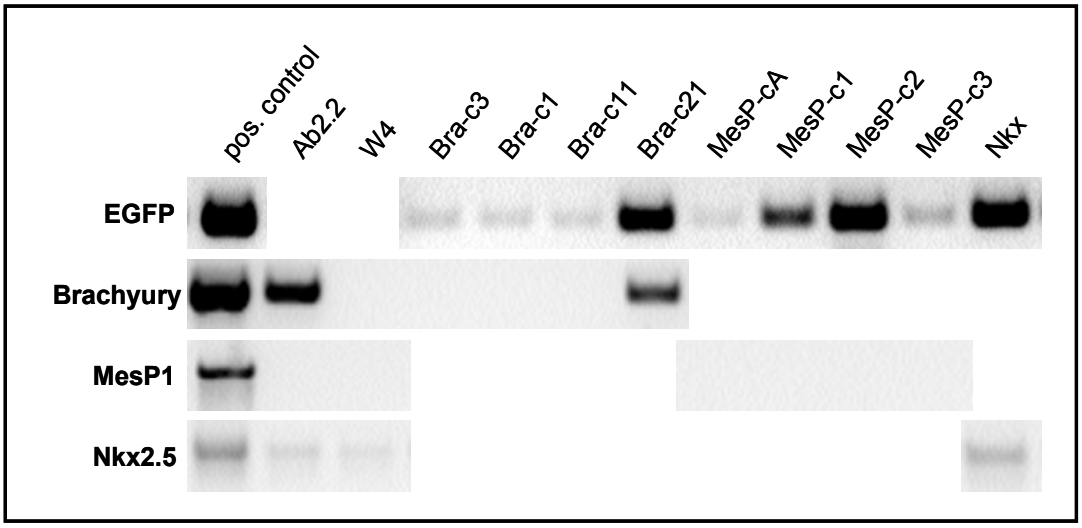

Figure 4.48: Correlation between reporter gene and gene of interest expression in **ESCs**. Semi-quantitative PCR analyses of *EGFP*, endogenous *Brachyury*, *MesP1* and *Nkx2.5* mRNA levels in undifferentiated ESC lines (Ab2.2 and W4) and Brachyury^{EGFP}, MesP1^{EGFP} or Nkx2.5^{EGFP} reporter ESC lines. Visualisation on agarose gel. Positive controls: plasmid MesP-EGFP for *EGFP* primers, cDNA of Ab2.2 cells on day 4.7 of differentiation generated by Julia Hoebaus for *Brachyury* and *MesP1* primers and cDNA of A5 cells on day 3 of differentiation generated by Jasmin Taubenschmid for *Nkx2.5* primers.

We then determined the integrated density levels of the mRNA PCR signals on the agarose gel mentioned and shown above using the software ImageJ and calculated the mean values of different PCR reactions.

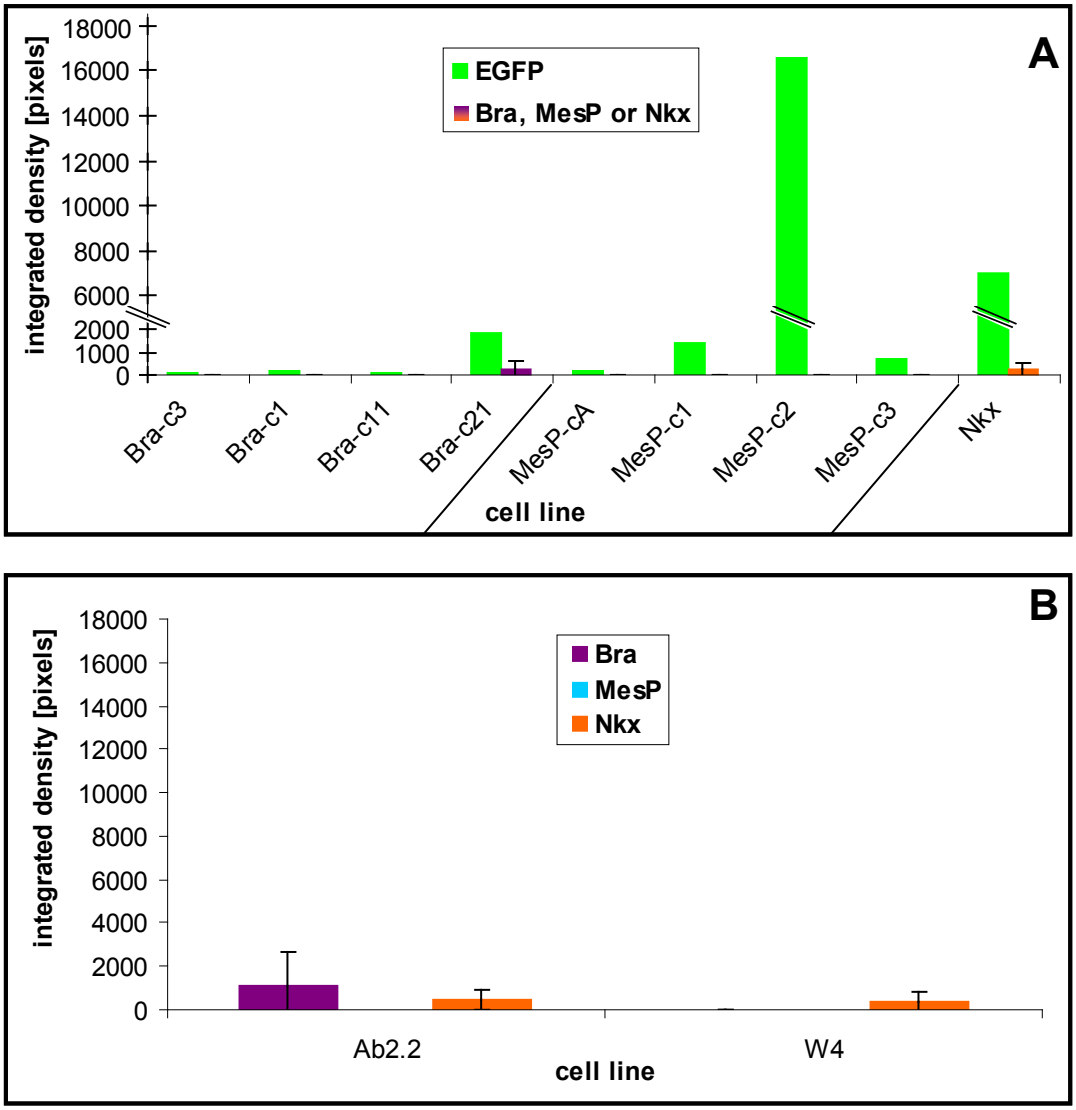

Figure 4.49: Correlation between reporter gene and gene of interest expression in **ESCs**. Semi-quantitative PCR analyses of *EGFP* (green bars) and endogenous *Brachyury* (purple bars), *MesP1* or *Nkx2.5* (orange bars) mRNA levels.

A) In Brachyury^{EGFP} (detection of *EGFP* and *Brachyury*), MesP1^{EGFP} (detection of *EGFP* and *MesP1*) or Nkx2.5^{EGFP} (detection of *EGFP* and *Nkx2.5*) reporter ESC lines.

B) In undifferentiated ESC lines (Ab2.2 and W4; detection of *Brachyury*, *MesP1* and *Nkx2.5*).

Mean values of levels of integrated density of PCR signals on agarose gels. Error bars: SD.

Undifferentiated clones c3, c1 and c11 of the Brachyury^{EGFP} ESC line did not express *Brachyury* mRNA and only low levels of *EGFP* mRNA, thus the expression levels of *Brachyury* and *EGFP* mRNA were comparable as shown in figures 4.48 and 4.49A. Low levels of *Brachyury* mRNA and higher levels of *EGFP* mRNA were found in clone c21 of the Brachyury^{EGFP} ESC line but the expression levels were still rather comparable.

None of the clones of the MesP1^{EGFP} ESC line expressed *MesP1* mRNA but they all expressed *EGFP* mRNA. In clones cA, c1 and c3 of the MesP1^{EGFP} ESC line *EGFP* mRNA levels were still rather low but in clone c2 *EGFP* mRNA was highly expressed and therefore clearly not comparable to endogenous *MesP1* mRNA levels.

Low levels of *Nkx2.5* mRNA were detected in the Nkx2.5^{EGFP} ESC line as well as surprisingly high levels of *EGFP* mRNA. Thus, *EGFP* and *Nkx2.5* mRNA levels did not seem to be comparable in the Nkx2.5^{EGFP} ESC line even though the EGFP gene was integrated into the NKX2.5 gene in this cell line. A possible explanation could be that the *Nkx2*.5 primers worked less efficiently than the *EGFP* primers which might have to be taken into account to accurately compare the expression of these two genes (see section 5.4).

As shown in figure 4.49B the ESC lines Ab2.2 and W4 both expressed low levels of *Nkx2*.5 mRNA but only the Ab2.2 cell line expressed *Brachyury* mRNA at slightly higher levels than *Nkx2*.5 mRNA. *MesP1* mRNA was not detected in these two ESC lines.

Nkx2.5 mRNA levels were quite similar in the Ab2.2 and W4 cell lines. As one *Nkx2.5* allele is disrupted in the Nkx2.5^{EGFP} reporter ESC line *Nkx2.5* mRNA levels in this cell line were only half of the same levels in the Ab2.2 cell line. The Ab2.2 cell line expressed higher levels of *Brachyury* mRNA than clone c21 of the Brachyury^{EGFP} ESC line (Figures 4.48 and 4.49).

Actually, W4 and Ab2.2 ESC lines normally should not express *Brachyury*, *MesP1* or *Nkx2.5* mRNA (Lauss et al., 2005; Liu et al., 2007). In the Nkx2.5^{EGFP} reporter ESC line or in the Ab2.2 ESC line and in clone c21 of the Brachyury^{EGFP} ESC line *Nkx2.5* mRNA or *Brachyury* mRNA, respectively, was only detected after one PCR reaction as indicated by the large error bars. However, in W4 and Ab2.2 cells *Nkx2.5* mRNA was found after both PCR reactions which could mean that these cells were not in a complete undifferentiated state.

FACS analysis

The proportion of *Brachyury^{EGFP}*, *MesP1^{EGFP}* or *Nkx2.5^{EGFP}* expressing cells in undifferentiated reporter ESC lines was determined and compared to *EGFP* mRNA levels as well as to endogenous *Brachyury*, *MesP1* and *Nkx2.5* mRNA levels in these cell lines to see whether these parameters correlated.

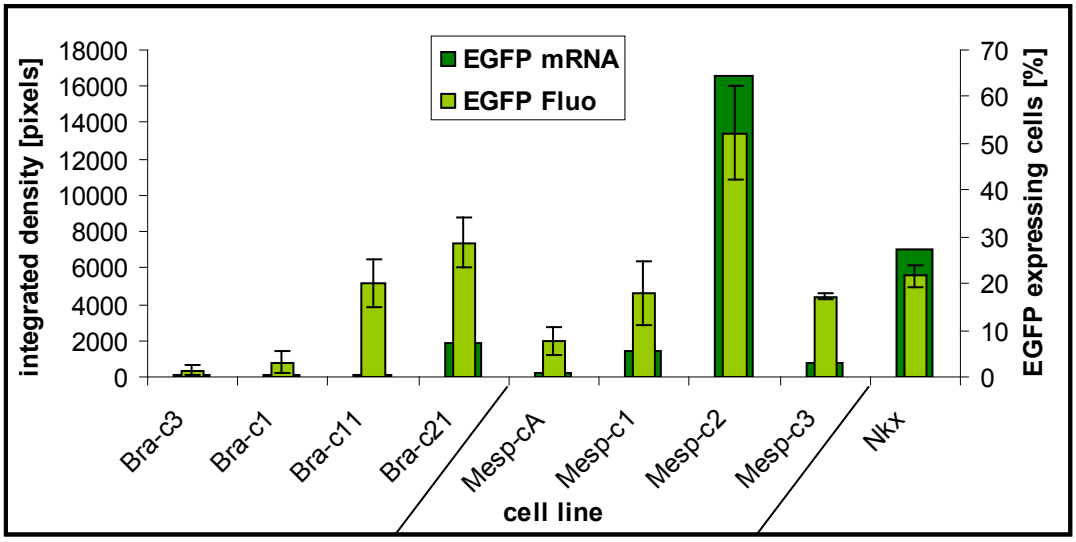

Figure 4.50: Reporter gene expression in **ESCs**. Comparison between *EGFP* mRNA and EGFP protein expression in Brachyury^{EGFP}, MesP1^{EGFP} and Nkx2.5^{EGFP} reporter ESC lines. Semi-quantitative PCR analyses of *EGFP* mRNA levels in Brachyury^{EGFP}, MesP1^{EGFP} or Nkx2.5^{EGFP} reporter ESC lines. Levels of integrated density of the PCR signal on an agarose gel (dark green bars). FACS analyses of undifferentiated Brachyury^{EGFP}, MesP1^{EGFP} and Nkx2.5^{EGFP} ESC reporter lines. Proportion of ESCs expressing *Brachyury^{EGFP}*, *MesP1^{EGFP}* or *Nkx2.5^{EGFP}* (light green bars). Error bars: SD.

FACS analysis detects fluorescence of the EGFP protein and does not detect mRNA. Also different units are used to express levels of mRNA and levels of fluorescence. Therefore, a comparison between EGFP fluorescence and mRNA levels of our genes of interest is not trivial.

As depicted in figure 4.50 the proportions of *Brachyury^{EGFP}* expressing cells in clones c3 and c1 of the Brachyury^{EGFP} ESC line were low as were the *EGFP* mRNA levels in these clones. No *Brachyury* mRNA was found in these clones as shown in figure 4.49A. Clone c3 of the Brachyury^{EGFP} ESC line was used for all other experiments with this cell line in this thesis. Therefore, we could confirm the assumption that *EGFP* and endogenous *Brachyury* expression correlated in these experiments at least on day 0 of differentiation. Also, the proportions of *Brachyury^{EGFP}* expressing cells were low in this clone on day 0 of differentiation showing that *Brachyury* expression was still correctly regulated in this clone as ESCs do not express *Brachyury* (Lauss et al., 2005; Liu et al., 2007).

Only in clone c21 of the Brachyury^{EGFP} ESC line *Brachyury* mRNA was detected at low levels and the proportion of *Brachyury^{EGFP}* expressing cells was higher in this clone than in all the other clones of the Brachyury^{EGFP} ESC line as demonstrated in figure 4.49A. However, the proportion of *Brachyury^{EGFP}* expressing cells in clone c11 of the Brachyury^{EGFP} ESC line also exceeded that of clones c3 and c1 of the same cell line but

clone c11 did not express *Brachyury* mRNA as depicted in figure 4.50. Therefore, the proportion of *Brachyury*^{EGFP} expressing cells and the Brachyury mRNA levels did clearly not correlate in clone c11 of the Brachyury^{EGFP} ESC line. The difference between *EGFP* mRNA and EGFP protein levels was quite high in clones c11 and c21.

In clone c2 of the MesP1^{EGFP} ESC line the proportion of *MesP1*^{EGFP} expressing cells was highest and in clone cA of the same cell line it was lowest compared to that in the other clones of this cell line which was comparable to *EGFP* mRNA levels as shown in figure 4.50. But none of the clones of the MesP1^{EGFP} ESC line was expressing *MesP1* mRNA as can be seen in figure 4.49A. In our other experiments we only used clone cA of the MesP1^{EGFP} ESC line which showed the lowest *EGFP* expression on both mRNA and protein level and therefore coming closest to the ideal situation in which *MesP1* and thus *EGFP* should not be expressed in undifferentiated ESCs.

The proportion of *Nkx2.5*^{EGFP} expressing cells in the Nkx2.5^{EGFP} ESC line was rather high as was the level of *EGFP* mRNA (Figure 4.50) while the level of *Nkx2.5* mRNA was very low (Figure 4.49A). Thus, the proportion of *Nkx2.5*^{EGFP} expressing cells and the level of *Nkx2.5* mRNA did not seem to correlate but might have to be compared using a different approach (see section 5.4).

We also tested the correlation of *Brachyury*^{EGFP}, *MesP1*^{EGFP} and Nkx2.5^{EGFP} expression intensity with *EGFP* mRNA levels as well as with endogenous *Brachyury*, *MesP1* and *Nkx2.5* mRNA levels in reporter ESC lines.

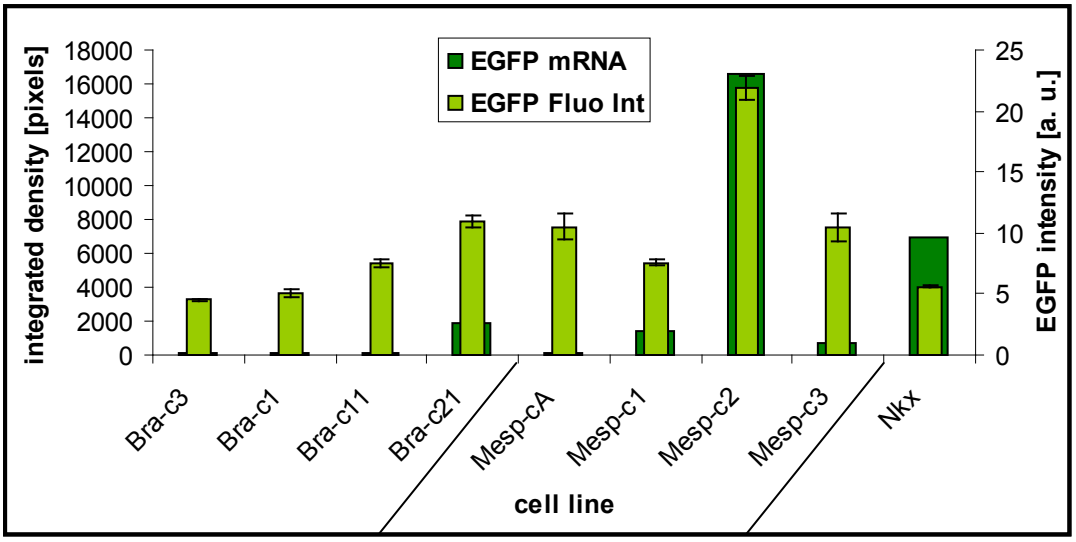

Figure 4.51: Reporter gene expression in **ESCs**. Comparison between *EGFP* mRNA and EGFP protein expression in Brachyury^{EGFP}, MesP1^{EGFP} and Nkx2.5^{EGFP} reporter ESC lines. Semi-quantitative PCR analyses of *EGFP* mRNA levels in Brachyury^{EGFP}, MesP1^{EGFP} or Nkx2.5^{EGFP} reporter ESC lines. Levels of integrated density of the PCR signal on an agarose gel (dark green bars). FACS analyses of undifferentiated Brachyury^{EGFP}, MesP1^{EGFP} and Nkx2.5^{EGFP} ESC reporter lines. Mean intensity of *Brachyury^{EGFP}*, *MesP1^{EGFP}* and *Nkx2.5^{EGFP}* expression in ESCs (light green bars). Error bars: SD.

As depicted in figure 4.51 the mean intensity of *Brachyury^{EGFP}* expression was highest in clone c21 of the Brachyury reporter ESC line as was the *EGFP* mRNA level compared to other clones of that cell line. This was also the only clone of the ESC Brachyury reporter cell line which expressed *Brachyury* mRNA but only at low levels as shown in figure 4.49A.

Generally, levels of mean *EGFP* expression intensity in all clones of the ESC Brachyury reporter cell line seemed to be too high to be comparable with *Brachyury* mRNA levels as well as *EGFP* mRNA levels in these clones. But as only a small number of cells was actually expressing *Brachyury^{EGFP}* in clones c3 and c1 of the ESC Brachyury reporter cell line the levels of the mean intensity of *Brachyury^{EGFP}* expression might not be statistically significant and might also have been overestimated. Therefore, the mean intensity of *Brachyury^{EGFP}* expression might still be comparable to endogenous *Brachyury* mRNA levels in these clones when a higher number of cells express *Brachyury^{EGFP}*.

Similar to the proportion of *MesP1^{EGFP}* expressing cells the mean intensity of *MesP1^{EGFP}* expression was highest in clone c2 of the ESC MesP1^{EGFP} reporter cell line in comparison to other clones of this cell line but it was lowest in clone c1 which was not the case for the proportion of *MesP1^{EGFP}* expressing cells as shown in figures 4.50 and 4.51. *EGFP* mRNA

levels were comparable with the mean *EGFP* intensity in clones c1 and c2 while *EGFP* mRNA levels significantly fall below intensity levels in clones cA and c3 (Figure 4.51).
Again, levels of mean intensity of *MesP1*^{EGFP} expression were not comparable to levels of endogenous *MesP1* mRNA as none of the clones of the ESC MesP1^{EGFP} reporter cell line did express *MesP1* mRNA (Figure 4.49A).
Figure 4.51 shows that the mean intensity of *Nkx2.5*^{EGFP} expression was rather low in the ESC Nkx2.5^{EGFP} reporter cell line and seemed to be more comparable to endogenous *Nkx2.5* mRNA levels (Figure 4.49A) than the proportion of *Nkx2.5*^{EGFP} expressing cells in this cell line (Figure 4.50). *EGFP* mRNA levels and the mean intensity of *Nkx2.5*^{EGFP} expression also seemed to correlate.

In former experiments with Brachyury^{EGFP} and MesP1^{EGFP} ESC reporter lines where cells were treated according to the hanging drop culture protocol the proportions of *Brachyury*^{EGFP} and *MesP1*^{EGFP} expressing ESCs were quite high on day 0 differentiation. As mentioned before this could be due to a stress response to trypsinisation on the previous day as it was required for the establishment of hanging drop cell culture but not for monolayer cell culture. Therefore, we analysed the differences between the proportions of *Brachyury*^{EGFP} and *MesP1*^{EGFP} expressing cells in different clones of reporter ESC lines treated according to the monolayer culture protocol and the same proportions in different clones of reporter ESC lines treated according to the EB protocol.

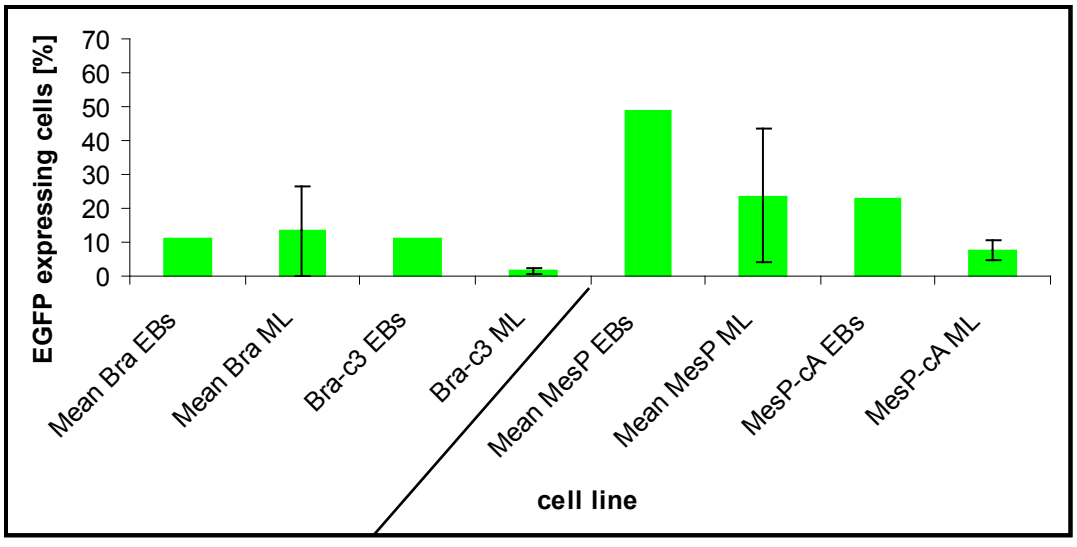

Figure 4.52: Reporter gene expression in **ESCs**. Comparison between EB and monolayer cell culture protocols. FACS analyses of undifferentiated Brachyury^{EGFP} and MesP1^{EGFP} ESC reporter lines either treated according to the hanging drop culture or the monolayer cell culture protocol. Proportion of ESCs expressing *Brachyury*^{EGFP} or *MesP1*^{EGFP}. Mean: Mean values of the proportions of ESCs expressing *Brachyury*^{EGFP} or *MesP1*^{EGFP} in different clones of Brachyury^{EGFP} or

MesP1^{EGFP} ESC reporter lines. Data for monolayer cell culture comprised of mean values of EGFP Fluo data from figure 4.50. Data for EBs was produced by Lucia Leitner in the course of her diploma thesis (Leitner, 2013). Error bars: SD. EBs: embryoid bodies. ML: monolayer.

When comparing the mean values of proportions of *Brachyury^{EGFP}* expressing ESCs of different clones of the Brachyury^{EGFP} ESC line, which were either treated according to the hanging drop culture or the monolayer cell culture protocol, these proportions were rather similar between the two protocols on day 0 of differentiation as depicted in figure 4.52. However, different clones were used in the two experiments except for clone c3 which was used in both experiments and showed a higher proportion of *Brachyury^{EGFP}* expressing ESCs on day 0 if cells had been treated according to the EB protocol.
Proportions of *MesP1^{EGFP}* expressing ESCs on day 0 of differentiation were always higher in cells which had been treated according to the hanging drop culture protocol (Figure 4.52).
These findings indicate that the high proportions of *Brachyury^{EGFP}* and *MesP1^{EGFP}* expressing ESCs on day 0 of differentiation in cells treated according to the EB protocol might be indeed caused by a stress reaction because of trypsinisation on the day before FACS analysis.

We also evaluated the proportions of dead cells in different clones of reporter ESC lines after treatment according to the monolayer protocol.

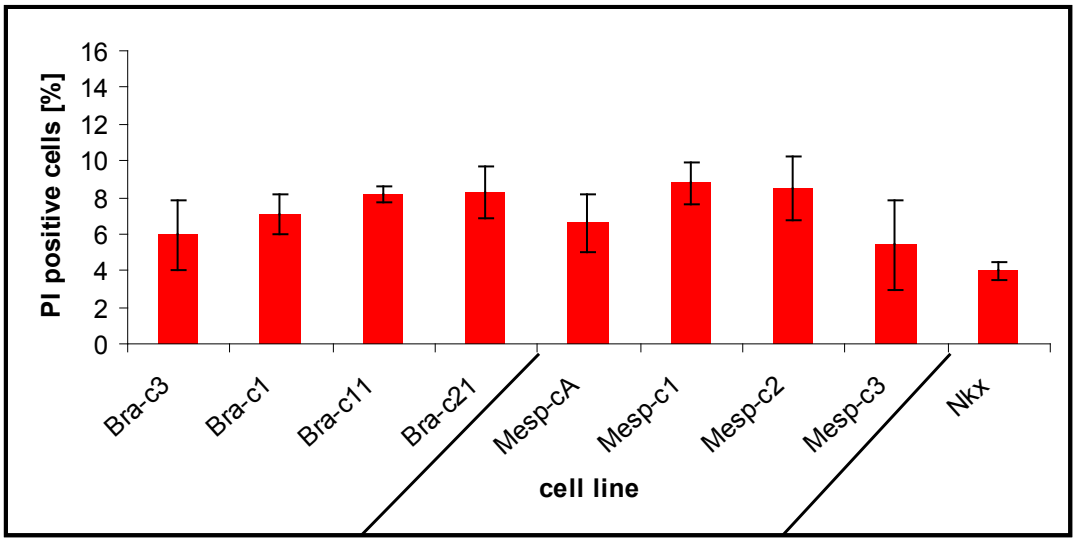

Figure 4.53: Reporter gene expression in **ESCs**. FACS analyses of undifferentiated Brachyury^{EGFP}, MesP1^{EGFP} and Nkx2.5^{EGFP} ESC reporter lines. Proportion of PI positive (dead) ESCs. Error bars: SD.

As shown in figure 4.53 the proportions of PI positive cells were rather low in all clones of the different undifferentiated ESC lines and the differences between them were only small.

We then compared the mean values of the proportions of dead cells between ESC reporter lines treated according to the monolayer and the same cell lines treated according to the EB protocol to analyse whether one of these methods led to enhanced cell death.

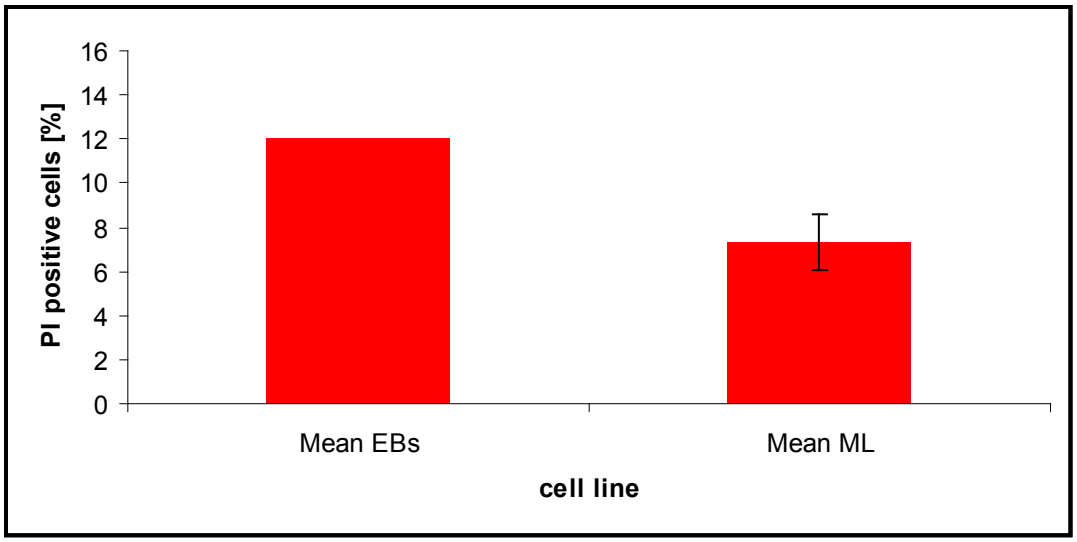

Figure 4.54: Reporter gene expression in **ESCs**. Comparison between EB and monolayer cell culture protocols. FACS analyses of undifferentiated Brachyury^{EGFP} and MesP1^{EGFP} ESC reporter lines either treated according to the hanging drop culture or the monolayer cell culture protocol. Mean: Mean values of the proportions of PI positive (dead) cells in different clones of undifferentiated Brachyury^{EGFP} and MesP1^{EGFP} ESC reporter lines in monolayer cell culture or in EBs. Data for monolayer cell culture comprises of mean values of portions of PI positive cells of Brachyury^{EGFP} and MesP1^{EGFP} ESC reporter lines presented in figure 4.53. Data for EBs was produced by Lucia Leitner in the course of her diploma thesis (Leitner, 2013). Error bars: SD. EBs: embryoid bodies. ML: monolayer.

In former experiments in which ESCs had been treated according to the EB protocol the proportion of PI positive cells was only slightly higher than in this experiment where ESCs had been treated according to the monolayer cell culture protocol as depicted in figure 4.54. Thus, there were not significantly more cells dying in former experiments in which cells had been trypsinised one day prior to FACS analysis.

4.5.2 Expression of reporter gene and gene of interest in cardiovascular progenitor Brachyury^{EGFP}, MesP1^{EGFP} and Nkx2.5^{EGFP} reporter or wild type cell lines

We also investigated the correlation of *Brachyury*^{EGFP}, *MesP1*^{EGFP} and *Nkx2.5*^{EGFP} expression with endogenous *Brachyury*, *MesP1* and *Nkx2.5* expression in undifferentiated reporter CVPC lines. For that purpose we analysed *EGFP*, *Brachyury*, *MesP1* and *Nkx2.5* mRNA levels, the proportions of *Brachyury*^{EGFP}, *MesP1*^{EGFP} and *Nkx2.5*^{EGFP} expressing cells and the mean intensity of *Brachyury*^{EGFP}, *MesP1*^{EGFP} and *Nkx2.5*^{EGFP} expression in undifferentiated reporter CVPC lines.

mRNA levels of *EGFP*, *Brachyury*, *MesP1* and *Nkx2.5*

First, we determined *Brachyury*, *MesP1* and *Nkx2.5* mRNA levels in different clones of Brachyury^{EGFP}, MesP1^{EGFP} and Nkx2.5^{EGFP} reporter CVPC lines and tested whether these levels correlated with *EGFP* mRNA levels in the same clones. We also analysed *Brachyury*, *MesP1* and *Nkx2.5* mRNA levels in the CVPC line A5 from which our CVPC reporter lines had been derived.

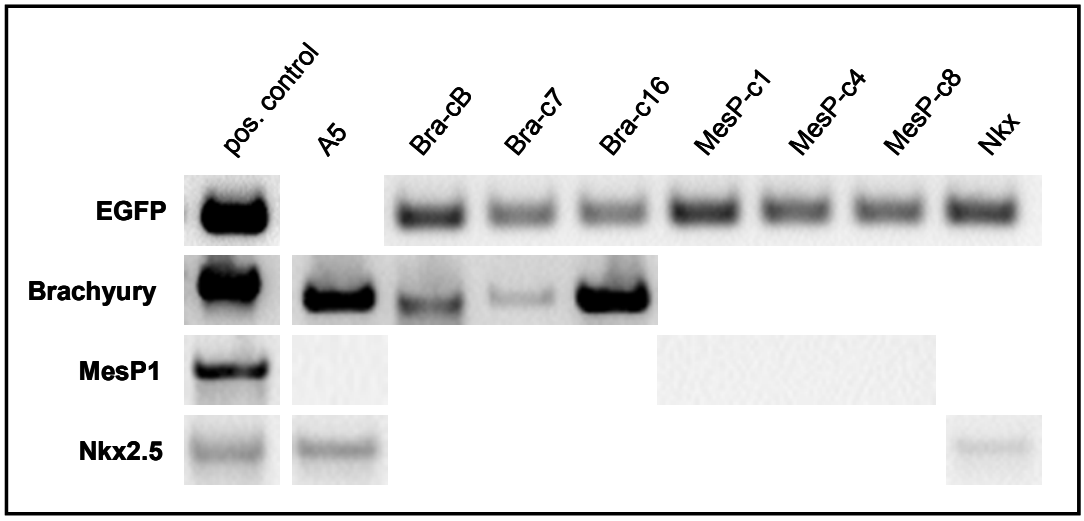

Figure 4.55: Correlation between reporter gene and gene of interest expression in **CVPCs**. Semi-quantitative PCR analyses of *EGFP*, endogenous *Brachyury*, *MesP1* and *Nkx2.5* mRNA levels in undifferentiated ESC lines and Brachyury^{EGFP}, MesP1^{EGFP} or Nkx2.5^{EGFP} reporter CVPC lines. Visualisation on agarose gel. Positive controls: plasmid MesP-EGFP for *EGFP* primers, cDNA of Ab2.2 cells on day 4.7 of differentiation generated by Julia Hoebaus for *Brachyury* and *MesP1* primers and cDNA of A5 cells on day 3 of differentiation generated by Jasmin Taubenschmid for *Nkx2.5* primers.

We then detected the integrated density levels of the PCR signals on the agarose gels of the mRNA levels mentioned and depicted above.

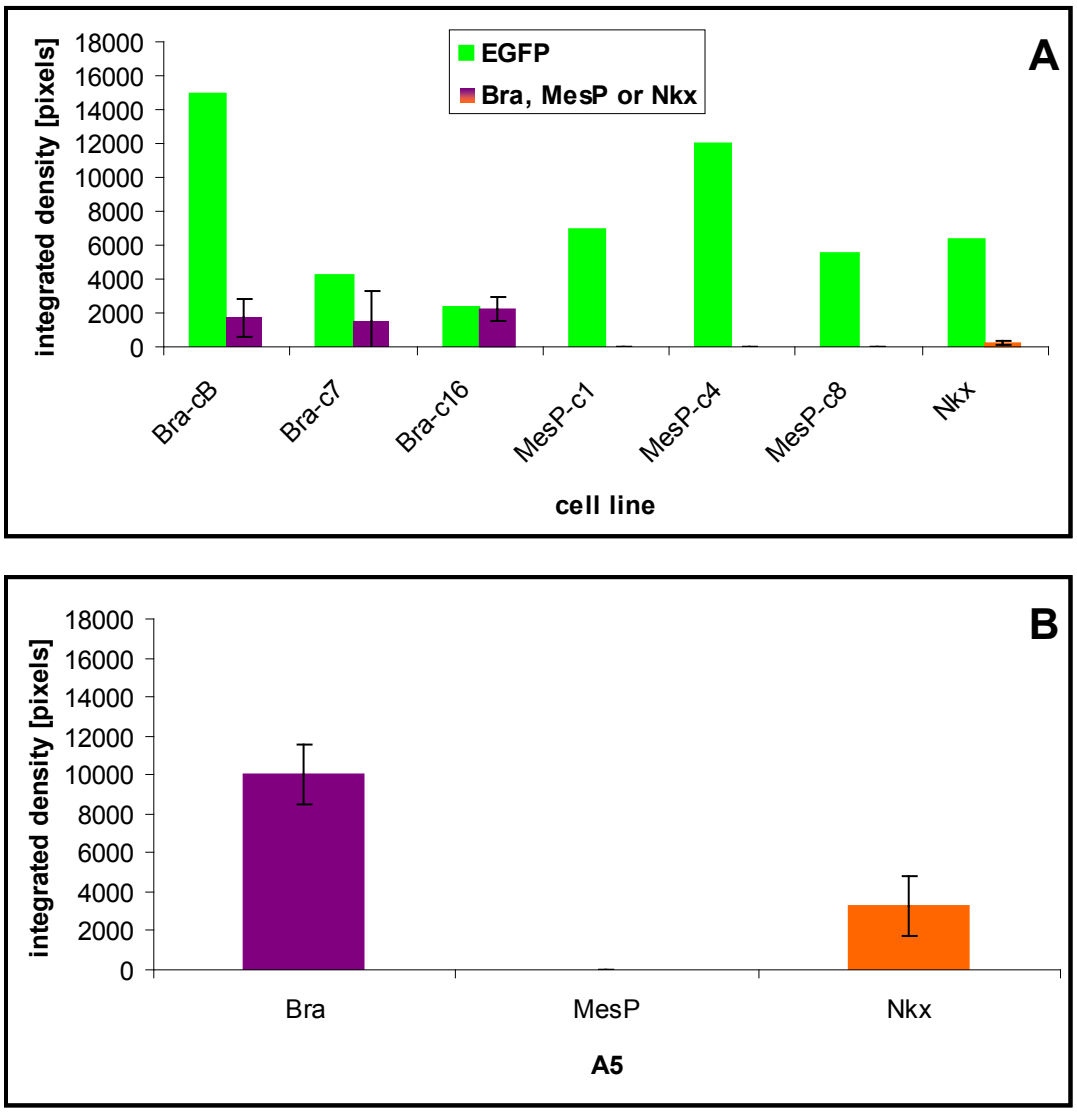

Figure 4.56: Correlation between reporter gene and gene of interest expression in **CVPCs**. Semi-quantitative PCR analyses of *EGFP* (green bars) and endogenous *Brachyury* (purple bars), *MesP1* or *Nkx2.5* (orange bars) mRNA levels.

A) In Brachyury^{EGFP} (detection of *EGFP* and *Brachyury*), MesP1^{EGFP} (detection of *EGFP* and *MesP1*) or Nkx2.5^{EGFP} (detection of *EGFP* and *Nkx2.5*) reporter CVPC lines.

B) In undifferentiated CVPC line (A5; detection of *Brachyury*, *MesP1* and *Nkx2.5*).

Levels of integrated density of the PCR signal on an agarose gel. Error bars: SD.

Unlike the clones of the Brachyury^{EGFP} ESC line all tested clones of the Brachyury^{EGFP} CVPC line expressed *Brachyury* mRNA in the undifferentiated state and levels were rather similar in the different clones as demonstrated in figure 4.56A. Levels of *EGFP* mRNA were comparable with levels of *Brachyury* mRNA in clones c7 and c16 of the Brachyury^{EGFP} CVPC line. However, in clone cB of the Brachyury^{EGFP} CVPC line, which

had been used in all the other experiments of this thesis, *EGFP* mRNA was much more highly expressed than *Brachyury* mRNA.

Exactly like the clones of the MesP1^{EGFP} ESC line, none of the clones of the MesP1^{EGFP} CVPC line expressed *MesP1* mRNA but they all expressed rather high levels of *EGFP* mRNA which were highest in clone c4 as shown in figure 4.56A. Therefore, levels of *EGFP* and *MesP1* mRNA were clearly not comparable in the MesP1^{EGFP} CVPC line.

In the Nkx2.5^{EGFP} CVPC line very low levels of *Nkx2.5* mRNA and rather high levels of *EGFP* mRNA were found as depicted in figure 4.56A. Levels of both *Nkx2.5* mRNA and *EGFP* mRNA were similar in the Nkx2.5^{EGFP} CVPC line and the Nkx2.5^{EGFP} ESC line (Figure 4.49A). Like in the Nkx2.5^{EGFP} ESC line levels of *Nkx2.5* mRNA and *EGFP* mRNA did not seem comparable despite the fact that the EGFP gene was directly integrated into the NKX2.5 gene. It might be possible that *EGFP* and *Nkx2.5* primers differed in their efficiency which might have to be considered for this comparison (see section 5.4).

In the A5 cell line high levels of *Brachyury* mRNA, lower levels of *Nkx2.5* mRNA and no *MesP1* mRNA were detected as shown in figure 4.56B. The levels of *Brachyury* mRNA in the A5 cell line were much higher than those in the Brachyury^{EGFP} CVPC (Figure 4.56A) and ESC lines (Figure 4.49A) as well as in the Ab2.2 and W4 cell lines (Figure 4.49B). As A5 cells are already more committed towards a certain cell type than W4 or Ab2.2 cells (ESCs) it is not surprising that they express higher levels of *Brachyury* mRNA. However, it is unexpected that A5 cells express higher levels of *Brachyury* mRNA than cells of the Brachyury^{EGFP} CVPC line and might indicate that the transgene interferes with physiological *Brachyury* expression.

Also *Nkx2.5* mRNA levels in the A5 cell line exceeded those in Nkx2.5^{EGFP} ESC and CVPC lines (Figure 4.56A) as well as those in W4 and Ab2.2 cell lines (Figure 4.49B). It was expected that the Nkx2.5^{EGFP} CVPC line would express lower levels of *Nkx2.5* mRNA than the A5 cell line because one allele of the NKX2.5 gene had been disrupted by the EGFP gene in the Nkx2.5^{EGFP} CVPC line. However, the Nkx2.5^{EGFP} CVPC line should still express approximately half of the *Nkx2.5* mRNA levels detected in the A5 cell line which was clearly not the case here.

The A5 cell line was previously shown to express *Brachyury*, *MesP1* and *Nkx2.5* mRNA (Hoebaus et al., 2013), yet no *MesP1* mRNA was detected in the A5 or the MesP1^{EGFP} CVPC lines in this experiment (Figure 4.56A and B). It can be excluded that the *MesP1* primers were defective as they produced a signal for the positive control (Figure 4.55).

FACS analysis

The proportions of *Brachyury*^{EGFP}, *MesP1*^{EGFP} and *Nkx2.5*^{EGFP} expressing cells in different clones of reporter CVPC lines were determined and compared with *EGFP* and endogenous *Brachyury*, *MesP1* and *Nkx2.5* mRNA levels.

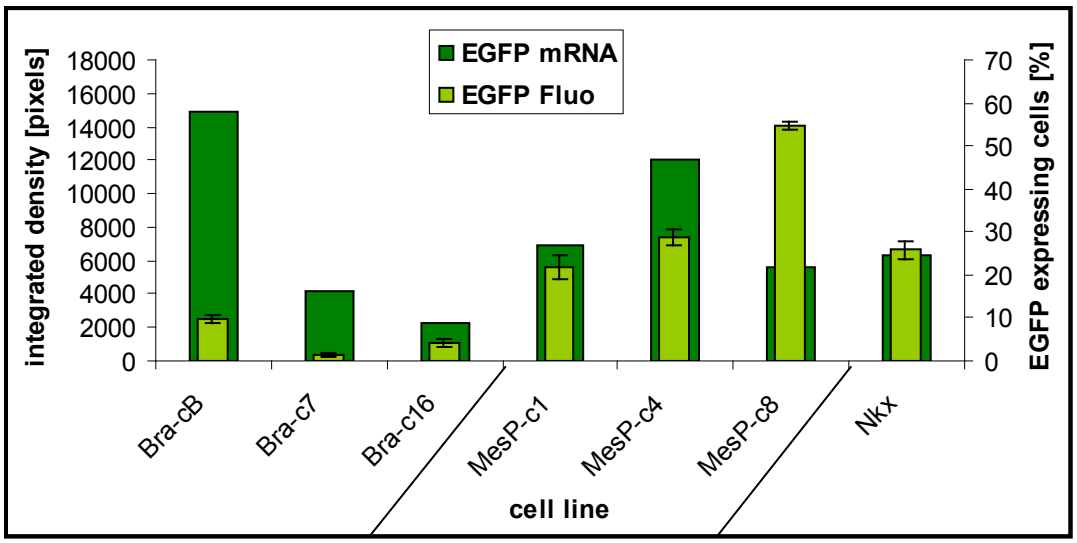

Figure 4.57: Reporter gene expression in **CVPCs**. Comparison between *EGFP* mRNA and EGFP protein expression in different clones of Brachyury^{EGFP}, MesP1^{EGFP} and Nkx2.5^{EGFP} reporter CVPC lines. Semi-quantitative PCR analyses of *EGFP* mRNA levels in Brachyury^{EGFP}, MesP1^{EGFP} or Nkx2.5^{EGFP} reporter CVPC lines. Levels of integrated density of the PCR signal on an agarose gel (dark green bars). FACS analyses of undifferentiated Brachyury^{EGFP}, MesP1^{EGFP} and Nkx2.5^{EGFP} CVPC reporter lines. Proportion of CVPCs expressing *Brachyury*^{EGFP}, *MesP1*^{EGFP} or *Nkx2.5*^{EGFP} (light green bars). Error bars: SD.

As depicted in figure 4.57 the proportion of *Brachyury*^{EGFP} expressing cells in clone cB of the Brachyury^{EGFP} CVPC line was higher than that in clones c7 and c16 of the same cell line. This trend was not reflected by *Brachyury* mRNA levels which were quite similar between the different clones of the Brachyury^{EGFP} CVPC line as shown in figure 4.56A but *EGFP* mRNA levels of clone cB of the Brachyury^{EGFP} CVPC line were also higher than those of the other two clones of the same cell line. Therefore, on day 0 of differentiation endogenous *Brachyury* mRNA levels in CVPCs and the proportion of CVPCs expressing Brachyury^{EGFP} protein could not be compared in the other experiments of this thesis in which only clone cB of the Brachyury^{EGFP} CVPC line was used. However, it might be possible that endogenous Brachyury protein levels were comparable to the proportion of *Brachyury*^{EGFP} expressing CVPCs, which we did not investigate here.

The highest proportion of *MesP1*^{EGFP} expressing cells in the MesP1^{EGFP} CVPC line could be detected in clone c8 whereas *EGFP* mRNA levels were highest in clone c4 as can be seen in figure 4.57. In the other clones the proportions of *MesP1*^{EGFP} expressing cells were also quite high while none of the clones was actually expressing *MesP1* mRNA (Figure 4.56A). But again, we did not analyse MesP1 protein expression in these cell lines which might be comparable to the proportion of *MesP1*^{EGFP} expressing CVPCs.
In the Nkx2.5^{EGFP} CVPC line a rather high proportion of *Nkx2.5*^{EGFP} expressing cells was detected (Figure 4.57) whereas levels of *Nkx2.5* mRNA were very low (Figure 4.56). Thus, levels of *Nkx2.5* mRNA and the proportion of *Nkx2.5*^{EGFP} expressing cells did not seem to be comparable in the Nkx2.5^{EGFP} CVPC line but might have to be compared with a different approach (see section 5.4). EGFP fluorescence and *EGFP* mRNA levels correlate well in the Nkx2.5^{EGFP} CVPC line.

The mean intensity of *Brachyury*^{EGFP}, *MesP1*^{EGFP} and *Nkx2.5*^{EGFP} expression in different clones of reporter CVPC lines was also detected and compared to *EGFP* and *Brachyury*, *MesP1* and *Nkx2.5* mRNA levels.

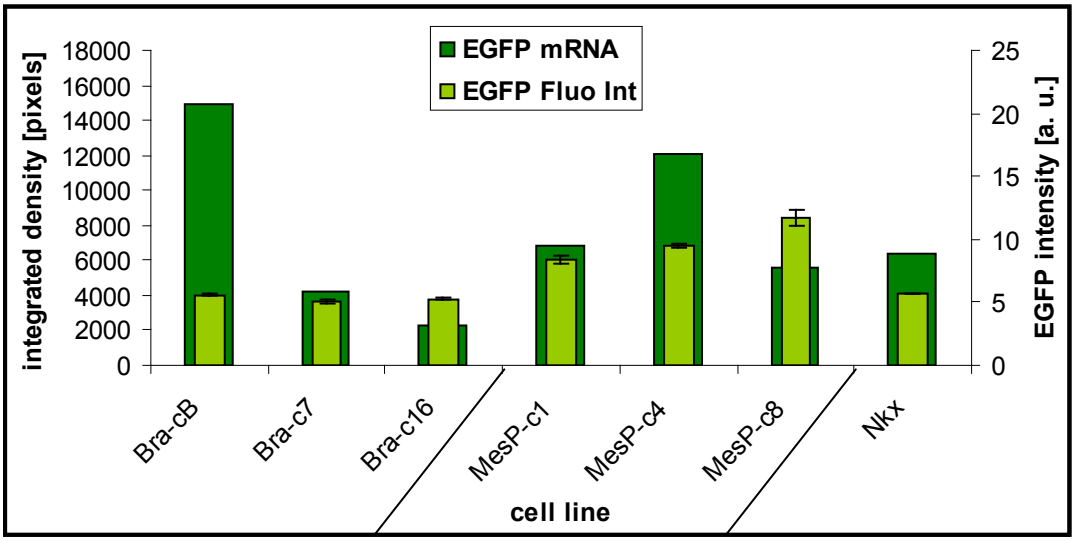

Figure 4.58: Reporter gene expression in **CVPCs**. Comparison between *EGFP* mRNA and EGFP protein expression in different clones of Brachyury^{EGFP}, MesP1^{EGFP} and Nkx2.5^{EGFP} reporter CVPC lines. Semi-quantitative PCR analyses of *EGFP* mRNA levels in Brachyury^{EGFP}, MesP1^{EGFP} or Nkx2.5^{EGFP} reporter CVPC lines. Levels of integrated density of the PCR signal on an agarose gel (dark green bars). FACS analyses of undifferentiated Brachyury^{EGFP}, MesP1^{EGFP} and Nkx2.5^{EGFP} CVPC reporter lines. Mean intensity of *Brachyury*^{EGFP}, *MesP1*^{EGFP} and *Nkx2.5*^{EGFP} expression in CVPCs (light green bars). Error bars: SD.

As shown in figure 4.58 levels of *EGFP* mRNA and the mean intensity levels of *Brachyury*^{EGFP} expression were comparable in clone c7 but did not correlate in clones cB and c16 of the CVPC Brachyury^{EGFP} reporter cell line. Generally, levels of mean intensity of *Brachyury*^{EGFP} expression were similar between different clones of the CVPC Brachyury^{EGFP} reporter cell line which was reflected by the *Brachyury* mRNA levels in this cell line (Figure 4.56A).

There was no great difference in the mean intensity of *MesP1*^{EGFP} expression in the different clones of the CVPC MesP1^{EGFP} reporter cell line but it was higher than that of the CVPC Brachyury^{EGFP} reporter cell line as depicted in figure 4.58. In clones c1 and c8 mean *EGFP* intensity levels correlated quite well with *EGFP* mRNA levels while *EGFP* intensity levels did not seem to be comparable with *EGFP* mRNA levels in clone c4. The mean intensity of *MesP1*^{EGFP} expression and *MesP1* mRNA levels were not comparable in the CVPC MesP1^{EGFP} reporter cell line as no *MesP1* mRNA was found in this cell line (Figure 4.56A) but it might be comparable to MesP1 protein levels which we did not analyse here.

Levels of mean *EGFP* intensity and *EGFP* mRNA levels correlated well in the CVPC Nkx2.5^{EGFP} reporter cell line as demonstrated in figure 4.58. In this cell line the mean intensity of *Nkx2.5*^{EGFP} expression was similar to *Brachyury*^{EGFP} expression intensity in the different clones of the CVPC Brachyury^{EGFP} reporter cell line. However, *Nkx2.5* mRNA levels in the CVPC Nkx2.5^{EGFP} reporter cell line were higher than *Brachyury* mRNA levels in the different clones of the CVPC Brachyury^{EGFP} reporter cell line (Figure 4.56A). Thus, the mean *EGFP* intensity and *Nkx2.5* mRNA levels did not seem to correlate in the CVPC Nkx2.5 reporter cell line but again there might be a correlation with NKX2.5 protein levels.

We also compared the proportions of *Brachyury*^{EGFP} and *MesP1*^{EGFP} expressing CVPCs between cells which had been treated according to the CB protocol and cells which had been treated according to the monolayer cell culture protocol.

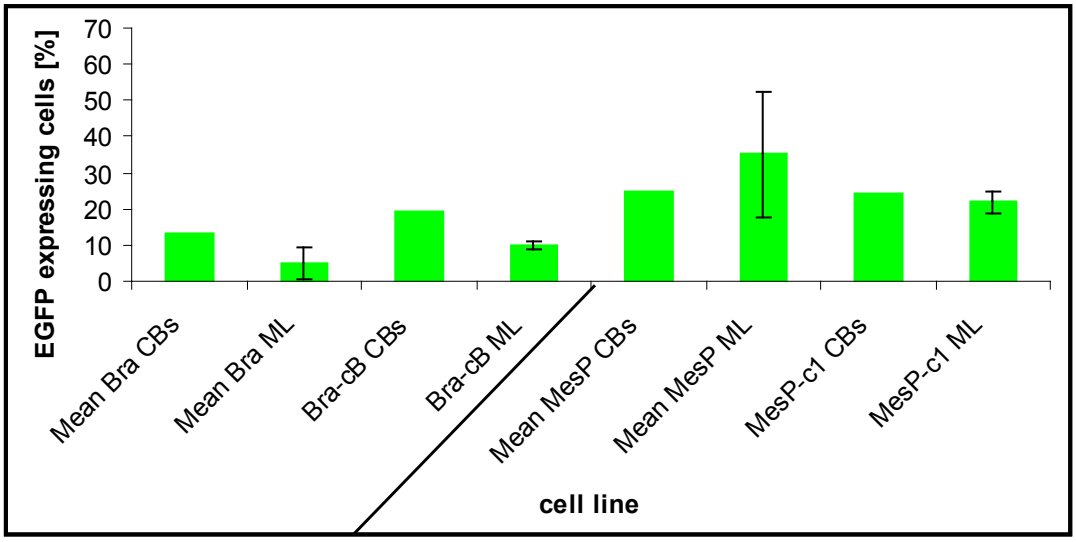

Figure 4.59: Reporter gene expression in **CVPCs**. Comparison between CB and monolayer cell culture protocols. FACS analyses of undifferentiated Brachyury^{EGFP} and MesP1^{EGFP} CVPC reporter lines either treated according to the hanging drop culture or the monolayer cell culture protocol. Proportion of CVPCs expressing *Brachyury^{EGFP}* or *MesP1^{EGFP}*. Mean: Mean values of the proportions of CVPCs expressing *Brachyury^{EGFP}* or *MesP1^{EGFP}* in different clones of Brachyury^{EGFP} or MesP1^{EGFP} CVPC reporter lines. Data for monolayer cell culture comprised of mean values of EGFP Fluo data from figure 4.57. Data for CBs was produced by Lucia Leitner in the course of her diploma thesis (Leitner, 2013). Error bars: SD. CBs: cardiac bodies. ML: monolayer.

The proportions of *Brachyury^{EGFP}* expressing CVPCs on day 0 of differentiation were higher in cells which had been treated according to the CB protocol than in cells treated according to the monolayer cell culture protocol as depicted in figure 4.59.
Mean values of the proportions of *MesP1^{EGFP}* expressing cells in different clones of the MesP1^{EGFP} CVPC line were lower in cells which had been treated according to the CB protocol. When only looking at clone cA of the MesP1^{EGFP} CVPC line, which had been used in both experiments, the proportions of *MesP1^{EGFP}* expressing CVPCs were similar for the two protocols.
In CVPCs treated according to the CB protocol the high proportions of *Brachyury^{EGFP}* and *MesP1^{EGFP}* expressing cells on day 0 of differentiation were probably only partially caused by a stress response to trypsinisation and were also due to the regular expression of *Brachyury* and *MesP1* in CVPCs which are already more committed towards a certain cell type than ESCs.

We assessed the proportions of dead cells in different clones of reporter CVPC lines after treatment according to the monolayer cell culture protocol.

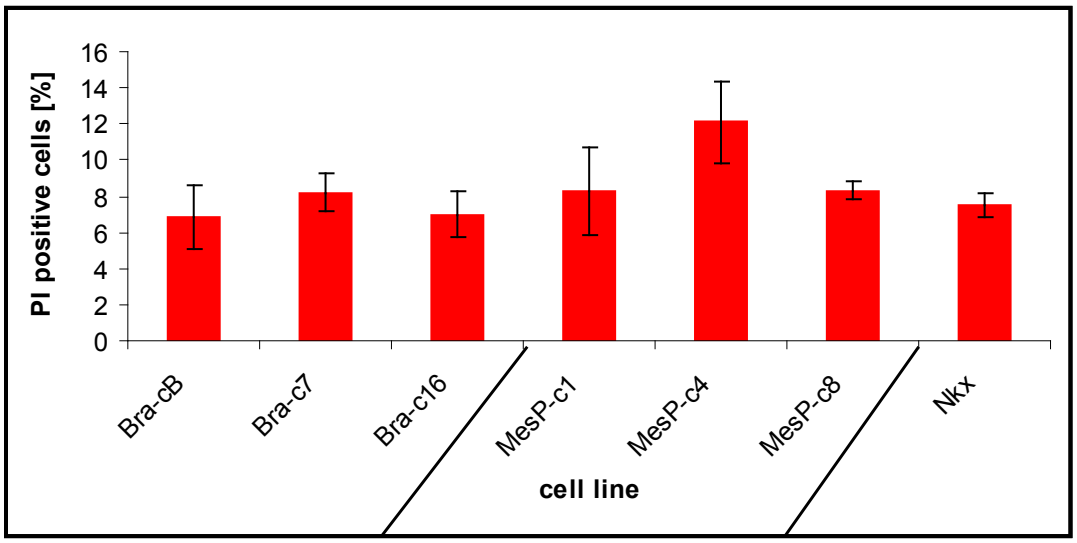

Figure 4.60: Reporter gene expression in **CVPCs**. FACS analyses of undifferentiated Brachyury^{EGFP}, MesP1^{EGFP} and Nkx2.5^{EGFP} CVPC reporter lines. Proportion of PI positive (dead) CVPCs. Error bars: SD.

The proportions of PI positive cells were rather low and quite similar in all the clones of the different CVPC reporter lines as shown in figure 4.60.

We then compared the mean values of the proportions of dead cells between CVPCs treated according to the monolayer cell culture method and CVPCs treated according to the hanging drop culture method.

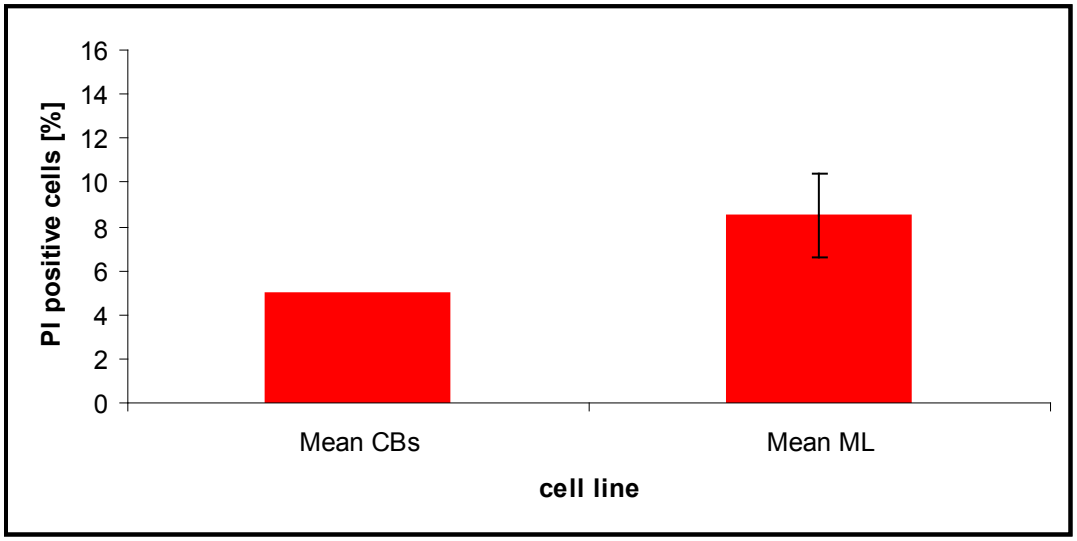

Figure 4.61: Reporter gene expression in **CVPCs**. Comparison between CB and monolayer cell culture protocols. FACS analyses of undifferentiated Brachyury^{EGFP} and MesP1^{EGFP} CVPC reporter lines either treated according to the hanging drop culture or the monolayer cell culture protocol. Mean: Mean values of the proportions of PI positive (dead) cells in different clones of undifferentiated Brachyury^{EGFP} and

MesP1^{EGFP} CVPC reporter lines in monolayer cell culture or in CBs. Data for monolayer cell culture comprises of mean values of portions of PI positive cells of Brachyury^{EGFP} and MesP1^{EGFP} CVPC reporter lines presented in figure 4.60. Data for CBs was produced by Lucia Leitner in the course of her diploma thesis (Leitner, 2013). Error bars: SD. CBs: cardiac bodies. ML: monolayer.

Figure 4.61 shows that the mean values of the proportions of dead cells in all the clones of Brachyury^{EGFP} and MesP1^{EGFP} reporter CVPC lines were lower in cells treated according to the CB protocol than in cells treated according to the monolayer protocol but the difference was rather small as shown in figure 4.61. Therefore, trypsinisation one day prior to the FACS analysis as required for the generation of CBs did not lead to enhanced cell death in CVPCs.

4.6 Wnt signalling in low volume monolayer ESC/CVPC culture

None of the reporter CVPC and ESC lines differentiated into contracting cardiomyocytes in any of the conditions we tested in low volume monolayer cell culture. We wanted to investigate whether ESCs and CVPCs still actively performed Wnt signalling or whether this signalling was hampered in low volume monolayer cell culture as Wnt signalling plays an important role in the induction of *Brachyury* expression and possibly also in the induction of *MesP1* expression. To address this question we used TOPflash reporter ESC and CVPC lines. These cell lines carry several copies of TCF/LEF sites upstream of a firefly luciferase open reading frame in their genome and can therefore be used to monitor transcriptional activation by β-catenin, hence active Wnt signalling, by measuring luminescence in a luciferase assay (see also section 1.5.4).

TOPflash ESC or CVPC lines were separated from feeder cells and $5x10^5$ or 10^5 cells per well, respectively, were placed onto gelatinised 48-well plates. Cells were either left untreated or treated with 2.5 µM CHIR99021 throughout the whole experiment to enhance the signal of possibly weak Wnt signalling in low volume monolayer cell culture.

Luminescence measurements were performed on days 0, 1, 3, 5, 7, 9, 11, 13, 15 and 16 of differentiation. Three aliquots of 50 µl were taken of each sample but only two aliquots were mixed 1:1 with the luciferase substrate so that one aliquot could serve as a negative control. The luminescence of each aliquot was measured three times. The limit of detection (LOD) was calculated from the mean value and standard deviation of all blank measurements. The readouts of empty wells as well as samples without luciferase substrate served as blanks.

4.6.1 Monitoring Wnt signalling at different time points of differentiation in untreated and CHIR99021 treated embryonic stem cells

To test whether canonical Wnt signalling is active in differentiating ESCs in low volume monolayer cell culture we performed luciferase assays at several time points of differentiation using an ESC TOPflash reporter cell line.

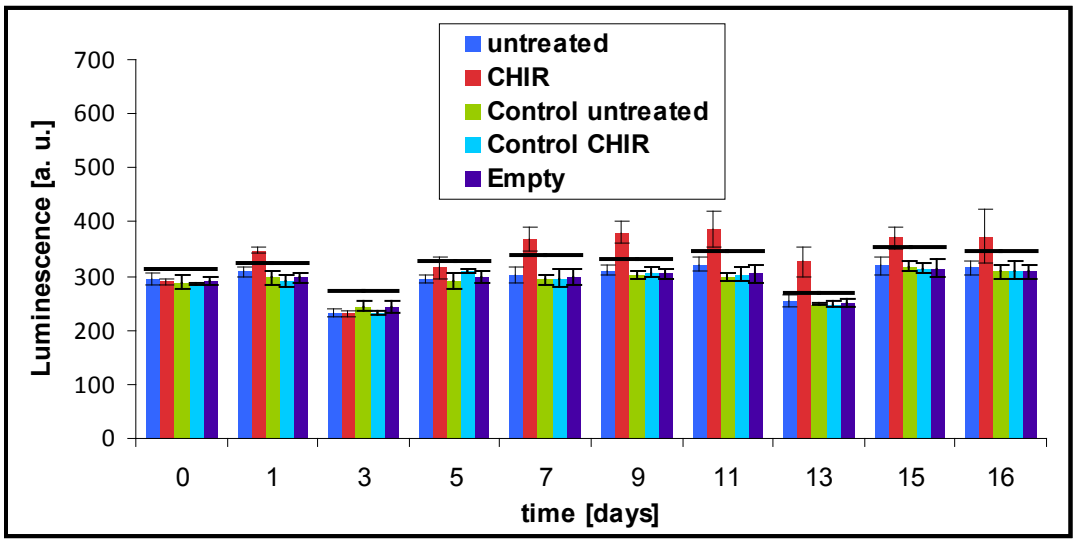

Figure 4.62: Wnt signalling in differentiating **ESCs** in monolayer cell culture. Luciferase assays of TOPflash reporter ESC line on days 0-16 of differentiation after treatment with 2.5 µM CHIR99021 for 0-16 days. Luminescence in untreated or CHIR99021 treated ESCs seeded on 48-well plates ($5x10^5$ cells per well) on day 0 of differentiation. Controls: cell suspension without luciferase substrate. Empty: empty well. Black horizontal lines: LOD. Error bars: SD.

As depicted in figure 4.62 Wnt signalling could be induced by CHIR treatment in differentiating ESCs in low volume cell culture at most time points of differentiation. Wnt signalling was most strongly induced in these cells between day 7 and 13 of differentiation. However, reporter TOPflash ESCs, which had not been treated with CHIR, did not show luminescence above control levels and the LOD meaning that β-catenin activity induced by Wnt signalling could not be detected in these cells at any time point of differentiation in low volume monolayer cell culture. No distinct peak of luminescence could be detected which this cell line showed in previous experiments with EBs on day 5 of differentiation (Figure 4.62; Leitner, 2013).

These findings indicate that Wnt signalling might be hindered in low volume monolayer ESC culture and that ESCs are only mildly responsive to external stimuli under these conditions as was already shown in the experiment of section 4.3.

4.6.2 Monitoring Wnt signalling at different time points of differentiation in untreated and CHIR99021 treated cardiovascular progenitor cells

The activity of canonical Wnt signalling was also assessed using luminescence assays in differentiating CVPCs in low volume monolayer cell culture at several time points of differentiation.

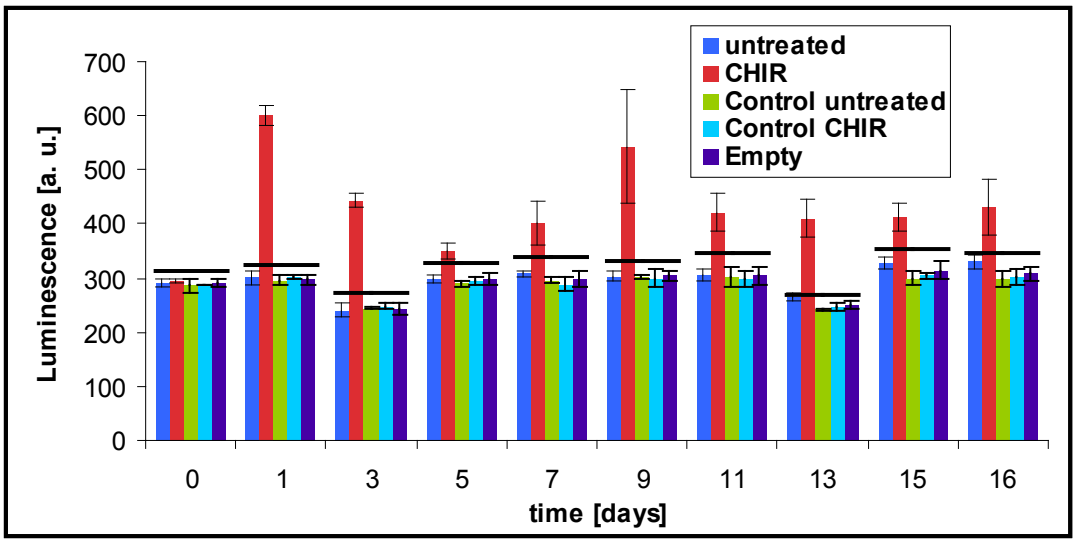

Figure 4.63: Wnt signalling in differentiating **CVPCs** in monolayer cell culture. Luciferase assays of TOPflash reporter ESC line on days 0-16 of differentiation after treatment with 2.5 µM CHIR99021 for 0-16 days. Luminescence in untreated or CHIR99021 treated CVPCs seeded on 48-well plates (10^5 cells per well) on day 0 of differentiation. Controls: cell suspension without luciferase substrate. Empty: empty wells. Black horizontal lines: LOD. Error bars: SD.

Figure 4.63 shows that enhanced levels of luminescence could be detected after CHIR treatment in this cell line at most time points of differentiation with these levels substantially exceeding the limit of detection on days 1, 3, 9 and 13 of differentiation. In contrast, luminescence levels above the LOD and above control levels could not be observed in the untreated TOPflash reporter CVPC line in low volume monolayer cell culture. There could not be observed a distinct peak of luminescence on a certain time point as it was detected on day 5 of differentiation in former experiments using CBs (Figure 4.63; Leitner, 2013).

Similar to the situation in ESCs Wnt signalling seemed to be blocked in CVPCs in the conditions provided by low volume monolayer cell culture. However, CVPCs seemed to be more responsive to CHIR treatment than ESCs. As CVPCs were most sensitive to CHIR treatment at early time points of differentiation and then again at later time points of

differentiation one could speculate that certain cells started to differentiate at later time points than other cells in the same culture system.

4.7 Preferential directions of differentiation of CVPCs in low volume monolayer cell culture

In low volume monolayer cell culture CVPCs were not capable to perform active Wnt signalling which probably plays an important role in the early stages of cardiomyogenesis. As already pointed out no contracting cardiomyocytes could be detected by light microscopy in low volume monolayer CVPC culture. However, CVPCs did differentiate under these conditions and an especially high number of endothelial cells could be observed using light microscopy. Thus, we wanted to further investigate this differentiation behaviour of CVPCs in low volume monolayer cell culture to see whether low volume monolayer cell culture promotes the differentiation of other cell types than cardiomyocytes.

Therefore, we compared the expression of the endothelial cell markers, *Cd31* and *Cd34* (Garlanda and Dejana, 1997), *c-Kit* (Rafii et al., 2002), *eNos* (Minami and Aird, 2005), *Pim1* (Walpen et al., 2012; Zippo et al., 2004) and *VE-cadherin* (Breier et al. 1996), of the cardiomyocyte markers, *Gata4* (Perrino and Rockman, 2006), *Desmin* (Milner et al., 1999), *Nkx2.5* (Schwartz and Olson, 1999), *Tropomyosin-α* (Muthuchamy et al., 1993) and *Mef2c* (Liu et al., 2001), and of the cardiac fibroblast markers, *Vimentin* (Ieda et al., 2009) and *Ddr2* (Goldsmith et al., 2004), between CBs and differentiating CVPCs in low volume monolayer cell culture.

The TOPflash reporter CVPC line was used for this experiment. mRNA was isolated from CBs and CVPCs in low volume monolayer cell culture on days 0, 3, 5, 7 and 9 of differentiation and was reverse transcribed into cDNA. Samples were normalised by semi-quantitative PCR analysis using primers for the housekeeping gene *Hprt* prior to semi-quantitative PCR analyses with primers for the marker genes mentioned above. PCR reactions were repeated once except for reactions with primers for *eNos*, *Nkx2.5* and *Mef2c* which were only done once. PCR samples were separated on an agarose gel and the intensity of the signal on the gel was detected by measuring its integrated density with the computer programme ImageJ and adjusting it to the background signal.

4.7.1 Expression of endothelial cell, cardiomyocyte and cardiac fibroblast markers in CBs and monolayer CVPC culture

To test whether the extent of endothelial cell differentiation differed between monolayer and hanging drop cell culture we investigated mRNA levels of several endothelial marker genes at various time points of differentiation in the two systems.

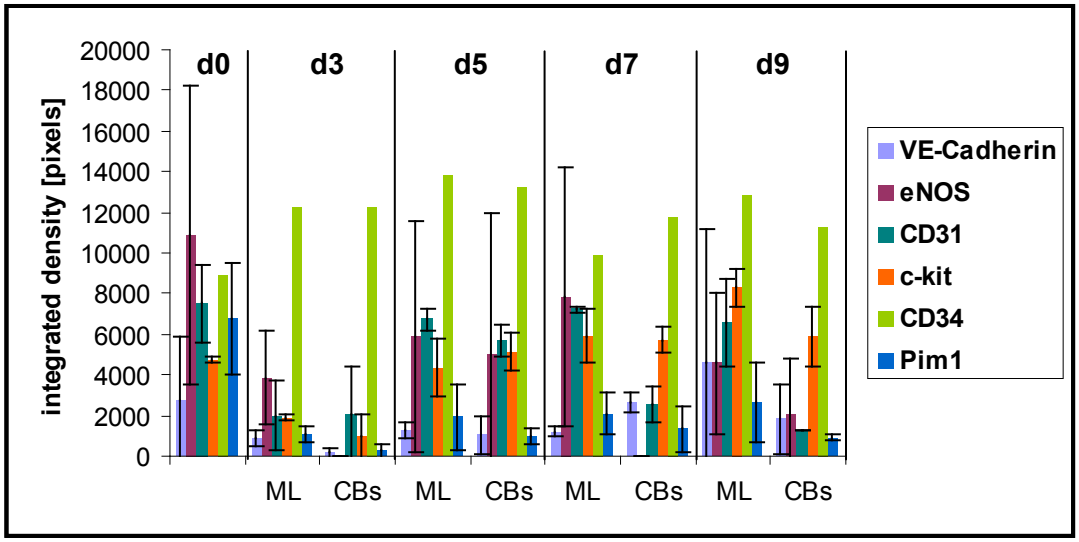

Figure 4.64: Semi-quantitative RT PCR analyses of endogenous *VE-cadherin*, *eNos*, *Cd31*, *c-Kit*, *Cd34* and *Pim1* (endothelial cell markers) mRNA levels in **CBs** and **CVPC** monolayer cell cultures of TOPflash CVPC line on days 0-9 of differentiation. Levels of integrated density of the PCR signal on an agarose gel. Error bars: SD. ML: monolayer. CBs: cardiac bodies.

As depicted in figure 4.64 most of the endothelial cell markers analysed here tended to be expressed at higher levels in monolayer cell culture than in CBs especially at later time points of differentiation. The difference was very significant for *Cd31* mRNA levels at later time points of differentiation. However, *Cd34* mRNA levels seemed to be similar in the two cell culture systems but this result could have also been caused by a quite high number of PCR cycles.

We also compared expression levels of cardiomyocyte markers between CBs and differentiating CVPCs in low volume monolayer cell culture at different time points of differentiation.

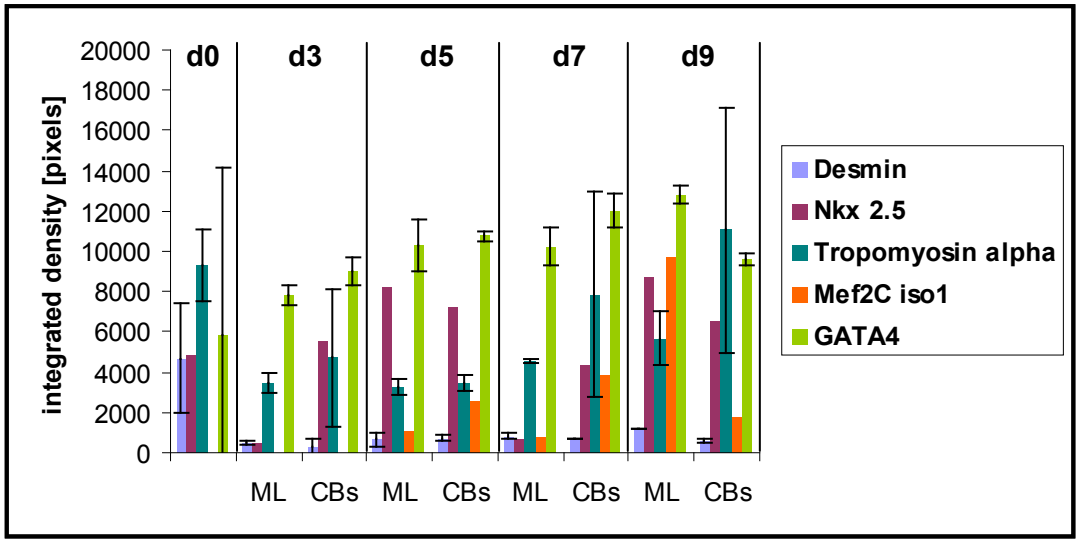

Figure 4.65: Semi-quantitative RT PCR analyses of endogenous *Desmin*, *Nkx2.5*, *Tropomyosin-α*, *Mef2c* and *Gata4* (cardiomyocyte markers) mRNA levels in **CBs** and **CVPC** monolayer cell cultures of TOPflash CVPC line on days 0-9 of differentiation. Levels of integrated density of the PCR signal on an agarose gel. Error bars: SD. ML: monolayer. CBs: cardiac bodies.

As can be seen in figure 4.65 the results were rather ambiguous for the cardiomyocyte markers. There was no big difference between the mRNA expression levels of *Gata4* and *Desmin* between CBs and monolayer cell culture. *Nkx2.5* and *Mef2c* were more highly expressed in CBs on certain time points of differentiation but were surprisingly highly expressed in monolayer cell culture on day 9 of differentiation. However, *Tropomyosin-α* clearly showed higher mRNA levels in CBs at later time points of differentiation.

Cardiac fibroblast marker expression levels were also investigated in differentiating CVPCs in both monolayer and hanging drop cell culture at several time points of differentiation.

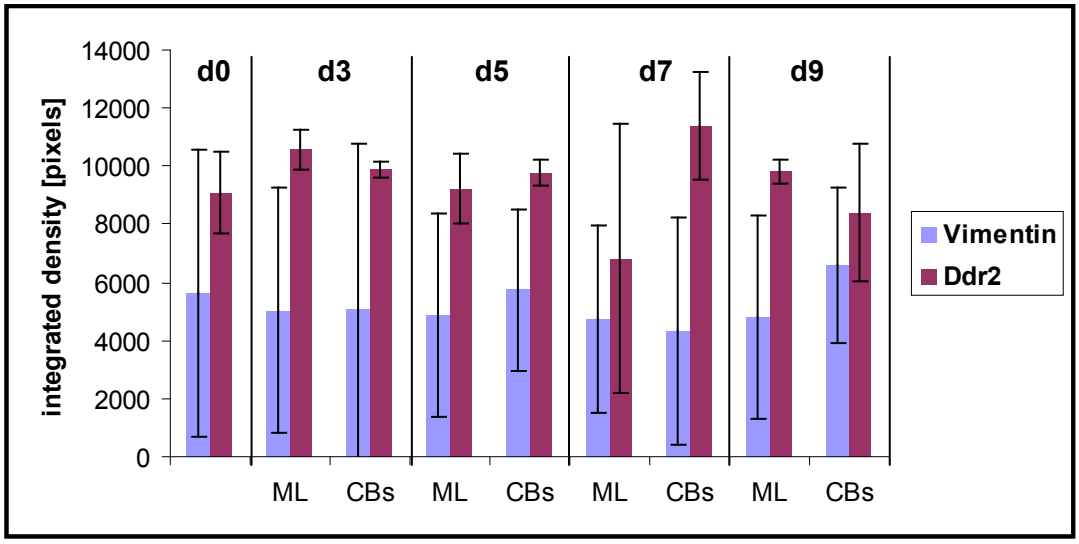

Figure 4.66: Semi-quantitative RT PCR analyses of endogenous *Vimentin* and *Ddr2* (cardiac fibroblast markers) mRNA levels in **CBs** and **CVPC** monolayer cell cultures of TOPflash CVPC line on days 0-9 of differentiation. Levels of integrated density of the PCR signal on an agarose gel. Error bars: SD. ML: monolayer. CBs: cardiac bodies.

Figure 4.66 shows that cardiac fibroblast markers were found to be similarly expressed in monolayer CVPC culture and CBs at most time points but *Vimentin* mRNA levels seemed to be slightly higher in CBs at a later time point of differentiation. The levels of *Ddr2* mRNA might have been overestimated as the number of PCR cycles was rather high.

All the markers were surprisingly highly expressed on day 0 of differentiation which might be a similar stress response as the one previously discussed to trypsinisation and the handling of the cells prior to mRNA isolation (Figures 4.64, 4.65 and 4.66).

These findings indicate that CVPCs preferentially differentiate into endothelial cells in low volume monolayer cell culture. However, a certain number of CVPCs still seem to differentiate towards cardiomyocytes as indicated by the expression of certain cardiac markers but seem to fail to successfully complete this differentiation.

5 Discussion

5.1 Development of contracting cardiomyocytes

As shown in figure 5.1, in none of the conditions applied in this thesis ESCs or CVPCs differentiated into contracting cardiomyocytes in low volume monolayer cell culture. However, in previous experiments CVPCs were shown to develop into beating cardiomyocytes in high volume (Hoebaus et al., 2013) as well as in medium volume monolayer cell culture (Hoebaus, 2009). In EBs or CBs both ESC and CVPC non-reporter (W4 and A5 cell lines) and Brachyury^{EGFP}, MesP1^{EGFP} and Nkx2.5^{EGFP} reporter cell lines used in this thesis developed very well into contracting cardiomyocytes (Gottschamel, 2010; Hoebaus et al., 2013; Lauss et al., 2005; Leitner, 2013; Figure 5.1).

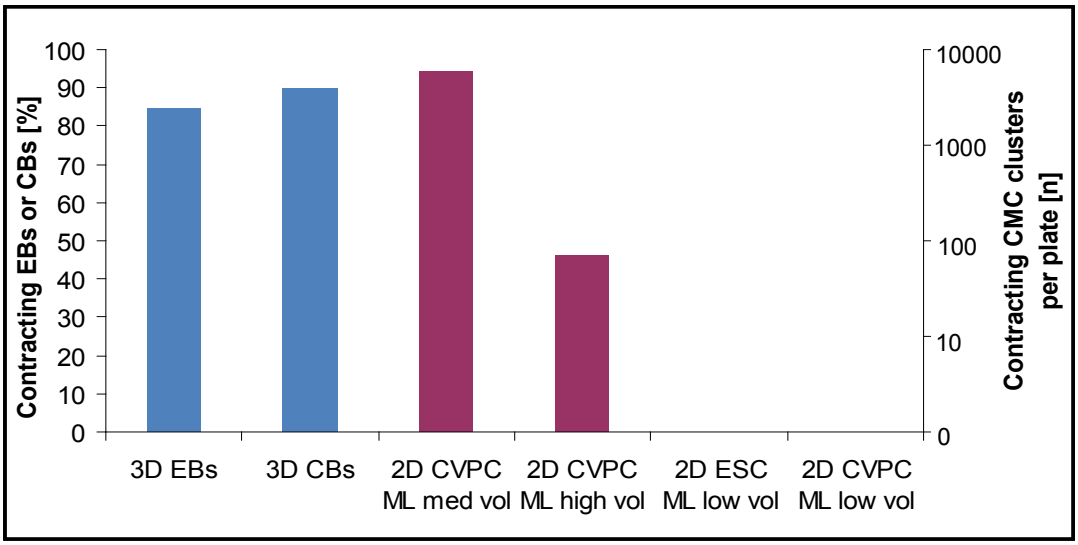

Figure 5.1: Quantification of contracting EBs and CBs (blue bars) or cardiomyocyte clusters (purple bars) in 3D hanging drop or 2D monolayer cell cultures in different volumes, respectively, using light microscopy. Data for EBs produced with W4 cell line by Lauss et al. (Lauss et al., 2005), data for CBs and high volume ML cell culture produced with A5 cell line by Hoebaus et al. (Hoebaus et al., 2013) and data for medium volume ML cell culture produced by Julia Hoebaus in the course of her diploma thesis (Hoebaus, 2009). Data for low volume ML cell culture comprised of all experiments in this thesis. ML: monolayer.

ESCs are not able to form beating cardiomyocytes in monolayer cell culture regardless of the volume. Apparently, the environment and the conditions created in EBs are more suitable for ESCs to differentiate into cardiomyocytes and come closer to the *in vivo*

situation. In EBs, a certain cell is surrounded by other cells in all directions and can directly communicate with and directly receive signals from these cells which seem to be essential requirements for cardiomyocyte differentiation of ESCs. Liu and co-workers compared gene expression profiles of differentiating ESCs cultured in either 2D monolayer culture or in different types of 3D cell culture and found certain extracellular matrix-related genes as well as several genes involved in cell growth, proliferation and differentiation to be more highly expressed in the 3D culture systems (Liu et al., 2006). However, human ESCs were shown to differentiate into contracting cardiomyocytes in monolayer cell culture under defined conditions (Laflamme et al., 2007; Lian et al., 2012).

CVPCs can develop into beating cardiomyocytes in high volume monolayer cell culture at rather high cell density with a starting cell number of approximately $1.7x10^6$ (Hoebaus et al., 2013) which probably partly mimics the 3D situation. High density EB culture also resulted in significantly enhanced cardiomyogenesis (Lee et al., 2011).

At high cell density the expression patterns of *Brachyury* and *MesP1* of ESCs and CVPCs in low volume monolayer cell culture comes closer to that observed in EBs and CBs. However, the number of dead cells rises dramatically, especially in CVPCs, at later time points of differentiation probably due to a lack of nutrients as only a small volume of medium can be administered (Section 4.4). Cells might die at high cell density in low volume monolayer cell culture before they can differentiate into contracting cardiomyocytes but it is also possible that the environment in low volume monolayer cell culture is simply not suited for cardiomyocyte development.

In contrast, in medium volume monolayer cell culture a starting cell number of $3x10^4$ cells was used (Hoebaus, 2009) and CVPCs differentiated more efficiently into cardiomyocytes compared to high volume monolayer cell culture. Thus, also at lower cell density successful cardiomyogenesis is possible. However, in this study the medium was only partially exchanged (Hoebaus, 2009) which was not possible for us due to the low volume of medium fitting in an 48-well and the concomitant high need of nutrients of cells grown at high cell density. The partial medium exchange probably resulted in a higher concentration of factors secreted by the cells in culture compared to full medium exchange as we performed it. One could speculate that, in high density low volume monolayer cell culture, the rising concentration of secreted factors produced by a higher number of cells compared to low density cell culture, might contribute to the assimilation of *Brachyury* and *MesP1* expression patterns towards those in EBs and CBs.

A possible strategy to induce cardiomyogenesis in low volume monolayer cell culture could be LIF treatment prior to monolayer culture establishment. In high and medium volume monolayer CVPC culture matrix-associated LIF (M-LIF) treatment for 30 days prior to the start of monolayer cell culture led to enhanced cardiomyocyte differentiation

(Hoebaus, 2009; Hoebaus et al., 2013). Furthermore, a combination treatment of LIF and BMP2 for 2 days stimulated expression of cardiomyocyte markers in ESCs (Rajasingh et al., 2007). Finally, in a mouse embryonic carcinoma cell line, LIF treatment for 15 minutes led to an induction of *Nkx2.5*, *Tbx5* and *Gata4* mRNA expression (Snyder et al., 2010).

5.2 *Brachyury*, *MesP1* and *Nkx2.5* expression patterns

In EBs, a clear peak of *Brachyury* and *MesP1* expression can be detected on day 5 of differentiation (Leitner, 2013) which is absent in differentiating ESCs in low volume monolayer cell culture as depicted in figure 4.8 and in table 5.1 (cell number $5x10^4$). Concomitantly, a higher percentage of cells is expressing *Brachyury* and especially *MesP1* in EBs (Leitner, 2013) than in low volume monolayer cell culture on day 5 of differentiation. These observations might indicate that certain stimuli which are responsible for the increase of *Brachyury* and *MesP1* expression in EBs are missing in monolayer cell culture and furthermore, that a lower proportion of ESCs differentiate into mesodermal progenitors and especially into cardiac progenitors in low volume monolayer cell culture compared to EBs. Interestingly, at the beginning of differentiation a higher proportion of cells express *Brachyury* and/or *MesP1* in monolayer cell culture than in EBs but this expression might not have been specific and these cells might not actually have differentiated into mesodermal or cardiac progenitors.

As shown in figure 4.10 the intensity of *Brachyury* expression was also lower at the beginning of differentiation in monolayer culture compared to EBs. Thus, expression levels in *Brachyury* expressing cells might have been too low for efficient further differentiation in low volume monolayer cell culture. However, *MesP1* expression levels were mostly similar in the two systems or even higher in monolayer cell culture. It is possible that ESCs differentiate into cardiac progenitors in low volume monolayer cell culture but that further development into cardiomyocytes is blocked.

This assumption is also supported by the observation that the proportion of *Nkx2.5* expressing cells is decreasing in the course of differentiation in monolayer cell culture as can be seen in figure 4.7 and in table 5.1. In contrast, at the beginning of differentiation the proportion of *Nkx2.5* expressing cells was quite high but this expression might have been not specific or too early for efficient cardiomyocyte differentiation. It is also possible that the expression levels of *Nkx2.5* were too low to propagate cardiomyocyte development. Figure 4.9 shows that the intensity of *Nkx2.5* expression stays constant during differentiation of ESCs in low volume monolayer cell culture. One could therefore speculate that there is a lack of external and/or internal stimuli which could influence *Nkx2.5* expression in low volume monolayer cell culture.

The proportion of *Brachyury* expressing cells is quite similar in differentiating CVPCs in monolayer cell culture and in CBs at the beginning of differentiation while it is higher in monolayer cell culture than in CBs later in development (Figure 4.13; cf. Leitner, 2013). It might be possible that certain CVPCs start to differentiate at a later time point in monolayer cell culture while the differentiation process is more temporally heterogenous in CBs. The level of *Brachyury* expression does not differ greatly between differentiating CVPCs in monolayer cell culture and CBs (cf. Leitner, 2013) except for later time points where the intensity of *Brachyury* expression increases in monolayer cell culture as shown in figure 4.15 which also supports the assumption of a later start of differentiation of certain cells in monolayer cell culture.

A higher percentage of differentiating CVPCs express *MesP1* in comparison to CBs (Figure 4.13; cf. Leitner, 2013). This proportion stays rather constant over time as shown in figure 4.12 and in table 5.1 (cell number $5x10^4$) and might indicate that these cells stay cardiac progenitors and do not differentiate further. The intensity of *MesP1* expression is higher in CBs (Figure 4.15; cf. Leitner, 2013) than in monolayer cell culture at most time points of differentiation which could mean that the level of *MesP1* expression is too low in differentiating CVPCs in low volume monolayer cell culture, especially at day 5 of differentiation, for an efficient differentiation into mature cardiomyocytes. At later time points of differentiation the intensity of *MesP1* expression rises in monolayer cell culture which might also be an indication for a late differentiation start of certain cells in this system.

The proportion of *Nkx2.*5 expressing cells is mostly lower in monolayer cell culture compared to CBs (Figure 4.13; cf. Walder, 2011) which might indicate that a lower proportion of cells differentiate towards the cardiac lineage in monolayer cell culture. Interestingly, a huge difference in the proportion of *Nkx2.5* expressing CVPCs can be observed between the two different studies on day 0 of differentiation, approximately 90 % of CVPCs expressed *Nkx2.5* in former experiments (cf. Walder, 2011) compared to only approximately 25 % in our experiments (Figure 4.13). This observation might be explained by the fact that different clones of the cell line were used in the different experiments.

In CBs, the proportion of *Nkx2.5* expressing cells is constantly declining (cf. Walder, 2011) while in monolayer cell culture an increase of *Nkx2.5* expression can be observed during the first three days of differentiation which is followed by a decrease of *Nkx2.5* expression as shown in figure 4.13 and in table 5.1. This constant decrease can probably be explained by the fact that CVPCs differentiate not only into cardiomyocytes but also into smooth muscle cells and endothelial cells in CBs. The different expression pattern of *Nkx2.5* in monolayer cell culture compared to CBs probably indicates that differentiation proceeds in a different way in monolayer cell culture than in CBs.

Similar to differentiating ESCs the intensity of *Nkx2.5* expression does not change to a great extent over time in differentiating CVPCs in low volume monolayer cell culture as depicted in figure 4.14 which further indicates that certain factors influencing *Nkx2.5* expression are absent in monolayer cell culture.

5.3 Impact of cell density on *Brachyury* and *MesP1* expression

As shown in table 5.1 and in section 4.4 cell density generally influences *Brachyury* and *MesP1* expression in low volume monolayer ESC and CVPC culture as *MesP1* and *Brachyury* expression patterns often vary greatly between different cell densities. This difference might be caused by different concentrations of secreted cellular factors dependent on cell density which influence gene expression in neighbouring cells. It is also possible that at higher cell densities secreted factors reach a higher number of cells. Different geometry of the whole cell culture system at different cell densities might also have an impact on gene expression.

At higher cell densities *MesP1* and *Brachyury* expression patterns in ESC and CVPC monolayer culture often resemble those in EBs and CBs to a greater extent compared to lower density monolayer cultures. For instance, the peak of the proportion of *Brachyury*^{EGFP} expressing cells in EBs can be mimicked in ESC monolayer culture at a cell number of 10^6 and differentiating ESCs in monolayer cell culture also exhibit this peak on day 6 at $5x10^5$ cells per well (Table 5.1, Figures 4.27 and 4.29). The peak of the proportion of *MesP1*^{EGFP} expressing cells in EBs cannot be detected in monolayer cell culture not even at high cell densities (Table 5.1, Figures 4.28 and 4.30).

However, EBs as well as differentiating ESCs in monolayer cell culture at a cell number of $5x10^5$ both show peaks of *MesP1*^{EGFP} intensity on day 5 of differentiation (Figures 4.32 and 4.34). The peak of *Brachyury*^{EGFP} intensity in EBs on day 5 of differentiation is also present in ESC monolayer culture at a cell number of $5x10^5$ (Figures 4.31 and 4.33).

The proportion of *Brachyury*^{EGFP} expressing cells is constantly declining over time in CBs while it is generally increasing starting from day 3 of differentiation in CVPC monolayer culture (Figure 4.39). However, at cell numbers of 10^5 and $5x10^5$ the proportion of *Brachyury*^{EGFP} expressing cells is decreasing at late time points of differentiation and it is already falling starting from day 7 of differentiation at a cell number of 10^6. Furthermore, the percentage of *Brachyury*^{EGFP} expressing cells is only increasing between day 5 and 7 of differentiation in low volume monolayer CVPC culture at a cell number of 10^6 (Table 5.1; Figure 4.37).

Similar to *Brachyury*^{EGFP} expression the proportion of *MesP1*^{EGFP} expressing cells is also mostly decreasing over time in CBs (Figure 4.40). As shown in table 5.1 and in figure 4.38

this pattern is mimicked in CVPC monolayer cell culture at lower cell density (cell number $5x10^4$) at most time points of differentiation. However, differentiating CVPCs in lower cell density monolayer cell culture show a peak of the proportion of *MesP1*^{EGFP} expressing cells on day 9 of differentiation which is absent in CBs and in CVPC monolayer culture at higher cell densities. At cell numbers 10^5 and $5x10^5$ the percentage of *MesP1*^{EGFP} expressing cells is decreasing starting from day 5 and 7, respectively, in monolayer CVPC culture. Thus, the *MesP1*^{EGFP} expression pattern in low density monolayer CVPC culture resembles that of CBs to a higher extent compared to high density monolayer CVPC culture. Nevertheless, the percentage values of *MesP1*^{EGFP} expressing cells are very similar between CBs and CVPC monolayer culture at cell number $5x10^5$ at late time points of differentiation (Figures 4.38 and 4.40).

The *Brachyury*^{EGFP} intensity patterns vary between CBs and CVPC monolayer culture at most time points of differentiation (Figure 4.43). However, peaks of *Brachyury*^{EGFP} expression intensity can be detected on day 9 of differentiation in both CVPC monolayer culture at cell number $5x10^5$ and in CBs (Figures 4.41 and 4.43).

Distinct peaks of *MesP1*^{EGFP} expression intensity can be observed both in CBs and in CVPC monolayer cell culture at cell number $5x10^5$ (Figures 4.42 and 4.44).

Even though the expression patterns of *Brachyury*^{EGFP} and *MesP1*^{EGFP} in high density monolayer cell culture are more similar to those in CBs compared to low density monolayer cell culture, the cells still fail to undergo successful cardiomyogenesis in high density monolayer cell culture. In CVPC monolayer culture this failure might be explained by the enhanced cell death at higher cell densities due to a lack of nutrients (Figures 4.45 and 4.46).

As already mentioned in section 5.1, strategies to overcome these problems might be only partial medium exchange when feeding the cells, which would have to involve shorter feeding intervals in low volume monolayer cell culture, or M-LIF treatment prior to the establishment of monolayer cell culture. Treating cells with CHIR99021 prior to the start of monolayer cell culture or at early time points of differentiation might also favour cardiomyocyte differentiation in low volume monolayer cell culture (see sections 5.5 and 5.6).

Cell type	Cell number	Gene	Expression pattern
ESC	$5x10^4$	*Brachyury*^{EGFP}	Peak on day 1 followed by constant decrease
ESC	10^5	*Brachyury*^{EGFP}	Distinct peak on day 1 followed by constant decrease
ESC	$5x10^5$	*Brachyury*^{EGFP}	Peak on day 1, increase after day 3 of differentiation, peak on day 6 followed by constant decrease
ESC	10^6	*Brachyury*^{EGFP}	Peak on day 1, increase after day 3 of differentiation, peak on day 5 followed by constant decrease
CVPC	$5x10^4$	*Brachyury*^{EGFP}	Decrease at early time points of differentiation, increase after day 3 of differentiation
CVPC	10^5	*Brachyury*^{EGFP}	Decrease at early time points of differentiation, increase after day 3 of differentiation, decrease at late time points of differentiation
CVPC	$5x10^5$	*Brachyury*^{EGFP}	Decrease at early time points of differentiation, increase after day 3 of differentiation, decrease at late time points of differentiation
CVPC	10^6	*Brachyury*^{EGFP}	Decrease at early time points of differentiation, increase after day 5 of differentiation, peak on day 7 followed by decrease
ESC	$5x10^4$	*MesP1*^{EGFP}	Small peak on day 1 followed by constant decrease
ESC	10^5	*MesP1*^{EGFP}	Constant decrease
ESC	$5x10^5$	*MesP1*^{EGFP}	Constant decrease
ESC	10^6	*MesP1*^{EGFP}	Constant decrease
CVPC	$5x10^4$	*MesP1*^{EGFP}	Distinct peak on day 1 of differentiation followed by steep decrease, then stays rather constant between days 3 and 11 of differentiation
CVPC	10^5	*MesP1*^{EGFP}	Increase at early time points of differentiation, distinct peak on day 5 followed by constant decrease
CVPC	$5x10^5$	*MesP1*^{EGFP}	Decrease at early time points of differentiation, increase after day 5, peak on day 7 followed by dramatic decrease
ESC	$5x10^4$	*Nkx2.5*^{EGFP}	Increase at early time points of differentiation, distinct peak on day 3 followed by constant decrease
CVPC	$5x10^4$	*Nkx2.5*^{EGFP}	Increase at early time points of differentiation, distinct peak on day 3 followed by constant decrease

Table 5.1: Expression patterns of *Brachyury*^{EGFP}, *MesP1*^{EGFP} and *Nkx2.5*^{EGFP} based on proportions of cells expressing these genes in differentiating ESCs and CVPCs in low volume monolayer cell culture at different cell numbers.

5.4 Correlation of transgene and endogenous gene expression

As *Brachyury*^{EGFP} and *MesP1*^{EGFP} transgenes were randomly integrated into the genome of ESCs and CVPCs we compared transgene expression with mRNA expression levels of the respective endogenous genes in undifferentiated ESCs and CVPCs to see whether

transgene expression reflects endogenous expression (see also section 4.5). Figure 5.2A shows that *EGFP* mRNA levels and endogenous *Brachyury* mRNA levels correlate quite well in clone c3 of the Brachyury^{EGFP} reporter ESC line which we used for most of the experiments of this thesis as well as in other clones of the same cell line.

MesP1 mRNA could not be detected in undifferentiated ESCs of the MesP1^{EGFP} cell line while *EGFP* was expressed in this cell line. Therefore, *EGFP* and *MesP1* mRNA levels do not correlate quite well in most clones of the MesP1^{EGFP} reporter ESC line. However, in clone cA of this cell line, which we mostly used for our experiments, *EGFP* mRNA levels are quite low and thus reflect endogenous *MesP1* expression at least to a certain extent (Figure 5.2B).

The Nkx2.5^{EGFP} reporter ESC line carries an *EGFP* knock-in in one allele of the NKX2.5 gene. Thus, *EGFP* and *Nkx2.5* expression should perfectly correlate. However, *EGFP* mRNA levels seem to be too high to be comparable to endogenous *Nkx2.5* mRNA levels but as one allele of the NKX2.5 gene is disrupted in the Nkx2.5 reporter ESC line *Nkx2.5* expression levels are below those in wild type cells. When taking this fact into account *EGFP* mRNA levels are comparable between the Nkx2.5^{EGFP} cell line and clone c21 of the Brachyury^{EGFP} cell line which both express similar levels of the respective endogenous gene. As *Brachyury* and *EGFP* expression seems to correlate quite well in clone c21 of the Brachyury^{EGFP} cell line we can probably assume that *EGFP* and *Nkx2.5* expression is also comparable in the Nkx2.5^{EGFP} cell line.

The general higher *EGFP* expression levels compared to expression levels of the analysed endogenous genes are probably caused by a higher efficiency of the *EGFP* primers compared to the other primers used.

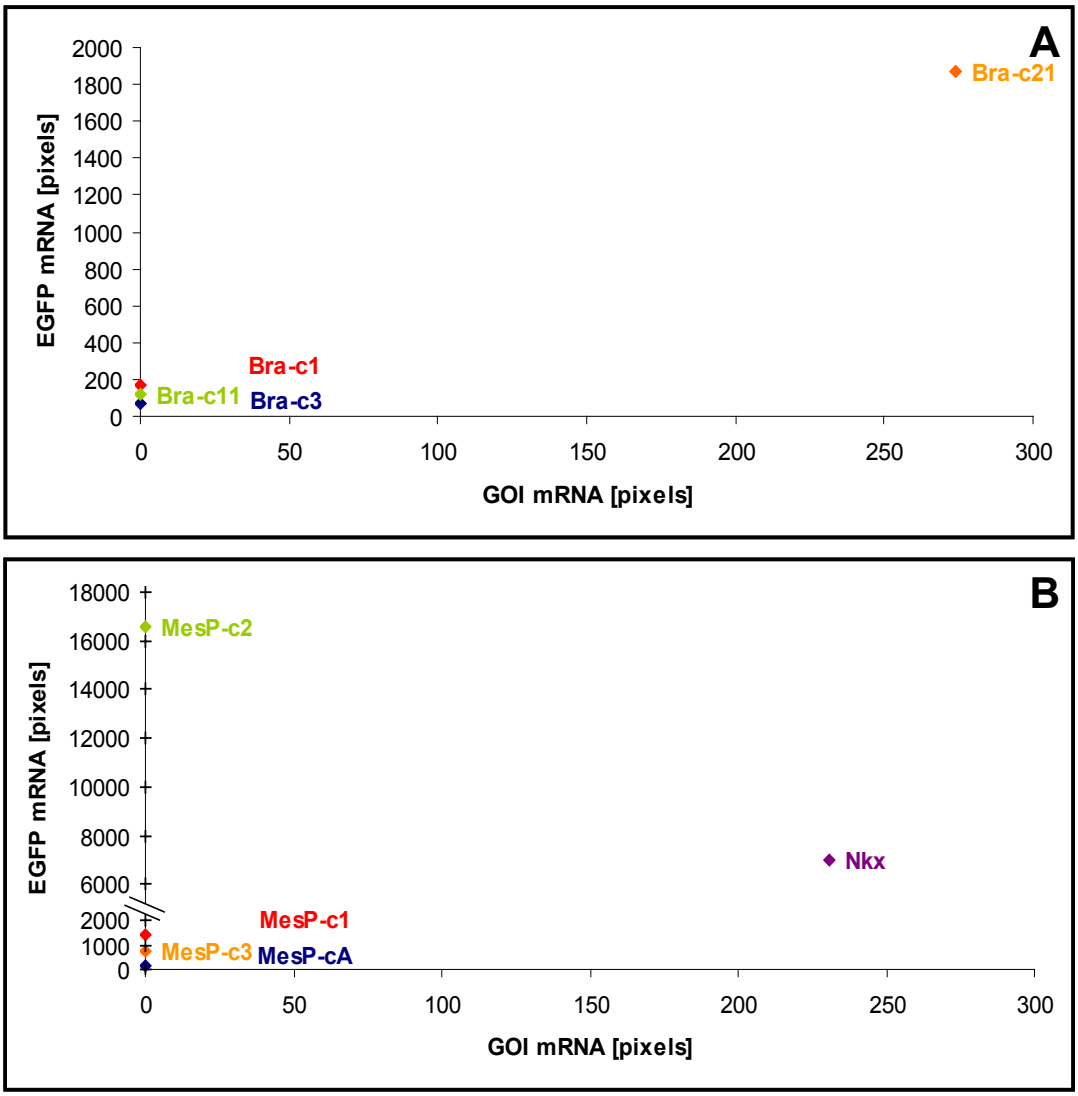

Figure 5.2: Correlation between reporter gene and gene of interest mRNA expression in ESCs.

A) Semi-quantitative PCR analyses of *EGFP* and endogenous *Brachyury* mRNA levels in undifferentiated Brachyury^{EGFP} ESC line.

B) Semi-quantitative PCR analyses of *EGFP* and *MesP1* or *Nkx2.5* mRNA levels in MesP1^{EGFP} or Nkx2.5^{EGFP} reporter ESC lines.

Levels of integrated density of the PCR signal on an agarose gel. GOI: Gene of interest, here *Brachyury*, *MesP1* or *Nkx2.5*.

As shown in figure 5.3A the percentage of *Brachyury^{EGFP}* expressing cells and endogenous *Brachyury* mRNA levels correlates best in clone c3 of the Brachyury^{EGFP} reporter ESC line, which we used for most of the experiments in this thesis, and it also correlates quite well in clones c1 and c21 of the same cell line. In contrast, the proportion of *Brachyury^{EGFP}* expressing cells is too high to be comparable with endogenous *Brachyury* expression levels in clone c11 of the Brachyury^{EGFP} ESC line.

In the MesP1^{EGFP} reporter ESC line the endogenous *MesP1* mRNA levels correlate very badly with the proportions of *MesP1^{EGFP}* expressing cells. However, compared to the other clones of the MesP1^{EGFP} cell line, *MesP1* mRNA levels and the proportion of *MesP1^{EGFP}* expressing cells are still quite comparable in clone cA, which we used mostly in this thesis (Figure 5.3B).

Endogenous *Nkx2.5* mRNA levels correlate quite well with the proportion of *Nkx2.5^{EGFP}* expressing cells in the Nkx2.5^{EGFP} ESC line (Figure 5.3B).

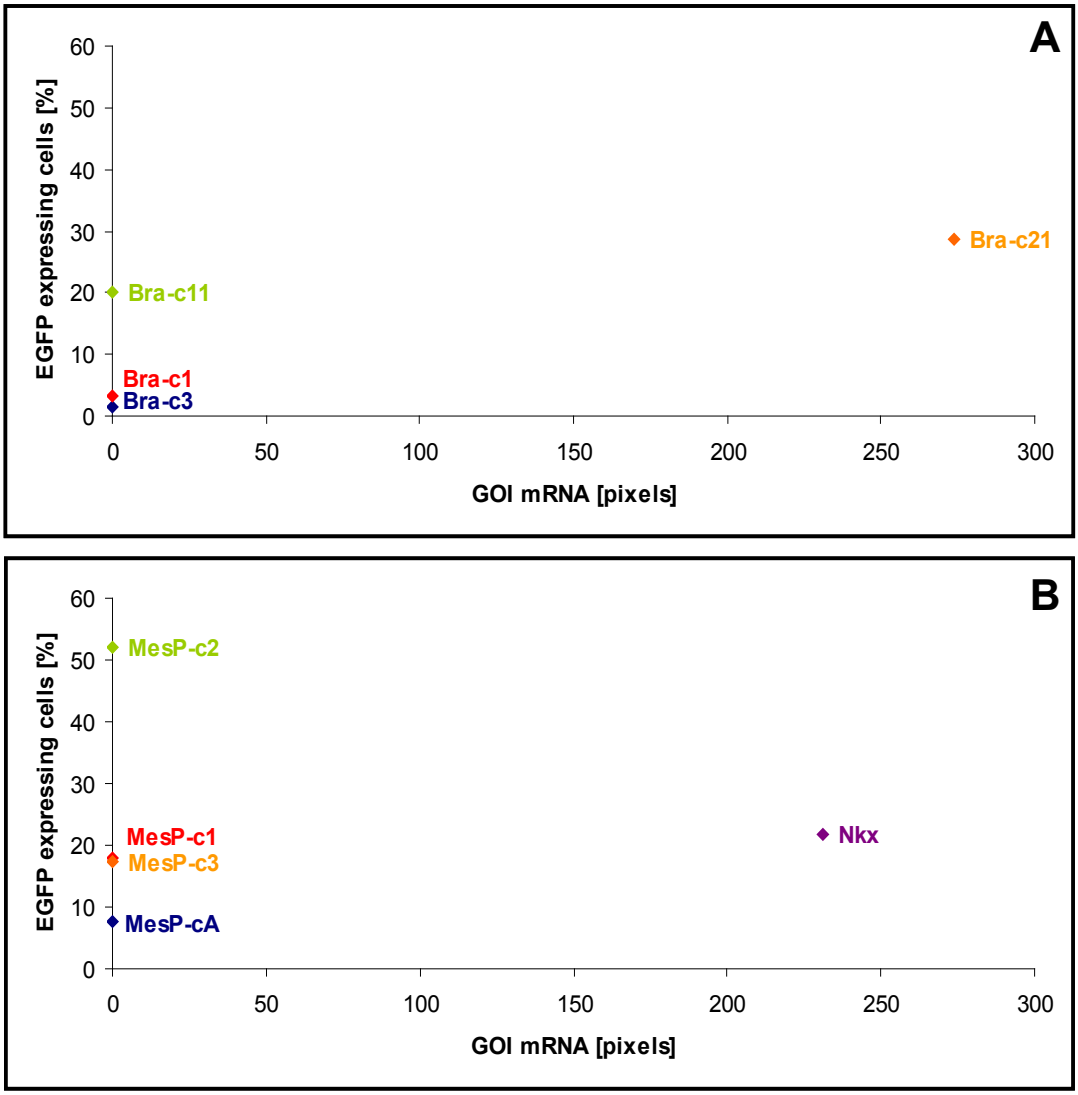

Figure 5.3: Correlation between proportion of cells expressing reporter gene and gene of interest mRNA expression in ESCs.

A) Semi-quantitative PCR analyses of endogenous *Brachyury* mRNA levels in undifferentiated Brachyury^{EGFP} ESC line. Levels of integrated density of the PCR signal on an agarose gel (x-axis). FACS analyses of undifferentiated Brachyury^{EGFP} ESC line. Proportion of ESCs expressing *Brachyury^{EGFP}* (y-axis).

B) Semi-quantitative PCR analyses of endogenous *MesP1* or *Nkx2.5* mRNA levels in MesP1^{EGFP} or Nkx2.5^{EGFP} reporter ESC lines. Levels of integrated density of the

PCR signal on an agarose gel (x-axis). FACS analyses of undifferentiated MesP1^{EGFP} and Nkx2.5^{EGFP} ESC reporter lines. Proportion of ESCs expressing *MesP1^{EGFP}* or *Nkx2.5^{EGFP}* (y-axis).

GOI: Gene of interest, here *Brachyury*, *MesP1* or *Nkx2.5*.

As depicted in figures 5.4A and B *EGFP* intensity levels and endogenous *Brachyury*, *MesP1* and *Nkx2.5* mRNA levels did not correlate very well. However, the mean intensity of *EGFP* expression only reflects the mean *EGFP* expression in EGFP positive cells and does not include cells which do not express *EGFP*. Thus, to truly compare the mean *EGFP* intensity levels with endogenous gene expression levels we would have to only analyse cells which already express *Brachyury*, *MesP1* or *Nkx2.5* or will differentiate into precursors expressing these genes.

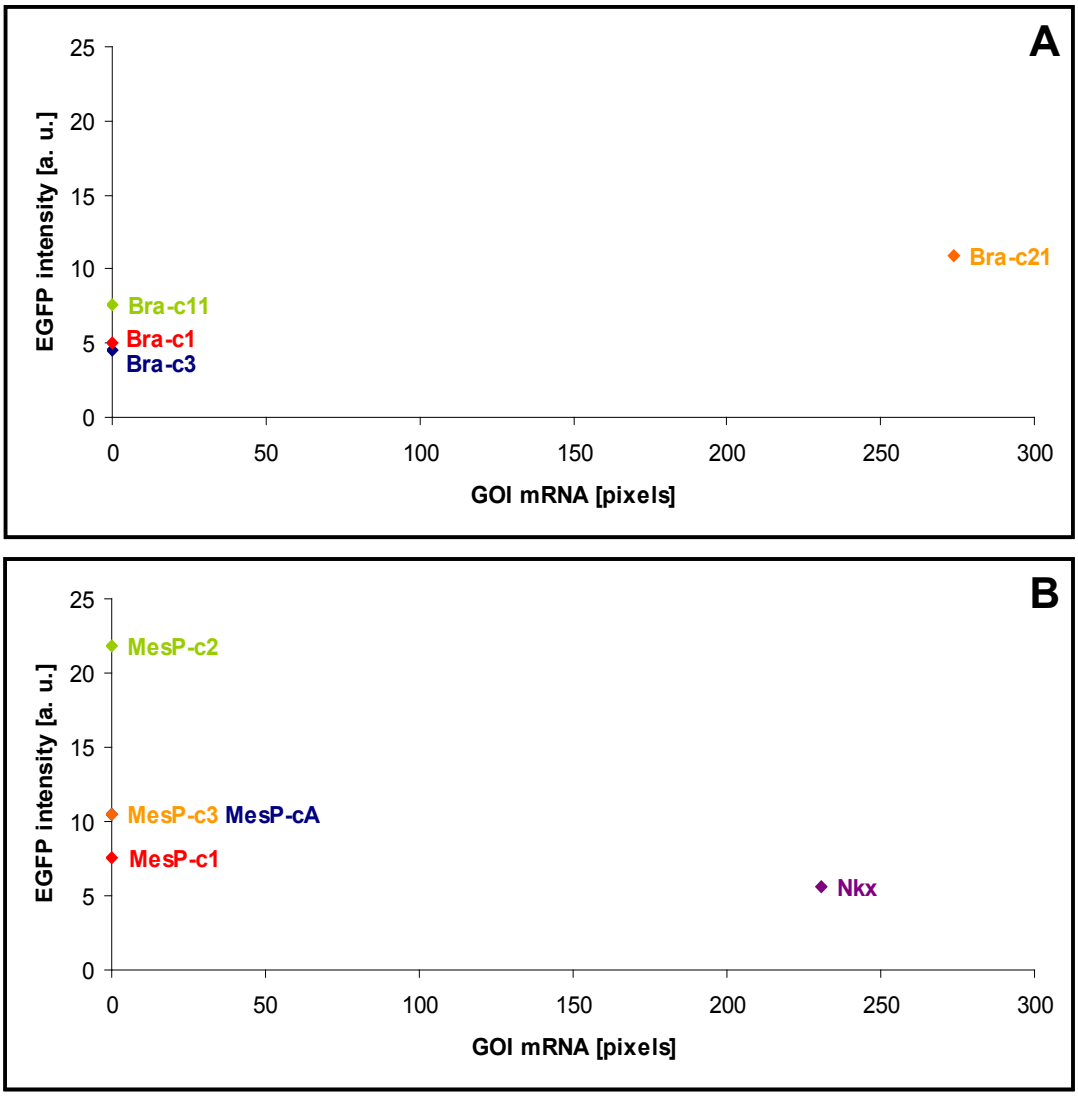

Figure 5.4: Correlation between reporter gene protein expression intensity per cell and gene of interest mRNA expression in ESCs.

A) Semi-quantitative PCR analyses of endogenous *Brachyury* mRNA levels. Levels of integrated density of the PCR signal on an agarose gel (x-axis). FACS analyses of undifferentiated Brachyury^{EGFP} ESC line. Mean intensity of *Brachyury*^{EGFP} expression (y-axis).

B) Semi-quantitative PCR analyses of endogenous *MesP1* or *Nkx2.5* mRNA levels in undifferentiated MesP1^{EGFP} or Nkx2.5^{EGFP} reporter ESC lines. Levels of integrated density of the PCR signal on an agarose gel (x-axis). FACS analyses of undifferentiated MesP1^{EGFP} and Nkx2.5^{EGFP} ESC reporter lines. Mean intensity of *MesP1*^{EGFP} and *Nkx2.5*^{EGFP} expression (y-axis).

GOI: Gene of interest, here *Brachyury*, *MesP1* or *Nkx2.5*.

In CVPCs, the *EGFP* mRNA and endogenous *Brachyury* mRNA levels correlate quite well in clone cB of the Brachyury^{EGFP} reporter cell line as apparent in figure 5.5A while the *EGFP* mRNA levels are too low to be comparable with endogenous Brachyury mRNA levels in the other clones.

Endogenous *MesP1* mRNA levels do not correlate with *EGFP* mRNA levels in all the analysed clones of the MesP1^{EGFP} CVPC line whereas *Nkx2.5* mRNA levels are comparable with *EGFP* mRNA levels in the Nkx2.5^{EGFP} reporter CVPC line (Figure 5.5B).

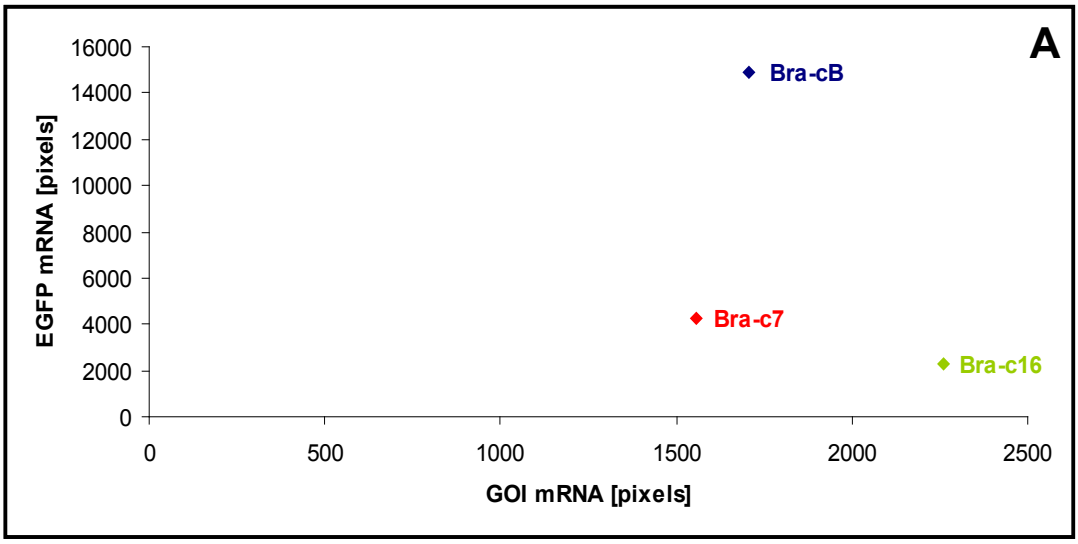

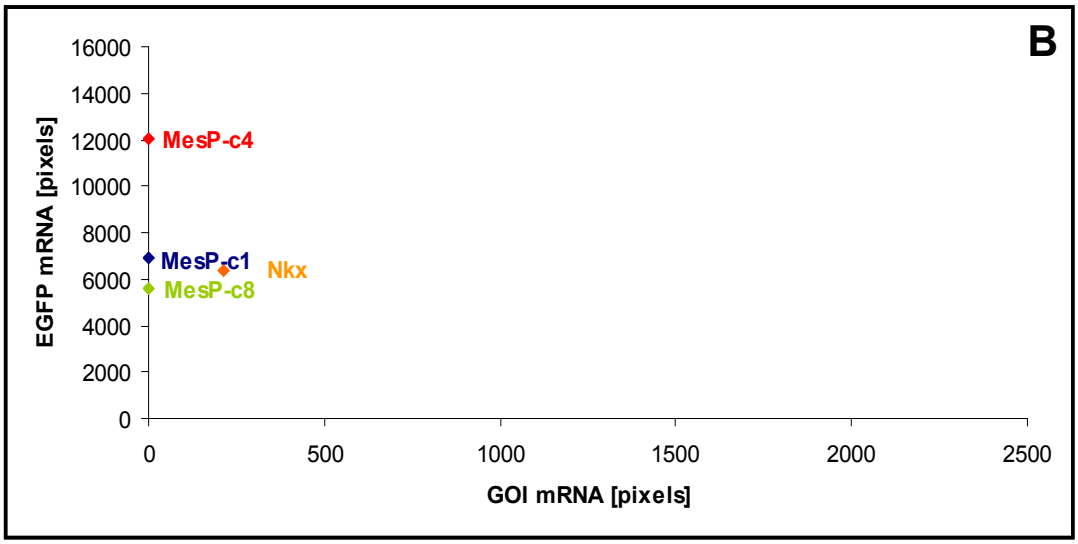

Figure 5.5: Correlation between reporter gene and gene of interest mRNA expression in CVPCs.

A) Semi-quantitative PCR analyses of *EGFP* and endogenous *Brachyury* mRNA levels in undifferentiated Brachyury^{EGFP} reporter CVPC line.

B) Semi-quantitative PCR analyses of *EGFP* and endogenous *MesP1* or *Nkx2.5* mRNA levels in undifferentiated MesP1^{EGFP} or Nkx2.5^{EGFP} reporter CVPC lines.

Levels of integrated density of the PCR signal on an agarose gel. GOI: Gene of interest, here *Brachyury*, *MesP1* or *Nkx2.5*.

As depicted in figures 5.6A and B the proportions of *EGFP* expressing cells do not correlate with endogenous *Brachyury* and *MesP1* mRNA levels in any clones of Brachyury^{EGFP} and MesP1^{EGFP} reporter CVPC lines, respectively. However, clone cB of the Brachyury^{EGFP} CVPC line and clone c1 of the MesP1^{EGFP} CVPC line, which we used for most experiments, still exhibit the best correlation compared to the other clones we investigated.

In contrast, the levels of *Nkx2.5* mRNA do correlate quite well with the proportion of *Nkx2.5*^{EGFP} expressing cells in the Nkx2.5 reporter CVPC line (Figure 5.6B).

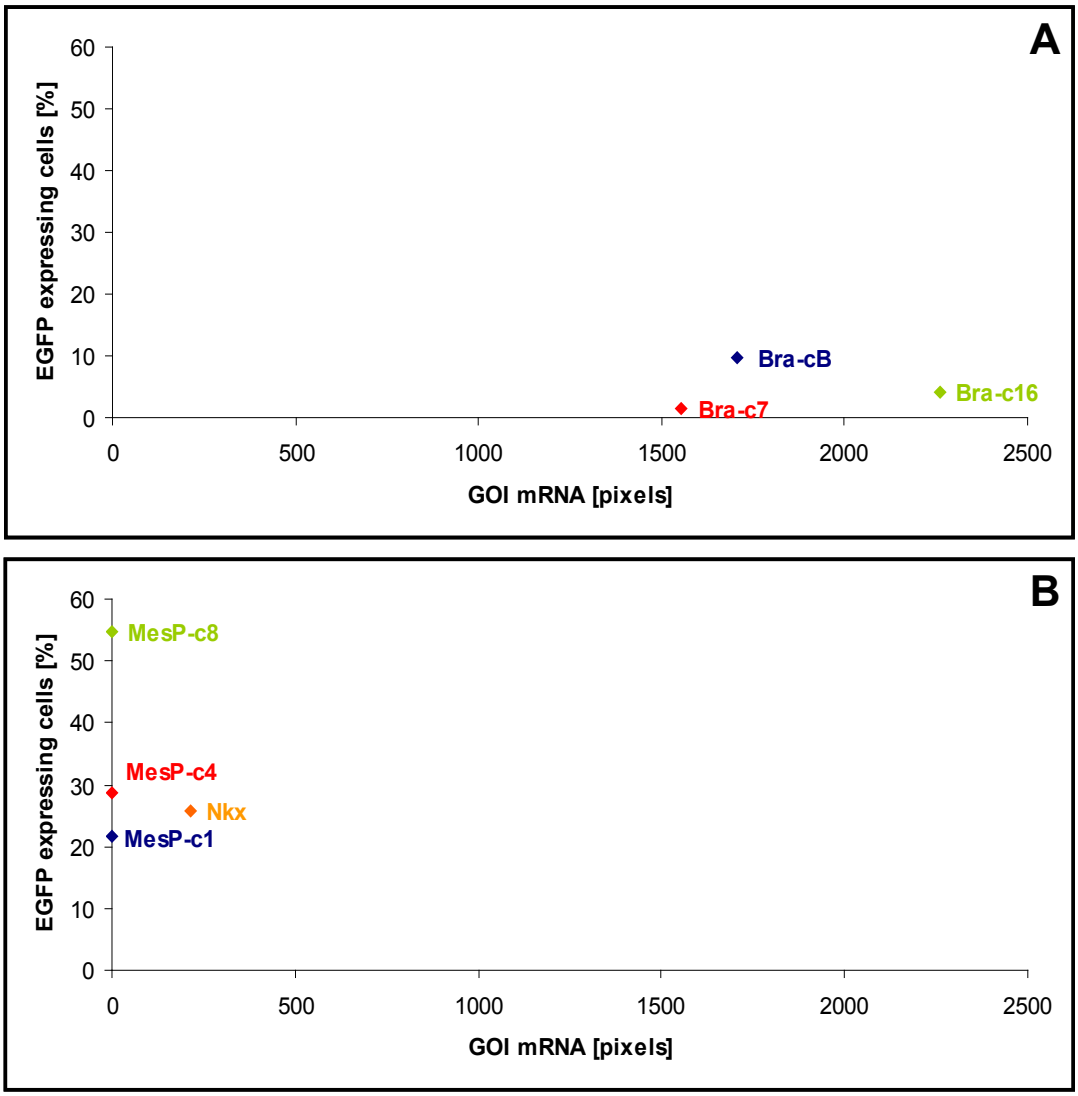

Figure 5.6: Correlation between reporter gene protein and gene of interest mRNA expression in CVPCs.

A) Semi-quantitative PCR analyses of endogenous *Brachyury* mRNA levels in undifferentiated Brachyury^{EGFP} reporter CVPC line. Levels of integrated density of the PCR signal on an agarose gel (x-axis). FACS analyses of undifferentiated Brachyury^{EGFP} CVPC reporter line. Proportion of CVPCs expressing *Brachyury^{EGFP}* (y-axis).

B) Semi-quantitative PCR analyses of endogenous *MesP1* or *Nkx2.5* mRNA levels in undifferentiated MesP1^{EGFP} or Nkx2.5^{EGFP} reporter CVPC lines. Levels of integrated density of the PCR signal on an agarose gel (x-axis). FACS analyses of undifferentiated MesP1^{EGFP} and Nkx2.5^{EGFP} CVPC reporter lines. Proportion of CVPCs expressing *MesP1^{EGFP}* or *Nkx2.5^{EGFP}* (y-axis).

GOI: Gene of interest, here *Brachyury*, *MesP1* or *Nkx2.5*.

EGFP intensity levels cannot be compared with *Brachyury*, *MesP1* or *Nkx2.5* mRNA levels in reporter CVPC lines as shown in figures 5.7A and B. But again as already mentioned above, we should have analysed only cells which do actually express

Brachyury, *MesP1* or *Nkx2.5* mRNA to be able to assess this correlation in a more meaningful way.

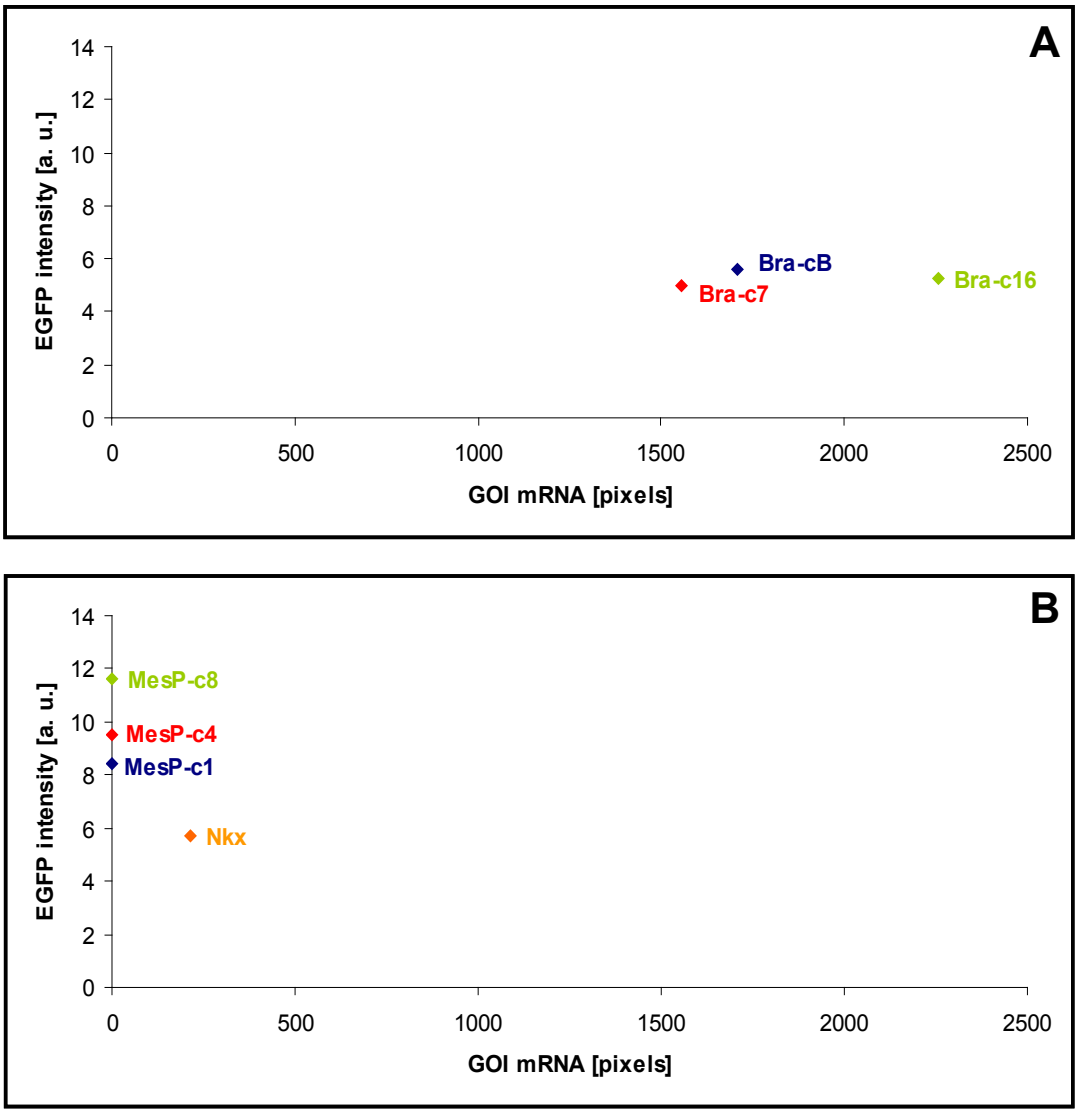

Figure 5.7: Correlation between reporter gene protein and gene of interest mRNA expression in CVPCs.

A) Semi-quantitative PCR analyses of endogenous *Brachyury* mRNA levels in undifferentiated Brachyury^{EGFP} reporter CVPC line. Levels of integrated density of the PCR signal on an agarose gel (x-axis). FACS analyses of undifferentiated Brachyury^{EGFP} CVPC reporter line. Mean intensity of *Brachyury^{EGFP}* expression (y-axis).

B) Semi-quantitative PCR analyses of endogenous *MesP1* or *Nkx2.5* mRNA levels in undifferentiated MesP1^{EGFP} or Nkx2.5^{EGFP} reporter CVPC lines. Levels of integrated density of the PCR signal on an agarose gel (x-axis). FACS analyses of undifferentiated MesP1^{EGFP} and Nkx2.5^{EGFP} CVPC reporter lines. Mean intensity of *MesP1^{EGFP}* and *Nkx2.5^{EGFP}* expression in CVPCs (y-axis).

GOI: Gene of interest, here *Brachyury*, *MesP1* or *Nkx2.5*.

In general, endogenous *Brachyury* and *Nkx2.5* mRNA levels correlated well with *EGFP* mRNA levels and proportions of *EGFP* expressing cells in both undifferentiated ESC and CVPC Brachyury^{EGFP} and Nkx2.5^{EGFP} reporter cell lines respectively, at least in the clones we used for most experiments of this thesis and we can therefore assume that the results from our FACS analyses resemble endogenous expression patterns.

In CVPCs, *Brachyury* mRNA levels and the percentages of Brachyury^{EGFP} expressing cells did not correlate that well. However, *EGFP* mRNA levels and endogenous *Brachyury* levels were comparable in clone cB of the Brachyury^{EGFP} CVPC line, which we used mostly in this thesis. Therefore, we can probably assume that Brachyury protein levels correlate with the proportion of *Brachyury^{EGFP}* expressing cells in the Brachyury^{EGFP} reporter CVPC line as the proportion of *EGFP* expressing cells actually reflects EGFP protein and not *EGFP* mRNA levels.

In ESCs, endogenous *MesP1* mRNA levels were still rather comparable with *EGFP* mRNA levels and the proportion of *MesP1^{EGFP}* expressing cells at least in clone cA of the MesP1^{EGFP} reporter cell line, which we used for most experiments. However, in CVPCs no correlation between endogenous *MesP1* mRNA levels and *EGFP* mRNA levels or proportions of *EGFP* expressing cells could be detected. It is possible that the *MesP1* primers we used did not efficiently amplify the respective cDNA molecules but the positive control actually showed a distinct signal (Figures 4.48 and 4.55).

Additionally, the MesP1^{EGFP} reporter cell lines carry a human and not a murine *MesP1* promoter sequence which might exhibit slightly different regulation patterns compared to the murine promoter even though the *MesP1* promoter sequence is highly conserved between human and mouse as well as other vertebrate species containing, for instance, conserved Brachyury responsive elements (David et al., 2011; 2013).

In *Drosophila*, a transgenic regulatory sequence was shown to enhance the expression of the corresponding endogenous gene even over a great distance (Johnston and Desplan, 2014). Thus, it might also be possible that the transgenic *MesP1* promoter negatively influences endogenous *MesP1* expression. Still, our analyses should be repeated with different *MesP1* primers to be able to exclude that low primer efficiency accounts for the missing correlation between endogenous *MesP1* mRNA levels and *EGFP* mRNA levels as well as proportions of *MesP1^{EGFP}* expressing cells.

EGFP expression levels differed in the different clones of Brachyury^{EGFP} and MesP1^{EGFP} reporter ESC and CVPC lines probably because the transgenes integrated at various sites in the different clones. Enhancers, silencers and insulators in proximity to the integration site might influence transgene expression (Eszterhas et al., 2002). Additionally, transgenes might be differently epigenetically regulated depending on their location in the genome. For instance, the DNA methylation as well as the histone acetylation status

varied in different transgenic pigs carrying the same transgene at different integration sites (Yin et al., 2012). However, most of the clones of the Brachyury^{EGFP} and MesP1^{EGFP} reporter cell lines we used for our experiments seem to be similarly regulated compared to their endogenous counterparts.

5.5 SPARC, α-SPARC and CHIR99021 treatment

In the experiment of this thesis SPARC did not influence cardiomyogenesis of differentiating ESCs or CVPCs as no contracting cardiomyocytes formed in low volume monolayer cell culture in any condition. In contrast, SPARC was shown to enhance cardiomyogenesis in EBs resulting in nearly 100 % EBs containing large areas of contracting cardiomyocytes compared to approximately 85 % when EBs were left untreated (Stary et al., 2005). Apparently SPARC is not able to induce cardiomyogenesis in a system unsupportive to cardiomyocyte differentiation like low volume monolayer culture but only to enhance cardiomyogenesis in a system which is already favourable for this development. It was also shown that SPARC required BMP2 for its positive influence on cardiomyogenesis (Stary et al., 2005) which might not have been expressed at this early time point of differentiation, day 1 of differentiation, when we started the SPARC treatment. Different studies could only demonstrate *Bmp2* expression in EBs as early as day 2 or 3 of differentiation (Doss et al., 2007; Rong et al., 2012).

Additionally, SPARC was added to EBs at a higher concentration than we used and treatment was started only at day 7 of differentiation while we already commenced at day 1 of differentiation. Probably SPARC can only influence cardiomyocyte development later in the differentiation process close to the onset of cardiomyogenesis which was also confirmed by a different study where SPARC treatment of EBs had a positive effect on cardiomyogenesis only on day 7 of differentiation but not on day 1, 3, 5 or 9 of differentiation (Hrabchak et al., 2008). In EBs SPARC is also secreted by the parietal endoderm (PE) (Stary et al., 2005) which is formed upon adhesion of EBs, hence approximately at day 4 of differentiation (Weitzer, 2006). SPARC secretion is enhanced when the PE undergoes EMT which occurs at some point between day 5 and day 8 of differentiation (Stary et al., 2005). Thus, in the natural situation SPARC action occurs later than at the time point we administered it. It is also possible that a higher concentration of SPARC is needed to cause an effect.

As depicted in figure 4.1 and in table 5.2 we observed a reduction in *Nkx2.5* expression upon SPARC treatment while in SPARC treated EBs an increase in *Nkx2.5* expression was detected. In the experiment using EBs SPARC was only administered at day 7 of differentiation while we used it at day 1 of differentiation (Stary et al., 2005). SPARC might

influence *Nkx2.5* expression differently during development dependent on the time point of its action. Additionally, *Nkx2.5* expression in EBs was analysed 4 hours after SPARC treatment (Stary et al., 2005) whereas we investigated *Nkx2.5* expression only after 24 hours of SPARC treatment. Short term influence of SPARC on *Nkx2.5* expression might therefore differ from long term influence of SPARC. Finally, we analysed NKX2.5 protein expression while Stary et al. investigated *Nkx2.5* mRNA expression (Stary et al., 2005) which might also contribute to the different outcome.

SPARC was also shown to increase cardiomyogenesis in CBs but only at the onset of cardiomyogenesis. Later in development the number of CBs containing beating cardiomyocytes was comparable between untreated and SPARC treated cells (Gottschamel, 2010). As the effect of SPARC was already only mild in conditions favourable for cardiomyogenesis it is probably not possible to induce cardiomyogenesis using SPARC in an environment apparently not well suited for cardiomyogenesis. However, SPARC treatment of CVPCs in 6-well plates at the beginning of differentiation led to an enhancement of cardiomyogenesis. But these conditions seem to be better suited for cardiomyocyte development than low volume monolayer cell culture as also untreated CVPCs differentiated into beating cardiomyocytes. Additionally, in the 6-well plate experiment cells were treated with SPARC for 4 days (Auner, 2012) while we performed SPARC treatment for only 24 hours. Thus, one could speculate that SPARC only exhibits its positive effects on cardiomyogenesis if administered for several days. Furthermore, it seems to be favourable to treat CVPCs – in contrast to ESCs – already early during differentiation as this increased cardiomyogenesis to a greater extent than treatment starting from day 4.7 of differentiation as it was performed in the CB experiment (Auner, 2012; Gottschamel, 2010).

We could not detect any influence of SPARC on *Brachyury*, *MesP1* or *Nkx2.5* expression in CVPCs as shown in figures 4.4, 4.5 and in table 5.2. In contrast, in a different study *Brachyury* and *Nkx2.5* expression was increased after 2-3 hours of SPARC treatment and *MesP1* expression was reduced after 2 hours but slightly enhanced after 3 hours (Gottschamel, 2010). Furthermore, *Nkx2.5* expression was increased in CVPCs at day 13 of differentiation after 3 hours of SPARC treatment (Walder, 2011). Therefore, SPARC treatment might only have a short term effect on the expression of the above mentioned genes in CVPCs. This assumption is further confirmed by different studies where no influence of SPARC on *Nkx2.5* expression in CVPCs could be determined neither after 48 hours (Hoebaus, 2009) nor after 24 hours in differentiating CVPCs (Walder, 2011). In contrast, if differentiating CVPCs in 6-well plates were treated with SPARC starting at day 4 of differentiation an increase in *Nkx2.5* expression could be detected after 24 hours (Auner, 2012). SPARC might therefore exhibit a longer lasting effect on *Nkx2.5*

expression only later in differentiation. Additionally, in the latter experiment *Nkx2.5* mRNA was detected (Auner, 2012) while we investigated NKX2.5 protein levels which might also explain the contradictory results.

Cell type	Gene	Effector molecule	Effect
ESC	*Brachyury*^{EGFP}	SPARC	No effect
ESC	*MesP1*^{EGFP}	SPARC	No effect
ESC	*Nkx2.5*^{EGFP}	SPARC	Decreased expression
CVPC	*Brachyury*^{EGFP}	SPARC	No effect
CVPC	*MesP1*^{EGFP}	SPARC	No effect
CVPC	*Nkx2.5*^{EGFP}	SPARC	No effect
ESC	*Brachyury*^{EGFP}	α-SPARC	No effect
CVPC	*Brachyury*^{EGFP}	α-SPARC	Decreased expression at late time points of differentiation
ESC	*Brachyury*^{EGFP}	CHIR	No effect
CVPC	*Brachyury*^{EGFP}	CHIR	Increased expression at most time points of differentiation

Table 5.2: Effects of SPARC, α-SPARC and CHIR99021 on *Brachyury*^{EGFP}, *MesP1*^{EGFP} and *Nkx2.5*^{EGFP} expression in differentiating ESCs or CVPCs in low volume monolayer cell culture.

Treatment with α-SPARC led to a reduction of cardiomyogenesis in EBs as well as in CBs in previous studies (Gottschamel, 2010; Stary et al., 2005). As neither untreated ESCs nor untreated CVPCs differentiated into contracting cardiomyocytes in low volume monolayer cell culture it was impossible for us to confirm these findings. Table 5.2 shows that α-SPARC did not influence *Brachyury* expression in differentiating ESCs in low volume monolayer cell culture (see also figures 4.18 and 4.20) while it reduced *Brachyury* expression in CVPCs in this system but only between days 9 and 11 of differentiation (see also figures 4.22 and 4.24). Thus, CVPCs seem to be more sensitive to α-SPARC treatment than ESCs in low volume monolayer cell culture. However, CVPCs only seem to react to α-SPARC treatment at later time points of differentiation which might indicate that CVPCs differentiate more slowly in low volume monolayer cell culture than in hanging drop culture. It is also possible that α-SPARC influences *Brachyury* expression only after long term treatment as cells were constantly treated with α-SPARC in our experiments. Interestingly, α-SPARC treatment resulted in a *Brachyury* expression pattern more similar to the one in CBs than the *Brachyury* expression pattern of untreated differentiating CVPCs which exhibits increased expression at late time points of differentiation (Figures 4.22 and 4.23; cf. Leitner, 2013).

As can be seen in table 5.2 CHIR treatment led to increased *Brachyury* expression in CVPCs in low volume monolayer cell culture at most time points of differentiation (see also figures 4.23 and 4.24) while it had no effect on *Brachyury* expression in ESCs in this system (see also figures 4.19 and 4.20). Apparently CVPCs are more sensitive to CHIR

treatment in low volume monolayer cell culture than ESCs which was also confirmed in the TOPflash cell lines where β-catenin mediated expression of luciferase was much stronger upon CHIR treatment in CVPCs than upon CHIR treatment of ESCs (see section 4.6). CHIR activates canonical Wnt signalling via inhibition of GSK-3β. It is possible that factors required for this CHIR mediated activation are absent in ESCs in low volume monolayer cell culture. In EBs, however, *Brachyury* expression increased upon CHIR treatment but was not influenced in CBs under the same conditions. In CBs the *Brachyury* expression levels were very low (Leitner, 2013), thus, it might be possible that CHIR treatment does not lead to induction of *Brachyury* expression but only to an enhancement of already present *Brachyury* expression.

Constant CHIR treatment led to a deregulation of differentiation in EBs and CBs and hampered cardiomyogenesis (Leitner, 2013). In CBs, CHIR treatment caused delayed and decreased cardiomyogenesis when administered between day 7 and 10 of differentiation but had no effect when added between day 0 and 4.7 of differentiation (Gottschamel, 2010). In contrast, if differentiating CVPCs on 6-well plates were treated with CHIR on the first 4 days of differentiation cardiomyocyte differentiation was inhibited (Auner, 2012). As neither CVPCs nor ESCs developed into contracting cardiomyocytes under any condition we could not confirm any of these results.

As activation of canonical Wnt signalling via WNT3A addition at early differentiation time points led to enhanced cardiomoyogenesis of ESCs (Ueno et al., 2007) one could speculate that CHIR treatment at early time points of differentiation might also be beneficial for cardiomyocyte development in monolayer cell culture and hanging drop culture. Indeed, Hartman and colleagues recently introduced a protocol for cardiomyocyte differentiation of ESCs where undifferentiated ESCs are first grown in the presence of CHIR and PD0325901, an inhibitor of MAPK/Extracellular-signal related kinase (ERK). Upon formation of EBs, cells are further grown in the presence of these two factors at reduced concentrations for 3 days. CHIR and PD0325901 are then removed and cells are treated with BMP4 and Activin A among other factors. This procedure results in the yield of 40 % cardiac Troponin positive cardiomyocytes (Hartman et al., 2014). In a different study with human ESCs, CHIR treatment prior to EB formation led to increased cardiomyogenesis (Lian et al., 2012).

5.6 Wnt signalling in monolayer cell culture

As depicted in figures 4.62 and 4.63 no active canonical Wnt signalling can be detected in low volume monolayer culture of neither ESCs nor CVPCs using the luciferase assay. However, luciferase activity and thus canonical Wnt signalling can be induced by CHIR

treatment in both differentiating ESCs and CVPCs in low volume monolayer cell culture This finding might indicate that factors of the canonical Wnt pathway generally are present in differentiating ESCs and CVPCs in low volume monolayer cell culture but that GSK-3β activity is too high for induction of canonical Wnt signalling.

While canonical Wnt signalling could only be activated to a small extent by CHIR in differentiating ESCs a significant induction of canonical Wnt signalling by CHIR could be observed in differentiating CVPCs in low volume monolayer cell culture at most time points. Similarly, canonical Wnt signalling was shown to be induced more strongly by CHIR treatment in differentiating CVPCs than in differentiating ESCs in the hanging drop system (Leitner, 2013) indicating that components of the Wnt pathway are more highly expressed in differentiating CVPCs than in differentiating ESCs.

The absence of canonical Wnt signalling in untreated differentiating ESCs and CVPCs in low volume monolayer cell culture might be an explanation why these cells fail to successfully undergo cardiomyogenesis in this system as canonical Wnt signalling is required at early time points of differentiation for successful cardiomyogenesis (Naito et al., 2006; Ueno et al., 2007) and furthermore, as it promotes expression of *Brachyury* (Yamaguchi et al., 1999), *MesP1* (Li et al., 2013) and probably also of *Nkx2.5* (Klaus et al., 2012; Liu et al., 2009). In EBs and CBs, canonical Wnt pathway activation peaks at day 5 of differentiation (Leitner, 2013). In ESCs Wnt signalling cannot be induced by CHIR treatment around this time point in low volume monolayer cell culture but activation of this pathway is possible in CVPCs at this time point. Therefore, short term CHIR treatment around day 5 of differentiation might promote cardiomyogenesis in differentiating CVPCs in low volume monolayer cell culture and also in differentiating ESCs in this system when administered at a slightly later time point.

It is possible that canonical Wnt signalling is not absent in low volume monolayer cell culture but shows only low activity in this system which we fail to detect with the TOPflash assay as the TCF/LEF sites upstream of the luciferase gene are not the only TCF/LEF sites in the genome of these cells. Additionally, β-catenin might also bind to binding sites other than TCF/LEF sites (Bottomly et al., 2010; Schuijers et al., 2014). Thus, if β-catenin levels are quite low due to low expression levels or because of high GSK-3β activity β-catenin is probably only recruited to a limited number of binding sites and might simply omit the TCF/LEF sites upstream of the luciferase open reading frame.

Other shortcomings of the TOPflash assay lie in the time span of several hours that the signal requires to develop (Vincent, 2014) and in the short half-life of the luciferase (Thompson et al., 1991; Wexler et al., 2009). It is therefore possible that we missed the time window of active canonical Wnt signalling in low volume monolayer cell culture as we performed the luciferase assay only every 48 hours. Finally, Wexler et al. also failed to

detect low canonical Wnt signalling activity in adult hippocampal progenitors but were able to observe Wnt activity using a different assay (Wexler et al., 2009).

5.7 Differentiation potential in monolayer cell culture

In low volume monolayer cell culture CVPCs preferentially differentiate into endothelial cells as shown in figure 4.64. In comparison to CVPCs in hanging drop cell culture differentiating CVPCs in low volume monolayer cell culture show higher expression levels of several endothelial cell markers especially at later time points of differentiation.

Expression levels of *Cd31* are clearly up-regulated on days 7 and 9 of differentiation in low volume monolayer cell culture compared to CBs. *Cd31* is already expressed by vascular progenitors and continues to be expressed in mature endothelial cells (Descamps and Emanueli, 2012) which are probably present on days 7 and 9 of differentiation. As *Cd31* expression did not differ greatly between monolayer and hanging drop cell culture at early time points of differentiation it is possible that a similar number of endothelial precursors is formed in the two systems but that the further generation of mature endothelial cells is more effective in monolayer cell culture than in CBs. *Cd31* is also expressed by certain haematopoietic cell types but CVPCs do not have the capacity to differentiate into this cell type (Hoebaus et al., 2013).

Levels of *eNos* expression are higher in differentiating CVPCs in monolayer cell culture than in hanging drop culture on days 3, 7 and 9 of differentiation. While *eNos* is only expressed at low levels in endothelial precursors it is highly expressed in mature endothelial cells (Ohtani et al., 2011) which are probably predominantly marked at later time points of differentiation. However, *eNos* is also expressed in cardiomyocytes (Bloch et al., 1999; Hare and Stamler, 1999) but at a much lower level than in endothelial cells (Shah and McCarthy, 2000). Thus, we can assume that *eNOS* predominantly marks endothelial cells.

VE-cadherin expression levels in monolayer cell culture exceed those in CBs on days 3 and 9 of differentiation. VE-Cadherin is regarded to be a late endothelial cell marker (Zippo et al., 2004) but *VE-cadherin* mRNA could be detected as early as day 2 of differentiation in EBs (Nsiah et al., 2014). However, in a different study *VE-cadherin* mRNA could be detected in EBs only starting from day 7 of differentiation (Kim et al., 2008). We observed only low levels of *VE-Cadherin* at early time points of differentiation which were specifically enhanced in monolayer cell culture at late time points of differentiation most probably marking mature endothelial cells.

The expression levels of *c-Kit* were higher in differentiating CVPCs in monolayer cell culture than in those in CBs on days 3 and 9 of differentiation. *C-Kit* is expressed in

endothelial precursor cells (Peichev et al., 2000; Rafii et al., 2002) as well as in mature endothelial cells (König et al., 1997; Peichev et al., 2000) which probable account for the highest proportion of c-KIT positive cells on day 9 of differentiation. However, *c-Kit* is also expressed by undifferentiated CVPCs (Hoebaus et al., 2013) which might explain the rather small differences in its expression level between monolayer and hanging drop cell culture.

Pim1 expression levels were rather low at most time points of differentiation in both monolayer and hanging drop culture but rose at later time points of differentiation in monolayer cell culture therefore significantly exceeding levels in CBs. *Pim1* is transiently expressed *in vivo* in endothelial cells during angiogenesis (Zippo et al., 2004) and is therefore a rather late endothelial cell marker assigning mature endothelial cells.

The levels of *Cd34* mRNA were similar in monolayer and hanging drop cell culture. However, as already mentioned the levels might have been overestimated due to a high level of PCR cycles. Furthermore, *Cd34* is also expressed by self-renewing CVPCs although at only low levels (Hoebaus et al., 2013).

The difference in the expression levels of cardiac markers between monolayer cell culture and CBs is not as distinct as the difference in endothelial markers. However, *Nkx2.5*, *Gata4* and *Mef2c* are already expressed in cardiac precursors (Edmondson et al., 1994; Heikinheimo et al., 1994; Svensson et al., 1999) therefore marking also immature cardiomyocytes. As mRNA levels of these factors rise over time in low volume monolayer cell culture CVPCs probably differentiate towards cardiomyocytes in this system but cannot complete maturation. This assumption is further enforced by the observation of higher levels of *Tropomyosin-α* expression in CBs compared to monolayer cell culture. Tropomyosin-α plays a vital role in the contraction of cardiomyocytes (Jagatheesan et al., 2010) and its low expression levels in monolayer cell culture in comparison to CBs might also be an explanation for the lack of contracting cardiomyocytes in low volume monolayer cell culture.

Canonical Wnt signalling is required for successful endothelial cell differentiation (Wang et al., 2007; Yang et al., 2009a). Thus, canonical Wnt signalling is probably active at least at low levels in low volume monolayer cell culture as already speculated above.

In conclusion, differentiation seems to be direct, synchronous and complete in CBs while in low volume monolayer CVPC culture cells seem to start differentiation at different times and to commence differentiating towards various types of precursors. However, at some point differentiation is switched predominantly towards endothelial cells in monolayer CVPC culture as illustrated in figure 5.8.

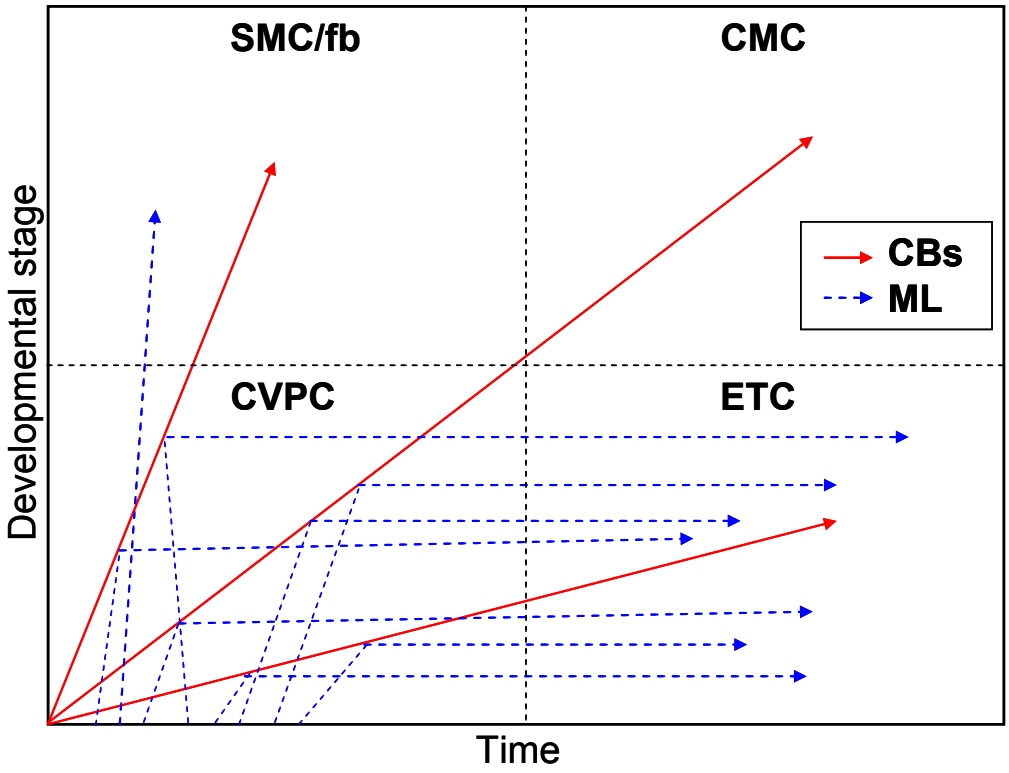

Figure 5.8: Model for differentiation processes in CBs and low volume monolayer CVPC culture. In CBs CVPCs seem to simultaneously start differentiation and to directly differentiate into mature cardiomyocytes, smooth muscle cells, cardiac fibroblasts and endothelial cells. On the other hand, in monolayer cell culture CVPCs seem to start differentiation towards all the aforesaid cell types in an asynchronous manner but at some point the differentiation process seems to be redirected primarily towards endothelial cells and to a smaller extent towards cardiac fibroblasts. CBs: cardiac bodies. CMC: cardiomyocyte. CVPC: cardiovascular progenitor. ETC: endothelial cell. fb: fibroblast. ML: monolayer cell culture. SMC: smooth muscle cell.

Successful endothelial cell differentiation does not seem to be dependent on a 3D system but to rather occur preferentially in a 2D low volume monolayer system. In different studies, ESCs also successfully differentiated into endothelial cells in monolayer cell culture under defined conditions (Blancas et al., 2011; McCloskey et al., 2003; Nishikawa et al., 2001). Monolayer cell culture is advantageous to hanging drop culture because it allows easier cell visualisation and a better control of the microenvironment (Blancas et al., 2011). Therefore, low volume monolayer cell culture is an excellent tool to study endothelial cell differentiation processes and their regulation.

6 References

Abdul-Ghani, M., Dufort, D., Stiles, R., De Repentigny, Y., Kothary, R., and Megeney, L.A. (2011). Wnt11 promotes cardiomyocyte development by caspase-mediated suppression of canonical Wnt signals. Mol. Cell. Biol. *31*, 163–178.

Adams, D.J., Quail, M.A., Cox, T., van der Weyden, L., Gorick, B.D., Su, Q., Chan, W., Davies, R., Bonfield, J.K., Law, F., et al. (2005). A genome-wide, end-sequenced 129Sv BAC library resource for targeting vector construction. Genomics *86*, 753–758.

Ai, D., Fu, X., Wang, J., Lu, M.-F., Chen, L., Baldini, A., Klein, W.H., and Martin, J.F. (2007). Canonical Wnt signaling functions in second heart field to promote right ventricular growth. Proc. Natl. Acad. Sci. U.S.A. *104*, 9319–9324.

Akazawa, H., and Komuro, I. (2005). Cardiac transcription factor Csx/Nkx2-5: Its role in cardiac development and diseases. Pharmacology & Therapeutics *107*, 252–268.

Alper, J. (2009). Geron gets green light for human trial of ES cell–derived product. Nature Biotechnology *27*, 213–214.

Amaya, E., Stein, P.A., Musci, T.J., and Kirschner, M.W. (1993). FGF signalling in the early specification of mesoderm in Xenopus. Development *118*, 477–487.

van Amerongen, R., Mikels, A., and Nusse, R. (2008). Alternative wnt signaling is initiated by distinct receptors. Sci Signal *1*, re9.

Anderson, R.H., Webb, S., Brown, N.A., Lamers, W., and Moorman, A. (2003). Development of the heart: (2) Septation of the atriums and ventricles. Heart *89*, 949–958.

Anversa, P., and Kajstura, J. (1998). Ventricular Myocytes Are Not Terminally Differentiated in the Adult Mammalian Heart. Circulation Research *83*, 1–14.

Arceci, R.J., King, A.A., Simon, M.C., Orkin, S.H., and Wilson, D.B. (1993). Mouse GATA-4: a retinoic acid-inducible GATA-binding transcription factor expressed in endodermally derived tissues and heart. Mol. Cell. Biol. *13*, 2235–2246.

Arnold, S.J., and Robertson, E.J. (2009). Making a commitment: cell lineage allocation and axis patterning in the early mouse embryo. Nat. Rev. Mol. Cell Biol. *10*, 91–103.

Asahina, K., Tsai, S.Y., Li, P., Ishii, M., Maxson, R.E., Sucov, H.M., and Tsukamoto, H. (2009). Mesenchymal origin of hepatic stellate cells, submesothelial cells, and perivascular mesenchymal cells during mouse liver development. Hepatology *49*, 998–1011.

Aubert, J., Dunstan, H., Chambers, I., and Smith, A. (2002). Functional gene screening in embryonic stem cells implicates Wnt antagonism in neural differentiation. Nat. Biotechnol. *20*, 1240–1245.

Augello, A., Kurth, T.B., and De Bari, C. (2010). Mesenchymal stem cells: a perspective from in vitro cultures to in vivo migration and niches. Eur Cell Mater *20*, 121–133.

Auner, H. (2012). Characterization and differentiation of cardiovascular progenitor cells. Diploma thesis. University of Vienna.

Bader, A., Gruss, A., Höllrigl, A., Al-Dubai, H., Capetanaki, Y., and Weitzer, G. (2001). Paracrine promotion of cardiomyogenesis in embryoid bodies by LIF modulated endoderm. Differentiation *68*, 31–43.

Bajolle, F., Zaffran, S., Kelly, R.G., Hadchouel, J., Bonnet, D., Brown, N.A., and Buckingham, M.E. (2006). Rotation of the myocardial wall of the outflow tract is implicated in the normal positioning of the great arteries. Circ. Res. *98*, 421–428.

Baker, M. (2011). Stem-cell pioneer bows out. Nature *479*, 459–459.

Baker, J.C., Beddington, R.S., and Harland, R.M. (1999). Wnt signaling in Xenopus embryos inhibits bmp4 expression and activates neural development. Genes Dev. *13*, 3149–3159.

Balza, R.O., and Misra, R.P. (2006). Role of the Serum Response Factor in Regulating Contractile Apparatus Gene Expression and Sarcomeric Integrity in Cardiomyocytes. Journal of Biological Chemistry *281*, 6498–6510.

Bartlett, H., Veenstra, G.J.C., and Weeks, D.L. (2010). Examining the Cardiac NK-2 Genes in Early Heart Development. Pediatric Cardiology *31*, 335–341.

Bearzi, C., Rota, M., Hosoda, T., Tillmanns, J., Nascimbene, A., De Angelis, A., Yasuzawa-Amano, S., Trofimova, I., Siggins, R.W., LeCapitaine, N., et al. (2007). Human cardiac stem cells. Proceedings of the National Academy of Sciences *104*, 14068–14073.

Bedzhov, I., Graham, S.J.L., Leung, C.Y., and Zernicka-Goetz, M. (2014). Developmental plasticity, cell fate specification and morphogenesis in the early mouse embryo. Philosophical Transactions of the Royal Society B: Biological Sciences *369*, 20130538–20130538.

Behr, R., Heneweer, C., Viebahn, C., Denker, H.-W., and Thie, M. (2005). Epithelial-mesenchymal transition in colonies of rhesus monkey embryonic stem cells: a model for processes involved in gastrulation. Stem Cells *23*, 805–816.

Belema Bedada, F., Technau, A., Ebelt, H., Schulze, M., and Braun, T. (2005). Activation of myogenic differentiation pathways in adult bone marrow-derived stem cells. Mol. Cell. Biol. *25*, 9509–9519.

Beltrami, A.P., Barlucchi, L., Torella, D., Baker, M., Limana, F., Chimenti, S., Kasahara, H., Rota, M., Musso, E., Urbanek, K., et al. (2003). Adult cardiac stem cells are multipotent and support myocardial regeneration. Cell *114*, 763–776.

Bendall, S.C., Stewart, M.H., Menendez, P., George, D., Vijayaragavan, K., Werbowetski-Ogilvie, T., Ramos-Mejia, V., Rouleau, A., Yang, J., Bossé, M., et al. (2007). IGF and FGF cooperatively establish the regulatory stem cell niche of pluripotent human cells in vitro. Nature *448*, 1015–1021.

Benson, D.W. (2010). Genetic Origins of Pediatric Heart Disease. Pediatric Cardiology *31*, 422–429.

Benson, D.W., Silberbach, G.M., Kavanaugh-McHugh, A., Cottrill, C., Zhang, Y., Riggs, S., Smalls, O., Johnson, M.C., Watson, M.S., Seidman, J.G., et al. (1999). Mutations in the cardiac transcription factor NKX2.5 affect diverse cardiac developmental pathways. J. Clin. Invest. *104*, 1567–1573.

Bergmann, O., Bhardwaj, R.D., Bernard, S., Zdunek, S., Barnabe-Heider, F., Walsh, S., Zupicich, J., Alkass, K., Buchholz, B.A., Druid, H., et al. (2009). Evidence for Cardiomyocyte Renewal in Humans. Science *324*, 98–102.

Biben, C., and Harvey, R.P. (1997). Homeodomain factor Nkx2-5 controls left/right asymmetric expression of bHLH gene eHand during murine heart development. Genes Dev. *11*, 1357–1369.

Blancas, A.A., Shih, A.J., Lauer, N.E., and McCloskey, K.E. (2011). Endothelial Cells from Embryonic Stem Cells in a Chemically Defined Medium. Stem Cells and Development *20*, 2153–2161.

Bloch, W., Fleischmann, B.K., Lorke, D.E., Andressen, C., Hops, B., Hescheler, J., and Addicks, K. (1999). Nitric oxide synthase expression and role during cardiomyogenesis. Cardiovasc. Res. *43*, 675–684.

Bodmer, R. (1993). The gene tinman is required for specification of the heart and visceral muscles in Drosophila. Development *118*, 719–729.

Boeuf, H., Hauss, C., De Graeve, F., Baran, N., and Kedinger, C. (1997). Leukemia inhibitory factor–dependent transcriptional activation in embryonic stem cells. The Journal of Cell Biology *138*, 1207–1217.

Boheler, K.R., Czyz, J., Tweedie, D., Yang, H.-T., Anisimov, S.V., and Wobus, A.M. (2002). Differentiation of Pluripotent Embryonic Stem Cells Into Cardiomyocytes. Circulation Research *91*, 189–201.

Boissière, A., Arnathau, C., Duperray, C., Berry, L., Lachaud, L., Renaud, F., Durand, P., and Prugnolle, F. (2012). Isolation of Plasmodium falciparum by flow-cytometry: implications for single-trophozoite genotyping and parasite DNA purification for whole-genome high-throughput sequencing of archival samples. Malar. J. *11*, 163.

Bolli, R., Chugh, A.R., D'Amario, D., Loughran, J.H., Stoddard, M.F., Ikram, S., Beache, G.M., Wagner, S.G., Leri, A., Hosoda, T., et al. (2011). Cardiac stem cells in

patients with ischaemic cardiomyopathy (SCIPIO): initial results of a randomised phase 1 trial. The Lancet *378*, 1847–1857.

Bondue, A., and Blanpain, C. (2010). Mesp1: a key regulator of cardiovascular lineage commitment. Circ. Res. *107*, 1414–1427.

Bondue, A., Lapouge, G., Paulissen, C., Semeraro, C., Iacovino, M., Kyba, M., and Blanpain, C. (2008). Mesp1 acts as a master regulator of multipotent cardiovascular progenitor specification. Cell Stem Cell *3*, 69–84.

Borowiak, M., Maehr, R., Chen, S., Chen, A.E., Tang, W., Fox, J.L., Schreiber, S.L., and Melton, D.A. (2009). Small molecules efficiently direct endodermal differentiation of mouse and human embryonic stem cells. Cell Stem Cell *4*, 348–358.

von Both, I., Silvestri, C., Erdemir, T., Lickert, H., Walls, J.R., Henkelman, R.M., Rossant, J., Harvey, R.P., Attisano, L., and Wrana, J.L. (2004). Foxh1 is essential for development of the anterior heart field. Dev. Cell *7*, 331–345.

Bottomly, D., Kyler, S.L., McWeeney, S.K., and Yochum, G.S. (2010). Identification of beta-catenin binding regions in colon cancer cells using ChIP-Seq. Nucleic Acids Res. *38*, 5735–5745.

Brade, T., Pane, L.S., Moretti, A., Chien, K.R., and Laugwitz, K.-L. (2013). Embryonic Heart Progenitors and Cardiogenesis. Cold Spring Harbor Perspectives in Medicine *3*, a013847–a013847.

Bradley, R.S., and Brown, A.M. (1995). A soluble form of Wnt-1 protein with mitogenic activity on mammary epithelial cells. Mol. Cell. Biol. *15*, 4616–4622.

Bratt-Leal, A.M., Carpenedo, R.L., and McDevitt, T.C. (2009). Engineering the embryoid body microenvironment to direct embryonic stem cell differentiation. Biotechnology Progress *25*, 43–51.

Breier, G., Breviario, F., Caveda, L., Berthier, R., Schnürch, H., Gotsch, U., Vestweber, D., Risau, W., and Dejana, E. (1996). Molecular cloning and expression of murine vascular endothelial-cadherin in early stage development of cardiovascular system. Blood *87*, 630–641.

Brown, M., and Wittwer, C. (2000). Flow cytometry: principles and clinical applications in hematology. Clinical Chemistry *46*, 1221–1229.

Bruneau, B.G., Bao, Z.Z., Tanaka, M., Schott, J.J., Izumo, S., Cepko, C.L., Seidman, J.G., and Seidman, C.E. (2000). Cardiac expression of the ventricle-specific homeobox gene Irx4 is modulated by Nkx2-5 and dHand. Dev. Biol. *217*, 266–277.

Bruneau, B.G., Nemer, G., Schmitt, J.P., Charron, F., Robitaille, L., Caron, S., Conner, D.A., Gessler, M., Nemer, M., Seidman, C.E., et al. (2001). A murine model of Holt-Oram syndrome defines roles of the T-box transcription factor Tbx5 in cardiogenesis and disease. Cell 10^6, 709–721.

Bu, L., Jiang, X., Martin-Puig, S., Caron, L., Zhu, S., Shao, Y., Roberts, D.J., Huang, P.L., Domian, I.J., and Chien, K.R. (2009). Human ISL1 heart progenitors generate diverse multipotent cardiovascular cell lineages. Nature *460*, 113–117.

Buchberger, A., Seidl, K., Klein, C., Eberhardt, H., and Arnold, H.H. (1998). cMeso-1, a novel bHLH transcription factor, is involved in somite formation in chicken embryos. Dev. Biol. *199*, 201–215.

Buchberger, A., Bonneick, S., Klein, C., and Arnold, H.-H. (2002). Dynamic expression of chicken cMeso2 in segmental plate and somites. Dev. Dyn. *223*, 108–118.

Buckingham, M., Meilhac, S., and Zaffran, S. (2005). Building the mammalian heart from two sources of myocardial cells. Nature Reviews Genetics *6*, 826–837.

Cadigan, K.M., and Nusse, R. (1997). Wnt signaling: a common theme in animal development. Genes Dev. *11*, 3286–3305.

Cai, C.-L., Liang, X., Shi, Y., Chu, P.-H., Pfaff, S.L., Chen, J., and Evans, S. (2003). Isl1 identifies a cardiac progenitor population that proliferates prior to differentiation and contributes a majority of cells to the heart. Developmental Cell *5*, 877–889.

Cambier, L., Plate, M., Sucov, H.M., and Pashmforoush, M. (2014). Nkx2-5 regulates cardiac growth through modulation of Wnt signaling by R-spondin3. Development *141*, 2959–2971.

Cambray, N., and Wilson, V. (2007). Two distinct sources for a population of maturing axial progenitors. Development *134*, 2829–2840.

Capo-chichi, C.D., Rula, M.E., Smedberg, J.L., Vanderveer, L., Parmacek, M.S., Morrisey, E.E., Godwin, A.K., and Xu, X.-X. (2005). Perception of differentiation cues by GATA factors in primitive endoderm lineage determination of mouse embryonic stem cells. Developmental Biology *286*, 574–586.

Casey, E.S., O'Reilly, M.A., Conlon, F.L., and Smith, J.C. (1998). The T-box transcription factor Brachyury regulates expression of eFGF through binding to a non-palindromic response element. Development *125*, 3887–3894.

Chan, S.S.-K., Shi, X., Toyama, A., Arpke, R.W., Dandapat, A., Iacovino, M., Kang, J., Le, G., Hagen, H.R., Garry, D.J., et al. (2013). Mesp1 Patterns Mesoderm into Cardiac, Hematopoietic, or Skeletal Myogenic Progenitors in a Context-Dependent Manner. Cell Stem Cell *12*, 587–601.

Chazaud, C., Yamanaka, Y., Pawson, T., and Rossant, J. (2006). Early lineage segregation between epiblast and primitive endoderm in mouse blastocysts through the Grb2-MAPK pathway. Dev. Cell *10*, 615–624.

Chen, C.Y., and Schwartz, R.J. (1996). Recruitment of the tinman homolog Nkx-2.5 by serum response factor activates cardiac alpha-actin gene transcription. Mol. Cell. Biol. *16*, 6372–6384.

Chen, J.N., and Fishman, M.C. (1996). Zebrafish tinman homolog demarcates the heart field and initiates myocardial differentiation. Development *122*, 3809–3816.

Chen, F., Kook, H., Milewski, R., Gitler, A.D., Lu, M.M., Li, J., Nazarian, R., Schnepp, R., Jen, K., Biben, C., et al. (2002). Hop is an unusual homeobox gene that modulates cardiac development. Cell *110*, 713–723.

Chen, V.C., Stull, R., Joo, D., Cheng, X., and Keller, G. (2008). Notch signaling respecifies the hemangioblast to a cardiac fate. Nat. Biotechnol. *26*, 1169–1178.

Chesley, P. (1935). Development of the short-tailed mutant in the house mouse. J. Exp. Zool. *70*, 429–459.

Chimutengwende-Gordon, M., and S Khan, W. (2012). Advances in the use of stem cells and tissue engineering applications in bone repair. Current Stem Cell Research & Therapy *7*, 122–126.

Chong, J.J.H., and Murry, C.E. (2014). Cardiac regeneration using pluripotent stem cells—Progression to large animal models. Stem Cell Research.

Chong, J.J.H., Chandrakanthan, V., Xaymardan, M., Asli, N.S., Li, J., Ahmed, I., Heffernan, C., Menon, M.K., Scarlett, C.J., Rashidianfar, A., et al. (2011). Adult Cardiac-Resident MSC-like Stem Cells with a Proepicardial Origin. Cell Stem Cell *9*, 527–540.

Chong, J.J.H., Reinecke, H., Iwata, M., Torok-Storb, B., Stempien-Otero, A., and Murry, C.E. (2013). Progenitor Cells Identified by PDGFR-Alpha Expression in the Developing and Diseased Human Heart. Stem Cells and Development *22*, 1932–1943.

Chong, J.J.H., Yang, X., Don, C.W., Minami, E., Liu, Y.-W., Weyers, J.J., Mahoney, W.M., Van Biber, B., Cook, S.M., Palpant, N.J., et al. (2014). Human embryonic-stem-cell-derived cardiomyocytes regenerate non-human primate hearts. Nature *510*, 273–277.

Christoffels, V.M., Habets, P.E., Franco, D., Campione, M., de Jong, F., Lamers, W.H., Bao, Z.Z., Palmer, S., Biben, C., Harvey, R.P., et al. (2000). Chamber formation and morphogenesis in the developing mammalian heart. Dev. Biol. *223*, 266–278.

Clements, D., Taylor, H.C., Herrmann, B.G., and Stott, D. (1996). Distinct regulatory control of the Brachyury gene in axial and non-axial mesoderm suggests separation of mesoderm lineages early in mouse gastrulation. Mech. Dev. *56*, 139–149.

Cohen, E.D., Wang, Z., Lepore, J.J., Lu, M.M., Taketo, M.M., Epstein, D.J., and Morrisey, E.E. (2007). Wnt/beta-catenin signaling promotes expansion of Isl-1-positive cardiac progenitor cells through regulation of FGF signaling. J. Clin. Invest. *117*, 1794–1804.

Cohen, E.D., Miller, M.F., Wang, Z., Moon, R.T., and Morrisey, E.E. (2012). Wnt5a and Wnt11 are essential for second heart field progenitor development. Development *139*, 1931–1940.

Collins, C.A., Olsen, I., Zammit, P.S., Heslop, L., Petrie, A., Partridge, T.A., and Morgan, J.E. (2005). Stem Cell Function, Self-Renewal, and Behavioral Heterogeneity of Cells from the Adult Muscle Satellite Cell Niche. Cell *122*, 289–301.

Combs, M.D., and Yutzey, K.E. (2009). Heart valve development: regulatory networks in development and disease. Circ. Res. 10^5, 408–421.

Conlon, F.L., Sedgwick, S.G., Weston, K.M., and Smith, J.C. (1996). Inhibition of Xbra transcription activation causes defects in mesodermal patterning and reveals autoregulation of Xbra in dorsal mesoderm. Development *122*, 2427–2435.

Coppola, A., Romito, A., Borel, C., Gehrig, C., Gagnebin, M., Falconnet, E., Izzo, A., Altucci, L., Banfi, S., Antonarakis, S.E., et al. (2014). Cardiomyogenesis is controlled by the miR-99a/let-7c cluster and epigenetic modifications. Stem Cell Research *12*, 323–337.

Corbo, J.C., Levine, M., and Zeller, R.W. (1997). Characterization of a notochord-specific enhancer from the Brachyury promoter region of the ascidian, Ciona intestinalis. Development *124*, 589–602.

Correa, R.G., Tergaonkar, V., Ng, J.K., Dubova, I., Izpisua-Belmonte, J.C., and Verma, I.M. (2004). Characterization of NF-kappa B/I kappa B proteins in zebra fish and their involvement in notochord development. Mol. Cell. Biol. *24*, 5257–5268.

Cortes-Bergoderi, M., Goel, K., Murad, M.H., Allison, T., Somers, V.K., Erwin, P.J., Sochor, O., and Lopez-Jimenez, F. (2013). Cardiovascular mortality in Hispanics compared to non-Hispanic whites: A systematic review and meta-analysis of the Hispanic paradox. European Journal of Internal Medicine *24*, 791–799.

Costello, I., Pimeisl, I.-M., Dräger, S., Bikoff, E.K., Robertson, E.J., and Arnold, S.J. (2011). The T-box transcription factor Eomesodermin acts upstream of Mesp1 to specify cardiac mesoderm during mouse gastrulation. Nat. Cell Biol. *13*, 1084–1091.

Dang, S.M., Kyba, M., Perlingeiro, R., Daley, G.Q., and Zandstra, P.W. (2002). Efficiency of embryoid body formation and hematopoietic development from embryonic stem cells in different culture systems. Biotechnol. Bioeng. *78*, 442–453.

Danos, M.C., and Yost, H.J. (1996). Role of notochord in specification of cardiac left-right orientation in zebrafish and Xenopus. Dev. Biol. *177*, 96–103.

David, R., Brenner, C., Stieber, J., Schwarz, F., Brunner, S., Vollmer, M., Mentele, E., Müller-Höcker, J., Kitajima, S., Lickert, H., et al. (2008). MesP1 drives vertebrate cardiovascular differentiation through Dkk-1-mediated blockade of Wnt-signalling. Nat. Cell Biol. *10*, 338–345.

David, R., Jarsch, V.B., Schwarz, F., Nathan, P., Gegg, M., Lickert, H., and Franz, W.-M. (2011). Induction of MesP1 by Brachyury(T) generates the common multipotent cardiovascular stem cell. Cardiovascular Research *92*, 115–122.

David, R., Schwarz, F., Rimmbach, C., Nathan, P., Jung, J., Brenner, C., Jarsch, V., Stieber, J., and Franz, W.-M. (2013). Selection of a common multipotent cardiovascular stem cell using the 3.4-kb MesP1 promoter fragment. Basic Research in Cardiology *108*.

Davies, O.R., Lin, C.-Y., Radzisheuskaya, A., Zhou, X., Taube, J., Blin, G., Waterhouse, A., Smith, A.J.H., and Lowell, S. (2013). Tcf15 Primes Pluripotent Cells for Differentiation. Cell Reports *3*, 472–484.

Denker, H.-W., Behr, R., Heneweer, C., Viebahn, C., and Thie, M. (2007). Epithelial-mesenchymal transition in Rhesus monkey embryonic stem cell colonies: a model for processes involved in gastrulation? Cells Tissues Organs (Print) *185*, 48–50.

Dentice, M., Cordeddu, V., Rosica, A., Ferrara, A.M., Santarpia, L., Salvatore, D., Chiovato, L., Perri, A., Moschini, L., Fazzini, C., et al. (2006). Missense mutation in the transcription factor NKX2-5: a novel molecular event in the pathogenesis of thyroid dysgenesis. J. Clin. Endocrinol. Metab. *91*, 1428–1433.

Descamps, B., and Emanueli, C. (2012). Vascular differentiation from embryonic stem cells: Novel technologies and therapeutic promises. Vascular Pharmacology *56*, 267–279.

Van Dilla, M.A., Trujillo, T.T., Mullaney, P.F., and Coulter, J.R. (1969). Cell microfluorometry: a method for rapid fluorescence measurement. Science *163*, 1213–1214.

Dittrich, W., and Göhde, W. (1969). [Impulse fluorometry of single cells in suspension]. Z. Naturforsch. B *24*, 360–361.

Dobrovolskaïa-Zavadskaïa, N. (1927). Sur la mortification spontanée de la queue chez la souris nouveau-née et sur l'existence d'un caractère (facteur) heriditaire "non-viable." C R Soc Biol *97*, 114–116.

Doetsch, F., Caille, I., Lim, D.A., García-Verdugo, J.M., and Alvarez-Buylla, A. (1999). Subventricular zone astrocytes are neural stem cells in the adult mammalian brain. Cell *97*, 703–716.

Doetschman, T.C., Eistetter, H., Katz, M., Schmidt, W., and Kemler, R. (1985). The in vitro development of blastocyst-derived embryonic stem cell lines: formation of visceral yolk sac, blood islands and myocardium. J Embryol Exp Morphol *87*, 27–45.

Doss, M.X., Chen, S., Winkler, J., Hippler-Altenburg, R., Odenthal, M., Wickenhauser, C., Balaraman, S., Schulz, H., Hummel, O., Hubner, N., et al. (2007). Transcriptomic and phenotypic analysis of murine embryonic stem cell derived BMP2+ lineage cells: an insight into mesodermal patterning. Genome Biol *8*, R184.

Dravid, G., Ye, Z., Hammond, H., Chen, G., Pyle, A., Donovan, P., Yu, X., and Cheng, L. (2005). Defining the role of Wnt/beta-catenin signaling in the survival, proliferation, and self-renewal of human embryonic stem cells. Stem Cells *23*, 1489–1501.

Durocher, D., Chen, C.Y., Ardati, A., Schwartz, R.J., and Nemer, M. (1996). The atrial natriuretic factor promoter is a downstream target for Nkx-2.5 in the myocardium. Mol. Cell. Biol. *16*, 4648–4655.

Durocher, D., Charron, F., Warren, R., Schwartz, R.J., and Nemer, M. (1997). The cardiac transcription factors Nkx2-5 and GATA-4 are mutual cofactors. EMBO J. *16*, 5687–5696.

Edmondson, D.G., Lyons, G.E., Martin, J.F., and Olson, E.N. (1994). Mef2 gene expression marks the cardiac and skeletal muscle lineages during mouse embryogenesis. Development *120*, 1251–1263.

Eisenberg, C.A., and Eisenberg, L.M. (1999). WNT11 promotes cardiac tissue formation of early mesoderm. Dev. Dyn. *216*, 45–58.

Eszterhas, S.K., Bouhassira, E.E., Martin, D.I.K., and Fiering, S. (2002). Transcriptional interference by independently regulated genes occurs in any relative arrangement of the genes and is influenced by chromosomal integration position. Mol. Cell. Biol. *22*, 469–479.

Evans, M.J., and Kaufman, M.H. (1981). Establishment in culture of pluripotential cells from mouse embryos. Nature *292*, 154–156.

Evans, A.L., Faial, T., Gilchrist, M.J., Down, T., Vallier, L., Pedersen, R.A., Wardle, F.C., and Smith, J.C. (2012). Genomic Targets of Brachyury (T) in Differentiating Mouse Embryonic Stem Cells. PLoS ONE *7*, e33346.

Fernandes, S., Naumova, A.V., Zhu, W.Z., Laflamme, M.A., Gold, J., and Murry, C.E. (2010). Human embryonic stem cell-derived cardiomyocytes engraft but do not alter cardiac remodeling after chronic infarction in rats. Journal of Molecular and Cellular Cardiology *49*, 941–949.

Flaherty, M.P., and Dawn, B. (2008). Noncanonical Wnt11 signaling and cardiomyogenic differentiation. Trends in Cardiovascular Medicine *18*, 260–268.

Flaherty, M.P., Abdel-Latif, A., Li, Q., Hunt, G., Ranjan, S., Ou, Q., Tang, X.-L., Johnson, R.K., Bolli, R., and Dawn, B. (2008). Noncanonical Wnt11 signaling is sufficient to induce cardiomyogenic differentiation in unfractionated bone marrow mononuclear cells. Circulation *117*, 2241–2252.

Fraidenraich, D., Stillwell, E., Romero, E., Wilkes, D., Manova, K., Basson, C.T., and Benezra, R. (2004). Rescue of cardiac defects in id knockout embryos by injection of embryonic stem cells. Science *306*, 247–252.

Francou, A., Saint-Michel, E., Mesbah, K., Théveniau-Ruissy, M., Rana, M.S., Christoffels, V.M., and Kelly, R.G. (2013). Second heart field cardiac progenitor cells in the early mouse embryo. Biochimica et Biophysica Acta (BBA) - Molecular Cell Research *1833*, 795–798.

Fromm, J.R., and Wood, B.L. (2012). Strategies for immunophenotyping and purifying classical Hodgkin lymphoma cells from lymph nodes by flow cytometry and flow cytometric cell sorting. Methods *57*, 368–375.

Fuchs, C., Scheinast, M., Pasteiner, W., Lagger, S., Hofner, M., Hoellrigl, A., Schultheis, M., and Weitzer, G. (2012). Self-Organization Phenomena in Embryonic Stem Cell-Derived Embryoid Bodies: Axis Formation and Breaking of Symmetry during Cardiomyogenesis. Cells Tissues Organs *195*, 377–391.

Fulwyler, M.J. (1965). Electronic separation of biological cells by volume. Science *150*, 910–911.

Galceran, J., Hsu, S.C., and Grosschedl, R. (2001). Rescue of a Wnt mutation by an activated form of LEF-1: regulation of maintenance but not initiation of Brachyury expression. Proc. Natl. Acad. Sci. U.S.A. *98*, 8668–8673.

Galli, D., Domínguez, J.N., Zaffran, S., Munk, A., Brown, N.A., and Buckingham, M.E. (2008). Atrial myocardium derives from the posterior region of the second heart field, which acquires left-right identity as Pitx2c is expressed. Development *135*, 1157–1167.

Galli, D., Gobbi, G., Carrubbi, C., Marcantonio, D., Benedetti, L., De Angelis, M.G.C., Meschi, T., Vaccarezza, M., Sampaolesi, M., Mirandola, P., et al. (2013). The role of PKCε-dependent signaling for cardiac differentiation. Histochemistry and Cell Biology *139*, 35–46.

Gardner, R.L., Papaioannou, V.E., and Barton, S.C. (1973). Origin of the ectoplacental cone and secondary giant cells in mouse blastocysts reconstituted from isolated trophoblast and inner cell mass. J Embryol Exp Morphol *30*, 561–572.

Garlanda, C., and Dejana, E. (1997). Heterogeneity of endothelial cells. Specific markers. Arterioscler. Thromb. Vasc. Biol. *17*, 1193–1202.

Gaspard, N., Bouschet, T., Hourez, R., Dimidschstein, J., Naeije, G., van den Ameele, J., Espuny-Camacho, I., Herpoel, A., Passante, L., Schiffmann, S.N., et al. (2008). An intrinsic mechanism of corticogenesis from embryonic stem cells. Nature *455*, 351–357.

Gaspard, N., Bouschet, T., Herpoel, A., Naeije, G., van den Ameele, J., and Vanderhaeghen, P. (2009). Generation of cortical neurons from mouse embryonic stem cells. Nat Protoc *4*, 1454–1463.

Gasperowicz, M., and Natale, D.R.C. (2011). Establishing Three Blastocyst Lineages--Then What? Biology of Reproduction *84*, 621–630.

Gentsch, G.E., Owens, N.D.L., Martin, S.R., Piccinelli, P., Faial, T., Trotter, M.W.B., Gilchrist, M.J., and Smith, J.C. (2013). In Vivo T-Box Transcription Factor Profiling Reveals Joint Regulation of Embryonic Neuromesodermal Bipotency. Cell Reports *4*, 1185–1196.

Gessert, S., and Kühl, M. (2010). The Multiple Phases and Faces of Wnt Signaling During Cardiac Differentiation and Development. Circulation Research *107*, 186–199.

Gilbert, S.F. (2014). Developmental biology.

Givan, A.L. (2011). Flow Cytometry: An Introduction. In Flow Cytometry Protocols, T.S. Hawley, and R.G. Hawley, eds. (Totowa, NJ: Humana Press), pp. 1–29.

Gluecksohn-Schoenheimer, S. (1938). The Development of Two Tailless Mutants in the House Mouse. Genetics *23*, 573–584.

Gluecksohn-Schoenheimer, S. (1944). The Development of Normal and Homozygous Brachy (T/T) Mouse Embryos in the Extraembryonic Coelom of the Chick. Proc. Natl. Acad. Sci. U.S.A. *30*, 134–140.

Go, A.S., Mozaffarian, D., Roger, V.L., Benjamin, E.J., Berry, J.D., Blaha, M.J., Dai, S., Ford, E.S., Fox, C.S., Franco, S., et al. (2014). Heart Disease and Stroke Statistics--2014 Update: A Report From the American Heart Association. Circulation *129*, e28–e292.

Goddeeris, M.M., Rho, S., Petiet, A., Davenport, C.L., Johnson, G.A., Meyers, E.N., and Klingensmith, J. (2008). Intracardiac septation requires hedgehog-dependent cellular contributions from outside the heart. Development *135*, 1887–1895.

Goldmuntz, E., Geiger, E., and Benson, D.W. (2001). NKX2.5 mutations in patients with tetralogy of fallot. Circulation *104*, 2565–2568.

Goldsmith, E.C., Hoffman, A., Morales, M.O., Potts, J.D., Price, R.L., McFadden, A., Rice, M., and Borg, T.K. (2004). Organization of fibroblasts in the heart. Developmental Dynamics *230*, 787–794.

Gottschamel, T. (2010). The effect of Desmin and SPARC on early cardiomyogenesis. Diploma thesis. University of Vienna.

Di Gregorio, A., and Levine, M. (1999). Regulation of Ci-tropomyosin-like, a Brachyury target gene in the ascidian, Ciona intestinalis. Development *126*, 5599–5609.

Gruneberg, H. (1958). Genetical studies on the skeleton of the mouse. XXIII. The development of brachyury and anury. J Embryol Exp Morphol *6*, 424–443.

Guo, L., Lynch, J., Nakamura, K., Fliegel, L., Kasahara, H., Izumo, S., Komuro, I., Agellon, L.B., and Michalak, M. (2001). COUP-TF1 antagonizes Nkx2.5-mediated activation of the calreticulin gene during cardiac development. J. Biol. Chem. *276*, 2797–2801.

Habets, P.E.M.H., Moorman, A.F.M., Clout, D.E.W., van Roon, M.A., Lingbeek, M., van Lohuizen, M., Campione, M., and Christoffels, V.M. (2002). Cooperative action of Tbx2 and Nkx2.5 inhibits ANF expression in the atrioventricular canal: implications for cardiac chamber formation. Genes Dev. *16*, 1234–1246.

Hackanson, B., and Waller, C.F. (2011). Long-term follow-up of patients with chronic myeloid leukemia having received autologous stem cell transplantation. Annals of Hematology *90*, 395–399.

Haegele, L., Ingold, B., Naumann, H., Tabatabai, G., Ledermann, B., and Brandner, S. (2003). Wnt signalling inhibits neural differentiation of embryonic stem cells by controlling bone morphogenetic protein expression. Mol. Cell. Neurosci. *24*, 696–708.

Hall, J., Guo, G., Wray, J., Eyres, I., Nichols, J., Grotewold, L., Morfopoulou, S., Humphreys, P., Mansfield, W., Walker, R., et al. (2009). Oct4 and LIF/Stat3 Additively Induce Krüppel Factors to Sustain Embryonic Stem Cell Self-Renewal. Cell Stem Cell *5*, 597–609.

Hare, J.M., and Stamler, J.S. (1999). NOS: modulator, not mediator of cardiac performance. Nat. Med. *5*, 273–274.

Harel, I., Nathan, E., Tirosh-Finkel, L., Zigdon, H., Guimarães-Camboa, N., Evans, S.M., and Tzahor, E. (2009). Distinct origins and genetic programs of head muscle satellite cells. Dev. Cell *16*, 822–832.

Hartman, M.E., Librande, J.R., Medvedev, I.O., Ahmad, R.N., Moussavi-Harami, F., Gupta, P.P., Chien, W.-M., and Chin, M.T. (2014). An optimized and simplified system of mouse embryonic stem cell cardiac differentiation for the assessment of differentiation modifiers. PLoS ONE *9*, e93033.

Harvey, R.P. (2002). Patterning the vertebrate heart. Nat. Rev. Genet. *3*, 544–556.

Harvey, S.A., Tümpel, S., Dubrulle, J., Schier, A.F., and Smith, J.C. (2010). no tail integrates two modes of mesoderm induction. Development *137*, 1127–1135.

Heikinheimo, M., Scandrett, J.M., and Wilson, D.B. (1994). Localization of transcription factor GATA-4 to regions of the mouse embryo involved in cardiac development. Dev. Biol. *164*, 361–373.

Hemmati-Brivanlou, A., and Melton, D.A. (1992). A truncated activin receptor inhibits mesoderm induction and formation of axial structures in Xenopus embryos. Nature *359*, 609–614.

Herrmann, B.G. (1991). Expression pattern of the Brachyury gene in whole-mount TWis/TWis mutant embryos. Development *113*, 913–917.

Herrmann, B.G., Labeit, S., Poustka, A., King, T.R., and Lehrach, H. (1990). Cloning of the T gene required in mesoderm formation in the mouse. Nature *343*, 617–622.

Hierlihy, A.M., Seale, P., Lobe, C.G., Rudnicki, M.A., and Megeney, L.A. (2002). The post-natal heart contains a myocardial stem cell population. FEBS Letters *530*, 239–243.

High, F.A., and Epstein, J.A. (2008). The multifaceted role of Notch in cardiac development and disease. Nat. Rev. Genet. *9*, 49–61.

Hiroi, Y., Kudoh, S., Monzen, K., Ikeda, Y., Yazaki, Y., Nagai, R., and Komuro, I. (2001). Tbx5 associates with Nkx2-5 and synergistically promotes cardiomyocyte differentiation. Nat. Genet. *28*, 276–280.

Hoebaus, J. (2009). Self-renewal and differentiation of cardiovascular progenitor cells. Diploma thesis. University of Vienna.

Hoebaus, J., Heher, P., Gottschamel, T., Scheinast, M., Auner, H., Walder, D., Wiedner, M., Taubenschmid, J., Miksch, M., Sauer, T., et al. (2013). Embryonic Stem Cells Facilitate the Isolation of Persistent Clonal Cardiovascular Progenitor Cell Lines and Leukemia Inhibitor Factor Maintains Their Self-Renewal and Myocardial Differentiation Potential in vitro. Cells Tissues Organs *197*, 249–268.

Hoffmann, A.D., Peterson, M.A., Friedland-Little, J.M., Anderson, S.A., and Moskowitz, I.P. (2009). sonic hedgehog is required in pulmonary endoderm for atrial septation. Development *136*, 1761–1770.

Hoogaars, W.M.H., Barnett, P., Moorman, A.F.M., and Christoffels, V.M. (2007). T-box factors determine cardiac design. Cell. Mol. Life Sci. *64*, 646–660.

Höpfl, G., Gassmann, M., and Desbaillets, I. (2004). Differentiating embryonic stem cells into embryoid bodies. Methods Mol. Biol. *254*, 79–98.

Hopstock, L.A., Fors, A.S., Bønaa, K.H., Mannsverk, J., Njølstad, I., and Wilsgaard, T. (2012). The effect of daily weather conditions on myocardial infarction incidence in a subarctic population: the Tromsø Study 1974-2004. J Epidemiol Community Health *66*, 815–820.

Hrabchak, C., Ringuette, M., and Woodhouse, K. (2008). Recombinant mouse SPARC promotes parietal endoderm differentiation and cardiomyogenesis in embryoid bodies. Biochem. Cell Biol. *86*, 487–499.

Hsu, Y.-C., and Fuchs, E. (2012). A family business: stem cell progeny join the niche to regulate homeostasis. Nature Reviews Molecular Cell Biology *13*, 103–114.

Hsu, W., Mohyeldin, A., Shah, S.R., ap Rhys, C.M., Johnson, L.F., Sedora-Roman, N.I., Kosztowski, T.A., Awad, O.A., McCarthy, E.F., Loeb, D.M., et al. (2011a). Generation of chordoma cell line JHC7 and the identification of Brachyury as a novel molecular target. J. Neurosurg. *115*, 760–769.

Hsu, Y.-C., Pasolli, H.A., and Fuchs, E. (2011b). Dynamics between Stem Cells, Niche, and Progeny in the Hair Follicle. Cell *144*, 92–10[5].

Hu, Y., Mintz, A., Shah, S.R., Quinones-Hinojosa, A., and Hsu, W. (2014). The FGFR/MEK/ERK/brachyury pathway is critical for chordoma cell growth and survival. Carcinogenesis *35*, 1491–1499.

Huelsken, J., Vogel, R., Brinkmann, V., Erdmann, B., Birchmeier, C., and Birchmeier, W. (2000). Requirement for beta-catenin in anterior-posterior axis formation in mice. J. Cell Biol. *148*, 567–578.

Hulett, H.R., Bonner, W.A., Barrett, J., and Herzenberg, L.A. (1969). Cell sorting: automated separation of mammalian cells as a function of intracellular fluorescence. Science *166*, 747–749.

Hutson, M.R., and Kirby, M.L. (2003). Neural crest and cardiovascular development: a 20-year perspective. Birth Defects Res. C Embryo Today *69*, 2–13.

Hwang, K., Park, C.-J., Jang, S., Chi, H.-S., Kim, D.-Y., Lee, J.-H., Lee, J.H., Lee, K.H., Im, H.-J., and Seo, J.-J. (2012). Flow cytometric quantification and immunophenotyping of leukemic stem cells in acute myeloid leukemia. Ann. Hematol. *91*, 1541–1546.

Ieda, M., Tsuchihashi, T., Ivey, K.N., Ross, R.S., Hong, T.-T., Shaw, R.M., and Srivastava, D. (2009). Cardiac Fibroblasts Regulate Myocardial Proliferation through β1 Integrin Signaling. Developmental Cell *16*, 233–244.

Ikeda, W., Nakanishi, H., Miyoshi, J., Mandai, K., Ishizaki, H., Tanaka, M., Togawa, A., Takahashi, K., Nishioka, H., Yoshida, H., et al. (1999). Afadin: A key molecule essential for structural organization of cell-cell junctions of polarized epithelia during embryogenesis. J. Cell Biol. *146*, 1117–1132.

Imajyo, I., Sugiura, T., Kobayashi, Y., Shimoda, M., Ishii, K., Akimoto, N., Yoshihama, N., Kobayashi, I., and Mori, Y. (2012). T-box transcription factor Brachyury expression is correlated with epithelial-mesenchymal transition and lymph node metastasis in oral squamous cell carcinoma. Int. J. Oncol. *41*, 1985–1995.

Isaacs, H.V., Pownall, M.E., and Slack, J.M. (1994). eFGF regulates Xbra expression during Xenopus gastrulation. EMBO J. *13*, 4469–4481.

Jackson, M., Taylor, A.H., Jones, E.A., and Forrester, L.M. (2010). The culture of mouse embryonic stem cells and formation of embryoid bodies. Methods Mol. Biol. *633*, 1–18.

Jagatheesan, G., Rajan, S., and Wieczorek, D.F. (2010). Investigations into tropomyosin function using mouse models. Journal of Molecular and Cellular Cardiology *48*, 893–898.

James, R.G., Conrad, W.H., and Moon, R.T. (2008). Beta-catenin-independent Wnt pathways: signals, core proteins, and effectors. Methods Mol. Biol. *468*, 131–144.

Jaspard, B., Couffinhal, T., Dufourcq, P., Moreau, C., and Duplàa, C. (2000). Expression pattern of mouse sFRP-1 and mWnt-8 gene during heart morphogenesis. Mech. Dev. *90*, 263–267.

Jay, P.Y., Harris, B.S., Maguire, C.T., Buerger, A., Wakimoto, H., Tanaka, M., Kupershmidt, S., Roden, D.M., Schultheiss, T.M., O'Brien, T.X., et al. (2004). Nkx2-5 mutation causes anatomic hypoplasia of the cardiac conduction system. J. Clin. Invest. *113*, 1130–1137.

Jessell, T.M. (2000). Neuronal specification in the spinal cord: inductive signals and transcriptional codes. Nature Reviews Genetics *1*, 20–29.

Johnson, M.H., and Ziomek, C.A. (1981). The foundation of two distinct cell lineages within the mouse morula. Cell *24*, 71–80.

Johnston, R.J., and Desplan, C. (2014). Interchromosomal communication coordinates intrinsically stochastic expression between alleles. Science *343*, 661–665.

Jollie, W.P. (1990). Development, morphology, and function of the yolk-sac placenta of laboratory rodents. Teratology *41*, 361–381.

Kalejta, R.F., Shenk, T., and Beavis, A.J. (1997). Use of a membrane-localized green fluorescent protein allows simultaneous identification of transfected cells and cell cycle analysis by flow cytometry. Cytometry *29*, 286–291.

Karsner, H.T., Saphir, O., and Todd, T.W. (1925). The state of the cardiac muscle in hypertrophy and atrophy. The American Journal of Pathology *1*, 351.

Kasahara, H., and Benson, D.W. (2004). Biochemical analyses of eight NKX2.5 homeodomain missense mutations causing atrioventricular block and cardiac anomalies. Cardiovasc. Res. *64*, 40–51.

Kasahara, H., Bartunkova, S., Schinke, M., Tanaka, M., and Izumo, S. (1998). Cardiac and extracardiac expression of Csx/Nkx2.5 homeodomain protein. Circ. Res. *82*, 936–946.

Kasahara, H., Lee, B., Schott, J.J., Benson, D.W., Seidman, J.G., Seidman, C.E., and Izumo, S. (2000). Loss of function and inhibitory effects of human CSX/NKX2.5 homeoprotein mutations associated with congenital heart disease. J. Clin. Invest. 10^6, 299–308.

Kasahara, H., Usheva, A., Ueyama, T., Aoki, H., Horikoshi, N., and Izumo, S. (2001a). Characterization of homo- and heterodimerization of cardiac Csx/Nkx2.5 homeoprotein. J. Biol. Chem. *276*, 4570–4580.

Kasahara, H., Wakimoto, H., Liu, M., Maguire, C.T., Converso, K.L., Shioi, T., Huang, W.-Y., Manning, W.J., Paul, D., Lawitts, J., et al. (2001b). Progressive atrioventricular

conduction defects and heart failure in mice expressing a mutant Csx/Nkx2.5 homeoprotein. Journal of Clinical Investigation *108*, 189–201.
Keller, G. (2005). Embryonic stem cell differentiation: emergence of a new era in biology and medicine. Genes Dev. *19*, 1129–1155.
Keller, G., Kennedy, M., Papayannopoulou, T., and Wiles, M.V. (1993). Hematopoietic commitment during embryonic stem cell differentiation in culture. Mol. Cell. Biol. *13*, 473–486.
Kelley, C., Blumberg, H., Zon, L.I., and Evans, T. (1993). GATA-4 is a novel transcription factor expressed in endocardium of the developing heart. Development *118*, 817–827.
Kelly, R.G. (2012). The second heart field. Curr. Top. Dev. Biol. *100*, 33–65.
Kelly, K.F., Ng, D.Y., Jayakumaran, G., Wood, G.A., Koide, H., and Doble, B.W. (2011). β-catenin enhances Oct-4 activity and reinforces pluripotency through a TCF-independent mechanism. Cell Stem Cell *8*, 214–227.
Kelly, O.G., Pinson, K.I., and Skarnes, W.C. (2004). The Wnt co-receptors Lrp5 and Lrp6 are essential for gastrulation in mice. Development *131*, 2803–2815.
Kelly, R.G., Brown, N.A., and Buckingham, M.E. (2001). The arterial pole of the mouse heart forms from Fgf10-expressing cells in pharyngeal mesoderm. Dev. Cell *1*, 435–440.
Kelly, R.G., Buckingham, M.E., and Moorman, A.F. (2014). Heart fields and cardiac morphogenesis. Cold Spring Harb Perspect Med *4*.
Kemler, R., Hierholzer, A., Kanzler, B., Kuppig, S., Hansen, K., Taketo, M.M., de Vries, W.N., Knowles, B.B., and Solter, D. (2004). Stabilization of beta-catenin in the mouse zygote leads to premature epithelial-mesenchymal transition in the epiblast. Development *131*, 5817–5824.
Kemp, C., Willems, E., Abdo, S., Lambiv, L., and Leyns, L. (2005). Expression of all Wnt genes and their secreted antagonists during mouse blastocyst and postimplantation development. Dev. Dyn. *233*, $10^6$4–1075.
Kemp, C.R., Willems, E., Wawrzak, D., Hendrickx, M., Agbor Agbor, T., and Leyns, L. (2007). Expression of Frizzled5, Frizzled7, and Frizzled10 during early mouse development and interactions with canonical Wnt signaling. Dev. Dyn. *236*, 2011–2019.
Kim, G.D., Kim, G.J., Seok, J.H., Chung, H.-M., Chee, K.-M., and Rhee, G.-S. (2008). Differentiation of endothelial cells derived from mouse embryoid bodies: A possible in vitro vasculogenesis model. Toxicology Letters *180*, 166–173.
King, T., Beddington, R.S., and Brown, N.A. (1998). The role of the brachyury gene in heart development and left-right specification in the mouse. Mech. Dev. *79*, 29–37.
Kirby, M.L., Gale, T.F., and Stewart, D.E. (1983). Neural crest cells contribute to normal aorticopulmonary septation. Science *220*, $10^5$9–$10^6$1.
Kispert, A., and Herrmann, B.G. (1993). The Brachyury gene encodes a novel DNA binding protein. EMBO J. *12*, 3211–3220.
Kispert, A., Koschorz, B., and Herrmann, B.G. (1995a). The T protein encoded by Brachyury is a tissue-specific transcription factor. EMBO J. *14*, 4763–4772.
Kispert, A., Ortner, H., Cooke, J., and Herrmann, B.G. (1995b). The chick Brachyury gene: developmental expression pattern and response to axial induction by localized activin. Dev. Biol. *168*, 406–415.
Kispert, A., Vainio, S., and McMahon, A.P. (1998). Wnt-4 is a mesenchymal signal for epithelial transformation of metanephric mesenchyme in the developing kidney. Development *125*, 4225–4234.
Kitaguchi, T., Mizugishi, K., Hatayama, M., Aruga, J., and Mikoshiba, K. (2002). Xenopus Brachyury regulates mesodermal expression of Zic3, a gene controlling left-right asymmetry. Dev. Growth Differ. *44*, 55–61.
Kitajima, S., Takagi, A., Inoue, T., and Saga, Y. (2000). MesP1 and MesP2 are essential for the development of cardiac mesoderm. Development *127*, 3215–3226.

Klaus, A., Saga, Y., Taketo, M.M., Tzahor, E., and Birchmeier, W. (2007). Distinct roles of Wnt/beta-catenin and Bmp signaling during early cardiogenesis. Proc. Natl. Acad. Sci. U.S.A. *104*, 18531–18536.

Klaus, A., Müller, M., Schulz, H., Saga, Y., Martin, J.F., and Birchmeier, W. (2012). Wnt/β-catenin and Bmp signals control distinct sets of transcription factors in cardiac progenitor cells. Proceedings of the National Academy of Sciences *109*, 10921–10926.

Klug, M.G., Soonpaa, M.H., Koh, G.Y., and Field, L.J. (1996). Genetically selected cardiomyocytes from differentiating embronic stem cells form stable intracardiac grafts. J. Clin. Invest. *98*, 216–224.

Kohn, A.D., and Moon, R.T. (2005). Wnt and calcium signaling: beta-catenin-independent pathways. Cell Calcium *38*, 439–446.

Kolios, G., and Moodley, Y. (2013). Introduction to Stem Cells and Regenerative Medicine. Respiration *85*, 3–10.

Komura, H., Ogita, H., Ikeda, W., Mizoguchi, A., Miyoshi, J., and Takai, Y. (2008). Establishment of cell polarity by afadin during the formation of embryoid bodies. Genes Cells *13*, 79–90.

Komuro, I., and Izumo, S. (1993). Csx: a murine homeobox-containing gene specifically expressed in the developing heart. Proc. Natl. Acad. Sci. U.S.A. *90*, 8145–8149.

König, A., Corbacioglu, S., Ballmaier, M., and Welte, K. (1997). Downregulation of c-kit expression in human endothelial cells by inflammatory stimuli. Blood *90*, 148–155.

Kørbling, M., and Estrov, Z. (2003). Adult stem cells for tissue repair - a new therapeutic concept? N. Engl. J. Med. *349*, 570–582.

Koshiba-Takeuchi, K., Mori, A.D., Kaynak, B.L., Cebra-Thomas, J., Sukonnik, T., Georges, R.O., Latham, S., Beck, L., Beck, L., Henkelman, R.M., et al. (2009). Reptilian heart development and the molecular basis of cardiac chamber evolution. Nature *461*, 95–98.

Kuehn, M.R., Bradley, A., Robertson, E.J., and Evans, M.J. (1987). A potential animal model for Lesch-Nyhan syndrome through introduction of HPRT mutations into mice. Nature *326*, 295–298.

Kühl, M. (2002). Non-canonical Wnt signaling in Xenopus: regulation of axis formation and gastrulation. Semin. Cell Dev. Biol. *13*, 243–249.

Kühl, M., Sheldahl, L.C., Malbon, C.C., and Moon, R.T. (2000a). Ca(2+)/calmodulin-dependent protein kinase II is stimulated by Wnt and Frizzled homologs and promotes ventral cell fates in Xenopus. J. Biol. Chem. *275*, 12701–12711.

Kühl, M., Sheldahl, L.C., Park, M., Miller, J.R., and Moon, R.T. (2000b). The Wnt/Ca2+ pathway: a new vertebrate Wnt signaling pathway takes shape. Trends Genet. *16*, 279–283.

Kwon, C., Arnold, J., Hsiao, E.C., Taketo, M.M., Conklin, B.R., and Srivastava, D. (2007). Canonical Wnt signaling is a positive regulator of mammalian cardiac progenitors. Proc. Natl. Acad. Sci. U.S.A. *104*, 10894–10899.

Kwon, C., Qian, L., Cheng, P., Nigam, V., Arnold, J., and Srivastava, D. (2009). A regulatory pathway involving Notch1/beta-catenin/Isl1 determines cardiac progenitor cell fate. Nat. Cell Biol. *11*, 951–957.

Kwon, G.S., Viotti, M., and Hadjantonakis, A.-K. (2008). The Endoderm of the Mouse Embryo Arises by Dynamic Widespread Intercalation of Embryonic and Extraembryonic Lineages. Developmental Cell *15*, 509–520.

Lacombe, F., and Belloc, F. (1996). Flow cytometry study of cell cycle, apoptosis and drug resistance in acute leukemia. Hematol Cell Ther *38*, 495–504.

Laflamme, M.A., Chen, K.Y., Naumova, A.V., Muskheli, V., Fugate, J.A., Dupras, S.K., Reinecke, H., Xu, C., Hassanipour, M., Police, S., et al. (2007). Cardiomyocytes derived from human embryonic stem cells in pro-survival factors enhance function of infarcted rat hearts. Nature Biotechnology *25*, 1015–1024.

Lahm, H., Deutsch, M.-A., Dreßen, M., Doppler, S., Werner, A., Hörer, J., Cleuziou, J., Schreiber, C., Böhm, J., Laugwitz, K.-L., et al. (2013). Mutational analysis of the

human MESP1 gene in patients with congenital heart disease reveals a highly variable sequence in exon 1. European Journal of Medical Genetics *56*, 591–598.
Lanier, L.L. (2014). Just the FACS. The Journal of Immunology *193*, 2043–2044.
Lanner, F., and Rossant, J. (2010). The role of FGF/Erk signaling in pluripotent cells. Development *137*, 3351–3360.
Latinkić, B.V., Umbhauer, M., Neal, K.A., Lerchner, W., Smith, J.C., and Cunliffe, V. (1997). The Xenopus Brachyury promoter is activated by FGF and low concentrations of activin and suppressed by high concentrations of activin and by paired-type homeodomain proteins. Genes Dev. *11*, 3265–3276.
Laugwitz, K.-L., Moretti, A., Lam, J., Gruber, P., Chen, Y., Woodard, S., Lin, L.-Z., Cai, C.-L., Lu, M.M., Reth, M., et al. (2005). Postnatal isl1+ cardioblasts enter fully differentiated cardiomyocyte lineages. Nature *433*, 647–653.
Lauss, M., Stary, M., Tischler, J., Egger, G., Puz, S., Bader-Allmer, A., Seiser, C., and Weitzer, G. (2005). Single inner cell masses yield embryonic stem cell lines differing in lifr expression and their developmental potential. Biochemical and Biophysical Research Communications *331*, 1577–1586.
Lee, M.Y., Cagavi Bozkulak, E., Schliffke, S., Amos, P.J., Ren, Y., Ge, X., Ehrlich, B.E., and Qyang, Y. (2011). High density cultures of embryoid bodies enhanced cardiac differentiation of murine embryonic stem cells. Biochemical and Biophysical Research Communications *416*, 51–57.
Lee, Y., Shioi, T., Kasahara, H., Jobe, S.M., Wiese, R.J., Markham, B.E., and Izumo, S. (1998). The cardiac tissue-restricted homeobox protein Csx/Nkx2.5 physically associates with the zinc finger protein GATA4 and cooperatively activates atrial natriuretic factor gene expression. Mol. Cell. Biol. *18*, 3120–3129.
Leitner, L.M. (2013). Establishment of reporter cell lines for the characterization of Brachyury and Mesp1 expression during in vitro cardiomyogenesis. Diploma thesis. University of Vienna.
Lerchner, W., Latinkic, B.V., Remacle, J.E., Huylebroeck, D., and Smith, J.C. (2000). Region-specific activation of the Xenopus brachyury promoter involves active repression in ectoderm and endoderm: a study using transgenic frog embryos. Development *127*, 2729–2739.
Leri, A., Kajstura, J., and Anversa, P. (2011). Role of Cardiac Stem Cells in Cardiac Pathophysiology: A Paradigm Shift in Human Myocardial Biology. Circulation Research *109*, 941–961.
Leri, A., Rota, M., Hosoda, T., Goichberg, P., and Anversa, P. (2014). Cardiac stem cell niches. Stem Cell Research.
Lewis, S.L., and Tam, P.P.L. (2006). Definitive endoderm of the mouse embryo: formation, cell fates, and morphogenetic function. Dev. Dyn. *235*, 2315–2329.
Li, L., and Clevers, H. (2010). Coexistence of Quiescent and Active Adult Stem Cells in Mammals. Science *327*, 542–545.
Li, Y., McClintick, J., Zhong, L., Edenberg, H.J., Yoder, M.C., and Chan, R.J. (2005). Murine embryonic stem cell differentiation is promoted by SOCS-3 and inhibited by the zinc finger transcription factor Klf4. Blood 10^5, 635–637.
Li, Y., Yu, W., Cooney, A.J., Schwartz, R.J., and Liu, Y. (2013). Brief Report: Oct4 and Canonical Wnt Signaling Regulate the Cardiac Lineage Factor Mesp1 Through a Tcf/Lef-Oct4 Composite Element. Stem Cells *31*, 1213–1217.
Lian, X., Hsiao, C., Wilson, G., Zhu, K., Hazeltine, L.B., Azarin, S.M., Raval, K.K., Zhang, J., Kamp, T.J., and Palecek, S.P. (2012). Robust cardiomyocyte differentiation from human pluripotent stem cells via temporal modulation of canonical Wnt signaling. Proc. Natl. Acad. Sci. U.S.A. *109*, E1848–E1857.
Liberatore, C.M., Searcy-Schrick, R.D., Vincent, E.B., and Yutzey, K.E. (2002). Nkx-2.5 gene induction in mice is mediated by a Smad consensus regulatory region. Dev. Biol. *244*, 243–256.
Lien, C.-L., Wu, C., Mercer, B., Webb, R., Richardson, J.A., and Olson, E.N. (1999). Control of early cardiac-specific transcription of Nkx2-5 by a GATA-dependent enhancer. Development *126*, 75–84.

Lien, C.-L., McAnally, J., Richardson, J.A., and Olson, E.N. (2002). Cardiac-specific activity of an Nkx2-5 enhancer requires an evolutionarily conserved Smad binding site. Dev. Biol. *244*, 257–266.

Lin, C.-J., Lin, C.-Y., Chen, C.-H., Zhou, B., and Chang, C.-P. (2012). Partitioning the heart: mechanisms of cardiac septation and valve development. Development *139*, 3277–3299.

Lin, L., Cui, L., Zhou, W., Dufort, D., Zhang, X., Cai, C.-L., Bu, L., Yang, L., Martin, J., Kemler, R., et al. (2007). Beta-catenin directly regulates Islet1 expression in cardiovascular progenitors and is required for multiple aspects of cardiogenesis. Proc. Natl. Acad. Sci. U.S.A. *104*, 9313–9318.

Lindsley, R.C., Gill, J.G., Kyba, M., Murphy, T.L., and Murphy, K.M. (2006). Canonical Wnt signaling is required for development of embryonic stem cell-derived mesoderm. Development *133*, 3787–3796.

Lindsley, R.C., Gill, J.G., Murphy, T.L., Langer, E.M., Cai, M., Mashayekhi, M., Wang, W., Niwa, N., Nerbonne, J.M., Kyba, M., et al. (2008). Mesp1 Coordinately Regulates Cardiovascular Fate Restriction and Epithelial-Mesenchymal Transition in Differentiating ESCs. Cell Stem Cell *3*, 55–68.

Linke, A., Müller, P., Nurzynska, D., Casarsa, C., Torella, D., Nascimbene, A., Castaldo, C., Cascapera, S., Böhm, M., Quaini, F., et al. (2005). Stem cells in the dog heart are self-renewing, clonogenic, and multipotent and regenerate infarcted myocardium, improving cardiac function. Proceedings of the National Academy of Sciences of the United States of America *102*, 8966–8971.

Lints, T.J., Parsons, L.M., Hartley, L., Lyons, I., and Harvey, R.P. (1993). Nkx-2.5: a novel murine homeobox gene expressed in early heart progenitor cells and their myogenic descendants. Development *119*, 419–431.

Liu, C., Nakamura, E., Knezevic, V., Hunter, S., Thompson, K., and Mackem, S. (2003). A role for the mesenchymal T-box gene Brachyury in AER formation during limb development. Development *130*, 1327–1337.

Liu, H., Lin, J., and Roy, K. (2006). Effect of 3D scaffold and dynamic culture condition on the global gene expression profile of mouse embryonic stem cells. Biomaterials *27*, 5978–5989.

Liu, P., Wakamiya, M., Shea, M.J., Albrecht, U., Behringer, R.R., and Bradley, A. (1999). Requirement for Wnt3 in vertebrate axis formation. Nat. Genet. *22*, 361–365.

Liu, W., Medeiros, L.J., Lin, P., Romaguera, J.E., Wang, S.A., and Jorgensen, J.L. (2012). Usefulness of flow cytometric immunophenotyping for bone marrow staging in patients with mantle cell lymphoma after therapy. Am. J. Clin. Pathol. *137*, 634–640.

Liu, Y., Asakura, M., Inoue, H., Nakamura, T., Sano, M., Niu, Z., Chen, M., Schwartz, R.J., and Schneider, M.D. (2007). Sox17 is essential for the specification of cardiac mesoderm in embryonic stem cells. Proc. Natl. Acad. Sci. U.S.A. *104*, 3859–3864.

Liu, Z., Li, T., Liu, Y., Jia, Z., Li, Y., Zhang, C., Chen, P., Ma, K., Affara, N., and Zhou, C. (2009). WNT signaling promotes Nkx2.5 expression and early cardiomyogenesis via downregulation of Hdac1. Biochimica et Biophysica Acta (BBA) - Molecular Cell Research *1793*, 300–311.

Liu, Z.-P., Nakagawa, O., Nakagawa, M., Yanagisawa, H., Passier, R., Richardson, J.A., Srivastava, D., and Olson, E.N. (2001). CHAMP, A Novel Cardiac-Specific Helicase Regulated by MEF2C. Developmental Biology *234*, 497–509.

Lolas, M., Valenzuela, P.D.T., Tjian, R., and Liu, Z. (2014). Charting Brachyury-mediated developmental pathways during early mouse embryogenesis. Proceedings of the National Academy of Sciences *111*, 4478–4483.

Lomax, B., Tang, S., Separovic, E., Phillips, D., Hillard, E., Thomson, T., and Kalousek, D.K. (2000). Comparative genomic hybridization in combination with flow cytometry improves results of cytogenetic analysis of spontaneous abortions. Am. J. Hum. Genet. *66*, 1516–1521.

Lomonico, M.P., Moore, G.W., and Hutchins, G.M. (1986). Rotation of the junction of the outflow tract and great arteries in the embryonic human heart. Anat. Rec. *216*, 544–549.

Lu, C.C., Brennan, J., and Robertson, E.J. (2001). From fertilization to gastrulation: axis formation in the mouse embryo. Curr. Opin. Genet. Dev. *11*, 384–392.

Lu, J., Hou, R., Booth, C.J., Yang, S.-H., and Snyder, M. (2006). Defined culture conditions of human embryonic stem cells. Proc. Natl. Acad. Sci. U.S.A. *103*, 5688–5693.

Lyons, I., Parsons, L.M., Hartley, L., Li, R., Andrews, J.E., Robb, L., and Harvey, R.P. (1995). Myogenic and morphogenetic defects in the heart tubes of murine embryos lacking the homeo box gene Nkx2-5. Genes Dev. *9*, 1654–1666.

MacDonald, B.T., Tamai, K., and He, X. (2009). Wnt/beta-catenin signaling: components, mechanisms, and diseases. Dev. Cell *17*, 9–26.

Makkar, R.R., Smith, R.R., Cheng, K.E., Malliaras, K., Thomson, L.E., Berman, D., Czer, L.S., Marbán, L., Mendizabal, A., Johnston, P.V., et al. (2012). Intracoronary cardiosphere-derived cells for heart regeneration after myocardial infarction (CADUCEUS): a prospective, randomised phase 1 trial. The Lancet *379*, 895–904.

Malbon, C.C., Wang, H., and Moon, R.T. (2001). Wnt signaling and heterotrimeric G-proteins: strange bedfellows or a classic romance? Biochem. Biophys. Res. Commun. *287*, 589–593.

Maltsev, V.A., Wobus, A.M., Rohwedel, J., Bader, M., and Hescheler, J. (1994). Cardiomyocytes differentiated in vitro from embryonic stem cells developmentally express cardiac-specific genes and ionic currents. Circ. Res. *75*, 233–244.

Männer, J. (2000). Cardiac looping in the chick embryo: a morphological review with special reference to terminological and biomechanical aspects of the looping process. Anat. Rec. *259*, 248–262.

Männer, J., Pérez-Pomares, J.M., Macías, D., and Muñoz-Chápuli, R. (2001). The origin, formation and developmental significance of the epicardium: a review. Cells Tissues Organs (Print) *169*, 89–103.

Maranca-Hüwel, B., and Denker, H.-W. (2010). Epithelial-mesenchymal transition in rhesus monkey embryonic stem cell colonies: the role of culturing conditions. In Vitro Cell. Dev. Biol. Anim. *46*, 516–528.

Maretto, S., Cordenonsi, M., Dupont, S., Braghetta, P., Broccoli, V., Hassan, A.B., Volpin, D., Bressan, G.M., and Piccolo, S. (2003). Mapping Wnt/beta-catenin signaling during mouse development and in colorectal tumors. Proc. Natl. Acad. Sci. U.S.A. *100*, 3299–3304.

Marone, M., De Ritis, D., Bonanno, G., Mozzetti, S., Rutella, S., Scambia, G., and Pierelli, L. (2002). Cell cycle regulation in human hematopoietic stem cells: from isolation to activation. Leuk. Lymphoma *43*, 493–501.

Martello, G., Bertone, P., and Smith, A. (2013). Identification of the missing pluripotency mediator downstream of leukaemia inhibitory factor. The EMBO Journal *32*, 2561–2574.

Martin, C.M., Meeson, A.P., Robertson, S.M., Hawke, T.J., Richardson, J.A., Bates, S., Goetsch, S.C., Gallardo, T.D., and Garry, D.J. (2004). Persistent expression of the ATP-binding cassette transporter, Abcg2, identifies cardiac SP cells in the developing and adult heart. Developmental Biology *265*, 262–275.

Martin, R.M., Leonhardt, H., and Cardoso, M.C. (2005). DNA labeling in living cells. Cytometry Part A *67A*, 45–52.

Marvin, M.J., Di Rocco, G., Gardiner, A., Bush, S.M., and Lassar, A.B. (2001). Inhibition of Wnt activity induces heart formation from posterior mesoderm. Genes Dev. *15*, 316–327.

Matar, A.A., and Chong, J.J. (2014). Stem cell therapy for cardiac dysfunction. SpringerPlus *3*, 440.

Maurer, J., Nelson, B., Ceceña, G., Bajpai, R., Mercola, M., Terskikh, A., and Oshima, R.G. (2008). Contrasting expression of keratins in mouse and human embryonic stem cells. PLoS ONE *3*, e3451.

Maye, P., Zheng, J., Li, L., and Wu, D. (2004). Multiple mechanisms for Wnt11-mediated repression of the canonical Wnt signaling pathway. J. Biol. Chem. *279*, 24659–24665.

McBratney-Owen, B., Iseki, S., Bamforth, S.D., Olsen, B.R., and Morriss-Kay, G.M. (2008). Development and tissue origins of the mammalian cranial base. Dev. Biol. *322*, 121–132.

McCloskey, K.E., Lyons, I., Rao, R.R., Stice, S.L., and Nerem, R.M. (2003). Purified and proliferating endothelial cells derived and expanded in vitro from embryonic stem cells. Endothelium *10*, 329–336.

McCormick, J.B., and Huso, H.A. (2010). Stem Cells and Ethics: Current Issues. Journal of Cardiovascular Translational Research *3*, 122–127.

McCoy, J.P., and Carey, J.L. (1990). Recent advances in flow cytometric techniques for cancer detection and prognosis. Immunol. Ser. *53*, 171–187.

McElhinney, D.B., Geiger, E., Blinder, J., Benson, D.W., and Goldmuntz, E. (2003). NKX2.5 mutations in patients with congenital heart disease. J. Am. Coll. Cardiol. *42*, 1650–1655.

McMahon, A.P., and Bradley, A. (1990). The Wnt-1 (int-1) proto-oncogene is required for development of a large region of the mouse brain. Cell *62*, 1073–1085.

Meilhac, S.M., Esner, M., Kelly, R.G., Nicolas, J.-F., and Buckingham, M.E. (2004). The clonal origin of myocardial cells in different regions of the embryonic mouse heart. Dev. Cell *6*, 685–698.

Menten, B., Swerts, K., Delle Chiaie, B., Janssens, S., Buysse, K., Philippé, J., and Speleman, F. (2009). Array comparative genomic hybridization and flow cytometry analysis of spontaneous abortions and mors in utero samples. BMC Med. Genet. *10*, 89.

Mesnard, D., Guzman-Ayala, M., and Constam, D.B. (2006). Nodal specifies embryonic visceral endoderm and sustains pluripotent cells in the epiblast before overt axial patterning. Development *133*, 2497–2505.

Messina, E., De Angelis, L., Frati, G., Morrone, S., Chimenti, S., Fiordaliso, F., Salio, M., Battaglia, M., Latronico, M.V.G., Coletta, M., et al. (2004). Isolation and Expansion of Adult Cardiac Stem Cells From Human and Murine Heart. Circulation Research *95*, 911–921.

Meysen, S., Marger, L., Hewett, K.W., Jarry-Guichard, T., Agarkova, I., Chauvin, J.P., Perriard, J.C., Izumo, S., Gourdie, R.G., Mangoni, M.E., et al. (2007). Nkx2.5 cell-autonomous gene function is required for the postnatal formation of the peripheral ventricular conduction system. Dev. Biol. *303*, 740–753.

De Miguel, M.P., Fuentes-Julián, S., and Alcaina, Y. (2010). Pluripotent Stem Cells: Origin, Maintenance and Induction. Stem Cell Reviews and Reports *6*, 633–649.

Mikels, A.J., and Nusse, R. (2006). Purified Wnt5a protein activates or inhibits beta-catenin-TCF signaling depending on receptor context. PLoS Biol. *4*, e115.

Milner, D.J., Taffet, G.E., Wang, X., Pham, T., Tamura, T., Hartley, C., Gerdes, A.M., and Capetanaki, Y. (1999). The absence of desmin leads to cardiomyocyte hypertrophy and cardiac dilation with compromised systolic function. J. Mol. Cell. Cardiol. *31*, 2063–2076.

Min, J.-Y., Yang, Y., Converso, K.L., Liu, L., Huang, Q., Morgan, J.P., and Xiao, Y.-F. (2002). Transplantation of embryonic stem cells improves cardiac function in postinfarcted rats. J. Appl. Physiol. *92*, 288–296.

Minami, T., and Aird, W.C. (2005). Endothelial cell gene regulation. Trends in Cardiovascular Medicine *15*, 174–e1.

Miquerol, L., and Kelly, R.G. (2013). Organogenesis of the vertebrate heart. Wiley Interdiscip Rev Dev Biol *2*, 17–29.

Miyabayashi, T., Teo, J.-L., Yamamoto, M., McMillan, M., Nguyen, C., and Kahn, M. (2007). Wnt/beta-catenin/CBP signaling maintains long-term murine embryonic stem cell pluripotency. Proc. Natl. Acad. Sci. U.S.A. *104*, 5668–5673.

Mjaatvedt, C.H., Nakaoka, T., Moreno-Rodriguez, R., Norris, R.A., Kern, M.J., Eisenberg, C.A., Turner, D., and Markwald, R.R. (2001). The outflow tract of the heart is recruited from a novel heart-forming field. Dev. Biol. *238*, 97–109.

Mohamed, O.A., Clarke, H.J., and Dufort, D. (2004). Beta-catenin signaling marks the prospective site of primitive streak formation in the mouse embryo. Dev. Dyn. *231*, 416–424.

Mommersteeg, M.T.M., Soufan, A.T., de Lange, F.J., van den Hoff, M.J.B., Anderson, R.H., Christoffels, V.M., and Moorman, A.F.M. (2006). Two distinct pools of mesenchyme contribute to the development of the atrial septum. Circ. Res. *99*, 351–353.

Monkley, S.J., Delaney, S.J., Pennisi, D.J., Christiansen, J.H., and Wainwright, B.J. (1996). Targeted disruption of the Wnt2 gene results in placentation defects. Development *122*, 3343–3353.

Monzen, K., Shiojima, I., Hiroi, Y., Kudoh, S., Oka, T., Takimoto, E., Hayashi, D., Hosoda, T., Habara-Ohkubo, A., Nakaoka, T., et al. (1999). Bone morphogenetic proteins induce cardiomyocyte differentiation through the mitogen-activated protein kinase kinase kinase TAK1 and cardiac transcription factors Csx/Nkx-2.5 and GATA-4. Mol. Cell. Biol. *19*, 7096–7105.

Moorman, A., Webb, S., Brown, N.A., Lamers, W., and Anderson, R.H. (2003). Development of the heart: (1) formation of the cardiac chambers and arterial trunks. Heart *89*, 806–814.

Morley, R.H., Lachani, K., Keefe, D., Gilchrist, M.J., Flicek, P., Smith, J.C., and Wardle, F.C. (2009). A gene regulatory network directed by zebrafish No tail accounts for its roles in mesoderm formation. Proc. Natl. Acad. Sci. U.S.A. *106*, 3829–3834.

Moskowitz, I.P.G., Kim, J.B., Moore, M.L., Wolf, C.M., Peterson, M.A., Shendure, J., Nobrega, M.A., Yokota, Y., Berul, C., Izumo, S., et al. (2007). A molecular pathway including Id2, Tbx5, and Nkx2-5 required for cardiac conduction system development. Cell *129*, 1365–1376.

Mouquet, F., Pfister, O., Jain, M., Oikonomopoulos, A., Ngoy, S., Summer, R., Fine, A., and Liao, R. (2005). Restoration of Cardiac Progenitor Cells After Myocardial Infarction by Self-Proliferation and Selective Homing of Bone Marrow-Derived Stem Cells. Circulation Research *97*, 1090–1092.

Müller, C.W., and Herrmann, B.G. (1997). Crystallographic structure of the T domain-DNA complex of the Brachyury transcription factor. Nature *389*, 884–888.

Müller, J.G., Thompson, J.T., Edmonson, A.M., Rackley, M.S., Kasahara, H., Izumo, S., McQuinn, T.C., Menick, D.R., and O'Brien, T.X. (2002). Differential regulation of the cardiac sodium calcium exchanger promoter in adult and neonatal cardiomyocytes by Nkx2.5 and serum response factor. J. Mol. Cell. Cardiol. *34*, 807–821.

Murray, P., and Edgar, D. (2001). Regulation of the differentiation and behaviour of extra-embryonic endodermal cells by basement membranes. J. Cell. Sci. *114*, 931–939.

Muthuchamy, M., Pajak, L., Howles, P., Doetschman, T., and Wieczorek, D.F. (1993). Developmental analysis of tropomyosin gene expression in embryonic stem cells and mouse embryos. Molecular and Cellular Biology *13*, 3311–3323.

Nadal-Ginard, B., Kajstura, J., Leri, A., and Anversa, P. (2003). Myocyte Death, Growth, and Regeneration in Cardiac Hypertrophy and Failure. Circulation Research *92*, 139–150.

Nagy, I.I., Railo, A., Rapila, R., Hast, T., Sormunen, R., Tavi, P., Räsänen, J., and Vainio, S.J. (2010). Wnt-11 signalling controls ventricular myocardium development by patterning N-cadherin and beta-catenin expression. Cardiovasc. Res. *85*, 100–109.

Naito, A.T., Tominaga, A., Oyamada, M., Oyamada, Y., Shiraishi, I., Monzen, K., Komuro, I., and Takamatsu, T. (2003). Early stage-specific inhibitions of cardiomyocyte differentiation and expression of Csx/Nkx-2.5 and GATA-4 by phosphatidylinositol 3-kinase inhibitor LY294002. Exp. Cell Res. *291*, 56–69.

Naito, A.T., Shiojima, I., Akazawa, H., Hidaka, K., Morisaki, T., Kikuchi, A., and Komuro, I. (2006). Developmental stage-specific biphasic roles of Wnt/beta-catenin signaling

in cardiomyogenesis and hematopoiesis. Proc. Natl. Acad. Sci. U.S.A. *103*, 19812–19817.

Nakamura, T., Sano, M., Songyang, Z., and Schneider, M.D. (2003). A Wnt- and beta -catenin-dependent pathway for mammalian cardiac myogenesis. Proc. Natl. Acad. Sci. U.S.A. *100*, 5834–5839.

Nakano, T., Kodama, H., and Honjo, T. (1994). Generation of lymphohematopoietic cells from embryonic stem cells in culture. Science *265*, 1098–1101.

Nakashima, Y., Ono, K., Yoshida, Y., Kojima, Y., Kita, T., Tanaka, M., and Kimura, T. (2009). The search for Nkx2–5-regulated genes using purified embryonic stem cell-derived cardiomyocytes with Nkx2–5 gene targeting. Biochemical and Biophysical Research Communications *390*, 821–826.

Nascimento, B.R., Brant, L.C.C., Moraes, D.N., and Ribeiro, A.L.P. (2014). Global health and cardiovascular disease. Heart *100*, 1743–1749.

Nelson, A.C., Pillay, N., Henderson, S., Presneau, N., Tirabosco, R., Halai, D., Berisha, F., Flicek, P., Stemple, D.L., Stern, C.D., et al. (2012). An integrated functional genomics approach identifies the regulatory network directed by brachyury (T) in chordoma. J. Pathol. *228*, 274–285.

NHLBI, NIH - How Is Coronary Heart Disease Treated? url as of 1.10.2015: http://www.nhlbi.nih.gov/health/health-topics/topics/cad/treatment

Nichols, M., Townsend, N., Scarborough, P., and Rayner, M. (2014). Cardiovascular disease in Europe 2014: epidemiological update. European Heart Journal.

Nishikawa, S.-I., Hirashima, M., Nishikawa, S., and Ogawa, M. (2001). Cell biology of vascular endothelial cells. Annals of the New York Academy of Sciences *947*, 35–41.

Nishikawa, S.-I., Jakt, L.M., and Era, T. (2007). Embryonic stem-cell culture as a tool for developmental cell biology. Nature Reviews Molecular Cell Biology *8*, 502–507.

Nishioka, N., Yamamoto, S., Kiyonari, H., Sato, H., Sawada, A., Ota, M., Nakao, K., and Sasaki, H. (2008). Tead4 is required for specification of trophectoderm in pre-implantation mouse embryos. Mech. Dev. *125*, 270–283.

Niwa, H., Ogawa, K., Shimosato, D., and Adachi, K. (2009). A parallel circuit of LIF signalling pathways maintains pluripotency of mouse ES cells. Nature *460*, 118–122.

Northrop, J., Woods, A., Seger, R., Suzuki, A., Ueno, N., Krebs, E., and Kimelman, D. (1995). BMP-4 regulates the dorsal-ventral differences in FGF/MAPKK-mediated mesoderm induction in Xenopus. Dev. Biol. *172*, 242–252.

Noseda, M., Peterkin, T., Simões, F.C., Patient, R., and Schneider, M.D. (2011). Cardiopoietic factors: extracellular signals for cardiac lineage commitment. Circ. Res. *108*, 129–152.

Nowotschin, S., and Hadjantonakis, A.-K. (2010). Cellular dynamics in the early mouse embryo: from axis formation to gastrulation. Current Opinion in Genetics & Development *20*, 420–427.

Nsiah, B.A., Ahsan, T., Griffiths, S., Cooke, M., Nerem, R.M., and McDevitt, T.C. (2014). Fluid Shear Stress Pre-Conditioning Promotes Endothelial Morphogenesis of Embryonic Stem Cells Within Embryoid Bodies. Tissue Engineering Part A *20*, 954–965.

Oakley, G.J., Fuhrer, K., and Seethala, R.R. (2008). Brachyury, SOX-9, and podoplanin, new markers in the skull base chordoma vs chondrosarcoma differential: a tissue microarray-based comparative analysis. Mod. Pathol. *21*, 1461–1469.

Oh, H., Bradfute, S.B., Gallardo, T.D., Nakamura, T., Gaussin, V., Mishina, Y., Pocius, J., Michael, L.H., Behringer, R.R., Garry, D.J., et al. (2003). Cardiac progenitor cells from adult myocardium: homing, differentiation, and fusion after infarction. Proceedings of the National Academy of Sciences *100*, 12313–12318.

Ohtani, K., Vlachojannis, G.J., Koyanagi, M., Boeckel, J.-N., Urbich, C., Farcas, R., Bonig, H., Marquez, V.E., Zeiher, A.M., and Dimmeler, S. (2011). Epigenetic Regulation of Endothelial Lineage Committed Genes in Pro-Angiogenic Hematopoietic and Endothelial Progenitor Cells. Circulation Research *109*, 1219–1229.

Onizuka, T., Yuasa, S., Kusumoto, D., Shimoji, K., Egashira, T., Ohno, Y., Kageyama, T., Tanaka, T., Hattori, F., Fujita, J., et al. (2012). Wnt2 accelerates cardiac myocyte differentiation from ES-cell derived mesodermal cells via non-canonical pathway. Journal of Molecular and Cellular Cardiology *52*, 650–659.

Oyama, Y., Craig, R.M., Traynor, A.E., Quigley, K., Statkute, L., Halverson, A., Brush, M., Verda, L., Kowalska, B., Krosnjar, N., et al. (2005). Autologous hematopoietic stem cell transplantation in patients with refractory Crohn's disease. Gastroenterology *128*, 552–563.

Palena, C., Roselli, M., Litzinger, M.T., Ferroni, P., Costarelli, L., Spila, A., Cavaliere, F., Huang, B., Fernando, R.I., Hamilton, D.H., et al. (2014). Overexpression of the EMT driver brachyury in breast carcinomas: association with poor prognosis. J. Natl. Cancer Inst. 10^6.

Pandur, P., Läsche, M., Eisenberg, L.M., and Kühl, M. (2002). Wnt-11 activation of a non-canonical Wnt signalling pathway is required for cardiogenesis. Nature *418*, 636–641.

Parlakian, A., Tuil, D., Hamard, G., Tavernier, G., Hentzen, D., Concordet, J.-P., Paulin, D., Li, Z., and Daegelen, D. (2004). Targeted inactivation of serum response factor in the developing heart results in myocardial defects and embryonic lethality. Mol. Cell. Biol. *24*, 5281–5289.

Parr, B.A., and McMahon, A.P. (1994). Wnt genes and vertebrate development. Curr. Opin. Genet. Dev. *4*, 523–528.

Pashmforoush, M., Lu, J.T., Chen, H., Amand, T.S., Kondo, R., Pradervand, S., Evans, S.M., Clark, B., Feramisco, J.R., Giles, W., et al. (2004). Nkx2-5 pathways and congenital heart disease; loss of ventricular myocyte lineage specification leads to progressive cardiomyopathy and complete heart block. Cell *117*, 373–386.

Pauken, C.M., and Capco, D.G. (2000). The expression and stage-specific localization of protein kinase C isotypes during mouse preimplantation development. Dev. Biol. *223*, 411–421.

Pearl, J.I., Lee, A.S., Leveson-Gower, D.B., Sun, N., Ghosh, Z., Lan, F., Ransohoff, J., Negrin, R.S., Davis, M.M., and Wu, J.C. (2011). Short-Term Immunosuppression Promotes Engraftment of Embryonic and Induced Pluripotent Stem Cells. Cell Stem Cell *8*, 309–317.

Peichev, M., Naiyer, A.J., Pereira, D., Zhu, Z., Lane, W.J., Williams, M., Oz, M.C., Hicklin, D.J., Witte, L., Moore, M.A., et al. (2000). Expression of VEGFR-2 and AC133 by circulating human CD34(+) cells identifies a population of functional endothelial precursors. Blood *95*, 952–958.

Perea-Gomez, A., Meilhac, S.M., Piotrowska-Nitsche, K., Gray, D., Collignon, J., and Zernicka-Goetz, M. (2007). Regionalisation of the mouse visceral endoderm as the blastocyst transforms into the egg cylinder. BMC Developmental Biology *7*, 96.

Perrino, C., and Rockman, H.A. (2006). GATA4 and the Two Sides of Gene Expression Reprogramming. Circulation Research *98*, 715–716.

Pfeufer, A., van Noord, C., Marciante, K.D., Arking, D.E., Larson, M.G., Smith, A.V., Tarasov, K.V., Müller, M., Sotoodehnia, N., Sinner, M.F., et al. (2010). Genome-wide association study of PR interval. Nat. Genet. *42*, 153–159.

Pfister, S., Steiner, K.A., and Tam, P.P.L. (2007). Gene expression pattern and progression of embryogenesis in the immediate post-implantation period of mouse development. Gene Expr. Patterns *7*, 558–573.

Pinto, F., Pértega-Gomes, N., Pereira, M.S., Vizcaíno, J.R., Monteiro, P., Henrique, R.M., Baltazar, F., Andrade, R.P., and Reis, R.M. (2014). T-box transcription factor brachyury is associated with prostate cancer progression and aggressiveness. Clin. Cancer Res. *20*, 4949–4961.

Plaks, V., Birnberg, T., Berkutzki, T., Sela, S., BenYashar, A., Kalchenko, V., Mor, G., Keshet, E., Dekel, N., Neeman, M., et al. (2008). Uterine DCs are crucial for decidua formation during embryo implantation in mice. J. Clin. Invest. *118*, 3954–3965.

Plusa, B., Frankenberg, S., Chalmers, A., Hadjantonakis, A.-K., Moore, C.A., Papalopulu, N., Papaioannou, V.E., Glover, D.M., and Zernicka-Goetz, M. (2005). Downregulation of Par3 and aPKC function directs cells towards the ICM in the preimplantation mouse embryo. J. Cell. Sci. *118*, 505–515.

Prall, O.W.J., Menon, M.K., Solloway, M.J., Watanabe, Y., Zaffran, S., Bajolle, F., Biben, C., McBride, J.J., Robertson, B.R., Chaulet, H., et al. (2007). An Nkx2-5/Bmp2/Smad1 Negative Feedback Loop Controls Heart Progenitor Specification and Proliferation. Cell *128*, 947–959.

Presneau, N., Shalaby, A., Ye, H., Pillay, N., Halai, D., Idowu, B., Tirabosco, R., Whitwell, D., Jacques, T.S., Kindblom, L.-G., et al. (2011). Role of the transcription factor T (brachyury) in the pathogenesis of sporadic chordoma: a genetic and functional-based study. J. Pathol. *223*, 327–335.

Puett, R.C., Hart, J.E., Yanosky, J.D., Paciorek, C., Schwartz, J., Suh, H., Speizer, F.E., and Laden, F. (2009). Chronic Fine and Coarse Particulate Exposure, Mortality, and Coronary Heart Disease in the Nurses' Health Study. Environmental Health Perspectives *117*, 1697–1701.

Qi, X., Yang, G., Yang, L., Lan, Y., Weng, T., Wang, J., Wu, Z., Xu, J., Gao, X., and Yang, X. (2007). Essential role of Smad4 in maintaining cardiomyocyte proliferation during murine embryonic heart development. Dev. Biol. *311*, 136–146.

Qyang, Y., Martin-Puig, S., Chiravuri, M., Chen, S., Xu, H., Bu, L., Jiang, X., Lin, L., Granger, A., Moretti, A., et al. (2007). The renewal and differentiation of Isl1+ cardiovascular progenitors are controlled by a Wnt/beta-catenin pathway. Cell Stem Cell *1*, 165–179.

Rafii, S., Lyden, D., Benezra, R., Hattori, K., and Heissig, B. (2002). Vascular and haematopoietic stem cells: novel targets for anti-angiogenesis therapy? Nature Reviews Cancer *2*, 826–835.

Rajasingh, J., Bord, E., Hamada, H., Lambers, E., Qin, G., Losordo, D.W., and Kishore, R. (2007). STAT3-Dependent Mouse Embryonic Stem Cell Differentiation Into Cardiomyocytes: Analysis of Molecular Signaling and Therapeutic Efficacy of Cardiomyocyte Precommitted mES Transplantation in a Mouse Model of Myocardial Infarction. Circulation Research *101*, 910–918.

Ramírez-Solis, R., Liu, P., and Bradley, A. (1995). Chromosome engineering in mice. Nature *378*, 720–724.

Rashbass, P., Cooke, L.A., Herrmann, B.G., and Beddington, R.S. (1991). A cell autonomous function of Brachyury in T/T embryonic stem cell chimaeras. Nature *353*, 348–351.

Ratajczak, M., Zuba-Surma, E., Kucia, M., Poniewierska, A., Suszynska, M., and Ratajczak, J. (2012). Pluripotent and multipotent stem cells in adult tissues. Advances in Medical Sciences *57*, 1–17.

Reamon-Buettner, S.M., and Borlak, J. (2010). NKX2-5: an update on this hypermutable homeodomain protein and its role in human congenital heart disease (CHD). Human Mutation *31*, 1185–1194.

Reifers, F., Walsh, E.C., Léger, S., Stainier, D.Y., and Brand, M. (2000). Induction and differentiation of the zebrafish heart requires fibroblast growth factor 8 (fgf8/acerebellar). Development *127*, 225–235.

Reya, T., O'Riordan, M., Okamura, R., Devaney, E., Willert, K., Nusse, R., and Grosschedl, R. (2000). Wnt signaling regulates B lymphocyte proliferation through a LEF-1 dependent mechanism. Immunity *13*, 15–24.

Riccardi, C., and Nicoletti, I. (2006). Analysis of apoptosis by propidium iodide staining and flow cytometry. Nature Protocols *1*, 1458–1461.

Rieger, A.M., Nelson, K.L., Konowalchuk, J.D., and Barreda, D.R. (2011). Modified Annexin V/Propidium Iodide Apoptosis Assay For Accurate Assessment of Cell Death. Journal of Visualized Experiments.

Rivera-Pérez, J.A., and Magnuson, T. (2005). Primitive streak formation in mice is preceded by localized activation of Brachyury and Wnt3. Dev. Biol. *288*, 363–371.

Rivkees, S.A., Chen, M., Kulkarni, J., Browne, J., and Zhao, Z. (1999). Characterization of the murine A1 adenosine receptor promoter, potent regulation by GATA-4 and Nkx2.5. J. Biol. Chem. *274*, 14204–14209.

Rong, L., Liu, J., Qi, Y., Graham, A.M., Parmacek, M.S., and Li, S. (2012). GATA-6 promotes cell survival by up-regulating BMP-2 expression during embryonic stem cell differentiation. Molecular Biology of the Cell *23*, 3754–3763.

De Rooij, D.G., and Grootegoed, J.A. (1998). Spermatogonial stem cells. Current Opinion in Cell Biology *10*, 694–701.

Roselli, M., Fernando, R.I., Guadagni, F., Spila, A., Alessandroni, J., Palmirotta, R., Costarelli, L., Litzinger, M., Hamilton, D., Huang, B., et al. (2012). Brachyury, a driver of the epithelial-mesenchymal transition, is overexpressed in human lung tumors: an opportunity for novel interventions against lung cancer. Clin. Cancer Res. *18*, 3868–3879.

Rossant, J. (2001). Stem cells from the mammalian blastocyst. Stem Cells *19*, 477–482.

Rowley, T. (2012). Flow Cytometry - A Survey and the Basics. Materials and Methods *2*, 125.

Roy, A., Lin, Y.-N., Agno, J.E., DeMayo, F.J., and Matzuk, M.M. (2009). Tektin 3 is required for progressive sperm motility in mice. Molecular Reproduction and Development *76*, 453–459.

Rula, M.E., Cai, K.Q., Moore, R., Yang, D.-H., Staub, C.M., Capo-Chichi, C.D., Jablonski, S.A., Howe, P.H., Smith, E.R., and Xu, X.-X. (2007). Cell autonomous sorting and surface positioning in the formation of primitive endoderm in embryoid bodies. Genesis *45*, 327–338.

Ryan, T., Shelton, M., Lambert, J.-P., Malecova, B., Boisvenue, S., Ruel, M., Figeys, D., Puri, P.L., and Skerjanc, I.S. (2013). Myosin Phosphatase Modulates the Cardiac Cell Fate by Regulating the Subcellular Localization of Nkx2. 5 in a Wnt/Rho–Associated Protein Kinase–Dependent Pathway. Circulation Research *112*, 257–266.

Saga, Y., Hata, N., Kobayashi, S., Magnuson, T., Seldin, M.F., and Taketo, M.M. (1996). MesP1: a novel basic helix-loop-helix protein expressed in the nascent mesodermal cells during mouse gastrulation. Development *122*, 2769–2778.

Saga, Y., Miyagawa-Tomita, S., Takagi, A., Kitajima, S., Miyazaki, J. i, and Inoue, T. (1999). MesP1 is expressed in the heart precursor cells and required for the formation of a single heart tube. Development *126*, 3437–3447.

Saga, Y., Kitajima, S., and Miyagawa-Tomita, S. (2000). Mesp1 expression is the earliest sign of cardiovascular development. Trends Cardiovasc. Med. *10*, 345–352.

Saka, Y., Tada, M., and Smith, J.C. (2000). A screen for targets of the Xenopus T-box gene Xbra. Mech. Dev. *93*, 27–39.

Saka, Y., Hagemann, A.I., Piepenburg, O., and Smith, J.C. (2007). Nuclear accumulation of Smad complexes occurs only after the midblastula transition in Xenopus. Development *134*, 4209–4218.

Saneyoshi, T., Kume, S., Amasaki, Y., and Mikoshiba, K. (2002). The Wnt/calcium pathway activates NF-AT and promotes ventral cell fate in Xenopus embryos. Nature *417*, 295–299.

Sangoi, A.R., Karamchandani, J., Lane, B., Higgins, J.P., Rouse, R.V., Brooks, J.D., and McKenney, J.K. (2011). Specificity of brachyury in the distinction of chordoma from clear cell renal cell carcinoma and germ cell tumors: a study of 305 cases. Mod. Pathol. *24*, 425–429.

Sato, N., Meijer, L., Skaltsounis, L., Greengard, P., and Brivanlou, A.H. (2004). Maintenance of pluripotency in human and mouse embryonic stem cells through activation of Wnt signaling by a pharmacological GSK-3-specific inhibitor. Nat. Med. *10*, 55–63.

Satou, Y., Imai, K.S., and Satoh, N. (2004). The ascidian Mesp gene specifies heart precursor cells. Development *131*, 2533–2541.

Sawada, A., Fritz, A., Jiang, Y.J., Yamamoto, A., Yamasu, K., Kuroiwa, A., Saga, Y., and Takeda, H. (2000). Zebrafish Mesp family genes, mesp-a and mesp-b are

segmentally expressed in the presomitic mesoderm, and Mesp-b confers the anterior identity to the developing somites. Development *127*, 1691–1702.
Schleiffarth, J.R., Person, A.D., Martinsen, B.J., Sukovich, D.J., Neumann, A., Baker, C.V.H., Lohr, J.L., Cornfield, D.N., Ekker, S.C., and Petryk, A. (2007). Wnt5a is required for cardiac outflow tract septation in mice. Pediatr. Res. *61*, 386–391.
Schmidt, C., Wilson, V., Stott, D., and Beddington, R.S. (1997). T promoter activity in the absence of functional T protein during axis formation and elongation in the mouse. Dev. Biol. *189*, 161–173.
Schneider, V.A., and Mercola, M. (2001). Wnt antagonism initiates cardiogenesis in Xenopus laevis. Genes Dev. *15*, 304–315.
Schott, J.J., Benson, D.W., Basson, C.T., Pease, W., Silberbach, G.M., Moak, J.P., Maron, B.J., Seidman, C.E., and Seidman, J.G. (1998). Congenital heart disease caused by mutations in the transcription factor NKX2-5. Science *281*, 108–111.
Schroeder, J.A., Jackson, L.F., Lee, D.C., and Camenisch, T.D. (2003). Form and function of developing heart valves: coordination by extracellular matrix and growth factor signaling. J. Mol. Med. *81*, 392–403.
Schuijers, J., Mokry, M., Hatzis, P., Cuppen, E., and Clevers, H. (2014). Wnt-induced transcriptional activation is exclusively mediated by TCF/LEF. The EMBO Journal *33*, 146–156.
Schulte-Merker, S., and Smith, J.C. (1995). Mesoderm formation in response to Brachyury requires FGF signalling. Curr. Biol. *5*, 62–67.
Schulte-Merker, S., Ho, R.K., Herrmann, B.G., and Nüsslein-Volhard, C. (1992). The protein product of the zebrafish homologue of the mouse T gene is expressed in nuclei of the germ ring and the notochord of the early embryo. Development *116*, 1021–1032.
Schulte-Merker, S., van Eeden, F.J., Halpern, M.E., Kimmel, C.B., and Nüsslein-Volhard, C. (1994). no tail (ntl) is the zebrafish homologue of the mouse T (Brachyury) gene. Development *120*, 1009–1015.
Schultheiss, T.M., Xydas, S., and Lassar, A.B. (1995). Induction of avian cardiac myogenesis by anterior endoderm. Development *121*, 4203–4214.
Schultheiss, T.M., Burch, J.B., and Lassar, A.B. (1997). A role for bone morphogenetic proteins in the induction of cardiac myogenesis. Genes Dev. *11*, 451–462.
Schwartz, R.J., and Olson, E.N. (1999). Building the heart piece by piece: modularity of cis-elements regulating Nkx2-5 transcription. Development *126*, 4187–4192.
Schwartz, S.D., Hubschman, J.-P., Heilwell, G., Franco-Cardenas, V., Pan, C.K., Ostrick, R.M., Mickunas, E., Gay, R., Klimanskaya, I., and Lanza, R. (2012). Embryonic stem cell trials for macular degeneration: a preliminary report. The Lancet *379*, 713–720.
Searcy, R.D., Vincent, E.B., Liberatore, C.M., and Yutzey, K.E. (1998). A GATA-dependent nkx-2.5 regulatory element activates early cardiac gene expression in transgenic mice. Development *125*, 4461–4470.
Sepulveda, J.L., Belaguli, N., Nigam, V., Chen, C.Y., Nemer, M., and Schwartz, R.J. (1998). GATA-4 and Nkx-2.5 coactivate Nkx-2 DNA binding targets: role for regulating early cardiac gene expression. Mol. Cell. Biol. *18*, 3405–3415.
Sepulveda, J.L., Vlahopoulos, S., Iyer, D., Belaguli, N., and Schwartz, R.J. (2002). Combinatorial expression of GATA4, Nkx2-5, and serum response factor directs early cardiac gene activity. J. Biol. Chem. *277*, 25775–25782.
Shah, A.M., and MacCarthy, P.A. (2000). Paracrine and autocrine effects of nitric oxide on myocardial function. Pharmacol. Ther. *86*, 49–86.
Sheldahl, L.C., Slusarski, D.C., Pandur, P., Miller, J.R., Kühl, M., and Moon, R.T. (2003). Dishevelled activates Ca2+ flux, PKC, and CamKII in vertebrate embryos. J. Cell Biol. *161*, 769–777.
Shimoda, M., Sugiura, T., Imajyo, I., Ishii, K., Chigita, S., Seki, K., Kobayashi, Y., and Shirasuna, K. (2012). The T-box transcription factor Brachyury regulates epithelial-mesenchymal transition in association with cancer stem-like cells in adenoid cystic carcinoma cells. BMC Cancer *12*, 377.

Shin, C.H., Liu, Z.-P., Passier, R., Zhang, C.-L., Wang, D.-Z., Harris, T.M., Yamagishi, H., Richardson, J.A., Childs, G., and Olson, E.N. (2002). Modulation of cardiac growth and development by HOP, an unusual homeodomain protein. Cell *110*, 725–735.

Shiojima, I., Komuro, I., Oka, T., Hiroi, Y., Mizuno, T., Takimoto, E., Monzen, K., Aikawa, R., Akazawa, H., Yamazaki, T., et al. (1999). Context-dependent transcriptional cooperation mediated by cardiac transcription factors Csx/Nkx-2.5 and GATA-4. J. Biol. Chem. *274*, 8231–8239.

Shiojima, I., Oka, T., Hiroi, Y., Nagai, R., Yazaki, Y., and Komuro, I. (2000). Transcriptional regulation of human cardiac homeobox gene CSX1. Biochem. Biophys. Res. Commun. *272*, 749–757.

Showell, C., Binder, O., and Conlon, F.L. (2004). T-box genes in early embryogenesis. Dev. Dyn. *229*, 201–218.

Si, L., Shi, J., Gao, W., Zheng, M., Liu, L., Zhu, J., and Tian, J. (2014). Smad4 mediated BMP2 signal is essential for the regulation of GATA4 and Nkx2.5 by affecting the histone H3 acetylation in H9c2 cells. Biochemical and Biophysical Research Communications *450*, 81–86.

Simmons, D.G., and Cross, J.C. (2005). Determinants of trophoblast lineage and cell subtype specification in the mouse placenta. Developmental Biology *284*, 12–24.

Simmons, D.G., Fortier, A.L., and Cross, J.C. (2007). Diverse subtypes and developmental origins of trophoblast giant cells in the mouse placenta. Dev. Biol. *304*, 567–578.

Singh, A.M., Li, F.-Q., Hamazaki, T., Kasahara, H., Takemaru, K., and Terada, N. (2007). Chibby, an antagonist of the Wnt/beta-catenin pathway, facilitates cardiomyocyte differentiation of murine embryonic stem cells. Circulation *115*, 617–626.

Sirk, D.P., Zhu, Z., Wadia, J.S., and Mills, L.R. (2003). Flow cytometry and GFP: a novel assay for measuring the import and turnover of nuclear-encoded mitochondrial proteins in live PC12 cells. Cytometry A *56*, 15–22.

Slusarski, D.C., Corces, V.G., and Moon, R.T. (1997). Interaction of Wnt and a Frizzled homologue triggers G-protein-linked phosphatidylinositol signalling. Nature *390*, 410–413.

Smalley, M.J., and Dale, T.C. (1999). Wnt signalling in mammalian development and cancer. Cancer Metastasis Rev. *18*, 215–230.

Smith, J.C. (2001). Making mesoderm--upstream and downstream of Xbra. Int. J. Dev. Biol. *45*, 219–224.

Smith, J.C. (2004). Role of T-box genes during gastrulation. In Gastrulation: From Cells to Embryo, (Cold Spring Harbor, N.Y.: Cold Spring Harbor Laboratory Press), p. 731.

Smith, R., and McLaren, A. (1977). Factors affecting the time of formation of the mouse blastocoele. J Embryol Exp Morphol *41*, 79–92.

Smith, A.G., Heath, J.K., Donaldson, D.D., Wong, G.G., Moreau, J., Stahl, M., and Rogers, D. (1988). Inhibition of pluripotential embryonic stem cell differentiation by purified polypeptides. Nature *336*, 688–690.

Smith, J.C., Price, B.M., Green, J.B., Weigel, D., and Herrmann, B.G. (1991). Expression of a Xenopus homolog of Brachyury (T) is an immediate-early response to mesoderm induction. Cell *67*, 79–87.

Snarr, B.S., O'Neal, J.L., Chintalapudi, M.R., Wirrig, E.E., Phelps, A.L., Kubalak, S.W., and Wessels, A. (2007). Isl1 expression at the venous pole identifies a novel role for the second heart field in cardiac development. Circ. Res. *101*, 971–974.

Snarr, B.S., Kern, C.B., and Wessels, A. (2008). Origin and fate of cardiac mesenchyme. Dev. Dyn. *237*, 2804–2819.

Snyder, M., Huang, X.-Y., and Zhang, J.J. (2010). Stat3 Directly Controls the Expression of Tbx5, Nkx2.5, and GATA4 and Is Essential for Cardiomyocyte Differentiation of P19CL6 Cells. Journal of Biological Chemistry *285*, 23639–23646.

Solnica-Krezel, L., and Sepich, D.S. (2012). Gastrulation: Making and Shaping Germ Layers. Annual Review of Cell and Developmental Biology *28*, 687–717.

Sparrow, D.B., Jen, W.C., Kotecha, S., Towers, N., Kintner, C., and Mohun, T.J. (1998). Thylacine 1 is expressed segmentally within the paraxial mesoderm of the

Xenopus embryo and interacts with the Notch pathway. Development *125*, 2041–2051.
Später, D., Hansson, E.M., Zangi, L., and Chien, K.R. (2014). How to make a cardiomyocyte. Development *141*, 4418–4431.
Stallmeyer, B., Fenge, H., Nowak-Göttl, U., and Schulze-Bahr, E. (2010). Mutational spectrum in the cardiac transcription factor gene NKX2.5 (CSX) associated with congenital heart disease. Clin. Genet. *78*, 533–540.
Stanley, E.G., Biben, C., Elefanty, A., Barnett, L., Koentgen, F., Robb, L., and Harvey, R.P. (2002). Efficient Cre-mediated deletion in cardiac progenitor cells conferred by a 3'UTR-ires-Cre allele of the homeobox gene Nkx2-5. Int. J. Dev. Biol. *46*, 431–439.
Stark, K., Vainio, S., Vassileva, G., and McMahon, A.P. (1994). Epithelial transformation of metanephric mesenchyme in the developing kidney regulated by Wnt-4. Nature *372*, 679–683.
Stary, M., Pasteiner, W., Summer, A., Hrdina, A., Eger, A., and Weitzer, G. (2005). Parietal endoderm secreted SPARC promotes early cardiomyogenesis in vitro. Experimental Cell Research *310*, 331–343.
Stennard, F.A., Costa, M.W., Elliott, D.A., Rankin, S., Haast, S.J.P., Lai, D., McDonald, L.P.A., Niederreither, K., Dolle, P., Bruneau, B.G., et al. (2003). Cardiac T-box factor Tbx20 directly interacts with Nkx2-5, GATA4, and GATA5 in regulation of gene expression in the developing heart. Dev. Biol. *262*, 206–224.
Stower, M.J., and Srinivas, S. (2014). Heading forwards: anterior visceral endoderm migration in patterning the mouse embryo. Philosophical Transactions of the Royal Society B: Biological Sciences *369*, 20130546–20130546.
Strutt, D. (2003). Frizzled signalling and cell polarisation in Drosophila and vertebrates. Development *130*, 4501–4513.
Sun, X., Pang, L., Shi, M., Huang, J., and Wang, Y. (2015). HIF2α induces cardiomyogenesis via Wnt/β-catenin signaling in mouse embryonic stem cells. Journal of Translational Medicine *13*.
Sun, Y., Liang, X., Najafi, N., Cass, M., Lin, L., Cai, C.-L., Chen, J., and Evans, S.M. (2007). Islet 1 is expressed in distinct cardiovascular lineages, including pacemaker and coronary vascular cells. Dev. Biol. *304*, 286–296.
Suzuki, A., Raya, A., Kawakami, Y., Morita, M., Matsui, T., Nakashima, K., Gage, F.H., Rodríguez-Esteban, C., and Izpisúa Belmonte, J.C. (2006a). Maintenance of embryonic stem cell pluripotency by Nanog-mediated reversal of mesoderm specification. Nat Clin Pract Cardiovasc Med *3 Suppl 1*, S114–S122.
Suzuki, A., Raya, A., Kawakami, Y., Morita, M., Matsui, T., Nakashima, K., Gage, F.H., Rodríguez-Esteban, C., and Izpisúa Belmonte, J.C. (2006b). Nanog binds to Smad1 and blocks bone morphogenetic protein-induced differentiation of embryonic stem cells. Proc. Natl. Acad. Sci. U.S.A. *103*, 10294–10299.
Svensson, E.C., Tufts, R.L., Polk, C.E., and Leiden, J.M. (1999). Molecular cloning of FOG-2: A modulator of transcription factor GATA-4 in cardiomyocytes. PNAS *96*, 956–961.
Tada, M., and Smith, J.C. (2000). Xwnt11 is a target of Xenopus Brachyury: regulation of gastrulation movements via Dishevelled, but not through the canonical Wnt pathway. Development *127*, 2227–2238.
Tada, M., and Smith, J.C. (2001). T-targets: clues to understanding the functions of T-box proteins. Dev. Growth Differ. *43*, 1–11.
Tada, M., Casey, E.S., Fairclough, L., and Smith, J.C. (1998). Bix1, a direct target of Xenopus T-box genes, causes formation of ventral mesoderm and endoderm. Development *125*, 3997–4006.
Tada, M., Concha, M.L., and Heisenberg, C.P. (2002). Non-canonical Wnt signalling and regulation of gastrulation movements. Semin. Cell Dev. Biol. *13*, 251–260.
Tai, C.-I., and Ying, Q.-L. (2013). Gbx2, a LIF/Stat3 target, promotes reprogramming to and retention of the pluripotent ground state. Journal of Cell Science *126*, 1093–1098.

Takaoka, K., and Hamada, H. (2012). Cell fate decisions and axis determination in the early mouse embryo. Development *139*, 3–14.

Takaoka, K., Yamamoto, M., Shiratori, H., Meno, C., Rossant, J., Saijoh, Y., and Hamada, H. (2006). The mouse embryo autonomously acquires anterior-posterior polarity at implantation. Dev. Cell *10*, 451–459.

Takaoka, K., Yamamoto, M., and Hamada, H. (2011). Origin and role of distal visceral endoderm, a group of cells that determines anterior-posterior polarity of the mouse embryo. Nat. Cell Biol. *13*, 743–752.

Takashima, Y., and Suzuki, A. (2013). Regulation of organogenesis and stem cell properties by T-box transcription factors. Cellular and Molecular Life Sciences *70*, 3929–3945.

Takeuchi, J.K., Mileikovskaia, M., Koshiba-Takeuchi, K., Heidt, A.B., Mori, A.D., Arruda, E.P., Gertsenstein, M., Georges, R., Davidson, L., Mo, R., et al. (2005). Tbx20 dose-dependently regulates transcription factor networks required for mouse heart and motoneuron development. Development *132*, 2463–2474.

Talbot, W.S., Trevarrow, B., Halpern, M.E., Melby, A.E., Farr, G., Postlethwait, J.H., Jowett, T., Kimmel, C.B., and Kimelman, D. (1995). A homeobox gene essential for zebrafish notochord development. Nature *378*, 150–157.

Tam, P.P.L., and Loebel, D.A.F. (2007). Gene function in mouse embryogenesis: get set for gastrulation. Nat. Rev. Genet. *8*, 368–381.

Tam, P.P., Parameswaran, M., Kinder, S.J., and Weinberger, R.P. (1997). The allocation of epiblast cells to the embryonic heart and other mesodermal lineages: the role of ingression and tissue movement during gastrulation. Development *124*, 1631–1642.

Tam, P.P., Loebel, D.A., and Tanaka, S.S. (2006). Building the mouse gastrula: signals, asymmetry and lineages. Current Opinion in Genetics & Development *16*, 419–425.

Tanaka, M., Chen, Z., Bartunkova, S., Yamasaki, N., and Izumo, S. (1999). The cardiac homeobox gene Csx/Nkx2.5 lies genetically upstream of multiple genes essential for heart development. Development *126*, 1269–1280.

Tanaka, S.S., Kojima, Y., Yamaguchi, Y.L., Nishinakamura, R., and Tam, P.P.L. (2011). Impact of WNT signaling on tissue lineage differentiation in the early mouse embryo: WNT signaling on tissue lineage differentiation. Development, Growth & Differentiation *53*, 843–856.

Tarkowski, A.K., and Wróblewska, J. (1967). Development of blastomeres of mouse eggs isolated at the 4- and 8-cell stage. J Embryol Exp Morphol *18*, 155–180.

Tateishi, K., Ashihara, E., Takehara, N., Nomura, T., Honsho, S., Nakagami, T., Morikawa, S., Takahashi, T., Ueyama, T., Matsubara, H., et al. (2007). Clonally amplified cardiac stem cells are regulated by Sca-1 signaling for efficient cardiovascular regeneration. Journal of Cell Science *120*, 1791–1800.

Telford, W.G., Hawley, T., Subach, F., Verkhusha, V., and Hawley, R.G. (2012). Flow cytometry of fluorescent proteins. Methods *57*, 318–330.

Terada, R., Warren, S., Lu, J.T., Chien, K.R., Wessels, A., and Kasahara, H. (2011). Ablation of Nkx2-5 at mid-embryonic stage results in premature lethality and cardiac malformation. Cardiovascular Research *91*, 289–299.

Terami, H., Hidaka, K., Katsumata, T., Iio, A., and Morisaki, T. (2004). Wnt11 facilitates embryonic stem cell differentiation to Nkx2.5-positive cardiomyocytes. Biochem. Biophys. Res. Commun. *325*, 968–975.

Thattaliyath, B.D., Firulli, B.A., and Firulli, A.B. (2002). The basic-helix-loop-helix transcription factor HAND2 directly regulates transcription of the atrial naturetic peptide gene. J. Mol. Cell. Cardiol. *34*, 1335–1344.

The Lancet Editors (2014). Expression of concern: the SCIPIO trial. Lancet *383*, 1279.

Thiery, J.P., Acloque, H., Huang, R.Y.J., and Nieto, M.A. (2009). Epithelial-mesenchymal transitions in development and disease. Cell *139*, 871–890.

Thompson, J.F., Hayes, L.S., and Lloyd, D.B. (1991). Modulation of firefly luciferase stability and impact on studies of gene regulation. Gene *103*, 171–177.

Thomson, J.A., Itskovitz-Eldor, J., Shapiro, S.S., Waknitz, M.A., Swiergiel, J.J., Marshall, V.S., and Jones, J.M. (1998). Embryonic Stem Cell Lines Derived from Human Blastocysts. Science *282*, 1145–1147.

Tian, Y., Cohen, E.D., and Morrisey, E.E. (2010). The Importance of Wnt Signaling in Cardiovascular Development. Pediatric Cardiology *31*, 342–348.

Tonissen, K.F., Drysdale, T.A., Lints, T.J., Harvey, R.P., and Krieg, P.A. (1994). XNkx-2.5, a Xenopus gene related to Nkx-2.5 and tinman: evidence for a conserved role in cardiac development. Dev. Biol. *162*, 325–328.

Topol, L., Jiang, X., Choi, H., Garrett-Beal, L., Carolan, P.J., and Yang, Y. (2003). Wnt-5a inhibits the canonical Wnt pathway by promoting GSK-3-independent beta-catenin degradation. J. Cell Biol. *162*, 899–908.

Tortelote, G.G., Hernández-Hernández, J.M., Quaresma, A.J.C., Nickerson, J.A., Imbalzano, A.N., and Rivera-Pérez, J.A. (2013). Wnt3 function in the epiblast is required for the maintenance but not the initiation of gastrulation in mice. Developmental Biology *374*, 164–173.

Trivedi, H.L., Vanikar, A.V., Thakker, U., Firoze, A., Dave, S.D., Patel, C.N., Patel, J.V., Bhargava, A.B., and Shankar, V. (2008). Human Adipose Tissue-Derived Mesenchymal Stem Cells Combined With Hematopoietic Stem Cell Transplantation Synthesize Insulin. Transplantation Proceedings *40*, 1135–1139.

Tzahor, E., and Lassar, A.B. (2001). Wnt signals from the neural tube block ectopic cardiogenesis. Genes Dev. *15*, 255–260.

Ueno, S., Weidinger, G., Osugi, T., Kohn, A.D., Golob, J.L., Pabon, L., Reinecke, H., Moon, R.T., and Murry, C.E. (2007). Biphasic role for Wnt/beta-catenin signaling in cardiac specification in zebrafish and embryonic stem cells. Proc. Natl. Acad. Sci. U.S.A. *104*, 9685–9690.

Ueyama, T., Kasahara, H., Ishiwata, T., Nie, Q., and Izumo, S. (2003). Myocardin expression is regulated by Nkx2.5, and its function is required for cardiomyogenesis. Mol. Cell. Biol. *23*, 9222–9232.

Unno, K., Jain, M., and Liao, R. (2012). Cardiac Side Population Cells: Moving Toward the Center Stage in Cardiac Regeneration. Circulation Research *110*, 1355–1363.

Urbanek, K., Rota, M., Cascapera, S., Bearzi, C., Nascimbene, A., De Angelis, A., Hosoda, T., Chimenti, S., Baker, M., Limana, F., et al. (2005). Cardiac Stem Cells Possess Growth Factor-Receptor Systems That After Activation Regenerate the Infarcted Myocardium, Improving Ventricular Function and Long-Term Survival. Circulation Research *97*, 663–673.

Vallier, L., Alexander, M., and Pedersen, R.A. (2005). Activin/Nodal and FGF pathways cooperate to maintain pluripotency of human embryonic stem cells. Journal of Cell Science *118*, 4495–4509.

Verschueren, K., Remacle, J.E., Collart, C., Kraft, H., Baker, B.S., Tylzanowski, P., Nelles, L., Wuytens, G., Su, M.T., Bodmer, R., et al. (1999). SIP1, a novel zinc finger/homeodomain repressor, interacts with Smad proteins and binds to 5'-CACCT sequences in candidate target genes. J. Biol. Chem. *274*, 20489–20498.

Vincent, J.-P. (2014). Modulating and measuring Wingless signalling. Methods *68*, 194–198.

Vincent, S.D., and Buckingham, M.E. (2010). How to Make a Heart. In Current Topics in Developmental Biology, (Elsevier), pp. 1–41.

Vincentz, J.W., Barnes, R.M., Firulli, B.A., Conway, S.J., and Firulli, A.B. (2008). Cooperative interaction of Nkx2.5 and Mef2c transcription factors during heart development. Dev. Dyn. *237*, 3809–3819.

Vinot, S., Le, T., Ohno, S., Pawson, T., Maro, B., and Louvet-Vallée, S. (2005). Asymmetric distribution of PAR proteins in the mouse embryo begins at the 8-cell stage during compaction. Dev. Biol. *282*, 307–319.

Vittet, D., Prandini, M.H., Berthier, R., Schweitzer, A., Martin-Sisteron, H., Uzan, G., and Dejana, E. (1996). Embryonic stem cells differentiate in vitro to endothelial cells through successive maturation steps. Blood *88*, 3424–3431.

Vonica, A., and Gumbiner, B.M. (2002). Zygotic Wnt activity is required for Brachyury expression in the early Xenopus laevis embryo. Dev. Biol. *250*, 112–127.

Wagner, R.T., Xu, X., Yi, F., Merrill, B.J., and Cooney, A.J. (2010). Canonical Wnt/β-catenin regulation of liver receptor homolog-1 mediates pluripotency gene expression. Stem Cells *28*, 1794–1804.

Walder, D. (2011). Differentiation potential of cardiovascular progenitor cell line and somatic stem cell line isolated from the mouse. Diploma thesis. University of Vienna.

Waldo, K.L., Kumiski, D.H., Wallis, K.T., Stadt, H.A., Hutson, M.R., Platt, D.H., and Kirby, M.L. (2001). Conotruncal myocardium arises from a secondary heart field. Development *128*, 3179–3188.

Waldo, K.L., Hutson, M.R., Ward, C.C., Zdanowicz, M., Stadt, H.A., Kumiski, D., Abu-Issa, R., and Kirby, M.L. (2005). Secondary heart field contributes myocardium and smooth muscle to the arterial pole of the developing heart. Dev. Biol. *281*, 78–90.

Wallukat, G., and Wobus, A.M. (1991). Use of spontaneously beating heart muscle cells differentiating from pluripotential embryonic stem cells for testing of chronotropic agents. Arch. Toxicol. Suppl. *14*, 136–139.

Walpen, T., Peier, M., Haas, E., Kalus, I., Schwaller, J., Battegay, E., and Humar, R. (2012). Loss of Pim1 Imposes a Hyperadhesive Phenotype on Endothelial Cells. Cellular Physiology and Biochemistry *30*, 1083–1096.

Wang, H., Gilner, J.B., Bautch, V.L., Wang, D.-Z., Wainwright, B.J., Kirby, S.L., and Patterson, C. (2007). Wnt2 coordinates the commitment of mesoderm to hematopoietic, endothelial, and cardiac lineages in embryoid bodies. J. Biol. Chem. *282*, 782–791.

Wang, H., Hao, J., and Hong, C.C. (2011). Cardiac Induction of Embryonic Stem Cells by a Small Molecule Inhibitor of Wnt/β-Catenin Signaling. ACS Chemical Biology *6*, 192–197.

Webb, S., Brown, N.A., and Anderson, R.H. (1996). The structure of the mouse heart in late fetal stages. Anat. Embryol. *194*, 37–47.

Weisel, K.C., Kopp, H.-G., Moore, M.A.S., Studer, L., and Barberi, T. (2010). Wnt1 Overexpression Leads to Enforced Cardiomyogenesis and Inhibition of Hematopoiesis in Murine Embryonic Stem Cells. Stem Cells and Development *19*, 745–751.

Weitzer, G. (2006). Embryonic stem cell-derived embryoid bodies: an in vitro model of eutherian pregastrulation development and early gastrulation. Handb Exp Pharmacol *174*, 21–51.

Wessels, A., and Pérez-Pomares, J.M. (2004). The epicardium and epicardially derived cells (EPDCs) as cardiac stem cells. The Anatomical Record *276A*, 43–57.

Wessels, A., and Sedmera, D. (2003). Developmental anatomy of the heart: a tale of mice and man. Physiol. Genomics *15*, 165–176.

Wessels, A., Markman, M.W., Vermeulen, J.L., Anderson, R.H., Moorman, A.F., and Lamers, W.H. (1996). The development of the atrioventricular junction in the human heart. Circ. Res. *78*, 110–117.

Westfall, T.A., Brimeyer, R., Twedt, J., Gladon, J., Olberding, A., Furutani-Seiki, M., and Slusarski, D.C. (2003). Wnt-5/pipetail functions in vertebrate axis formation as a negative regulator of Wnt/beta-catenin activity. J. Cell Biol. *162*, 889–898.

Wexler, E.M., Paucer, A., Kornblum, H.I., Palmer, T.D., and Geschwind, D.H. (2009). Endogenous Wnt Signaling Maintains Neural Progenitor Cell Potency. Stem Cells *27*, 1130–1141.

WHO | Cardiovascular diseases (CVDs). url as of 11/09/15: http://www.who.int/mediacentre/factsheets/fs317/en/.

Wiles, M.V. (1993). Embryonic stem cell differentiation in vitro. Meth. Enzymol. *225*, 900–918.

Wilkinson, D.G., Bhatt, S., and Herrmann, B.G. (1990). Expression pattern of the mouse T gene and its role in mesoderm formation. Nature *343*, 657–659.

Williams, M., Burdsal, C., Periasamy, A., Lewandoski, M., and Sutherland, A. (2012). Mouse primitive streak forms in situ by initiation of epithelial to mesenchymal transition without migration of a cell population. Dev. Dyn. *241*, 270–283.

Williams, R.L., Hilton, D.J., Pease, S., Willson, T.A., Stewart, C.L., Gearing, D.P., Wagner, E.F., Metcalf, D., Nicola, N.A., and Gough, N.M. (1988). Myeloid leukaemia inhibitory factor maintains the developmental potential of embryonic stem cells. Nature *336*, 684–687.

Wilson, V., and Beddington, R. (1997). Expression of T protein in the primitive streak is necessary and sufficient for posterior mesoderm movement and somite differentiation. Dev. Biol. *192*, 45–58.

Wilson, V., Rashbass, P., and Beddington, R.S. (1993). Chimeric analysis of T (Brachyury) gene function. Development *117*, 1321–1331.

Wilson, V., Manson, L., Skarnes, W.C., and Beddington, R.S. (1995). The T gene is necessary for normal mesodermal morphogenetic cell movements during gastrulation. Development *121*, 877–886.

Wobus, A.M., and Boheler, K.R. (2005). Embryonic stem cells: prospects for developmental biology and cell therapy. Physiol. Rev. *85*, 635–678.

Wu, J.I., Centilli, M.A., Vasquez, G., Young, S., Scolnick, J., Durfee, L.A., Spearow, J.L., Schwantz, S.D., Rennebeck, G., and Artzt, K. (2007). Tint maps to mouse chromosome 6 and may interact with a notochordal enhancer of Brachyury. Genetics *177*, 1151–1161.

Yagi, R., Kohn, M.J., Karavanova, I., Kaneko, K.J., Vullhorst, D., DePamphilis, M.L., and Buonanno, A. (2007). Transcription factor TEAD4 specifies the trophectoderm lineage at the beginning of mammalian development. Development *134*, 3827–3836.

Yamagishi, H., Yamagishi, C., Nakagawa, O., Harvey, R.P., Olson, E.N., and Srivastava, D. (2001). The combinatorial activities of Nkx2.5 and dHAND are essential for cardiac ventricle formation. Dev. Biol. *239*, 190–203.

Yamaguchi, T.P., Takada, S., Yoshikawa, Y., Wu, N., and McMahon, A.P. (1999). T (Brachyury) is a direct target of Wnt3a during paraxial mesoderm specification. Genes Dev. *13*, 3185–3190.

Yamanaka, Y., Tamplin, O.J., Beckers, A., Gossler, A., and Rossant, J. (2007). Live Imaging and Genetic Analysis of Mouse Notochord Formation Reveals Regional Morphogenetic Mechanisms. Developmental Cell *13*, 884–896.

Yamanaka, Y., Lanner, F., and Rossant, J. (2010). FGF signal-dependent segregation of primitive endoderm and epiblast in the mouse blastocyst. Development *137*, 715–724.

Yamashita, J.K., Takano, M., Hiraoka-Kanie, M., Shimazu, C., Peishi, Y., Yanagi, K., Nakano, A., Inoue, E., Kita, F., and Nishikawa, S.-I. (2005). Prospective identification of cardiac progenitors by a novel single cell-based cardiomyocyte induction. FASEB J. *19*, 1534–1536.

Yanagisawa, K.O. (1990). Does the T gene determine the anteroposterior axis of a mouse embryo? Jpn. J. Genet. *65*, 287–297.

Yang, D.-H., Yoon, J.-Y., Lee, S.-H., Bryja, V., Andersson, E.R., Arenas, E., Kwon, Y.-G., and Choi, K.-Y. (2009a). Wnt5a is required for endothelial differentiation of embryonic stem cells and vascularization via pathways involving both Wnt/beta-catenin and protein kinase Calpha. Circ. Res. *104*, 372–379.

Yang, L., Cai, C.-L., Lin, L., Qyang, Y., Chung, C., Monteiro, R.M., Mummery, C.L., Fishman, G.I., Cogen, A., and Evans, S. (2006). Isl1Cre reveals a common Bmp pathway in heart and limb development. Development *133*, 1575–1585.

Yang, X.R., Ng, D., Alcorta, D.A., Liebsch, N.J., Sheridan, E., Li, S., Goldstein, A.M., Parry, D.M., and Kelley, M.J. (2009b). T (brachyury) gene duplication confers major susceptibility to familial chordoma. Nat. Genet. *41*, 1176–1178.

Yasunaga, M., Tada, S., Torikai-Nishikawa, S., Nakano, Y., Okada, M., Jakt, L.M., Nishikawa, S., Chiba, T., Era, T., and Nishikawa, S.-I. (2005). Induction and

monitoring of definitive and visceral endoderm differentiation of mouse ES cells. Nature Biotechnology *23*, 1542–1550.
Yasuo, H., and Satoh, N. (1993). Function of vertebrate T gene. Nature *364*, 582–583.
Yin, Z., Kong, Q.R., Zhao, Z.P., Wu, M.L., Mu, Y.S., Hu, K., and Liu, Z.H. (2012). Position effect variegation and epigenetic modification of a transgene in a pig model. Genetics and Molecular Research *11*, 355–369.
Ying, Q.-L., Nichols, J., Chambers, I., and Smith, A. (2003a). BMP induction of Id proteins suppresses differentiation and sustains embryonic stem cell self-renewal in collaboration with STAT3. Cell *115*, 281–292.
Ying, Q.-L., Stavridis, M., Griffiths, D., Li, M., and Smith, A. (2003b). Conversion of embryonic stem cells into neuroectodermal precursors in adherent monoculture. Nat. Biotechnol. *21*, 183–186.
Yoshida, K., Chambers, I., Nichols, J., Smith, A., Saito, M., Yasukawa, K., Shoyab, M., Taga, T., and Kishimoto, T. (1994). Maintenance of the pluripotential phenotype of embryonic stem cells through direct activation of gp130 signalling pathways. Mech. Dev. *45*, 163–171.
Yoshida, T., Vivatbutsiri, P., Morriss-Kay, G., Saga, Y., and Iseki, S. (2008). Cell lineage in mammalian craniofacial mesenchyme. Mech. Dev. *125*, 797–808.
Young, R.A. (2011). Control of the Embryonic Stem Cell State. Cell *144*, 940–954.
Yusen, R.D., Edwards, L.B., Kucheryavaya, A.Y., Benden, C., Dipchand, A.I., Dobbels, F., Goldfarb, S.B., Levvey, B.J., Lund, L.H., Meiser, B., et al. (2014). The Registry of the International Society for Heart and Lung Transplantation: Thirty-first Adult Lung and Heart–Lung Transplant Report—2014; Focus Theme: Retransplantation. The Journal of Heart and Lung Transplantation *33*, 1009–1024.
Zaffran, S., Kelly, R.G., Meilhac, S.M., Buckingham, M.E., and Brown, N.A. (2004). Right ventricular myocardium derives from the anterior heart field. Circ. Res. *95*, 261–268.
Zakin, L.D., Mazan, S., Maury, M., Martin, N., Guénet, J.L., and Brûlet, P. (1998). Structure and expression of Wnt13, a novel mouse Wnt2 related gene. Mech. Dev. *73*, 107–116.
Zaman, M.J., and Bhopal, R.S. (2013). New answers to three questions on the epidemic of coronary mortality in south Asians: incidence or case fatality? Biology or environment? Will the next generation be affected? Heart *99*, 154–158.
Zaruba, M.M., Soonpaa, M., Reuter, S., and Field, L.J. (2010). Cardiomyogenic Potential of C-Kit+-Expressing Cells Derived From Neonatal and Adult Mouse Hearts. Circulation *121*, 1992–2000.
Zeisberg, E.M., Ma, Q., Juraszek, A.L., Moses, K., Schwartz, R.J., Izumo, S., and Pu, W.T. (2005). Morphogenesis of the right ventricle requires myocardial expression of Gata4. J. Clin. Invest. *115*, 1522–1531.
Zhang, C.-L., Zou, Y., He, W., Gage, F.H., and Evans, R.M. (2008a). A role for adult TLX-positive neural stem cells in learning and behaviour. Nature *451*, 1004–1007.
Zhang, K., Li, L., Huang, C., Shen, C., Tan, F., Xia, C., Liu, P., Rossant, J., and Jing, N. (2010). Distinct functions of BMP4 during different stages of mouse ES cell neural commitment. Development *137*, 2095–210^{5}.
Zhang, L., Nomura-Kitabayashi, A., Sultana, N., Cai, W., Cai, X., Moon, A.M., and Cai, C.-L. (2014). Mesodermal Nkx2.5 is necessary and sufficient for early second heart field development. Developmental Biology *390*, 68–79.
Zhang, P., Li, J., Tan, Z., Wang, C., Liu, T., Chen, L., Yong, J., Jiang, W., Sun, X., Du, L., et al. (2008b). Short-term BMP-4 treatment initiates mesoderm induction in human embryonic stem cells. Blood *111*, 1933–1941.
Zhang, S.C., Wernig, M., Duncan, I.D., Brüstle, O., and Thomson, J.A. (2001). In vitro differentiation of transplantable neural precursors from human embryonic stem cells. Nat. Biotechnol. *19*, 1129–1133.
Zheng, M., Zhu, J., Lv, T., Liu, L., Sun, H., and Tian, J. (2013). Bone morphogenetic protein-2 enhances the expression of cardiac transcription factors by increasing histone H3 acetylation in H9c2 cells. Mol Med Rep *7*, 953–958.

Zhou, B., von Gise, A., Ma, Q., Rivera-Feliciano, J., and Pu, W.T. (2008). Nkx2-5- and Isl1-expressing cardiac progenitors contribute to proepicardium. Biochem. Biophys. Res. Commun. *375*, 450–453.

Zhou, B., Honor, L.B., He, H., Ma, Q., Oh, J.-H., Butterfield, C., Lin, R.-Z., Melero-Martin, J.M., Dolmatova, E., Duffy, H.S., et al. (2011). Adult mouse epicardium modulates myocardial injury by secreting paracrine factors. Journal of Clinical Investigation *121*, 1894–1904.

Zhou, W., Lin, L., Majumdar, A., Li, X., Zhang, X., Liu, W., Etheridge, L., Shi, Y., Martin, J., Van de Ven, W., et al. (2007). Modulation of morphogenesis by noncanonical Wnt signaling requires ATF/CREB family-mediated transcriptional activation of TGFbeta2. Nat. Genet. *39*, 1225–1234.

Zhu, S., Wurdak, H., Wang, J., Lyssiotis, C.A., Peters, E.C., Cho, C.Y., Wu, X., and Schultz, P.G. (2009). A small molecule primes embryonic stem cells for differentiation. Cell Stem Cell *4*, 416–426.

Zippo, A., De Robertis, A., Bardelli, M., Galvagni, F., and Oliviero, S. (2004). Identification of Flk-1 target genes in vasculogenesis: Pim-1 is required for endothelial and mural cell differentiation in vitro. Blood *103*, 4536–4544.

Zou, Y., Evans, S., Chen, J., Kuo, H.C., Harvey, R.P., and Chien, K.R. (1997). CARP, a cardiac ankyrin repeat protein, is downstream in the Nkx2-5 homeobox gene pathway. Development *124*, 793–804.

7 Appendix

Different clones of Brachyury^{EGFP} and MesP1^{EGFP} reporter ESC and CVPC lines were tested for the presence of *Brachyury^{EGFP}* and *MesP1^{EGFP}* transgenes, respectively, in the genome using PCR. Genomic DNA was isolated and PCR reactions with appropriate primers were performed.

Figures 6.1 and 6.2 depict where the individual primers bind to the transgenes. Table 6.1 shows for which clones and primer pairs PCR amplification was successful.

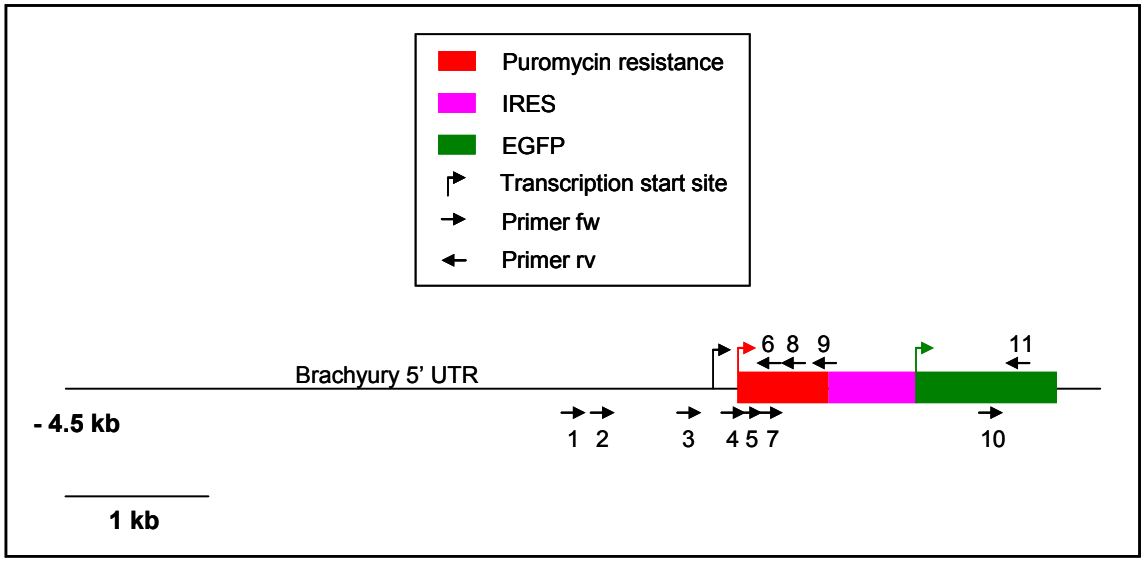

Figure 6.1: Brachyury^{EGFP} transgene. Small black arrows mark primer binding sites on the transgene.

1: primer T-NK1 fw. 2: primer Bra-Vektor 3 fw. 3: Bra-Vektor fw. 4: Bra-Vektor 2 fw. 5: Puro fw. 6: Puro 3 rv. 7: Puro 2 fw. 8: Puro 2 rv. 9: Puro rv. 10: EGFP fw. 11: EGFP rv. fw: forward. kb: kilobase. rv: reverse. UTR: untranslated region.

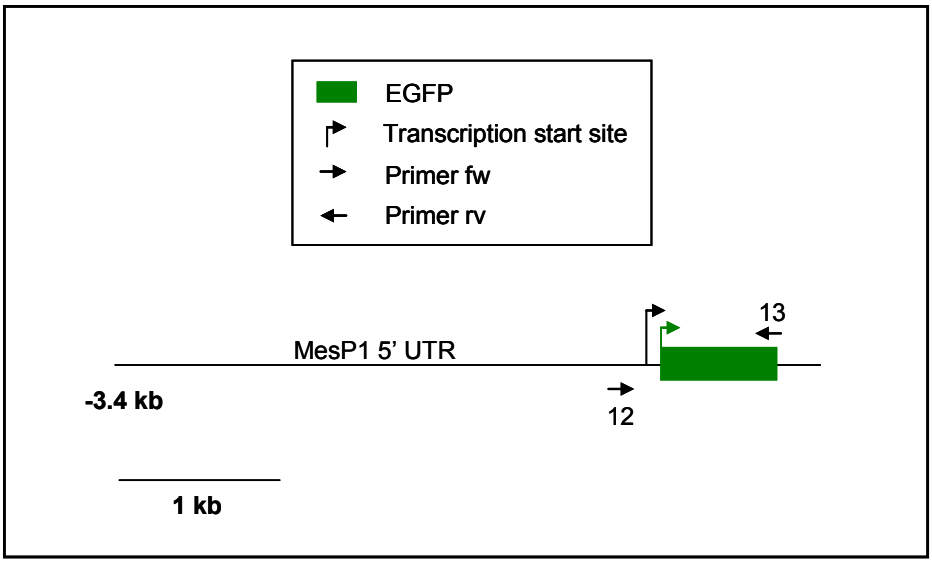

Figure 6.2: MesP1^{EGFP} transgene. Small black arrows mark primer binding sites on the transgene.

12: Mesp-Vektor fw. 13: EGFP rv.

fw: forward. kb: kilobase. rv: reverse. UTR: untranslated region.

Cell line + clone	Primers	Successful amplification
W4-bra-R-c3	T-NK1 fw (1) Puro 3 rv (6)	X
W4-bra-R-c1		X
W4-bra-R-c11		✓
W4-bra-R-c21		✓
A5-bra-R-cB		X
A5-bra-R-c7		X
A5-bra-R-c16		✓
W4-bra-R-c3	Bra-Vektor 3 fw (2) Puro 3 rv (6)	X
W4-bra-R-c1		X
W4-bra-R-c11		✓
W4-bra-R-c21		✓
A5-bra-R-cB		✓
A5-bra-R-c7		X
A5-bra-R-c16		✓
W4-bra-R-c3	Bra-Vektor fw (3) Puro 3 rv (6)	✓
W4-bra-R-c1		X
W4-bra-R-c11		✓
W4-bra-R-c21		✓
A5-bra-R-cB		✓
A5-bra-R-c7		X
A5-bra-R-c16		✓
W4-bra-R-c3	Bra-Vektor 2 fw (4) Puro 3 rv (6)	✓
W4-bra-R-c1		✓
W4-bra-R-c11		✓
W4-bra-R-c21		✓
A5-bra-R-c7		✓
W4-bra-R-c3	Puro fw (5) Puro rv (9)	✓
W4-bra-R-c1		✓
W4-bra-R-c11		✓
W4-bra-R-c21		X

Cell line + clone	Primers	Successful amplification
W4-bra-R-c3	Puro 2 fw (7) Puro 2 rv (8)	✓
W4-bra-R-c1		✓
W4-bra-R-c11		✓
W4-bra-R-c21		✓
A5-bra-R-c7		✓
W4-bra-R-c3	EGFP fw (10) EGFP rv (11)	✓
W4-bra-R-c1		✓
W4-bra-R-c11		✓
W4-bra-R-c21		✓
A5-bra-R-c7		✓
W4-MesP-R-cA	Mesp-Vektor fw (12) EGFP rv (13)	✓
W4-MesP-R-c1		✓
W4-MesP-R-c2		✓
W4-MesP-R-c3		✓
A5-MesP-R-c1		✓
A5-MesP-R-c2		X
A5-MesP-R-c4		✓
A5-MesP-R-c8		✓

Table 6.1: Results of test for the presence of parts of Brachyury^{EGFP} and MesP1^{EGFP} transgenes in the genome of different clones of Brachyury^{EGFP} and MesP1^{EGFP} ESC and CVPC lines.

✓**:** PCR amplification successful. X: PCR amplification unsuccessful. Numbers refer to figures 6.1 and 6.2.

W4-bra-R: Brachyury^{EGFP} reporter ESC line. A5-bra-R: Brachyury^{EGFP} reporter CVPC line. W4-MesP-R: MesP1^{EGFP} reporter ESC line. A5-MesP-R: MesP1^{EGFP} reporter CVPC line.

Abstract

In vitro-cardiomyogenesis of embryonic stem cells (ESCs) or cardiovascular progenitor cells (CVPCs) is usually triggered by placing these cells in hanging drop cultures in which they form 3D spheroids. However, this method is very laborious and cost-intensive. We therefore investigated the possibility to study cardiomyogenesis and its molecular regulation in low volume 2D monolayer culture, a less time consuming and less expensive method.

We assessed the capacity of ESCs and CVPCs to differentiate into contracting cardiomyocytes in low volume monolayer cell culture mainly by investigating *Brachyury*, *MesP1* and *Nkx2.5* expression patterns of differentiating ESCs and CVPCs in low volume monolayer cell culture. Brachyury is a very well characterised mesodermal marker and its expression is down-regulated upon further specialisation. MesP1 is the earliest known marker of cardiac progenitors. *Nkx2.5* is also expressed in early cardiac progenitors but remains to be expressed to some extent in the adult heart.

Unfortunately, neither ESCs nor CVPCs differentiated into mature cardiomyocytes in low volume monolayer cell culture. Nevertheless, *Brachyury*, *MesP1* and *Nkx2*.5 as well as other cardiac marker expression profiles indicate that differentiation into cardiac precursors is possible and that only the last steps of cardiomyogenesis are hampered in the monolayer system. However, CVPCs seem to preferentially develop towards the endothelial cell lineage in monolayer cell culture as endothelial marker gene expression levels are significantly higher in monolayer culture compared to hanging drop culture.

Monolayer cell culture allows for efficient endothelial differentiation and is advantageous to hanging drop culture not only regarding time and cost factors but also regarding cell visualisation and microenvironment control. Therefore, low volume monolayer cell culture provides an excellent tool to study endothelial cell differentiation processes and their regulation.

Zusammenfassung

In-vitro Kardiomyogenese von embryonalen Stammzellen (ESZ) oder kardiovaskulären Vorläuferzellen (KVZ) wird üblicherweise durch Überführung dieser Zellen in das so genannte „hanging drop“ Zellkultursystem ausgelöst, in welchem die Zellen 3D Spheroide ausbilden. Diese Methode ist allerdings sehr arbeits- und kostenintensiv. Darum haben wir untersucht, ob die Erforschung der Kardiomyogenese und ihrer molekularen Regulierung auch mittels einer weniger zeitaufwändigen und billigeren Methode, der 2D Monoschichtzellkultur in niedrigem Volumen, möglich ist.

Wir evaluierten die Fähigkeit der ESZ und KVZ zur Differenzierung in kontrahierende Kardiomyozyten vor allem mittels Analyse von Expressionsmustern der Gene *Brachyury*, *MesP1* und *Nkx2.5* in differenzierenden ESZ und KVZ in Monoschichtzellkultur in niedrigem Volumen. Brachyury ist ein sehr gut charakterisierter Marker des Mesoderms dessen Expression in der weiteren Entwicklung hinunter reguliert wird. MesP1 ist der früheste bekannte Marker von Herzvorläuferzellen. *Nkx2.5* wird auch in Herzvorläuferzellen exprimiert. Seine Expression bleibt allerdings in einem gewissen Ausmaß auch im adulten Herzen erhalten.

Leider differenzierten weder ESZ noch KVZ in voll entwickelte Kardiomyozyten in 2D Monoschichtzellkultur in niedrigem Volumen. Es lässt sich aber auf Grund der Expressionsprofile von *Brachyury*, *MesP1* und *Nkx2.5* als auch von anderen Herzmarkergenen darauf schließen, dass Herzvorläuferzellen sehr wohl in diesem System entstehen und nur die letzten Schritte der Kardiomyogenese nicht durchlaufen werden. Allerdings entwickeln sich KVZ bevorzugt in Endothelzellen in Monoschichtzellkultur, worauf deutlich höhere Expressionsniveaus von Endothelmarkergenen in der Monoschichtzellkultur im Vergleich zur „hanging drop“ Zellkultur hinweisen.

Monoschichtzellkultur ermöglicht effiziente Endothelzelldifferenzierung und bietet Vorteile gegenüber der „hanging drop“ Zellkultur nicht nur den Zeit- und Kostenfaktor betreffend sondern auch in Bezug auf Zellvisualisierung und auf die Kontrolle der Mikroumgebung. Deshalb stellt Monoschichtzellkultur in niedrigem Volumen ein hervorragendes Modell zur Untersuchung von Endotheldifferenzierungsprozessen und deren Regulierung dar.

Curriculum vitae

Name	Marie-Thérèse Konrad

Education

1997 – 2005	Gymnasium Realgymnasium 1 Stubenbastei 1010 Vienna, Austria
2005 – 2012	University of Vienna Bachelor Studies Biology
01/2009 – 06/2009	Université Paul Sabatier, Toulouse, France Exchange Semester
2012 – present	University of Vienna Master Studies Molecular Biology
05/2013 – 05/2014	Master's thesis (Research group of Georg Weitzer) Department of Medical Biochemistry Max F. Perutz Laboratories Medical University of Vienna

Scientific Symposia and Poster presentation

09/2013	Attendance at 5th Annual ÖGMBT meeting, Innsbruck, Austria
09/2014	Poster presentation at 6th Annual ÖGMBT meeting, Vienna, Austria *Can we study cardiomyogenesis in monolayer embryonic stem cell or cardiovascular progenitor cell cultures?* Konrad, M. and Weitzer, G.